Doctoral Thesis

NEW POTENTIAL NANOTECHNOLOGY-BASED THERAPIES FOR THE TREATMENT OF RHEUMATOID ARTHRITIS

Nataliya Storozhylova

Doctoral Program in Nanomedicine and Pharmaceutical Innovation

Faculty of Pharmacy

SANTIAGO DE COMPOSTELA

2018

USC
UNIVERSIDADE
DE SANTIAGO
DE COMPOSTELA

UNIVERSIDAD DE SANTIAGO DE COMPOSTELA

FACULTAD DE FARMACIA

DEPARTAMENTO DE FARMACOLOGÍA, FARMACIA Y TECNOLOGÍA FARMACÉUTICA

UNIVERSITÉ DE NANTES

FACULTÉ DES SCIENCES ET TECHNIQUES

Doctoral Thesis

NEW POTENTIAL NANOTECHNOLOGY-BASED THERAPIES FOR THE TREATMENT OF RHEUMATOID ARTHRITIS

Nataliya Storozhylova

Doctoral Program in Nanomedicine and Pharmaceutical Innovation

SANTIAGO DE COMPOSTELA

2018

USC
UNIVERSIDADE
DE SANTIAGO
DE COMPOSTELA

Prof. María José Alonso Fernández, Full Professor at the Department of Pharmacology, Pharmacy and Pharmaceutical Technology in the University of Santiago de Compostela, Spain

Dr. José Crecente Campo, Research Scientist at the Department of Pharmacology, Pharmacy and Pharmaceutical Technology in the University of Santiago de Compostela, Spain

Dr. **Cyrille Grandjean,** Chargé de Recherche CNRS – Unité Fonctionnalité et Ingénierie des Protéines (UFIP), UMR 6286, Université de Nantes, France / Researcher at French National Centre for Scientific Research (CNRS), UFIP, UMR 6286, University of Nantes, France.

Report:

That the experimental dissertation entitled: "**New potential nanotechnology-based therapies for the treatment of rheumatoid arthritis"** presented by **Nataliya Storozhylova** was conducted under their supervision at the Department of Pharmacology, Pharmacy and Pharmaceutical Technology at the University of Santiago de Compostela and at the Faculty of Sciences and Techniques, Unit of Functionality and Proteins Engineering, UMR CNRS 6286 at the University of Nantes, France. Being completed, they authorize its presentation, evaluation by the assigned jury members, considering that it meets the requirements demanded in article 34 of the Regulation of Doctoral Studies of the USC, and that as supervisors of this thesis they do not incur in the abstention causes established by the law 40/2015.

And for the record, they issue and sign the present certificate in Santiago de Compostela, February th and Nantes, February th 2018.

Prof. María José Alonso Fernández	Dr. José Crecente Campo	Dr. Cyrille Grandjean

USC
UNIVERSIDADE
DE SANTIAGO
DE COMPOSTELA

DECLARACIÓN DO AUTOR/A DA TESE

New potential nanotechnology-based therapies for the treatment of rheumatoid arthritis

D./Dna. Nataliya Storozhylova

Presento a miña tese, seguindo o procedemento axeitado ao Regulamento, e declaro que:

1) A tese abarca os resultados da elaboración do meu traballo.
2) De selo caso, na tese faise referencia ás colaboracións que tivo este traballo.
3) A tese é a versión definitiva presentada para a súa defensa e coincide coa versión enviada en formato electrónico.
4) Confirmo que a tese non incorre en ningún tipo de plaxio doutros autores nin de traballos presentados por min para a obtención doutros títulos.

En Santiago de Compostela, 05 de febrero de 2018

Asdo..

USC
UNIVERSIDADE
DE SANTIAGO
DE COMPOSTELA

To the memory of my Godmother,
who has always put her faith in me
and who has passed away before
I could find a medicine to her.

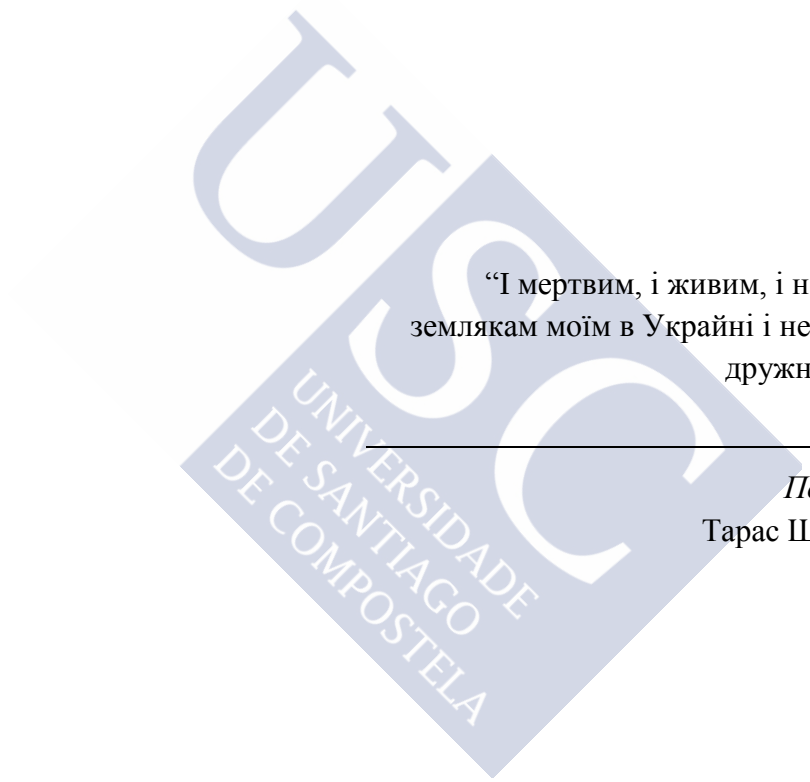

"І мертвим, і живим, і ненародженним
землякам моїм в Украйні і не в Украйні моє
дружнєє посланіє…"

Поема-послання
Тарас Шевченко, 1845

USC
UNIVERSIDADE
DE SANTIAGO
DE COMPOSTELA

And I asked them, "So what are your concerns?" "The same as the whole science concerns are, - answered a hawk-nosed man, - human happiness”

Monday Begins on Saturday,
Strugatski Brothers, 1964

USC
UNIVERSIDADE
DE SANTIAGO
DE COMPOSTELA

Acknowledgements

There are no words to express my endless gratitude to international doctorate program in Nanomedicine and pharmaceutical innovation “NanoFar” and Erasmus Mundus foundation that selected and supported my candidacy in the person of Prof. Frank Boury, “the father” of “NanoFar”, who opened a door to European high quality science to a Ukrainian girl with big ambitions and let me learn from the outstanding European researchers, who are making the modern history of science.

I would like to cordially and deeply thank my thesis directors: Prof. María José Alonso Fernández, Dr. Cyrille Grandjean and Dr. José Crecente Campo for their supervision, their high demands to implement this multidisciplinary project as well as to prepare the thesis manuscript as good as I could, for our fruitful discussions, their corrections, freedom of thoughts during the project, for the opportunities to extend my knowledge and have broad trainings to become a part of the superior scientific teams. They knew that making a thesis in two countries distinctive from the homeland and in the field much different from my Master studies was quite a challenge by itself. Thus, I am infinitely grateful for their wisdom, patience and support.

I would like to give thanks to the members of my follow-up thesis committee Prof. Veronique Préat and Prof. Eduardo Fernández Megía for their time, attention to my project, interesting discussions, insightful advices, and huge source of inspiration.

My immense gratitude and kowtow belongs to a person, who rendered big assistance, but remained behind the stage, his name is Dr. Samir Dahbi, who taught me the basics of carbohydrate synthesis and helped me to successfully start my project in France.

Furthermore, my both research teams at the University of Nantes and University of Santiago de Compostela deserve great praise and recognition for our team spirit, fantastic working days and social life together. I would like to mention these people: Johann, Amelie, Emilie, Jorge, José, Maria Jo, Inma, Belén, Fernando, Lena, Mati, Sara, Carmen, Irene, Tamara, “Lu” (Lungile), Niu, “Howl” (Wei-Hsin Hsu), both Sonias, Migui (Miguel), “Au” (Surasa), Sofìa, Andrea, Ana, Carla, Bhanu, Maruthi, Franchesco, Vanessas, and Desi. Many thanks for invaluable assistance of Puri and Marion in administrative issues and technical support of Belén, Balby and Rafa.

Lots of special thanks are directed to José, I greatly appreciated your priceless advices, not limited only to lab dilemmas, but also out-of-lab puzzles, for your willingness to help to make my life in Spain more comfortable.

My sincere gratitude also belongs to our collaborators Dr. Luis Lugo and Dr. David Cabaleiro from the University of Vigo, who helped me to study the rheological behavior and properties of my drug delivery system and also Dr. Sandra Isabel Dias Simões from the University of Lisbon, where I had a possibility to perform my successful *in vivo* experiments.

I express my appreciation to many honorable researchers (Prof. Nicholas Peppas, Sir Richard Timothy Hunt, Prof. Edgar Boo, Prof. Denis deBlois and others), whose insightful lectures I was able to attend during my PhD times, who illuminate the scientific horizon, inspired me with fresh ideas and let me think of my research from different perspectives.

Also I cannot miss the opportunity to express my deep gratitude to my research team at the German Rheumatism Research Centre at Charité hospital, in Berlin, where I have had the pleasure to perform my PhD-expert internship, especially to Dr. Ute Hoffmann for giving me so much of her time, for sharing with me priceless knowledge in immunology, molecular and cell biology of autoimmunity, for enabling to learn maximum of methods and techniques in such a short time, for our productive discussions; to TA Uta Lauer, PhD students Elisabeth Kenngott, Jennifer Pfeil and Matthias, who during only three months made me feel at home.

Among all, I would like to focus my attention on people, who became my second families in France and Spain, their names are engraved on my heart: Maria and Frederic Tobie with their fantastic kids, Elena Van Povedskaya and Juan José Ballesteros Pérez, correspondingly. I express my sincere gratitude to them for their continuous presence and psychological support in my life abroad, for family dinners and holidays together. May God abundantly bless you for your kindness.

Millions of thanks to my friends in France: Abood, Jean-Benoît, Fuliya, Ghazi, and Cemile, and also my Spanish “esmeraldas”: Alba, Raul, Carlos, Merche, Mano and Jorge, who made my life abroad easier, comfortable and colorful; for our unforgettable small trips, outdoor sports after work and entertaining tabletop games during some rainy weekends. I am extremely grateful to my German friends: Teona, Holger, Stephan, Marcus, Jenny and Vika with whom we spent a lot of training evenings, honing the skills of Latin and Standart Ballroom dances in the most professional dance-sport club, who returned me the taste of my pre-PhD life and who were coming to visit and exhilarate me even after I left Berlin.

Between the other a big cordial thanks to my Ukrainian Friends all over the world, who are like stars on the night sky – you don't always see them, but you know they are there

for you, going through the life with me shoulder to shoulder, for their presence, understanding, and moral support personally and by skype – to Lencha Steshenko, Iryna Chubareva, Vsevolod & Julia Lynyovy, Olena Markarian and many others. Thanks for our incredible stories and ideas that were motivating me along my thesis summit attempt. At those times one quote from the book "*Into Thin Air*" by Jon Krakauer has often appeared in my mind: "With enough determination, any bloody idiot can get up this hill," Hall observed. "The trick is to get back down alive." You all helped me to go all the way. Additional recognition goes to "Ryvok" (an Effort) fitness team: Maks Yaroshenko, Tania and Tos, who recharged my inner batteries (mind and body) and increased my coefficient of efficiency upon the final manuscript preparation. We pushed back the limits of our abilities every time.

I am grateful to my beloved parents – Liudmyla and Sergii Storozhylovy and to my angel-sister Yulia, who being so far from me have been always giving to me huge moral support, understanding and never impeding my decisions.

My deepest gratitude among all belongs to a very special person – Viktor Vasianovych, who even being very far from me during most of my PhD, has been always giving me a hand, inspired and amazed me, has been sharing my triumphs as well as my darkest hours and never leaving me alone, who bravely endured my constant presence at work, showing wisdom and patience during my long PhD-life journey abroad. I also wish to gratitude his parents – Emilia and Sergii Vasianovych, who took care of me as if I was their God daughter.

And last, but not least, I would like to acknowledge my former mentors in Ukraine at the National University of "Kyiv-Mohyla Academy" Dr. Lucia Zabava, Dr. Vitaly Nesterenko and Prof. Anatoly Burban, and to my creative supervisor Prof. Eduard Lugovskoy and Dr. Yevgen Makogonenko at the Institute of Biochemistry NASU, who planted the seed of love to natural and life sciences and research in my heart and helped it to grow up.

Ultimately, I admire the special traditional atmosphere and "a alma" of Galicia, where I have spent most of my thesis time, for the moments of enlightenment and willingness to go ahead! People, who ever lived in Galicia, will always miss it! No doubts, I will warmly remember these tough times and beautiful places (only the view from the lab windows worth a lot!), where I was able to stay during my project, and most of all people ("mis esmeraldas"), whom I have met during this life path. And I will definitely make "camino" one day with all my big family to show them the place of my second home.

Thanks awfully! Merci beaucoup! Muchas gracias! Moitas grazas! Muito obrigada! Vielen Dank! Большое спасибо! Щиро дякую!

Acknowledgements

As a Fellowship holder of the Nanofar: European Doctorate in Nanomedicine and pharmaceutical innovation, I would also like to extend my gratitude and great appreciation to the financial support from the European Commission, Education, Audiovisual and Culture Executive Agency (EACEA), Erasmus Mundus programme and pay obeisance to our consortium: the University of Angers (UA) and the University of Nantes (UN), The University of Louvain (UCL) and the University of Liège (ULg), the University of Nottingham (UNott), the University of Santiago de Compostela (USC).

Contents

USC
UNIVERSIDADE
DE SANTIAGO
DE COMPOSTELA

Abstract

Some other trifling particulars might be mentioned, but they are all of slight importance and have nothing to do with the true relation of the history; and no history can be bad so long as it is true.

Miguel de Cervantes Saavedra, 1605

USC
UNIVERSIDADE
DE SANTIAGO
DE COMPOSTELA

ABSTRACT

The local administration of drugs into the intra-articular cavity is beneficial for the treatment of a number of joints pathologies. Unfortunately, despite this interest, the efficient intra-articular delivery of drugs represents a challenge, which is mainly associated to the fast drug elimination from the synovial cavity. Therefore, there is a clear need to develop advanced controlled release technologies that may overcome this limitation. At the same time, the discovery of novel immunotherapeutic targets has prompted the design and development of highly specific antagonists for effective therapies. This is the case of the extracellular protein galectin-3 (Gal-3), which has been recently identified as a primer trigger of the pro-inflammatory cascade in arthritis. The inhibition of Gal-3 could block the whole inflammatory cascade, prevent further joints degradation and alleviate the inflammatory joint diseases.

In this work we have developed a novel drug delivery system (DDS) composed of an *in situ* forming hydrogel combined with hyaluronic acid (HA) nanocapsules (NCs). HA NCs consisting of an olive oil core surrounded by a HA shell were prepared by the solvent displacement technique. The NCs exhibited a particle size of 135 ± 9 nm, a negative surface charge and a modest capacity to encapsulate dexamethasone, which was used as a model drug. Thereafter, two injectable *in situ* hydrogels systems composed of HA-fibrin and fortified HA-fibrin (with crosslinker factor XIII and α2-antiplasmin) were developed. Both gels displayed easily adjustable gelation time and mechanical properties. These NCs-containing hydrogels showed the capacity to control the release of dexamethasone in simulated synovial fluid for up to 72 h.

On the other hand, an antagonist of Gal-3 was designed, synthesized and characterized. It was based on its natural ligand type II lactosamine [Galβ(1→4)-GlcN] core, modified with aromatic substituents to greatly increase its affinity and specificity. Gal-3 inhibitor revealed high affinity to Gal-3 (K_d = 0.59 μM at 4 °C) and selectivity among Gal-1/ Gal-3/Gal-7. This compound was further encapsulated within HA NCs (531 ± 5 μg/mL), dispersed within the *in situ* HA-fibrin hydrogel and tested in a carrageenan-induced acute knee joint synovitis rat model. Both, groups with drug-loaded NCs alone and in the gel, administrated intra-articularly at microgram scale doses (200 and 55 μg/kg), showed a remarkable suppression of inflammation compared with the non-treated control. These findings highlight the potential of Gal-3 inhibitor as a lead compound for the treatment of rheumatoid arthritis. In addition, the *in vitro* and *in vivo* experiments showed the interest of the nanotechnology-based DDS for intra-articular application.

USC
UNIVERSIDADE
DE SANTIAGO
DE COMPOSTELA

Resumen

Otras algunas menudencias había que advertir, pero todas son de poca importancia y que no hacen al caso a la verdadera relación de la historia, que ninguna es mala como sea verdadera.

Miguel de Cervantes Saavedra, 1605

USC
UNIVERSIDADE
DE SANTIAGO
DE COMPOSTELA

RESUMEN

La administración local de fármacos en la cavidad intra-articular puede ser beneficiosa para el tratamiento de ciertas patologías asociadas a las articulaciones. Sin embargo, a pesar de su interés, la liberación intra-articular de fármacos eficiente representa un desafío, principalmente debido a su rápida eliminación de la cavidad sinovial. Por lo tanto, hay una clara necesidad de desarrollar tecnologías de liberación controlada avanzadas que puedan superar estas dificultades. Al mismo tiempo, el descubrimiento de nuevas dianas inmunoterapéuticas ha suscitado el diseño y desarrollo de antagonistas altamente específicos con el fin de obtener terapias efectivas. Este es el caso de la proteína extracelular galectina-3 (Gal-3), que ha sido identificada recientemente como un iniciador principal de la cascada pro-inflamatoria en la artritis. La inhibición de Gal-3 podría bloquear toda la cascada inflamatoria, prevenir una mayor degradación de la articulación y aliviar las enfermedades inflamatorias de las articulaciones.

En este trabajo hemos desarrollado un sistema de liberación de fármacos compuesto por un hidrogel, que se forma *in situ*, combinado con nanocápsulas (NCs) de ácido hialurónico (HA). Las NCs de HA consisten en un núcleo oleoso de aceite de oliva rodeado por una cubierta de HA y fueron preparadas por el método de desplazamiento de disolvente. Las NCs presentan un tamaño de 135 ± 9 nm, una carga superficial negativa y una capacidad modesta de encapsular dexametasona, usada en este estudio como fármaco modelo. Posteriormente, se desarrollaron dos sistemas tipo hidrogel formados por HA-fibrina y HA-fibrina reforzado (con el entrecruzante factor XIII y α2-antiplasmina). Ambos geles muestran tiempos de gelificación y propiedades mecánicas fácilmente modulables. Los hidrogeles cargados de NCs permitieron la liberación controlada de dexametasona en fluido sinovial simulado durante 72 h.

Por otro lado, se ha diseñado, sintetizado y caracterizado un antagonista de la Gal-3. Dicho antagonista se basa en su ligando natural, con un núcleo tipo II de lactosamina [Galβ(1→4)-GlcN], modificado con sustituyentes aromáticos para incrementar en mayor medida su afinidad y especificidad. El inhibidor de Gal-3 mostró elevada afinidad por la Gal-3 (K_d = 0.59 μM a 4 °C) y selectividad entre Gal-1/Gal-3/Gal-7. Posteriormente, este compuesto fue encapsulado en NCs de HA (531 ± 5 μg/mL), que a su vez fueron dispersadas en un hidrogel de HA-fibrina y el conjunto evaluado en ratas, en un modelo de sinovitis aguda de rodilla inducida por carragenano. Tanto el grupo tratado con las NCs cargadas de fármaco como el grupo tratado con dichas NCs dispersadas en el gel, administrados intra-

articularmente (200 and 55 μg/kg), dieron lugar a una reducción destacable de la inflamación, comparados con el grupo control no tratado. Estos resultados muestran el interés del inhibidor de Gal-3 como un compuesto lider a candidato a fármaco con potencial indicación en el tratamiento de la artritis reumatoide. Al mismo tiempo, los experimentos *in vitro* e *in vivo* muestran el potencial de las nanocapsulas dispersas en el gel como sistema de liberación de fármacos a nivel intra-articular.

ABBREVIATION LIST

α2-AP	α2-antiplasmin
aa	Amino acids
Ac	Acetate
ADAMTS5	A Disintegrin And Metalloproteinase with Thrombospondin Motifs
CRD	Carbohydrate recognition domain
DD	Drug delivery
DDS	Drug delivery system
3,5-diMeOBn	3,5-dimethoxybenzyl
DLS	Dynamic light scattering
DXM	Dexamethasone
EE	Encapsulation efficiency
ECM	Extracellular matrix
ELISA	Enzyme-linked immunosorbent assay
Et_3Si	Triethylsilyl
FESEM	Field emission scanning electron microscopy
Fg	Fibrinogen
FITC	Fluorescein isothiocyanate
Fn	Fibrin
FXIII	Factor XIII
Galβ	Galactose
Gal	Galectin
Gal-3i	Galectin-3 inhibitor
GlcN	Glucosamine
HA	Hyaluronic acid, sodium hyaluronate
H&E	Haematoxylin and eosin staining
hGal-1	Human Gal-1
hGal-3-CRD	Human Gal-3 CRD
hGal-7	Human Gal-7
HPLC	High-performance liquid chromatography
IA	Intra-articular
IFN-γ	Interferon gamma

IL-1β	Interleukin-1 beta
IL-6	Interleukin-6
ITC	Isothermal titration calorimetry
Lec	Lecithin
LacNAc	N-acetyllactosamine
LN1	Type I lactosamine
LN2	Type II lactosamine
HRMS	High-resolution mass spectra
MMP	Matrix metalloproteinases
MW	Molecular weight
NMR	Nuclear magnetic resonance
NCs	Nanocapsules
NPs	Nanoparticles
OA	Osteoarthritis
OAm	Oleylamine
MeOBn	3-methoxybenzyl
MeOBz	3-methoxybenzoyl
OO	Olive oil
PDI	Polydispersity index
PhSe	Phenylselenium
py	Pyridine
RA	Rheumatoid arthritis
RA SF	Rheumatoid arthritis synovial fluid
RT	Room temperature
SEM	Scanning electron microscopy
SSF	Simulated synovial fluid
TE	Tissue engineering
TEM	Transmission electron microscopy
TNF-α	Tumor necrosis factor-α
Thr	Thrombin
FDA	Food and Drug Administration
UV-VIS	Ultraviolet-visible spectrophotometry

RESUMEN IN *EXTENSO*

Nuevas terapias basadas en la nanotecnología para el tratamiento de la artritis reumatoide

Tal com'as nubes
.....Qu'impele o vento,
Y agora asombran, u agora alegran
Os espaços inmensos d'o ceo,
.....Así as ideas
.....Loucas que'eu teño,
as imaẍes de múltiples formas
D'estranas feituras, de cores incertos,
.....Agora asombran,
.....Agora acraran,
O fondo sin fondo d'o meu pensamento.

Rosalía de Castro, 1880

USC
UNIVERSIDADE
DE SANTIAGO
DE COMPOSTELA

1. Introducción

En general, las cavidades de las articulaciones diartrodiales son adecuadas para la inyección intraarticular (IA) de fármacos. Por ello, en las últimas décadas, esta modalidad de administración ha sido aceptada como una vía directa que puede mejorar la eficacia de los tratamientos de las enfermedades articulares.[1–4] Los beneficios de la administración IA sobre la oral o intravenosa se reflejan en un aumento de la eficacia y en una reducción de la toxicidad del fármaco asociada a la exposición sistémica. Los principales fármacos actualmente disponibles en el mercado para el tratamiento de las artropatías y la mejora de la homeostasis de la rodilla son antagonistas de COX-2, TNF-α, IL-1 y IL-6, administrados de forma sistémica. Las principales limitaciones de estos fármacos son la falta de especificidad y la aparición de considerables efectos secundarios,[2,5–7] haciendo de la administración IA una alternativa atractiva.

Los avances en el área de biofarmacia durante las últimas décadas han permitido el desarrollo de sistemas de liberación controlada de fármacos, que disminuyen la toxicidad sistémica de los mismos y ofrecen un mayor tiempo de permanencia en el lugar de acción, con una liberación controlada y prolongada del fármaco directamente en el lugar requerido.[2,4] Sin embargo, la administración IA de fármacos sigue siendo un reto, principalmente debido a la eliminación prematura del fármaco de la cavidad sinovial junto con la rápida renovación del líquido sinovial, la internalización celular y la invasividad de la ruta.[2]

Se han desarrollado distintos tipos de sistemas de liberación controlada de fármacos para el tratamiento local de artropatías, con énfasis en nano-/microsistemas e hidrogeles,[2,4,6,8] siendo las formulaciones más prometedoras y avanzadas una combinación de ambos sistemas.[9–14] Dichos sistemas permiten una retención suficiente y una liberación prolongada de fármacos de bajo peso molecular (PM), cuyo tiempo de permanencia en las articulaciones es normalmente corto cuando se administran en disoluciones.[2,15]

El cartílago articular tiene una capacidad limitada para su auto-regeneración.[16–18] Además, el líquido sinovial pierde en gran medida sus funciones intrínsecas en las patologías articulares.[19] Teniendo esto en cuenta, los vehículos de administración de fármacos multifuncionales deben diseñarse para contribuir a la curación de la diartrosis. En este sentido, pueden no sólo permitir una liberación del fármaco controlada y prolongada, sino que también pueden estar compuestos de materiales resistentes a la deformación para permanecer en la cavidad articular y evitar una descomposición enzimática rápida.

Simultáneamente, los sistemas de liberación controlada pueden tener una papel de viscosuplementación, para mejorar la homeostasis de la rodilla, y servir de andamiajes celulares *in situ* para la regeneración del tejido del cartílago.

Al mismo tiempo, el descubrimiento de nuevas dianas terapéuticas ha suscitado grandes esfuerzos dirigidos hacia el diseño y desarrollo de pequeñas moléculas antagonistas altamente específicas para conseguir terapias eficaces (en particular para diferentes tipos de cáncer, enfermedades autoinmunes, diabetes, etcétera).[20–23] Este es el caso de la proteína extracelular galectina-3 (Gal-3), que ha sido recientemente identificada como desencadenante de la inflamación.[24,25] Además, esta proteína favorece la secreción de citocinas pro-inflamatorias, quimiocinas[24] y metaloproteinasas de la matriz extracelular,[26] que están involucradas en la remodelación del cartílago y la desmineralización ósea.[5,27]

2. Hipótesis

1. El uso de nanocápsulas (NCs) cargadas con fármacos dispersas en hidrogeles puede aumentar sustancialmente el tiempo de retención intra-articular de dichos fármacos. Las NCs pueden actuar como reservorios de fármacos lipófilos, permitiendo su liberación controlada, mientras que el hidrogel formado *in situ* podría proteger a las NCs de una rápida descomposición, endocitosis y eliminación de la cavidad sinovial, modulando también la liberación del fármaco. Dicha formulación inyectable de NCs combinadas con un hidrogel también podría contribuir a la homeostasis de la rodilla, debido al núcleo de aceite de oliva de las NCs y al recubrimiento de ácido hialurónico (HA) de 700 kDa, ambos con propiedades antiinflamatorias.[28–31] Además, el hidrogel 3D de fibrina fortalecida con ácido hialurónico podría actuar como viscosuplemento, con propiedades elásticas adecuadas para su permanencia en la cavidad articular y como soporte para la regeneración del cartílago.[32–34]

2. Dado que el bloqueo tradicional de COX-2 y las citocinas pro-inflamatorias TNF-α, IL-1 e IL-6, ha demostrado una efectividad limitada en las enfermedades inflamatorias de las articulaciones,[2,4,35–37] planteamos la hipótesis de que la inhibición de la diana galectina-3, podría bloquear toda la cascada inflamatoria y evitar la posterior degradación de las articulaciones.

3. **Objetivos**

Basándonos en los antecedentes bibliográficos y en las hipótesis anteriormente expuestas, el objetivo de esta tesis ha sido doble, por un lado, el de desarrollar un nuevo hidrogel que se forma *in situ* tras la inyección y que posee nano-reservorios que permiten la liberación prolongada de fármacos en la cavidad intraarticular; por otro lado, un objetivo adicional ha sido el de sintetizar un nuevo antagonista de la galactina-3 y su incorporación en el hidrogel antes mencionado para una evaluación *in vivo*.

Con este propósito, los objetivos generales se dividen en los siguientes objetivos específicos:

1) Desarrollo y evaluación *in vitro* de un nuevo sistema de liberación de fármacos destinado a la administración intra-articular

En el desarrollo de este objetivo se han cubierto las siguientes fases de trabajo:

1. Formulación de NCs de ácido hialurónico, cargadas con dexametasona (fármaco modelo), y posterior caracterización con respecto a sus propiedades fisicoquímicas, estabilidad en líquido sinovial simulado y estabilidad en almacenamiento.
2. Diseño y desarrollo de un hidrogel destinado a gelificar *in situ* tras la administración intraarticular, y estudio de la influencia de los parámetros que pueden modificar su tiempo de gelificación, propiedades mecánicas y evaluar su capacidad de ser inyectado.
3. Estudio de la formación del hidrogel en presencia de las NCs, análisis de su capacidad de carga y de la modificación de las propiedades reológicas del hidrogel en presencia de las NCs. Caracterización del comportamiento reológico tanto de los hidrogeles blancos como de los cargados con NCs, su estructura superficial y porosidad.
4. Optimización y caracterización de dos hidrogeles cargados con NCs, que difieren en el grado de entrecruzamiento de la red del hidrogel, diseñados para tratar la inflamación aguda y crónica de las articulaciones usando modelos *in vivo* de rata.
5. Evaluación del perfil de liberación *in vitro* de la dexametasona a partir del gel cargado con NCs.

Los resultados correspondientes a estos objetivos se presentan en el **Capítulo 1**: "An injectable, *in situ* forming hydrogel containing nanocapsules for intra-articular drug delivery".

2) Síntesis de un nuevo compuesto anti-inflamatorio, incorporación en el sistema de liberación de fármacos desarrollado y evaluación de su actividad *in vivo*

En el desarrollo de este objetivo se han cubierto las siguientes fases de trabajo:

6. Diseño y síntesis un nuevo candidato a fármaco antiinflamatorio – un antagonista de la galectina-3 extracelular (Gal-3), usando como núcleo su ligando natural, la lactosamina de tipo II [Galβ(1→4)-GlcN], modificado con sustituyentes aromáticos para aumentar en mayor medida su afinidad y especificidad.
7. Caracterización del inhibidor de Gal-3 obtenido, a través de la valoración de su afinidad y selectividad entre Gal-1/Gal-3/Gal-7, comparación con el primer inhibidor de bajo peso molecular de la Gal-3 comercializado (TD139) y selección del inhibidor sintético más potente para su posterior evaluación *in vivo*.
8. Incorporación del inhibidor de Gal-3 en las NCs cargadas en el hidrogel, posterior caracterización de sus propiedades fisicoquímicas y evaluación de su actividad antiinflamatoria *in vivo* en un modelo en rata con sinovitis aguda de rodilla inducida por carragenano.

Los resultados relacionados con este trabajo se presentan en el **Capítulo 2**: "New galectin-3 inhibitor as a lead compound for anti-inflammatory drug candidates".

4. Resultados y discusión

1. Gal-3i como compuesto líder candidato a fármaco en el tratamiento de la artritis reumatoide

Teniendo en cuenta su participación en la fisiopatología de la artritis reumatoide, la galectina-3 (Gal-3) se presenta como una nueva diana inmunoterapéutica,[24,27,38–40] cuyo bloqueo podría prevenir toda la cascada inflamatoria y la posterior degradación de las articulaciones. Con este objetivo, se han diseñado, sintetizado y caracterizado antagonistas de bajo peso molecular de la Gal-3 extracelular. Los compuestos se basaron en el núcleo que posee el ligando natural de Gal-3: una lactosamina tipo II [Galβ(1→4)-GlcN], modificado con sustituyentes aromáticos para aumentar de manera considerable su afinidad y especificidad. Sus estructuras, denominadas oxazolina y Gal-3i, se comparan en la **Figura 1** con otros inhibidores de la Gal-3 que han sido evaluados en ensayos clínicos para el tratamiento de diferentes patologías.[41–48]

Gal-3i, oxazolina y TD139 (el primer antagonista de Gal-3 de bajo PM aprobado por la FDA), testados en un ensayo de polarización de fluorescencia directo y competitivo, revelaron selectividad entre Gal-1/Gal-3/Gal-7. Gal-3i demostró una afinidad 7,5 veces mayor a la Gal-3 (K_d = 0,59 μM a 4 °C y 2,99 μM a 25 °C) que la oxazolina (K_d = 4,4 μM a 4 °C y 23 μM a 25 °C) y se seleccionó para su evaluación *in vivo*.

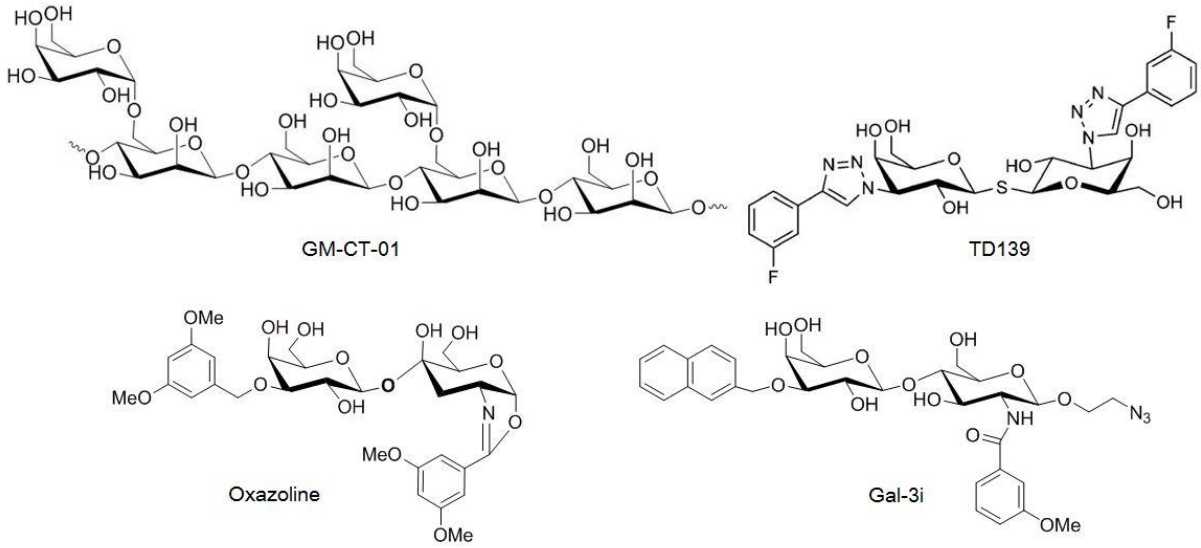

Figura 1. Estructuras de dos inhibidores comerciales de Gal-3: GM-CT-01 (DAVANAT®) y TD139; junto a la oxazolina y el Gal-3i sintetizados en este trabajo.

2. Desarrollo y caracterización de un sistema de liberación de controlada de fármacos para la aplicación intraarticular

Para evitar los dos principales desafíos que afrontan los sistemas de administración IA de fármacos, la internalización celular y la rápida eliminación de la cavidad sinovial,[2,15] se desarrolló un sistema compuesto de NCs dispersadas en un hidrogel formado *in situ* (**Figura 2**).

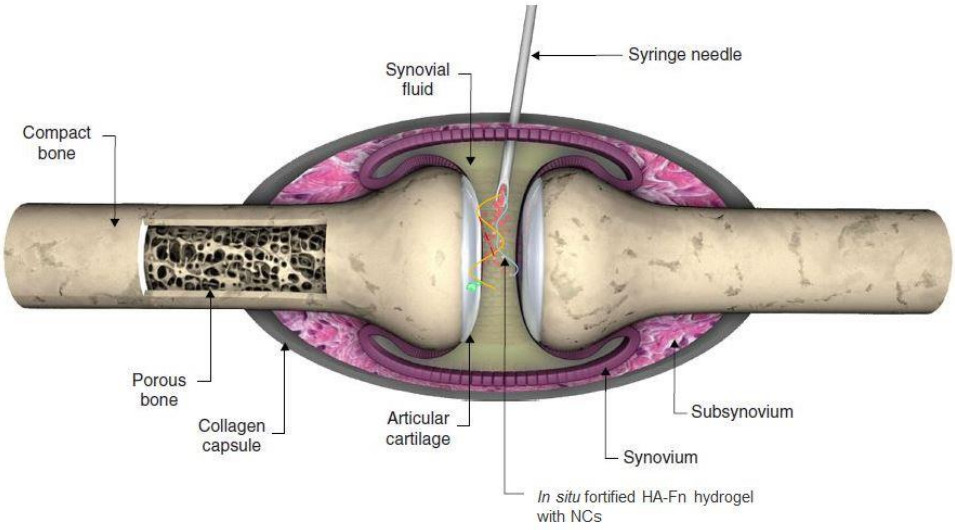

Figura 2. Ilustración esquemática de la estructura de una articulación sinovial y la inyección intraarticular de un hidrogel formado *in situ* combinado con nanocápsulas cargadas con un fármaco lipofílico. Adaptada y modificada con el permiso,[15] Copyright© 2009, Taylor & Francis.

Las NCs, preparadas mediante la técnica de desplazamiento de disolvente, están compuestas de aceite de oliva (OO), tensioactivos biodegradables y biocompatibles: lecitina de soja (Lec) y oleilamina (OAm) y, finalmente, HA de 700 kDa como polímero de cubierta. Nuestro objetivo era desarrollar NCs con un tamaño de ~130 nm, que no se espera que causen daño en el cartílago u otros daños mecánicos en la articulación[11] y que permitan encapsular la cantidad suficiente de fármacos lipofílicos (un fármaco modelo – dexametasona [DXM] y el nuevo compuesto Gal-3i). En la **Tabla 1** se resumen el tamaño de partícula, el potencial zeta y la eficacia de encapsulación de las formulaciones.

Las NCs fueron estables en condiciones de almacenamiento a 4 °C durante un período de al menos 1 mes. Sin embargo, la estabilidad de las NCs se vio comprometida tanto en PBS como en líquido sinovial simulado. Por lo tanto, desarrollamos un hidrogel inyectable, formado en presencia de NCs, para mejorar su estabilidad y aumentar su retención en la

cavidad articular (evitando la internalización celular y su rápida eliminación de la articulación). Al mismo tiempo, el hidrogel permitiría la liberación prolongada del fármaco.

Para la preparación del gel se seleccionaron los biopolímeros HA y fibrina que forman una red 3D interpenetrante (IPN),[33,49–52] debido a la afinidad del HA de alto PM por la fibrina.[32,53] La formación del hidrogel se basa en la activación enzimática del fibrinógeno por la trombina (Thr), y permite diseñar por etapas una IPN en presencia de HA de diferentes PM, de agentes entrecruzantes de fibrina (el factor XIII y la α2-antiplasmina) y de NCs cargadas con el fármaco.

Tabla 1. Propiedades fisicoquímicas de las NCs de HA de 700 kDa blancas y cargadas con fármaco (media ± SD, n = 6). OO = aceite de oliva, Lec = lecitina de soja, OAm = oleilamina, PDI = índice de polidispersión

Tipo de NCs			OO (mg)	Lec (mg)	OAm (mg)	Tamaño de partícula (nm)	PDI	Potencial ζ (mV)	Concentración de fármaco (mg/mL)
Blancas		prototipo 1	15	3,75	0,75	128 ± 13	0,2	−27 ± 3	n/a
		prototipo 2	22	5,625	1,125	121 ± 10	0,2	−30 ± 3	n/a
Cargadas con el fármaco	DXM	prototipo 1	15	3,75	0,75	160 ± 12	0,2	−20 ± 4	0,75 ± 0,13
		prototipo 2	22	5,625	1,125	135 ± 9	0,2	−31 ± 5	5,60 ± 0,40
	Gal-3i	prototipo 2	22	5,625	1,125	122 ± 11	0,2	−29 ± 5	0,53 ± 0,05

La formación de los geles se monitorizó mediante análisis de turbidez (λ = 350 nm) y estudios reológicos que permitieron identificar la fase de retardo, el punto de gelificación (**Figura 3**) y la evolución del gel en el tiempo.

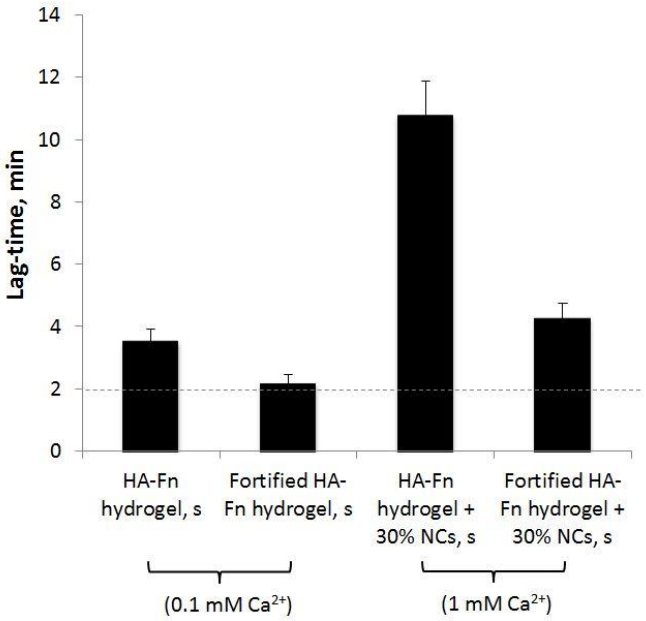

Figura 3. Resumen de la determinación del punto de gelificación mediante reología en los diferentes sistemas: geles blancos de "HA-fibrina" y de "HA-fibrina fortalecido" y estos geles con NCs al 30%. La línea de trazos y puntos refleja la fase de retardo requerida de 2 minutos. Las mediciones se llevaron a cabo a 37 ºC. Expresado como media ± SD; n = 3.

La modificación de la concentración de distintos compuestos, como la Thr, HAs, NCs, Ca^{2+}, factor XIII y α2-antiplasmina han permitido una modificación controlada de la microarquitectura del gel y de su tiempo de gelificación, obteniendo un tiempo de retardo de la gelificación adecuado para los estudios *in vivo*. Los geles permitieron albergar un 30% (v/v) de NCs en su estructura durante su autoensamblaje, con una distribución homogénea dentro del gel y con poros bien definidos (7,29 ± 1,23 μm y 4,88 ± 1,12 μm, respectivamente para los geles de HA-fibrina y HA-fibrina reforzado con 30% (v/v) de NCs). Los valores iniciales de viscosidad de la mezcla física HA-fibrina (sin adición la Thr) fueron 118,9 m*Pa·s* y 81,3 mPa·*s* a 20 °C y 37 °C, respectivamente, significativamente más bajos que los viscosuplementos comerciales,[54,55] por lo que se puede anticipar una fácil inyección, previa a la formación *in situ* del hidrogel, en los estudios *in vivo*. El hidrogel formado presentó características reológicas tanto de material elástico como de tipo sólido, adecuado para sostener las deformaciones intra-articulares. En resumen, hemos desarrollado dos sistemas de liberación controlada: "un gel de HA-fibrina con 30% de NCs" y "un gel reforzado de HA-fibrina con 30% de NCs" (**Figura 3**), que podrían ser adecuados para tratar inflamaciones articulares agudas y crónicas, respectivamente.

El perfil de liberación *in vitro* de la dexametasona desde el gel de HA-fibrina con 30% de NCs se prolongó hasta 72 h en fluido sinovial simulado, lo que podría ser altamente ventajoso para la administración intraarticular del fármaco (**Figura 4**).

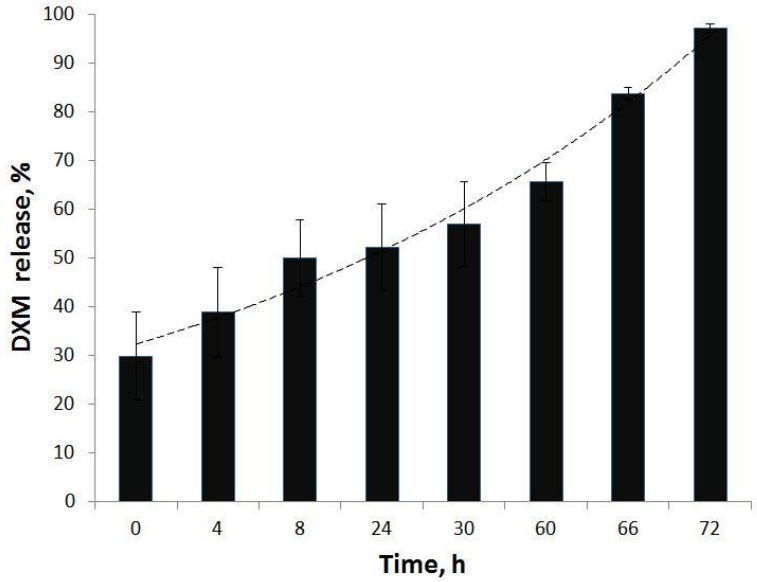

Figura 4. Liberación de dexametasona (DXM) desde el hidrogel de ácido hialurónico-fibrina con 30% de NCs en líquido sinovial simulado, 37 ºC, 72 h.

3. Actividad antiinflamatoria *in vivo* del inhibidor de Gal-3

Para evaluar la actividad biológica del Gal-3i, se empleó un modelo de inflamación aguda inducida por carragenano en ratas,[56] ampliamente usado para testar nuevos fármacos antiinflamatorios.[57]

Los animales con sinovitis inducida se distribuyeron en tres grupos de acuerdo con el tratamiento recibido (100 µL, IA): NCs blancas utilizadas como vehículo control (grupo 1), NCs cargadas con Gal-3i a una dosis de 200 µg/kg (grupo 2) y NCs cargadas con Gal-3i dispersadas (30% v/v) en el gel de HA-fibrina reforzado a una dosis de 55 µg/kg (grupo 3). La actividad del fármaco se controló a las 4 horas después de la inducción de la sinovitis, cuando se observa el pico de la inflamación.[56] Los datos de las mediciones de la hinchazón de la rodilla, los análisis de sangre, el análisis histopatológico y la cuantificación de los marcadores pro-inflamatorios del plasma sanguíneo, demostraron una actividad anti-inflamatoria pronunciada del Gal-3i y la mejora del estado de las articulaciones. Los datos de hinchazón de la rodilla (**Figura 5**) mostraron una reducción del diámetro de la rodilla en: 1,6

veces (grupo 1), 3,5 veces (grupo 2) y 7 veces (grupo 3) en comparación con el control de carragenano.

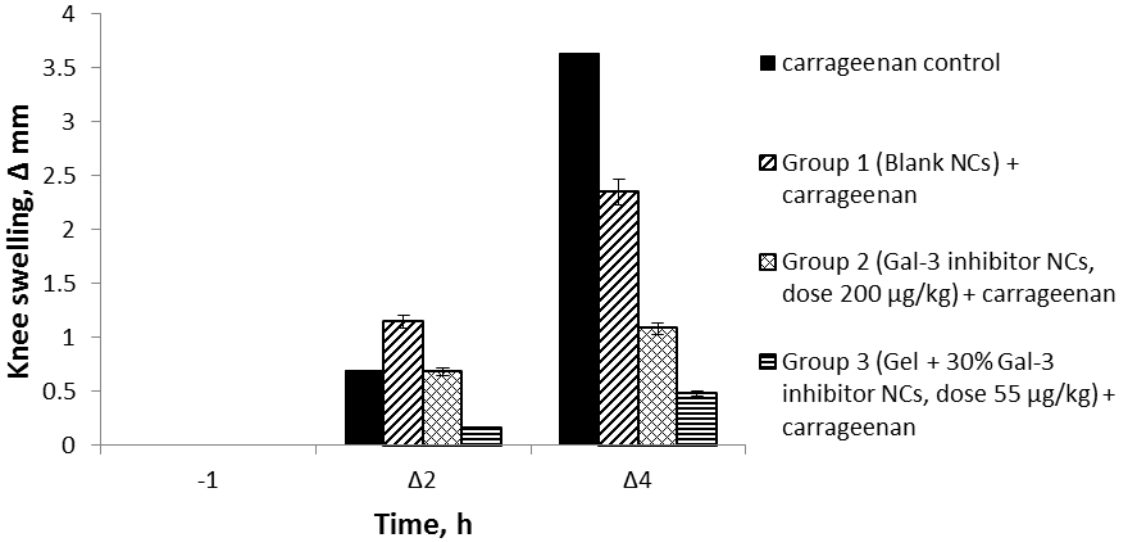

Figura 5. Efecto del tratamiento con el inhibidor de Gal-3 en el modelo de inflamación de la articulación inducido por carragenano usando las NCs y las NCs en gel comparado con NCs blancas y el control de carragenano (n = 5 para los grupos 1-3, n = 1 para el control de carragenano). Δ es la diferencia en el diámetro de la rodilla en diferentes momentos antes y después de la inyección de carragenano, expresada en mm. Datos expresados como media ± SEM.

Este hallazgo resulta más notable si se considera que la dosis del grupo 3 (NCs cargadas con Gal-3i en el gel a una dosis de 55 µg/kg), es considerablemente más baja que en el grupo 2 (NCs cargadas con Gal-3i a una dosis de 200 µg/kg). Posiblemente, el hidrogel de HA-Fibrina mantiene de manera efectiva las NCs dentro de la cavidad articular, modula la liberación y, por sí mismo, tiene un efecto beneficioso en la curación de las articulaciones, incluso en el modelo de inflamación aguda en ratas.

Los resultados obtenidos en este ensayo preliminar *in vivo* demostraron una notable supresión de la inflamación debida al Gal-3i encapsulado en el hidrogel y administrado de manera intraarticular en dosis de microgramos. Los resultados presentan al Gal-3i como un compuesto líder candidato a fármaco inmunoterapéutico para las enfermedades de la rodilla, en particular para la artritis reumatoide. Es de destacar, que el hidrogel con NCs sin fármaco también demostró una tendencia a contribuir a la curación de las articulaciones y a reducir la inflamación sinovial, gracias, probablemente, al núcleo de aceite de oliva y al ácido hialurónico presente en su composición.[28,29,58] Al mismo tiempo, el hidrogel de ácido hialurónico-fibrina podría, potencialmente, funcionar como un viscosuplemento, con

propiedades elásticas adecuadas para la permanencia intra-articular y como una estructura adhesiva *in situ* con alto grado de citocompatibilidad para la regeneración del cartílago.

5. Conclusiones

El objetivo de esta tesis ha sido el diseño y desarrollo de un nuevo sistema inyectable destinado a prolongar el tiempo de residencia intraarticular y lograr una liberación controlada de fármacos. El sistema consiste en un hidrogel con nanocápsulas dispersas en él, sirviendo como multireservorio para diferentes fármacos antiinflamatorios y lipófilos, tales como i) la dexametasona, empleada en este estudio como fármaco modelo y ii) un nuevo candidato a fármaco – un antagonista de la galectina-3 (Gal-3). Los resultados experimentales obtenidos condujeron a las siguientes conclusiones:

1) En este estudio, se desarrolló y sintetizó un nuevo inhibidor monovalente altamente afín, potente y selectivo de la Gal-3, formado por dos restos diferentes ensamblados a un núcleo de lactosamina modificado. Su K_d hacia la Gal-3, medido en un ensayo de polarización de fluorescencia directo y competitivo, fue de 0,59 μM a 4 °C (2,99 μM a 25 °C), mientras que el inhibidor de Gal-3 marcado con fluoresceína mostró una afinidad muy alta hacia la Gal-3, K_d = 14 nM a 4 °C (82 nM a 25 °C), ciertamente más alta que la del inhibidor comercial de Gal-3 DAVANAT®. Una característica importante de este compuesto es la capacidad de discriminar entre Gal-1/Gal-3/Gal-7, mientras que DAVANAT® difícilmente discrimina entre Gal-1 y Gal-3. Por otro lado, se ha confirmado experimentalmente que un primer antagonista de Gal-3 de bajo PM TD139, aprobado por la FDA, con el núcleo de tio-digalactósido modificado, medido en el mismo ensayo, tiene una alta afinidad, con una K_d (Gal-3) = 0,036 μM a 4 °C (0,166 μM a 25 °C) y alta selectividad entre Gal-1/Gal-3/Gal-7. Teniendo en cuenta los datos de K_d prometedores del compuesto que hemos desarrollado y sintetizado, consideramos interesante estudiar *in vivo* la eficacia de este inhibidor de la Gal-3 de bajo PM.

2) Se prepararon exitosamente nuevas nanocápsulas (NCs) con núcleo de aceite de oliva y recubrimiento de ácido hialurónico, utilizando para ello el método de desplazamiento de disolvente. Estas NCs tienen la capacidad de encapsular dexametasona (5,6 ± 0,4 mg/mL)

y el inhibidor de Gal-3 (531 ± 5 μg/mL), tamaño nanométrico (135 ± 9 nm y 122 ± 11 nm, correspondientemente), carga superficial negativa y forma esférica regular.

3) Se han desarrollado dos sistemas inyectables basados en hidrogeles de ácido hialurónico y fibrina, así como ácido hialurónico-fibrina reticulado con el factor XIII y la α2-antiplasmina. Los hidrogeles mostraron un tiempo de gelificación, microestructura y propiedades mecánicas fácilmente ajustables. Además, los geles permitieron un 30% (v/v) de carga de las NCs durante su formación. La viscosidad inicial del sistema fue significativamente más baja en comparación con los viscosuplementos comerciales, lo que permitió una buena inyección a través de jeringa. Las propiedades reológicas de los hidrogeles ensamblados revelaron resistencia a altas deformaciones, presentando características de materiales tanto de tipo elástico como sólido, y adecuados para preservar las deformaciones intra-articulares. Con respecto a su estructura, la formulación presenta poros bien definidos, con NCs dispersas homogéneamente dentro del gel. Este sistema de administración de fármacos intra-articular permitió un perfil de liberación del fármaco *in vitro* controlado y prolongado, evitando la descomposición rápida de las NCs en fluido sinovial simulado.

4) Se ha llevado a cabo un estudio preliminar *in vivo*, en modelo de ratas con sinovitis aguda en la articulación de la rodilla inducida por carragenano. En estos estudios el inhibidor de Gal-3 demostró una notable supresión de la inflamación. Tanto el grupo tratado con NCs cargadas con el fármaco, como el grupo tratado con las NCs cargadas con el fármaco dispersadas en el gel, se administraron a dosis de microgramos (55 and 200 μg/kg), y brindaron mejores resultados en comparación con el grupo control no tratado. Estos resultados confirman al inhibidor de Gal-3 como un compuesto líder candidato a fármaco inmunoterapéutico para condiciones inflamatorias de la rodilla, en particular para la artritis reumatoide. Es de destacar, que los hidrogeles sin fármaco también mostraron una tendencia a contribuir a la curación de las articulaciones y a reducir la inflamación sinovial.

En términos generales, el trabajo aquí presentado describe el desarrollo y caracterización de un nuevo sistema biodegradable de liberación de fármacos formado por un hidrogel inyectable en la cavidad articular y que se forma *in situ*. El hidrogel sirve como un depósito para las NCs cargadas con el fármaco, impidiendo su dispersión, internalización

celular y rápida eliminación de la cavidad de la articulación, pudiendo liberar el fármaco de forma prolongada en el tiempo. Las propiedades reológicas del sistema inicial permitieron una buena jeringabilidad y unas características mecánicas deseables para la aplicación intraarticular. La actividad preliminar *in vivo* del inhibidor de la galectina-3 confirmó a la galectina-3 como una diana inmunoterapéutica potencial para las enfermedades inflamatorias de las articulaciones, tales como la artritis reumatoide.

Referencias:

1. Edwards, S. H. R., Cake, M. a, Spoelstra, G. & Read, R. a. Biodistribution and clearance of intra-articular liposomes in a large animal model using a radiographic marker. *J. Liposome Res.* **17,** 249–261 (2007).

2. Evans, C. H., Kraus, V. B. & Setton., L. A. Progress in intra-articular therapy. *Nat. Rev. Rheumatol.* **10,** 11–22 (2015).

3. Gerwin, N., Hops, C. & Lucke, A. Intraarticular drug delivery in osteoarthritis. *Adv. Drug Deliv. Rev.* **58,** 226–242 (2006).

4. Kang, M. L. & Im, G.-I. Drug delivery systems for intra-articular treatment of osteoarthritis. *Expert Opin. Drug Deliv.* **11,** 269–82 (2014).

5. Quan, L.-D., Thiele, G. M., Tian, J. & Wang, D. The Development of Novel Therapies for Rheumatoid Arthritis. *Expert Opin. Ther. Pat.* **18,** 723–738 (2008).

6. Kapoor, B., Singh, S. K., Gulati, M., Gupta, R. & Vaidya, Y. Application of liposomes in treatment of rheumatoid arthritis: Quo vadis. *Sci. World J.* **2014,** (2014).

7. Butoescu, N., Jordan, O. & Doelker, E. Intra-articular drug delivery systems for the treatment of rheumatic diseases: A review of the factors influencing their performance. *Eur. J. Pharm. Biopharm.* **73,** 205–218 (2009).

8. Evans, C. H., Kraus, V. B. & Setton, L. a. Progress in intra-articular therapy. *Nat. Rev. Rheumatol.* **10,** 11–22 (2014).

9. Vorvolakos, K., Isayeva, I. S., do Luu, H. M., Patwardhan, D. V. & Pollack, S. K. Ionically cross-linked hyaluronic

acid: Wetting, lubrication, and viscoelasticity of a modified adhesion barrier gel. *Med. Devices Evid. Res.* **4,** 1–10 (2011).

10. Turker, S. *et al.* Gamma-irradiated liposome/noisome and lipogelosome/niogelosome formulations for the treatment of rheumatoid arthritis. *Interv. Med. Appl. Sci.* **5,** 60–69 (2013).

11. Morgen, M. *et al.* Nanoparticles for improved local retention after intra-articular injection into the knee joint. *Pharm. Res.* **30,** 257–268 (2013).

12. Kim, S. R. *et al.* Cationic PLGA/eudragit RL nanoparticles for increasing retention time in synovial cavity after intra-articular injection in knee joint. *Int. J. Nanomedicine* **10,** 5263–5271 (2015).

13. Wu, Q. *et al.* Thermosensitive hydrogel containing dexamethasone micelles for preventing postsurgical adhesion in a repeated-injury model. *Sci. Rep.* **5,** 13553 (2015).

14. Webber, M. J., Matson, J. B., Tamboli, V. K. & Stupp, S. I. Controlled release of dexamethasone from peptide nanofiber gels to modulate inflammatory response. *Biomaterials* **33,** 6823–6832 (2012).

15. Burt, H. M., Tsallas, A., Gilchrist, S. & Liang, L. S. Intra-articular drug delivery systems: Overcoming the shortcomings of joint disease therapy. *Expert Opin. Drug Deliv.* **6,** 17–26 (2009).

16. Spiller, K. L., Maher, S. a & Lowman, A. M. Hydrogels for the repair of articular cartilage defects. *Tissue Eng. Part B. Rev.* **17,** 281–99 (2011).

17. Ahearne, M., Buckley, C. T. & Kelly, D. J. A growth factor delivery system for chondrogenic induction of infrapatellar fat pad-derived stem cells in fibrin hydrogels. *Biotechnol. Appl. Biochem.* **58,** 345–352 (2011).

18. Jiang, Y., Chen, J., Deng, C., Suuronen, E. J. & Zhong, Z. Click hydrogels, microgels and nanogels: Emerging platforms for drug delivery and tissue engineering. *Biomaterials* **35,** 4969–4985 (2014).

19. Lipowitz, A. J. in *Textbook of Small Animal Orthopaedics* (1985).

20. Klyosov, A. A. in *Galectin Therapeutics* (2012).

21. Roy, R., Murphy, P. V. & Gabius, H. J. Multivalent carbohydrate-lectin interactions: How synthetic chemistry enables insights into nanometric recognition. *Molecules* **21,** (2016).

22. Oberg, C. T., Leffler, H. & Nilsson, U. J. Inhibition of galectins with small molecules. *Chimia (Aarau).* **65,** 18–23 (2011).

23. St-Pierre, C. *et al.* Galectin-1-specific inhibitors as a new class of compounds to treat HIV-1 infection. *Antimicrob. Agents Chemother.* **56,** 154–162 (2012).

24. Hu, Y., Yéléhé-Okouma, M., Ea, H. K., Jouzeau, J. Y. & Reboul, P. Galectin-3: A key player in arthritis. *Jt. Bone Spine* **84,** 15–20 (2017).

25. Janelle-Montcalm, A. *et al.* Extracellular localization of galectin-3 has a deleterious role in joint tissues. *Arthritis Res. Ther.* **9,** R20 (2007).

26. Palmer, M., Stanford, E. & Murray, M. M. The effect of synovial fluid enzymes on the biodegradability of collagen and fibrin clots. *Materials (Basel).* **4,** 1469–1482 (2011).

27. Page-McCaw, A., Ewald, A. J. & Werb, Z. Matrix metalloproteinases and the regulation of tissue. *Nat Rev Mol Cell Biol.* **8,** 221–233 (2007).

28. Fezai, M., Senovilla, L., Jemaà, M., Ben-Attia, M. & Ben-Attia, M. Analgesic, Anti-Inflammatory and Anticancer Activities of Extra Virgin Olive Oil. *J. Lipids* **2013,** 1–7 (2013).

29. Ghosh, P. & Guidolin, D. Potential mechanism of action of intra-articular hyaluronan therapy in osteoarthritis: Are the effects molecular weight dependent? *Semin. Arthritis Rheum.* **32,** 10–37 (2002).

30. Aly, M. N. S. Intra-articular drug delivery: a fast growing approach. *Recent Pat. Drug Deliv. Formul.* **2,** 231–7 (2008).

31. Mehta, D. P., Shodhan, K., Modi, R. I. & Ghosh, P. K. Sodium hyaluronate of defined molecular size for treating osteoarthritis. *Curr. Sci.* **92,** 209–213 (2007).

32. LeBoeuf, R. D., Raja, R. H., Fuller, G. M. & Weigel, P. H. Human fibrinogen specifically binds hyaluronic acid. *J. Biol. Chem.* **261,** 12586–12592 (1986).

33. Zhang, Y., Heher, P., Hilborn, J., Redl, H. & Ossipov, D. a. Hyaluronic acid-fibrin interpenetrating double network hydrogel prepared in situ by orthogonal disulfide cross-linking reaction for biomedical applications. *Acta Biomater.* **38,** 23–32 (2016).

34. Snyder, T. N., Madhavan, K., Intrator, M., Dregalla, R. C. & Park, D. A fibrin/hyaluronic acid hydrogel for the delivery of mesenchymal stem cells and potential for articular cartilage repair. *J. Biol. Eng.* **8,** 10 (2014).

35. Li, S., Yu, Y., Koehn, C. D., Zhang, Z. & Su, K. Galectins in the pathogenesis of rheumatoid arthritis. *J Clin Cell Immunol* **4,** 164 (2013).

36. De Oliveira, F. L. *et al.* Galectin-3 in autoimmunity and autoimmune diseases. *Exp. Biol. Med.* (2015). doi:10.1177/1535370215593826

37. Chen, H. Y., Liu, F.-T. & Yang, R.-Y. Roles of galectin-3 in immune responses. *Arch. Immunol. Ther. Exp. (Warsz).* **53,** 497–504 (2005).

38. Lepur, A. Functional properties of Galectin-3. Beyond the sugar binding. *Lund University, University of Zagreb* (2012).

39. Thiemann, S. & Baum, L. G. Galectins and Immune Responses—Just How Do They Do Those Things They Do? *Annu. Rev. Immunol* **34,** 243–64 (2016).

40. Rabinovich, G. A. & Toscano, M. A. Turning 'sweet' on immunity: galectin-glycan interactions in immune tolerance and inflammation. *Nat. Rev. Immunol.* **9,** 338–352 (2009).

41. Klyosov, A., Zomer, E. & Platt, D. in *Glycobiology and Drug Design* **1102,** 89–130 (American Chemical Society, 2012).

42. Klyosov, A. a. Galectins as New Therapeutic Targets for Galactose-Containing Polysaccharides. *Bull. Georg. Natl. Acad. Sci.* **8,** 5–17 (2014).

43. ClinicalTrials. A New Agent GM-CT-01 in Combination With 5-FU, Avastin and Leucovorin in Subjects With Colorectal A New. 10–12 (2016).

44. Harrison, S. a. *et al.* Randomised clinical study: GR-MD-02, a galectin-3 inhibitor, vs. placebo in patients having non-alcoholic steatohepatitis with advanced fibrosis. *Aliment. Pharmacol. Ther.* **44,** 1183–1198 (2016).

45. ClinicalTrials. RCT (Randomized Control Trial) of TD139 vs Placebo in HV's (Human Volunteers) and IPF Patients Purpose. 10–12 (2016).

46. Hsieh, T. *et al.* Dual thio-digalactoside-binding modes of human galectins as the structural basis for the design of potent and selective inhibitors. *Sci. Rep.* **6,** 29457 (2016).

47. ClinicalTrials. An Open-Label , Phase 2a Study to Evaluate Safety and Efficacy of GR-MD-02 for Treatment of Psoriasis An Open-Label. 12–14 (2017).

48. ClinicalTrials. Clinical Trial to Evaluation the Safety and Efficacy of GR-MD-02 for the Treatment of Liver Fibrosis and Resultant Portal Hypertension in Patients With Nash Cirrhosis (NASH-CX). 4–7 (2017).

49. Weigel, P. H., Frost, S. J., McGary, C. T. & LeBoeuf, R. D. The role of hyaluronic acid in inflammation and wound healing. *Int. J. Tissue React.* **10,** 355–365 (1988).

50. Frost, S. J. & Weigel, P. H. Binding of hyaluronic acid to mammalian fibrinogens. *BBA - Gen. Subj.* **1034,** 39–45 (1990).

51. Yang, C. L., Chen, H. W., Wang, T. C. & Wang, Y. J. A novel fibrin gel derived from hyaluronic acid-grafted fibrinogen. *Biomed. Mater.* **6,** 025009 (2011).

52. Lee, F. & Kurisawa, M. Formation and stability of interpenetrating polymer network hydrogels consisting of fibrin and hyaluronic acid for tissue engineering. *Acta Biomater.* **9,** 5143–5152 (2013).

53. Weigel, P. H., Fuller, G. M. & LeBoeuf, R. D. A model for the role of hyaluronic acid and fibrin in the early events during the inflammatory response and wound healing. *J. Theor. Biol.* **119,** 219–234 (1986).

54. *Instruction For Use Synvisc® (hylan G-F 20).* 1–6 (2014).

55. Eymard, F. *et al.* Predictors of response to viscosupplementation in patients with hip osteoarthritis: results of a prospective, observational, multicentre, open-label, pilot study. *BMC Musculoskelet. Disord.* **18,** 1–8 (2017).

56. Ekundi-Valentim, E. *et al.* Differing effects of exogenous and endogenous hydrogen sulphide in carrageenan-induced knee joint synovitis in the rat. *Br. J. Pharmacol.* **159,** 1463–1474 (2010).

57. Santos, J. M. *et al.* The role of human umbilical cord tissue-derived mesenchymal stromal cells (UCX®) in the treatment of inflammatory arthritis. *J. Transl. Med.* **11,** 18 (2013).

58. Cecerale, S. in *Olive oil - Constituents, Health Properties and Bioconversions* (INTECH, 2011).

RÉSUMÉ

De nouvelles thérapies basées sur les nanotechnologies pour le traitement de l'arthrite rhumatoïde

La seule chose qui compte, c'est l'effort.

Le Petit Prince,

Antoine de Saint-Exupéry, 1943

USC
UNIVERSIDADE
DE SANTIAGO
DE COMPOSTELA

1. Introduction

La plupart des articulations, en raison de leurs caractéristiques anatomiques, se prêtent aux injections intra-articulaires (IA). Ces dernières années, il a été démontré que l'administration locale de médicaments avec un mode d'action direct pouvait grandement améliorer l'efficacité des traitements des maladies articulaires.[1–4] Les avantages de l'administration intra-articulaire comparée aux voies orales ou intraveineuses sont les suivantes : (i) biodisponibilité accrue, (ii) réduction de la toxicité du médicament, (iii) l'obtention d'une concentration efficace avec une dose minimale de médicament, (iv) réduction de l'exposition systémique et des effets indésirables associés, (v) diminution de l'apparition de résistance, et (vi) réduction du coût total des médicaments. Les principaux médicaments utilisés pour le traitement des arthropathies et l'amélioration de l'hémostase du genou qui sont actuellement disponibles sur le marché sont la cyclooxygénase-2 (COX-2), les antagonistes des TNF-α, IL-1 et IL-6. Les principales limites de ces médicaments sont le manque de spécificité pour les articulations et l'apparition d'effets secondaires considérables[2,5–7] désignant l'administration IA comme une alternative intéressante.

Les progrès dans le domaine biopharmaceutique au cours des dernières décennies ont permis le développement de systèmes de délivrance des médicaments (SDMs) les rendant moins toxiques tout en offrant une libération contrôlée et prolongée des drogues directement au site d'action.[2,4] Cependant, l'administration de médicaments IA dans l'articulation reste complexe, principalement en raison d'efflux rapide dans la cavité synoviale allié à la rotation rapide du fluide synovial (FS), l'internalisation cellulaire et du caractère invasif de cette route d'administration.[2]

Différents SDMs ont été testés pour le traitement local des arthropathies à partir de nano-/microparticules et d'hydrogels.[2,4,6,8] Les formulations les plus prometteuses et avancées portent sur une combinaison des deux systèmes.[9–14] Ces SDMs permettent une rétention suffisante et la libération prolongée de médicaments de faible masse moléculaire (MM), connus pour avoir un temps de séjour court dans les articulations[2,15] lorsqu'ils sont administrés en solution IA.

Le cartilage articulaire a une capacité limitée pour l'auto-régénération.[16–18] En outre, le FS a largement perdu ses fonctions intrinsèques dans des conditions pathologiques des articulations.[19] Avec cela à l'esprit, le recours à des transporteurs de médicaments multifonctionnels devrait contribuer à la guérison des pathologies diartrosiques. Outre la

libération contrôlée et prolongée de médicament, ces systèmes composés de matériaux résistants à la déformation peuvent contribuer au maintien de la rotule et à la lutte contre les dégradations enzymatiques. Simultanément, les SDMs pourraient fonctionner comme agents de viscosupplémentation pour améliorer l'homéostase du genou et, comme échafaudages cellulaires pour la régénération *in situ* du tissu cartilagineux.

En même temps, la découverte de nouvelles cibles immunitaires a conduit à d'intenses efforts pour la conception et le développement de petites molécules antagonistes pour des thérapies efficaces (en particulier pour les différents types de cancer, les maladies auto-immunes, le diabète…).[20–23] Tel est le cas de la protéine galectine-3 (Gal-3), qui a récemment été identifié comme favorisant l'apparition de la réponse inflammatoire.[24,25] Entre autre, cette protéine favorise la sécrétion de cytokines pro-inflammatoires, chimiokines par les macrophages,[24] et l'expression de métalloprotéinases de la matrice,[26] qui sont impliquées dans le remodelage du cartilage et de la déminéralisation de l'os.[5,27]

2. Hypothèse

1. L'utilisation de nanocapsules (NCs) chargées avec des médicaments dans des hydrogels dispersés *in situ* peut sensiblement augmenter le temps de rétention intra-articulaire des drogues. Les NCs peuvent agir comme réservoirs pour de multiples drogues lipophiles, et permettre leur libération contrôlée, tandis que l'hydrogel *in situ* pourrait protéger les NCs d'une décomposition rapide, l'endocytose et l'efflux de la cavité synoviale tout en contribuant également à moduler la libération des drogues. De telles compositions injectables pourraient aussi contribuer à l'hémostase du genou si un noyau d'huile d'olive et un revêtement d'acide hyaluronique (HA) 700 kDa, connus pour posséder des propriétés anti-inflammatoires, sont utilisés.[28–31] Nous avons aussi imaginé qu'un l'hydrogel de fibrine en 3D renforcé avec de l'acide hyaluronique devrait servir de viscosupplément (chaînes réticulées de HA) avec des propriétés élastiques pour persister dans l'ariculation et servir de support pour la régénération du cartilage.[32–34]
2. Etant donné que le blocage traditionnel de la COX-2 et les cytokines pro-inflammatoires TNF-α, IL-1 et IL-6 n'a pas conduit à un soulagement adéquat des maladies articulaires inflammatoires,[2,4,35–37] nous avons émis l'hypothèse que le

ciblage d'une nouvelle cible, la galectine-3, pourrait aider à bloquer toute la cascade inflammatoire et prévenir la dégradation des articulations ultérieures du système immunitaire.

3. Objectifs

Sur la base des hypothèses décrites, l'objectif de cette thèse était double, d'une part, de développer un nouvel d'hydrogel avec des nano réservoirs injectables pour la libération prolongée de médicaments lipophiles dans la cavité intra-articulaire; d'autre part, la synthèse d'un nouvel antagoniste de la galectine-3 et son incorporation dans l'hydrogel mentionné ci-dessus pour l'évaluation *in vivo*.

La démarche adoptée pour atteindre les objectifs finaux a été décomposée comme suit :

1) Développement et validation de SDMs injectables

1. Formuler, optimiser et caractériser de nouveaux NCs, vides ou chargés avec de la dexaméthasone (en tant que médicament modèle), en termes de propriétés physico-chimiques, de stabilité dans un liquide synovial reconstitué et de stabilité au stockage.
2. Concevoir et développer un nouvel hydrogel injectable intra-articulaire et étudier l'influence des paramètres qui peuvent modifier leur temps de gélification, les propriétés mécaniques et évaluer leur seringabilité.
3. La formation d'hydrogel en présence de NCs, la capacité de charge et la modification de ses propriétés rhéologiques. Caractériser le comportement rhéologique des hydrogels formulés en résence ou en absence de NCs, en termes de surface et de tailles.
4. Optimiser et caractériser deux hydrogels *in situ* formulés avec des NCs destinés à étudier leur effet dans un modèle d'inflammation aiguë chez le rat induit par le carraghénane.
5. Test le profil de libération *in vitro* de dexaméthasone du gel *in situ* formulé avec les NCs.

Les résultats correspondant à ces tâches sont présentés au **Chapitre 1**:

"An injectable, *in situ* forming hydrogel containing nanocapsules for intra-articular drug delivery".

2) Synthèse du médicament anti-inflammatoire, l'incorporation dans le SDM développé et évaluation de l'activité *in vivo*

6. Concevoir et synthétiser un nouveau « lead » pour le traitement de l'inflammation – une petite molécule inhibitrice de la forme extracellulaire de la galectine-3 (Gal-3), dérivée de la lactosamine de type II [Galβ(1→4)-GlcN], motif naturel reconnu par cette lectine, décorée avec des substituants aromatiques en vue d'augmenter son affinité et sa spécificité.
7. Caractériser l'inhibiteur Gal-3 obtenu, vérifier son affinité et sa sélectivité vis-à-vis d'un panel de galectines, en comparaison avec une petite molécule inhibitrice dérivée de sucre connue, le *bis*-3-[(3-fluorophényl)triazolyl] thiodigalactoside (souvent désigné TD139) qui vient d'être favorablement évalué en étude clinique de phase II pour le traitement de la fibrose pulmonaire.
8. Ajouter l'inhibiteur Gal-3 dans le SDM développé, caractériser les propriétés physico-chimiques de la formulation obtenue et tester l'activité anti-inflammatoire de cet inhibiteur *in vivo* dans un modèle de synovite aigüe de l'articulation du genou induite par la carraghénane chez de rat.

Les résultats liés à ce travail sont présentés au **Chapitre 2**:

"New galectin-3 inhibitor as a lead compound for anti-inflammatory drug candidates."

4. Résultats et discussion

1. Gal-3i en tant que composé principal pour de nouveaux médicaments candidats pour le traitement de l'arthrite rhumatoïde

Compte tenu de son implication dans la physiopathologie de l'arthrite rhumatoïde, la galectine-3 (Gal-3) apparaît comme une nouvelle cible potentielle immunothérapeutique,[24,27,38–40] dont le blocage peut empêcher/éviter la cascade inflammatoire et la dégradation des articulations qui l'accompagne. Nous avons donc conçu

et réalisé la synthèse de petites molécules antagonistes de la galectine-3. Les composés ont été obtenus à partir d'un ligand naturel de la Gal-3, la lactosamine de type II [Galβ(1→4)-GlcN], modifié avec des substituants aromatiques. Leurs structures présentées dans la **Figure 1**, appelées oxazoline et Gal-3i, par rapport à d'autres inhibiteurs de Gal-3 sont comparées à d'autres structures qui font l'objet d'essais cliniques pour le traitement de diverses maladies.[44–51]

Gal-3i, oxazoline et TD139 (un premier antagoniste Gal-3 de faible poids moléculaire approuvé par la FDA), testé dans des essais de polarisation de fluorescence compétitive ont révélé une sélectivité entre Gal-1/Gal-3/Gal-7. Gal-3i a montré une affinité 7,5 fois plus grande pour Gal-3 (K_d = 0,59 µM à 4 °C et 2,99 µM à 25 °C) que l'oxazoline (K_d = 4,4 µM à 4 °C et 23 µM à 25 °C) et a été sélectionné en tant que composé principal pour évaluer l'inhibition de Gal-3 *in vivo*.

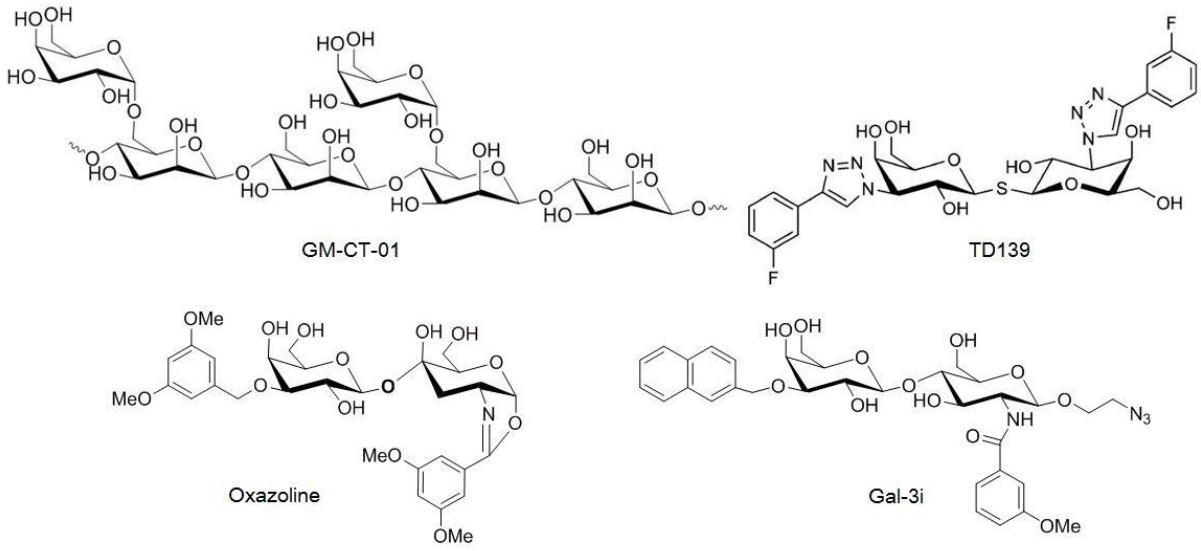

Figure 1. Les structures des deux inhibiteurs commerciaux Gal-3 : GM-CT-01 (DAVANAT®) TD139, oxazoline et Gal-3i synthétisé.

2. Développement et caractérisation d'une application SDM intra-articulaire

Afin de contourner deux des principaux écueils auxquels les systèmes délivrance de médicament IA doivent faire face, l'internalisation cellulaire et l'élimination rapide de la cavité synoviale,[2,15] nous avons développé un SDM composé de NCs dispersées dans un hydrogel *in situ* (**Figure 2**).

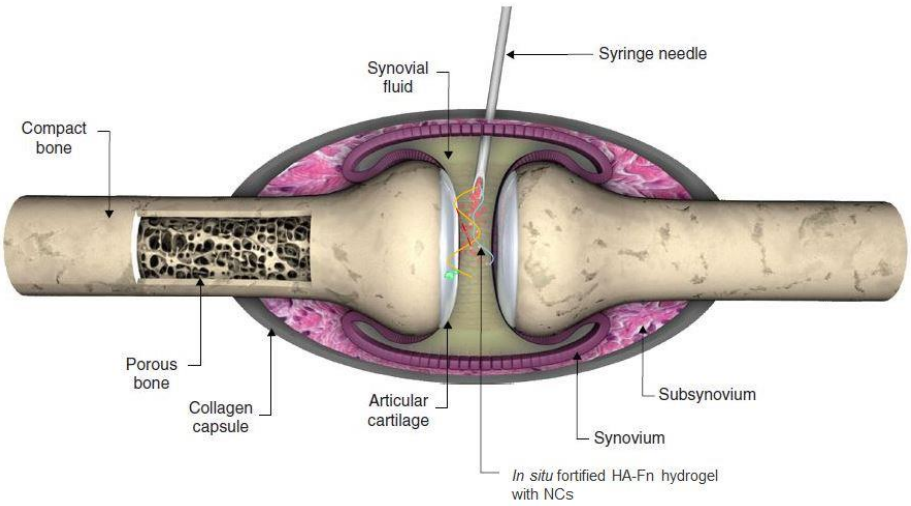

Figure 2. Représentation schématique de la structure d'une articulation synoviale et de l'injection intra-articulaire d'un hydrogel formé *in situ*, combiné à des nanocapsules chargées d'un médicament lipophile. Adapté et modifié avec l'autorisation de [15], Copyright© 2009, Taylor & Francis.

Les NCs reportés dans ce travail de thèse ont été préparées par une technique de déplacement de solvant et sont composées d'huile d'olive (OO), d'agents tensio-actifs biodégradables et biocompatibles - lécithine de soja (Lec) et oléylamine (OAm) et, finalement, d'acide hyaluronique (HA 700 kDa) en tant que polymère d'enveloppe. Nous avons développé des NCs ayant une taille d'environ ~130 nm propres à ne pas créer de dommages à l'articulation[11] tout en permettant d'encapsuler des drogues lipophiles en quantité suffisante (un anti-inflammatoire modèle – la dexaméthasone [DXM] et Gal-3i). La taille des particules, le potentiel zéta et l'efficacité d'encapsulation des formulations sont décrites dans le **Tableau 1**.

Les NCs sont stables dans des suspensions aqueuses stockées à 4 °C pendant une période d'au moins 1 mois. Les NCs maintiennent leur stabilité dans l'eau mais agrègent dans du PBS ou dans le liquide synovial reconstitué. Par conséquent, nous avons développé un hydrogel injectable *in situ*, en présence des NCs préformées pour améliorer la stabilité, avec maintien dans la cavité articulaire et une libération prolongée des drogues encapsulées.

Les gels ont été formés à partir de deux biopolymères HA et de la fibrine capables de former un réseau interpénétrant 3D (IPN)[33,52–55], en raison de l'affinité de HA de haut poids moléculaire pour la fibrine.[32,56] La formation d'hydrogel est basée sur l'activation enzymatique du fibrinogène par la thrombine (Thr), et permet de concevoir un IPN pas à pas, en présence de HA de différents poids moléculaires, d'agents renforçant la fibrine (facteur XIII et α2-antiplasmine) et les NCs chargées avec la drogue.

Tableau 1. Propriétés physico-chimiques des NCs vides ou chargées en drogue préparée avec HA 700 kDa (moyenne ± SD, n = 6). OO: d'huile d'olive, Lec: lécithine de soja, OAm: oléylamine, PDI: indice de polydispersité.

Type de NCs			OO (mg)	Lec (mg)	OAm (mg)	Taille de particule (nm)	PDI	ζ-potentiel (mV)	La concentration de drogue (mg/mL)
Blanc		prototype 1	15	3,75	0,75	128 ± 13	0,2	−27 ± 3	n/a
		prototype 2	22	5,625	1,125	121 ± 10	0,2	−30 ± 3	n/a
Chargé avec la drogue	DXM	prototype 1	15	3,75	0,75	160 ± 12	0,2	−20 ± 4	0,75 ± 0,13
		prototype 2	22	5,625	1,125	135 ± 9	0,2	−31 ± 5	5,60 ± 0,40
	Gal-3i	prototype 2	22	5,625	1,125	122 ± 11	0,2	−29 ± 5	0,53 ± 0,05

L'auto-assemblage des gels a été contrôlée par analyse de turbidité (λ = 350 nm) et des études rhéologiques qui identifient le retard de phase, déterminent le point de gel (**Figure 3**) et permettent d'observer l'évolution dans le temps du gel.

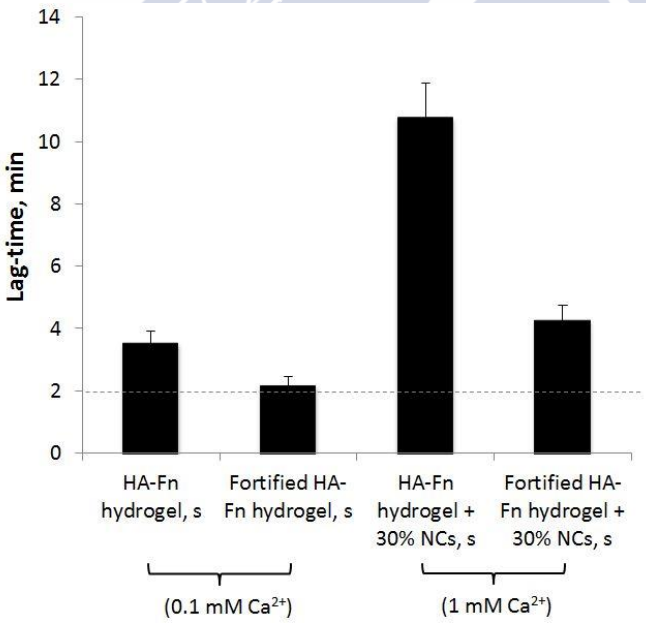

Figure 3. **Figure 3**. Résumé de la détermination du point de gélification par des mesures rhéologiques dans des systèmes différents: gels blancs "HA-fibrine" et "HA-fibrine renforcées" et ces gels 30% NCs. La ligne en pointillés représente le retard de phase requis 2 minutes. Les mesures ont été effectuées à 37 ° C Exprimé en moyenne ± SD; n = 3.

Nous avons obtenu un gel de microarchitecture et de temps de gel contrôlés en changeant la concentration du Thr, des NCs, des ions Ca^{2+}, du facteur XIII et de l'α2-antiplasmine afin d'obtenir une seringabilité adéquate pour les études *in vivo*. Un chargement des NCs de 30% (v/v) est observé au cours de l'auto-assemblage, et leur répartition homogène dans le gel avec des pores bien définis (7,29 ± 1,23 μm et 4,88 ± 1,12 μm, respectivement). Les valeurs de la viscosité initiale du mélange physique HA-fibrine (sans addition de Thr) étaient de 118,9 m*Pa·s* et 81,3 mPa·*s* à 20 °C et 37 °C, respectivement, et sont sensiblement plus faible par rapport aux viscosuppléments commerciaux[57,58], fournissant ainsi la seringabilité souhaitée pour une injection *in situ* de l'hydrogel pour des études *in vivo*. L'hydrogel formé *in situ* possède à la fois des caractéristiques rhéologiques d'un matériau élastique, adapté pour soutenir des déformations IA. Finalement, nous avons mis au point deux compositions de SDM, "le gel HA-fibrine pas renforcé avec 30% de NCs" et "le gel renforcé HA-fibrine avec 30% NCs" (**Figure 3**), pour d'évaluation chez le rat dans des modèles d'inflammation articulaire aiguë et chronique.

Le profil de libération *in vitro* de la dexaméthasone "gel HA-fibrine avec 30% de NCs" dans le liquide synovial reconstitué a été étendue à 72 h, ce qui peut être très avantageux pour l'administration intra-articulaire de la drogue (**Figure 4**).

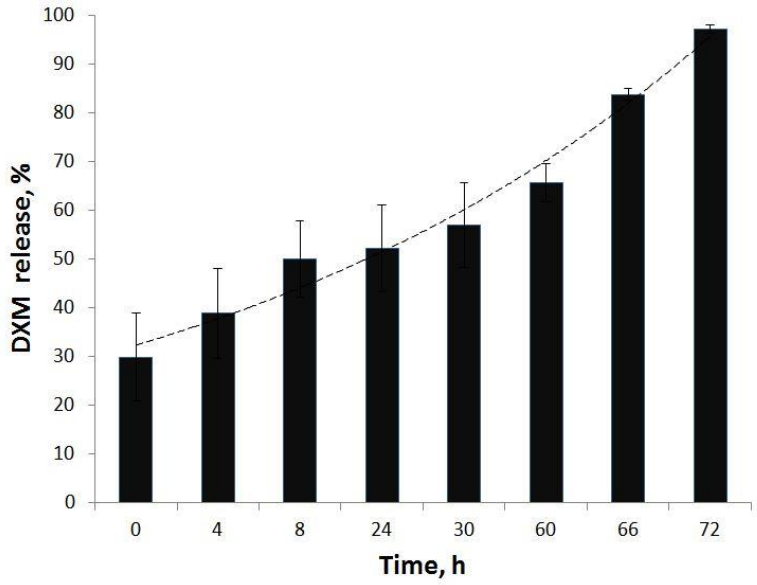

Figure 4. Libération de la dexaméthasone (DXM) à partir d'hydrogel HA-fibrine chargé avec 30% de NCs dans du liquide synovial simulé, 37 °C, 72 h.

3. L'activité anti-inflammatoire *in vivo* de l'inhibiteur de Gal-3

Dans une étude pilote, un modèle d'inflammation aiguë de courte durée induite par du carraghénane[59], qui fonctionne efficacement pour le criblage de nouveaux médicaments[60], a été choisi pour évaluer l'activité biologique de Gal-3i.

Les animaux avec une synovite induite ont été divisés en trois groupes selon le traitement reçu (100 µL, IA): des NCs vides utilisés comme véhicule contrôle (groupe 1), des NCs chargées avec Gal-3i à une dose de 200 µg/kg (groupe 2) et le gel HA-fibrine renforcé *in situ* contenat 30% de NCs chargées avec de la Gal- 3i à une dose de 55 µg/kg (groupe 3). Un animal de référence qui n'a pas été traité par du carraghénane a été utilisé en tant que contrôle négatif). L'activité de la drogue a été contrôlée à 4 heures après l'induction de la synovite, lorsque le pic de gonflement du genou est observé.[59] Les données de mesure du gonflement du genou et l'analyse histopathologique ont montré une activité anti-inflammatoire de Gal-3i et l'amélioration de l'état des articulations. Les données de gonflement du genou (**Figure 5**) ont montré une réduction du diamètre du genou: 1,6 fois (groupe 1), 3,5 fois (groupe 2) et 7 fois (groupe 3) par rapport au contrôle carraghénane.

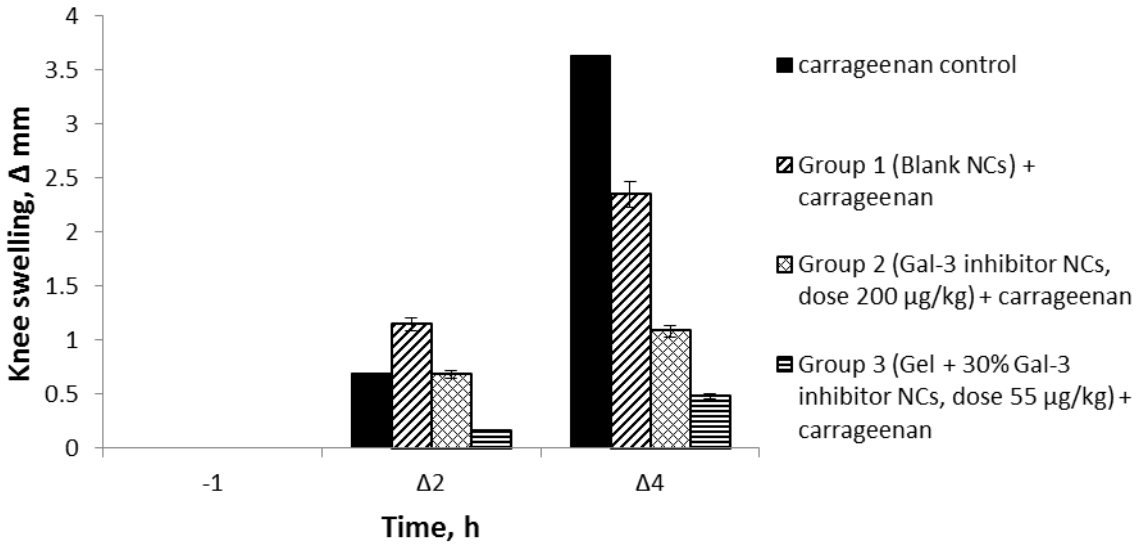

Figure 5. L'effet du traitement avec l'inhibiteur de Gal-3 dans le modèle de l'inflammation articulaire induite par la carraghénane en utilisant les NCs et les NCs un gel par rapport à NCs vides, et le contrôle de la carraghénane (n = 5 pour les groupes 1 3, n = 1 pour le carraghénane seul). Δ est la différence dans le diamètre du genou à différents moments avant et après l'injection de carraghénane, exprimée en mm. Les données sont exprimées en moyenne ± SEM.

Cette constatation est d'autant plus remarquable que la dose de Gal-3i (55 μg/kg) administrée au groupe 3 est nettement plus faible que celle administrée dans le groupe 2 (200 μg/kg). Finalement, l'hydrogel HA-fibrine semble maintenir de manière efficace les NCs dans la cavité articulaire et moduler la libération. Les NCs *per se* semblent avoir un effet bénéfique sur la cicatrisation des articulations.

Les résultats préliminaires obtenus dans le modèle de synovite aigüe induite chez le rat ont montré une suppression marquée de l'inflammation par le Gal-3i encapsulé dans l'hydrogel et administré à des doses de l'ordre du microgramme. Ces résultats suggèrent que Gal-3i peut être considéré comme un « lead » pour développer de nouvelles drogues immunothérapeutiques pour les maladies du genou, en particulier l'arthrite rhumatoïde. Il est à noter que le SDM contrôle a également montré une tendance à contribuer à prévenir l'inflammation des articulations probablement grâce aux effets protecteurs conjoints de l'huile d'olive et de l'acide hyaluronique dans la composition[28,29,61], tandis que l'hydrogel de fibrine de l'acide hyaluronique peut fonctionner en tant que potentielle viscosupplémentation pour ses propriétés élastiques, sa persistance dans l'articulation et en tant que structure adhérante *in situ* à haute cytocompatibilité pour la régénération du cartilage.

5. Conclusions

Le projet de thèse comprend la conception et le développement d'une nouvelle plate-forme de caractère nanotechnologique injectable pour prolonger le temps de séjour intra-articulaire et libération contrôlée de médicaments. Il est composé d'un hydrogel *in situ* dans lequel sont dispersées des nanocapsules, servant de réservoir pour divers drogues lipophiles anti-inflammatoires : i) un médicament modèle – la dexaméthasone; et ii) un nouveau composé en tant que molécule immunothérapeutique – un antagoniste de la galectine-3. Les résultats expérimentaux ont abouti aux conclusions suivantes :

1) Dans cette étude, un nouvel inhibiteur de haute affinité et sélectif de Gal-3 a été mis au point. Son K_d pour Gal-3 déterminé par polarisation de fluorescence est de 0,59 μM à 4 °C (2,99 μM a 25 °C). Une caractéristique importante de ce composé est d'être sélectif de Gal-3 par rapport à deux autres membres de cette famille de lectine Gal-1 et Gal-7.

2) De nouvelles nanocapsules (NCs) composées d'un cœur d'huile d'olive et d'un revêtement d'acide hyaluronique ont été préparées avec succès en utilisant une méthode simple de déplacement de solvant. Ces NCs ont la capacité d'encapsuler la dexaméthasone (5,6 ± 0,4 mg/mL) et l'inhibiteur de Gal-3 (531 ± 5 µg/mL). Ces dernières ont des tailles nanométriques (135 ± 9 nm et 122 ± 11 nm, respectivement), une charge de surface négative et une forme sphérique régulière.

3) Deux systèmes d'injection hydrogels *in situ* par un réseau interpénétrant composé d'acide hyaluronique-fibrine et d'acide hyaluronique-fibrine renforcée ont été développés. Les hydrogels ont montré un temps de gel, de microstructure et de propriétés mécaniques facilement modifiables. En outre, les gels permettent de charger des NCs à hauteur de 30% (v/v) lors leur auto-assemblage. La viscosité initiale du système est significativement plus faible par rapport à des viscosuppléments commerciaux, ce qui permet une bonne seringabilité. Les propriétés rhéologiques des hydrogels assemblés ont révélé une résistance à des tensions élevées, ce qui correspond à des caractéristiques à la fois de matériaux élastiques et de type solide, adapté pour persister intra-articulairement. En ce qui concerne leur structure, la formulation a des pores bien définis avec des NCs dispersées de manière homogène dans les de gel. Ce système de délivrance de médicament IA (SDM) a donné un profil de libération contrôlée et prolongée de drogue *in vitro*, en évitant une décomposition rapide des NCs dans le liquide synovial reconstitué.

4) Des études préliminaires *in vivo* réalisées dans un modèle de rat de synovite aiguë dans l'articulation du genou induite par le carraghénane a montré une suppression de l'inflammation par l'inhibiteur Gal-3 que ce soit pour les NCs chargé en inhibiteur que les NCs chargées en inhibiteur dispersées dans le gel. Ce résultat suggère que l'inhibiteur de la Gal-3 pouvait servir de composé de base pour concevoir des candidats médicaments pour le traitement de l'inflammation dans les articulations. Il est intéressant de noter que les NCs non chargées ont également montré une tendance à contribuer à réduire l'inflammation synoviale.

D'une manière générale, le travail présenté ici décrit le développement et la caractérisation d'un nouveau SDM biodégradable *in situ* comme potentiel hydrogel injectable intra-articulairement. Le système permet la distribution des médicaments lipophiles et devrait améliorer les thérapies actuelles des articulations. Les propriétés rhéologiques du système

initial offrent une bonne seringabilité et des caractéristiques mécaniques souhaitables pour l'application intra-articulaire. L'cctivité de l'inhibiteur de la galectine-3 dans une étude préliminaire *in vivo* a confirmé que la galectine-3 était une cible potentielle immunothérapeutique pour le traitement des maladies articulaires inflammatoires telles que l'arthrite rhumatoïde.

Références:

1. Edwards, S. H. R., Cake, M. a, Spoelstra, G. & Read, R. a. Biodistribution and clearance of intra-articular liposomes in a large animal model using a radiographic marker. *J. Liposome Res.* **17,** 249–261 (2007).
2. Evans, C. H., Kraus, V. B. & Setton., L. A. Progress in intra-articular therapy. *Nat. Rev. Rheumatol.* **10,** 11–22 (2015).
3. Gerwin, N., Hops, C. & Lucke, A. Intraarticular drug delivery in osteoarthritis. *Adv. Drug Deliv. Rev.* **58,** 226–242 (2006).
4. Kang, M. L. & Im, G.-I. Drug delivery systems for intra-articular treatment of osteoarthritis. *Expert Opin. Drug Deliv.* **11,** 269–82 (2014).
5. Quan, L.-D., Thiele, G. M., Tian, J. & Wang, D. The Development of Novel Therapies for Rheumatoid Arthritis. *Expert Opin. Ther. Pat.* **18,** 723–738 (2008).
6. Kapoor, B., Singh, S. K., Gulati, M., Gupta, R. & Vaidya, Y. Application of liposomes in treatment of rheumatoid arthritis: Quo vadis. *Sci. World J.* **2014,** (2014).
7. Butoescu, N., Jordan, O. & Doelker, E. Intra-articular drug delivery systems for the treatment of rheumatic diseases: A review of the factors influencing their performance. *Eur. J. Pharm. Biopharm.* **73,** 205–218 (2009).
8. Evans, C. H., Kraus, V. B. & Setton, L. Progress in intra-articular therapy. *Nat. Rev. Rheumatol.* **10,** 11–22 (2014).
9. Vorvolakos, K., Isayeva, I. S., do Luu, H. M., Patwardhan, D. V. & Pollack, S. K. Ionically cross-linked hyaluronic acid: Wetting, lubrication, and viscoelasticity of a modified adhesion barrier gel. *Med. Devices Evid. Res.* **4,** 1–10 (2011).
10. Turker, S. *et al.* Gamma-irradiated liposome/noisome and lipogelosome/niogelosome formulations for the treatment of rheumatoid arthritis. *Interv. Med. Appl. Sci.* **5,** 60–69 (2013).
11. Morgen, M. *et al.* Nanoparticles for improved local retention after intra-articular injection into the knee joint. *Pharm. Res.* **30,** 257–268 (2013).
12. Kim, S. R. *et al.* Cationic PLGA/eudragit RL nanoparticles for increasing retention time in synovial cavity after intra-articular injection in knee joint. *Int. J. Nanomedicine* **10,** 5263–5271 (2015).
13. Wu, Q. *et al.* Thermosensitive hydrogel containing dexamethasone micelles for preventing postsurgical adhesion in a repeated-injury model. *Sci. Rep.* **5,** 13553 (2015).
14. Webber, M. J., Matson, J. B., Tamboli, V. K. & Stupp, S. I. Controlled release of dexamethasone from peptide nanofiber gels to modulate inflammatory response. *Biomaterials* **33,** 6823–6832 (2012).
15. Burt, H. M., Tsallas, A., Gilchrist, S. & Liang, L. S. Intra-articular drug delivery systems: Overcoming the shortcomings of joint disease therapy. *Expert Opin. Drug Deliv.* **6,** 17–26 (2009).
16. Spiller, K. L., Maher, S. a & Lowman, A. M. Hydrogels for the repair of articular cartilage defects. *Tissue Eng. Part B. Rev.* **17,** 281–99 (2011).
17. Ahearne, M., Buckley, C. T. & Kelly, D. J. A growth factor delivery system for chondrogenic induction of infrapatellar fat pad-derived stem cells in fibrin hydrogels. *Biotechnol. Appl. Biochem.* **58,** 345–352 (2011).

18. Jiang, Y., Chen, J., Deng, C., Suuronen, E. J. & Zhong, Z. Click hydrogels, microgels and nanogels: Emerging platforms for drug delivery and tissue engineering. *Biomaterials* **35,** 4969–4985 (2014).

19. Lipowitz, A. J. in *Textbook of Small Animal Orthopaedics* (1985).

20. Klyosov, A. A. in *Galectin Therapeutics* (2012).

21. Roy, R., Murphy, P. V. & Gabius, H. J. Multivalent carbohydrate-lectin interactions: How synthetic chemistry enables insights into nanometric recognition. *Molecules* **21,** (2016).

22. Oberg, C. T., Leffler, H. & Nilsson, U. J. Inhibition of galectins with small molecules. *Chimia (Aarau).* **65,** 18–23 (2011).

23. St-Pierre, C. *et al.* Galectin-1-specific inhibitors as a new class of compounds to treat HIV-1 infection. *Antimicrob. Agents Chemother.* **56,** 154–162 (2012).

24. Hu, Y., Yéléhé-Okouma, M., Ea, H. K., Jouzeau, J. Y. & Reboul, P. Galectin-3: A key player in arthritis. *Jt. Bone Spine* **84,** 15–20 (2017).

25. Janelle-Montcalm, A. *et al.* Extracellular localization of galectin-3 has a deleterious role in joint tissues. *Arthritis Res. Ther.* **9,** R20 (2007).

26. Palmer, M., Stanford, E. & Murray, M. M. The effect of synovial fluid enzymes on the biodegradability of collagen and fibrin clots. *Materials (Basel).* **4,** 1469–1482 (2011).

27. Page-McCaw, A., Ewald, A. J. & Werb, Z. Matrix metalloproteinases and the regulation of tissue. *Nat Rev Mol Cell Biol.* **8,** 221–233 (2007).

28. Fezai, M., Senovilla, L., Jemaà, M., Ben-Attia, M. & Ben-Attia, M. Analgesic, Anti-Inflammatory and Anticancer Activities of Extra Virgin Olive Oil. *J. Lipids* **2013,** 1–7 (2013).

29. Ghosh, P. & Guidolin, D. Potential mechanism of action of intra-articular hyaluronan therapy in osteoarthritis: Are the effects molecular weight dependent? *Semin. Arthritis Rheum.* **32,** 10–37 (2002).

30. Aly, M. N. S. Intra-articular drug delivery: a fast growing approach. *Recent Pat. Drug Deliv. Formul.* **2,** 231–7 (2008).

31. Mehta, D. P., Shodhan, K., Modi, R. I. & Ghosh, P. K. Sodium hyaluronate of defined molecular size for treating osteoarthritis. *Curr. Sci.* **92,** 209–213 (2007).

32. LeBoeuf, R. D., Raja, R. H., Fuller, G. M. & Weigel, P. H. Human fibrinogen specifically binds hyaluronic acid. *J. Biol. Chem.* **261,** 12586–12592 (1986).

33. Zhang, Y., Heher, P., Hilborn, J., Redl, H. & Ossipov, D. a. Hyaluronic acid-fibrin interpenetrating double network hydrogel prepared in situ by orthogonal disulfide cross-linking reaction for biomedical applications. *Acta Biomater.* **38,** 23–32 (2016).

34. Snyder, T. N., Madhavan, K., Intrator, M., Dregalla, R. C. & Park, D. A fibrin/hyaluronic acid hydrogel for the delivery of mesenchymal stem cells and potential for articular cartilage repair. *J. Biol. Eng.* **8,** 10 (2014).

35. Li, S., Yu, Y., Koehn, C. D., Zhang, Z. & Su, K. Galectins in the pathogenesis of rheumatoid arthritis. *J Clin Cell Immunol* **4,** 164 (2013).

36. de Oliveira, F. L. *et al.* Galectin-3 in autoimmunity and autoimmune diseases. *Exp. Biol. Med.* (2015).

37. Chen, H. Y., Liu, F.-T. & Yang, R.-Y. Roles of galectin-3 in immune responses. *Arch. Immunol. Ther. Exp. (Warsz).* **53,** 497–504 (2005).

38. Haudek, K. C. *et al.* Dynamics of galectin-3 in the nucleus and cytoplasm. *Biochim. Biophys. Acta - Gen. Subj.* **1800,** 181–189 (2010).

39. Sörme, P., Arnoux, P., Kahl-Knutsson, B. & Leffler, H. Structural and Thermodynamic Studies on Cation− Π Interactions in Lectin− Ligand Complexes: High-Affinity Galectin-3 Inhibitors through Fine-Tuning of an Arginine− …. *J Am Chem …* 543–549 (2005). doi:10.1021/ja043475p

40. Lepur, A. Functional properties of Galectin-3. Beyond the sugar binding. *Lund University, University of Zagreb* (2012).

41. Thiemann, S. & Baum, L. G. Galectins and Immune Responses—Just How Do They Do Those Things They Do? *Annu. Rev. Immunol* **34,** 243–64 (2016).

42. Vasta, G. R. *et al.* Galectins as self/non-self recognition receptors in innate and adaptive immunity: An unresolved paradox. *Front. Immunol.* **3,** 1–14 (2012).

43. Rabinovich, G. A. & Toscano, M. A. Turning 'sweet' on immunity: galectin-glycan interactions in immune tolerance and inflammation. *Nat. Rev. Immunol.* **9,** 338–352 (2009).

44. Klyosov, A., Zomer, E. & Platt, D. in *Glycobiology and Drug Design* **1102,** 89–130 (American Chemical Society, 2012).

45. Klyosov, A. a. Galectins as New Therapeutic Targets for Galactose-Containing Polysaccharides. *Bull. Georg. Natl. Acad. Sci.* **8,** 5–17 (2014).

46. ClinicalTrials. A New Agent GM-CT-01 in Combination With 5-FU, Avastin and Leucovorin in Subjects With Colorectal A New. 10–12 (2016).

47. Harrison, S. a. *et al.* Randomised clinical study: GR-MD-02, a galectin-3 inhibitor, vs. placebo in patients having non-alcoholic steatohepatitis with advanced fibrosis. *Aliment. Pharmacol. Ther.* **44,** 1183–1198 (2016).

48. ClinicalTrials. RCT (Randomized Control Trial) of TD139 vs Placebo in HV's (Human Volunteers) and IPF Patients Purpose. 10–12 (2016).

49. Hsieh, T. *et al.* Dual thio-digalactoside-binding modes of human galectins as the structural basis for the design of potent and selective inhibitors. *Sci. Rep.* **6,** 29457 (2016).

50. ClinicalTrials. An Open-Label , Phase 2a Study to Evaluate Safety and Efficacy of GR-MD-02 for Treatment of Psoriasis An Open-Label , 12–14 (2017).

51. ClinicalTrials. Clinical Trial to Evaluation the Safety and Efficacy of GR-MD-02 for the Treatment of Liver Fibrosis and Resultant Portal Hypertension in Patients With Nash Cirrhosis (NASH-CX). 4–7 (2017).

52. Weigel, P. H., Frost, S. J., McGary, C. T. & LeBoeuf, R. D. The role of hyaluronic acid in inflammation and wound healing. *Int. J. Tissue React.* **10,** 355–365 (1988).

53. Frost, S. J. & Weigel, P. H. Binding of hyaluronic acid to mammalian fibrinogens. *BBA - Gen. Subj.* **1034,** 39–45 (1990).

54. Yang, C. L., Chen, H. W., Wang, T. C. & Wang, Y. J. A novel fibrin gel derived from hyaluronic acid-grafted fibrinogen. *Biomed. Mater.* **6,** 25009 (2011).

55. Lee, F. & Kurisawa, M. Formation and stability of interpenetrating polymer network

hydrogels consisting of fibrin and hyaluronic acid for tissue engineering. *Acta Biomater.* **9,** 5143–5152 (2013).

56. Weigel, P. H., Fuller, G. M. & LeBoeuf, R. D. A model for the role of hyaluronic acid and fibrin in the early events during the inflammatory response and wound healing. *J. Theor. Biol.* **119,** 219–234 (1986).
57. *Instruction For Use Synvisc® (hylan G-F 20)*. (2014).
58. Eymard, F. *et al.* Predictors of response to viscosupplementation in patients with hip osteoarthritis: results of a prospective, observational, multicentre, open-label, pilot study. *BMC Musculoskelet. Disord.* **18,** 1–8 (2017).
59. Ekundi-Valentim, E. *et al.* Differing effects of exogenous and endogenous hydrogen sulphide in carrageenan-induced knee joint synovitis in the rat. *Br. J. Pharmacol.* **159,** 1463–1474 (2010).
60. Santos, J. M. *et al.* The role of human umbilical cord tissue-derived mesenchymal stromal cells (UCX®) in the treatment of inflammatory arthritis. *J. Transl. Med.* **11,** 18 (2013).
61. Cecerale, S. in *Olive oil - Constituents, Health Properties and Bioconversions* (INTECH, 2011).

Intra-articular therapies for the treatment of rheumatoid arthritis

> Life can only be lived forwards, but must be understood backwards.
>
> *Søren Kierkegaard*

USC
UNIVERSIDADE
DE SANTIAGO
DE COMPOSTELA

1. Intra-articular therapies and local delivery of drugs

Over the last decades it has become clear that the local delivery of drugs in the intra-articular (IA) cavity can greatly improve the treatment schemes and effectiveness of joint-associated pathologies.[1–4] The current systemic therapies for these pathologies, administered by the oral or the intravenous routes, can be classified by the nature of the drug, as i) nonsteroidal anti-inflammatory drugs (NSAIDs), such as ibuprofen;[5] ii) corticosteroid anti-inflammatory drugs (*e.g.* dexamethasone);[6] iii) disease-modifying anti-rheumatic drugs (DMARDs), *e.g*. methotrexate;[7,8] iv) monoclonal antibodies (*e.g.* infliximab);[9] and v) natural agents, such as oils with anti-inflammatory and anti-oxidant properties.[10,11] Unfortunately, none of these drugs exhibit joint specificity.[2,12,13] Therefore, medication has considerable risks to humans due to the high doses required, with the subsequent systemic adverse effects (*e.g.* the cardiovascular, gastrointestinal complications, kidney dysfunction, skin and muscle atrophy, glaucoma, premature mortality).[12,14,15] Furthermore, after prolonged treatment, joints often become resistant to the systemic treatment.[1–3,16] Within this context, the intra-articular modality of administration offers the possibility to concentrate the drug locally,[2,17] and reduce the systemic toxicity.[2,12,18,19] Nevertheless, IA therapy still remains challenging due to a possible induction of septic arthritis (a risk controlled by careful handling of IA injections);[2,20,21] rapid drug elimination from the joint cavity,[2,22,23] and crystal-induced synovitis.[18,22,24] The latter two could be overcome by the development of drug delivery systems (DDSs) that display sufficient IA residence time with controlled and prolonged drug release profile.[2,16]

Anatomically, the human knee is a diarthrodial joint filled with 2 - 3.5 mL of synovial fluid (SF), a viscous liquid that plays an essential role in the knee homeostasis[3] (**Figure 1**), providing mechanical, nutritional and immune functions in the knee.[25] A key component of SF is high molecular weight (MW) hyaluronic acid (HA), present at an approximate concentration of 3 mg/mL.[26,27] In addition, HA reduces friction by lubricating the articulating joints and adsorbing shocks. Finally, the immune cells presented in the SF, mediated by HA, keep the immune control due to their high capacity of phagocytosis.[28–32]

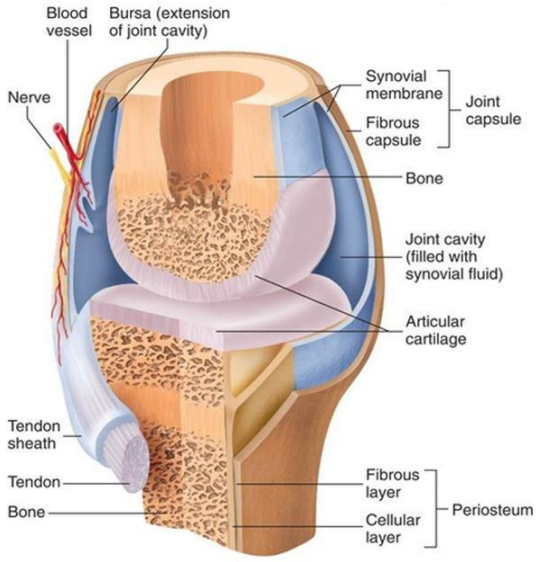

Figure 1. A schematic illustration of a knee joint. Reprinted with permission from The McGrow-Hill company, Inc, Copyright © 2009.

Given that in inflammatory conditions swollen knees accumulate between two and five times higher volumes of SF, the aspiration to remove the excess of fluid remains the first line treatment.[33–36] Besides, the administration of viscosupplementation agents, mainly HA or HA derivatives, has been widely used for improving the normal joints performance.[37,38] These products restore joint lubrication, provide elasticity and viscosity, improve the mobility, reduce pain, and protect the cartilage.[2,39–42] However, a limitation of this therapy is related to their high viscosity, causing intense IA pressure and pain in the knee joint.[43]

The marketed viscosupplements can be divided into non-crosslinked HA, that are normally highly viscous solutions, and crosslinked HA substances, usually injected as preformed hydrogels (**Table 1**).[2,44–54] These HA-based medical devices have shown significant improvement of viscoelastic properties of SF, increasing joint mobility, relieving the pain and inducing chondroprotective effect on osteoarthritis (OA).[55]

Generally, crosslinked HA has been reported to have a more prolonged residence time in the articular cavity, compared to the unmodified molecule.[2,48,56] As a result, these viscosupplements have shown long-lasting effects on OA (up to 26 weeks)[52–54,57–60] and, in some cases, have also been shown to alleviate rheumatoid arthritis (RA) symptoms, although they were not specifically designed for this pathology.[61] The longest therapeutic effect at OA was achieved by RenehaVis® (a course of 1-3 injections of a mixture of 1 and 2 MDa HAs, 12 months) and Crespine® Gel (a single injection of crosslinked HA, up to 6-8 months).

Table 1. Marketed intraarticular viscosupplements for arthropathies treatment.

Product name	Composition	Volume, dose and MW of HA	Number of injections per course	Company	Duration of therapeutic effect	Ref.
		Unmodified-HA viscosupplements				
Hyalgan®	0.5 – 0.73 MDa HA	2 mL, 20 mg	3	Sanofi-Aventis, USA	3 months	[45,62]
Supartz®	0.6 – 1.2 MDa HA	2.5 mL, 25 mg	3 – 5	Seikagaku Corp., Japan	3 – 6 months	[42,63]
Euflexxa®	2.4 – 3.6 MDa HA	2 mL, 20 mg	3	Ferring Pharmaceuticals Inc., USA	6 months	[45,64]
Orthovisc®	1.0 – 2.9 MDa HA	2 mL, 30 mg	3 – 4	Anika Therapeutics, Inc., USA	6 months	[65,66]
RenehaVis®	1 MDa (2.2%) and 2 MDa (1%) HA	0.7 mL, 15.4 mg (1 MDa), 0.7 mL, 7 mg (2 MDa)	1 – 3	MTD Int'l s.a., Switzerland	12 months	[46,67–70]
		Crosslinked HA hydrogels viscosupplements				
Synvisc-One®	Hylan[(a)] G-F20: a mixture of 80% (v/v) of Hylan A fluid, lightly crosslinked by formaldehyde and 20% (v/v) of Hylan B gel, crosslinked by sulfonyl-bis-ethyl	6 mL, 48 mg 6 MDa HA	1	Sanofi Biosurgery Inc, USA	Over 6 months	[47,48,71]
Gel-One®	HA crosslinked by dimers of cinnamic acid	3 mL, 30 mg High MW (not specified)	1	Seikagaku Corporation, Japan	Over 3 months	[44,72,73]
Durolane®	HA with 1,4-butane-diol diglycidyl ether crosslinker	3 mL, 60 mg High MW (not specified)	1	Bioventus Coöperatief U.A., Netherlands	Over 3 months (up to 9 months in some patients)	[49,74,75]

Monovisc®	Crosslinked HA (not disclosed)	4 mL, 88 mg 1 – 2.9 MDa HA	1	Anika Therapeutics, Inc., USA	Over 6 months	[50,51]
Hymovis® (HYADD®4)	A non-chemically crosslinked hexadecylamide derivative of HA	3 mL, 24 mg 500 – 730 kDa HA	2	Fidia Farmaceutici SpA, Italy	Over 6 months	[52–54,59,60]
Crespine® Gel	A mixture of non- and crosslinked HA by Covalent Reticulated Matrix (CRM®) technology HA	2 mL, 30 mg (MW not reported)	1	Biopolymer GmbH, Germany	6-8 months	[51,76]

(a) Hyalans (hyaluronan derivates) are produced by chemical crosslinking hyaluronan chains, without affecting the carboxylic and N-acetyl groups.[48,77]

When the degenerative illness has progressed, cartilage/osteochondral implants for hyaline cartilage or bone repair/substitution are the preferred treatments.[78–81] A variety of injectable *in situ* hydrogel/gel implants based on natural,[82–91] synthetic[92–99] and combined materials[100–107] were evaluated *in vivo* for articular tissues repair. Despite successful outcomes at the research level,[80,81,108] currently only one *in situ* hydrogel based on chitosan and glycerol phosphate (BST-CarGel®; Biosyntech, Canada)[109] is being tested on Phase IV clinical trials.[109–111]

2. Advanced drug delivery systems for intra-articular delivery

Drug-polymer conjugates constitute a more advanced treatment for IA pathologies compared with viscosupplements, which are actually considered as medical devices. They are designed to achieve combined effects: the action of the drug and the viscosupplementation of the polymer. In this regard, HA is the most used polymer in these products, although other examples are found, such as *N*-(2-hydroxypropyl)methacrylamide (HPMA)-dexamethasone.[63,112–115] It is worth mentioning the case of HA-methotrexate (DK226), designed specifically for the treatment of RA, which combines viscosupplementation agent with the methotrexate anti-inflammatory properties, showing a long lasting effect (24 days) in several RA rat models.[116,117]

The work in the area of IA drug delivery systems, aiming at prolonging the retention and controlling the drug release in the articular cavity, is currently moving in two principal directions: the development of nano-/microsystems and hydrogels (**Figure 2**).

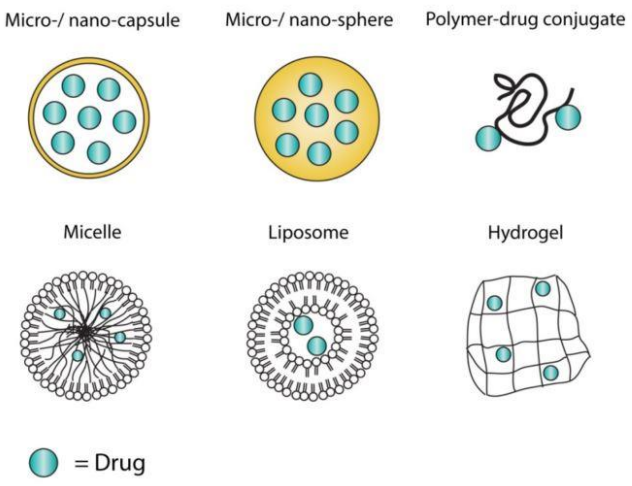

Figure 2. Different types of systems designed for IA administration. Reproduced with permission from[112] Copyright © 2014 Janssen *et al*., Creative Commons Attribution License.

2.1. Nano- and microsystems for IA delivery

Although a number of authors have described the potential use of nano-/microformulations for the IA delivery of drugs, the success of these DDS relies on their final fate. Nano-/microcarriers can show an increased joint retention time, which is size-dependent. Nanoparticles (NPs) injected into the joint cavity may penetrate into the cartilage extracellular matrix (ECM) and interact with collagen fibers when their particle size is generally below 100 nm.[4,118] For larger sizes, nanoparticles can be internalized by synovial macrophages, dendritic cells or chondrocytes,[23,119–121] or may suffer from a rapid efflux from the articular cavity.[2,16] Similarly, microparticles are also prone to be either phagocytized (< 20 μm) or remain in the SF, adhere to the cartilage and synovium or become entrapped within synovial folds (> 20 μm).[2,4,23,121] On the other hand, the diameter of blood capillaries (2-3 μm) and the lymph vessels (8-30 μm),[2,122,123] prevents the elimination of large particles.[2,112,124] An additional advantage of NPs vs. larger particles relies in the small size of the needle required for the injection and the fact that smaller particles are expected to cause no cartilage damage driven by mechanical damage in the joint.[124]

At present, only one liposomal formulation for IA application is available for the treatment of inflammatory osteoarthritis (OA) (**Table 2**). This formulation, Lipotalon®, which contains dexamethasone 21-palmitate,[125–127] has shown a maximal therapeutic effect on day 4 and the lowest disease activity index score at 16 days post-injection.[126,128,12] Another liposomal formulation, Clodrosome® (Encapsula NanoSciences LLC, USA), loaded with clodronate (antiosteoporotic cytotoxic drug), has been found to be effective in a preliminary clinical trial (7 days study) on patients with RA and has been marketed for non-human RA model studies (**Table 2**).[123,129,130] On the other hand, a new product PLGA microspheres (MS), namely Zilretta™/FX006 (Flexion Therapeutics, USA), which contains corticosteroid drug triamcinolone acetonide, has recently been approved by FDA and reached the market for OA treatment (**Table 2**).[131,132] The therapeutic effect of this formulation was maintained for up to 12 weeks.[131–134] Overall, these formulations have been shown to reduce the drug toxicity thanks to the improvement of its retention in the synovial cavity.

Table 2. Marketed formulations or in clinical trials based on nano-/microsystems for joints pathologies treatment by IA route.

Product name	Drug	Drug delivery systems	Indication	Phase of development	Ref.
Lipotalon®	Dexamethasone 21-palmitate (Corticosteroid anti-inflammatory)	Liposomes, ~200 nm	Inflammatory OA	Market, 2004	[125–127]
Zilretta™ (FX006)	Triamcinolone acetonide (Corticosteroid anti-inflammatory)	poly(D,L-lactic/glycolic acid) (PLGA) microspheres 9.7–10.3 μm	OA	Market, 2017	[131–135]
Clodrosome®	Clodronate disodium salt (Antiosteoporotic cytotoxic)	Liposomes, ~200 nm	RA, osteoporosis	Preliminary clinical trial on patients. Marketed for non-human RA model studies	[123,130,136]

The commercialization of these products has encompassed a quite active research activity in the field of liposomes and nano-/microparticles for intra-articular application made of a variety of biomaterials.[15,137–141] The most important recent advances with these formulations *in vivo* are summarized in **Table 3**. Overall, these liposomal or polymeric formulations containing anti-inflammatory or disease-modifying anti-rheumatic drugs have been evaluated *in vivo* providing in all cases the expected PK/PD changes of the associated drugs, extended residence time, reduced toxicity and prolonged effect.[121,142–159]

The drugs that have been more extensively studied are corticosteroids (i.e dexamethasone, betamethasone, prednisolone), NSAIDs (i.e. diclofenac, indomethacin), DMARDs cytotoxic drugs (i.e. methotrexate, paclitaxel, clodronate), and others, i.e. kartogenin, actarit, etc.[121,142–159] With regard to the composition of the nanosystems, in most cases they have been made of lipids (liposomes), polyesters (PLGA, PLA nanoparticles) and polysaccharides (i.e. chitosan nanoparticles). Despite of the positive initial *in vivo* data obtained with these formulations, their therapeutic responses have not been as long-lasting as expected. In fact, the longest response has been reported for the thermo-responsive Pluronic® F127/chitosan nanospheres for co-delivery of kartogenin and diclofenac (to achieve a dual chondroprotective and anti-inflammatory effect), and showed a 2-week retention time in

joints[159,160] (**Table 3**). A strategy to prolong the dwelling time of the nanoparticulated systems has relied on making them interactive with the surrounding environment. For example, cationic (Eudragit RL100 or PLGA/Eudragit RL) NPs, with the capacity to interact with endogenous HA, formed an *in situ* gel once injected to the rat joint cavity.[124,161] As a consequence, the NPs remained in the articular joints up to 28 days after the injection.[161]

Table 3. Formulations based on nano-/microsystems for the treatment of joints pathologies following IA administration.

Drug class		Drug	Drug delivery systems	*In vivo* model	Key observation	Ref.
Anti-inflammatory	Corticosteroids	Dexamethasone palmitate	Liposomes, 160 nm and 750 nm	Rabbit antigen-induced arthritis	750 nm liposomes have longer retention time. 30% of a drug dose found at 48 h	143
		Dexamethasone 21-acetate	Superparamagnetic iron oxide nanoparticles in PLGA microparticles, ~10 µm	A mouse dorsal air pouch	Release prolonged up to 6 days	162
		Betamethasone sodium phosphate	PLGA nanoparticles, 100–200 nm	Rats adjuvant-induced arthritis and mice with anti-type II collagen antibody induced arthritis	Almost complete remission of the inflammatory response after 1 week	152
		Betamethasone sodium phosphate	PLGA nanospheres, 300–490 nm	Rabbits with ovalbumin-induced chronic synovitis. A rat air pouch was used to evaluate the drug release	The drug release was prolonged to 7 days. The joint swelling decreased significantly during a 21-day period	151
		Prednisolone phosphate	Liposomes, 90–100 nm	Mice antigen-induced arthritis	At 24 h strongly suppressed pro-inflammatory markers of M1 phenotype macrophages, strongly diminished joint inflammation and destruction during 7 days of the study	144
		Diclofenac sodium	Radio-labelled liposomes, 235 nm	Rabbit antigen-induced arthritis	Scintigraphic imaging showed 60% retention of the formulations in the articular cavity at 24 h after the injection	163
		Diclofenac sodium	Radio-labelled BSA microspheres, ~15 µm	Rabbit antigen-induced arthritis	Scintigraphic imaging showed 99% microspheres retention at 4 h after injection. At day 30 some drug-loaded microspheres were still detectable in joints	164
	Non-steroidal	Indomethacin	Liposomes, 50–100 nm	Rat acute carrageenan-induced and chronic adjuvant-induced arthritis, (daily injections at days 1-14)	In short RA model the maximal paw edema inhibition was observed at 5 h; while in chronic RA model at day 21 liposomes could completely prevent the inflammation	146

		Indomethacin	Amphiphilic polyphosphazene micelles, size was not defined	Rat acute carrageenan-induced and chronic adjuvant induced arthritis	The drug released completely in 50 h (detected in plasma)	158
		Flurbiprofen	Chitosan microspheres crosslinked by genipin, 5.18–9.74 μm	Carrageenan-induced mono-articular arthritis (long RA model)	Concentration of the drug in microspheres was 8.7 folds higher than drug alone in the joints at 24 h after the injection	157
		Curcumin	Solid lipid nanoparticles, 135 nm	Complete adjuvant-induced arthritis in rats	Significantly and dose-dependently ameliorated various symptoms of arthritis, improved biochemical markers and preserved radiological alterations in joints of arthritic rats at 2 weeks	165
Disease-modifying anti-rheumatic	**Cytotoxic**	Methotrexate	Liposomes, 100 nm 1.8 μm	Rat antigen-induced arthritis	1.8 μm liposomes showed better joint retention and more effective suppression of inflammation compared to 100 nm ones. For 1.8 μm liposomes the knee diameter almost returned to normal state after 20 days. The treatment inhibited the cellular infiltration associated with the arthritis	148
		Methotrexate	poly(L-lactic acid) (PLA) microspheres, 30–100 μm	Healthy rabbit	After 24 h the drug concentration in the group treated with the microspheres is three fold higher compared with the group treated with the drug alone	155
		Paclitaxel	PLGA/PLA microspheres, 1–20 μm 10–35 μm 35–105 μm	Rabbit antigen-induced arthritis, carrageenan induced mono-articular arthritis	35–105 μm microspheres were biocompatible, whereas smaller ones (1–20 μm) produced an inflammatory response. PLA microspheres significantly reduced all measures of inflammation in the antigen arthritis rabbit model	156

	Antiosteoporotic	Clodronate	Liposomes, size was not defined	Rabbit antigen-induced arthritis	1 week joints retention, prevention of cartilage proteoglycan loss	149
	Chondrogenesis inducing	Kartogenin	Chitosan nano/microparticles kartogenin-conjugated 150 nm, 1.8 µm	Rat surgically induced osteoarthritis	Microparticles showed longer retention time in the knee joint than nanoparticles after IA injection. Both 150 nm and 1.8 µm particles showed much less degenerative changes than the untreated control or rats treated with unconjugated kartogenin	160
		Co-delivery of kartogenin and diclofenac	Thermo-responsive pluronic F127/chitosan nanospheres with kartogenin (covalently conjugated to outer shell) and diclofenac (encapsulated), 305 nm (37 °C) and 650 nm (4 °C)	Rat surgically induced osteoarthritis	The anti-inflammatory and chondroprotective effects were enhanced by cold treatment (4 ºC). Prolonged retention time in the joint up to 14 days	159,160
	Anti-rheumatic	Actarit	Solid lipid nanoparticles, 240 nm	Healthy mice (drug biodistribution), healthy rabbits (pharmacokinetic studies)	The actarit-loaded SLNs exhibited a longer mean retention time (13.53 h) compared with the actarit 50% propylene glycol solution (1.32 h)	166
	Hormones	Insulin	PLGA microspheres, 30–37 µm	Diabetic mice	Tested the effect of insulin on the diabetic cartilage. Microspheres allowed slow insulin release during 3 days. Insulin stimulated matrix synthesis in osteoarthritic cartilage. Local treatment with insulin overcame endogenous suppression of matrix synthesis in diabetic cartilage	167

	Photosensitizers	Anionic photosensitizers: 1) Tetra-phenyl-porphyrin-tetra-sulfonate; 2) tetra-phenyl-chlorin-tetra-carboxylic acid; 3) Chlorin e6	Chitosan-based nanogels decorated with hyaluronate, 40–140 nm	Mouse antigen-induced arthritis	Selective delivery of photosensitizers to macrophages and photodynamic destruction of macrophages. Efficient retention and decreasing the clearance of photosensitizers from the inflamed articular joints. For up to 24 h they were retained inside the cells and even at day 8 showed after light exposure showed efficacy of such a photodynamic therapy	168
Model drug	**Fluorescent probe**	A tetrapeptide labeled with fluorescein isothiocyanate	Eudragit RL100 NPs, 130 nm	Healthy rat	NPs injected to the synovial cavity form ionically cross-linked hydrogel with endogenous HA, allowing 7 days retention	124
		1,1′-dioctadecyl-3,3,3′,3′ tetramethylindotri carbocyanine iodide	PLGA/Eudragit RL NPs, 170 nm	Healthy mice	Microscopic imaging showed improved retention time in the knee joint with the filamentous NPs/HA aggregates, with over 50% preservation of the fluorescent signal 28 days after injection	161

2.2. Hydrogels

Hydrogels are insoluble crosslinked 3D structures of polymer chains with water or biological fluid swollen inside them. They can be designed with an adequate elasticity, mechanical strength, permeability and diffusivity, being versatile DDSs for arthropathies. Such hydrogels display highly porous networks, allowing the entrapment of drugs, nano-/ microcarriers or cells inside their pores and, depending on the material, the gels may support cell adhesion, proliferation, and differentiation.[112,169–172]

Hydrogels used for IA drug delivery are injectable pre-formed[173] or *in situ* forming hydrogels[174] with physically mixed[173] or chemically bound drugs.[175] For instance, a hydrogel with pre-mixed dexamethasone (DXM) has been shown to significantly reduced the inherent DXM toxicity in a rat OA model, providing an anti-inflammatory and chondroprotective effect at 12 weeks after the injection.[173]

A different strategy has relied on the design of *in situ* forming hydrogels that are easy to inject and exhibit a prolonged residence time in the articular cavity. Among them, it is worth mentioning a radiotherapeutical pH responsive Holmium-166-chitosan hydrogel,[176] in Phase II clinical trials for the treatment of knee synovitis typical for RA.[177] Another example, is a thermosensitive triblock poly(ε-caprolactone)-poly(ethylene glycol)-poly(ε-caprolactone) copolymer hydrogel, which has been proposed for the controlled delivery of methotrexate in rat joints. The complete drug clearance was monitored during 24 h in plasma and occurred slower compared to free methotrexate.[178]

2.3. Nano-/microsystems incorporated into hydrogels

Recent attention has been paid to the combination of drug loaded nano-/microsystems with hydrogels aiming at improving the residence time in the synovial cavity and the drug release profile.[80,179,180] These nano-/microcarrier-loaded hydrogels have been found to control the delivery of the associated drugs for about a month[174,181,182] or even longer.[183] Nevertheless, overall, the reported work of *in situ*-forming hydrogels containing drug-loaded nano-/microparticles is at a very early stage and only a few of these formulations have been tested *in vivo* (**Table 4**).[145,163,184]

In most of the cases these combined systems were tested in healthy animals what did not allow to adequately estimate the residence time and prolonged release at inflamed joints. However, radio-labelled liposomes (235 nm) incorporated into Carbopol® 940/carboxymethylcellulose gel evaluated at rabbit induced arthritis model demonstrated 67% retention in the articular cavity at 24 h after injection.[145,163] At healthy rat joints the

maximal sustained-released reached 42 days post IA injection by using amphotericin B precipitates/crystals suspended in glyceryl monooleate-HA hydrogel.[183]

An intra-articular DDS should fulfil a number of properties, such as biocompatibility, and biodegradability, in addition to an effective and prolonged disease improvement.[185] Another distinctive feature is bioadhesiveness,[81] which allows to increase the residence time of DDS in the synovial cavity and impart the chondroprotective effect.[186] Given the complexity of the joints anatomy, drug-loaded *in situ* hydrogels combined with nano-/microsystems might receive a significant benefit for IA drug delivery.

Table 4. Nano-/microsystems-loaded hydrogels for IA applications tested *in vivo.*

Drug	Drug delivery systems	*In vivo* model	Key observation	Ref.
Celecoxib (NSAID)	Precipitates/crystals (size non specified) dispersed in a poly(ε-caprolactone-co-lactide)-b-poly(ethylene glycol)-b-poly(ε-caprolactone-co-lactide) (PCLA-PEG-PCLA) gel network (*in situ*)	Healthy rat	The degradation and the release profiles were tested by different routes of administration: 1) In the articular cavity the DDS degraded between week 3 and 4. Release was not evaluated. 2) At subcutaneous injection in rats gel degradation happened in ~12 weeks, ~30 % celecoxib released during the first 3 days followed by a sustained release up to 4-8 weeks	174,181
Ibuprofen (NSAID)	Polyethylene glycol (PEG)-microspheres (40–100 μm) crosslinked by short PLGA chains to a hydrogel. Two populations: slow degradable and non-degradable	Healthy sheep shoulder joint	At 4 weeks non-degradable MS and not completely degraded MS were found, in synovial fluid and in the synovium. Degradable MS caused low inflammation compared to the non-degradable ones	182,187
Amphotericin B (Antifungal)	Precipitates/crystals (size non defined) suspended in glyceryl monooleate-HA hydrogel (*in situ*)	Healthy rat	This formulation showed sustained-released during 42 days after IA injection	183
Dexamethasone (Corticosteroid)	Monomethyl poly(ethylene glycol)-poly(ε-caprolactone) (MPEG-PCL) micelles (25 nm) incorporated into thermosensitive *in situ* PEG-PCL-PEG hydrogel (*in situ*)	Rat repeated-injury adhesion model	The gel biodegradation was evaluated upon subcutaneous injection and degraded in ~20 days	184
Diclofenac Sodium (Corticosteroid)	Lipogelosomes: Radio-labelled liposomes DMPC–CHOL–DCP (235 nm) incorporated into Carbopol® 940/carboxymethylcellulose gel	Rabbit antigen-induced arthritis	Scintigraphic imaging showed 67% retention of the formulations in the articular cavity at 24 h after injection	145,163

3. Galectin-3 role in pathophysiology of rheumatoid arthritis

Galectins are attracting more and more attention of scientists due to their presence in most of the tissues and their crucial role in biological processes and pathologies. Galectins are proteins able to bind to β-galactoside motifs (noteworthy, lactosamine [Galβ(1→3/4)-GlcN] types, so-called LN1 and LN2) by one or two conserved carbohydrate-recognition domains (CRDs) and lack of enzymatic activity.[188–190]

Galectins are widely distributed in the organism and they are continuously produced by different cell lines.[189,191] Their dual localization, intracellular (in nuclear and cytoplasmic compartments) and extracellular (at the cell membrane and extracellular matrix),[192,193] is associated with a wide range of biological processes, notably in cell cycle,[194195–197] cell migration,[198–201] inflammation, and immune response[202–207] (**Figure 3**). Overall, galectins synthesis can represent up to 1% of total protein in the producer cells.[207] However, during pathological processes the level of galectins can raise considerably. For instance, galectins local concentration at the inflammation site increases up to 40 mg/kg (of wet tissue), leaving the immune cells immersed in a sea of different galectins.[207] As a consequence, the deregulation of the galectins expression have been directly or indirectly associated with at least 137 pathologies headed by different cancer types, heart failure and RA, showing the potential of lectins as therapeutic targets.[208]

Currently, galectin family is represented by 15 members in mammals, which according to their architecture can be classified as: a) proto-, b) tandem-repeat-, and c) chimera-types (**Figure 3**).[191,209,210]

Proto-type galectins have one CRD and exist as monomers, but *in vivo* they are able to dimerize via non-covalent interactions to form homodimers. The tandem-repeat type is composed of two distinct, but homologous CRDs covalently linked to a dimer by a functional peptide. Finally, chimera-type galectins are made of one CRD that enables multimerization and *N*-terminal domain, including intermediate lateral collagen-like sequence, which implements alternative multimerization upon binding glycan ligands, mostly forming trimers and pentamers[207,211–213] (**Figure 3**).

Galectin-3 (Gal-3) is a key member of galectin family and a unique representative of the chimera-type.[202] It is present in vertebrates, protochordates, invertebrates, mushrooms, and viruses.[209] Human Gal-3 was found to be expressed in various tissues (gastrointestinal tract,[214] lung,[215,216] kidney,[217] skeletal tissues and brain[218]) and cell lines (immune

cells,[206,207,213] osteoblasts,[219,220] chondrocytes,[221,222] fibroblasts,[223] epithelial,[224–226] and endotelial cells).[227]

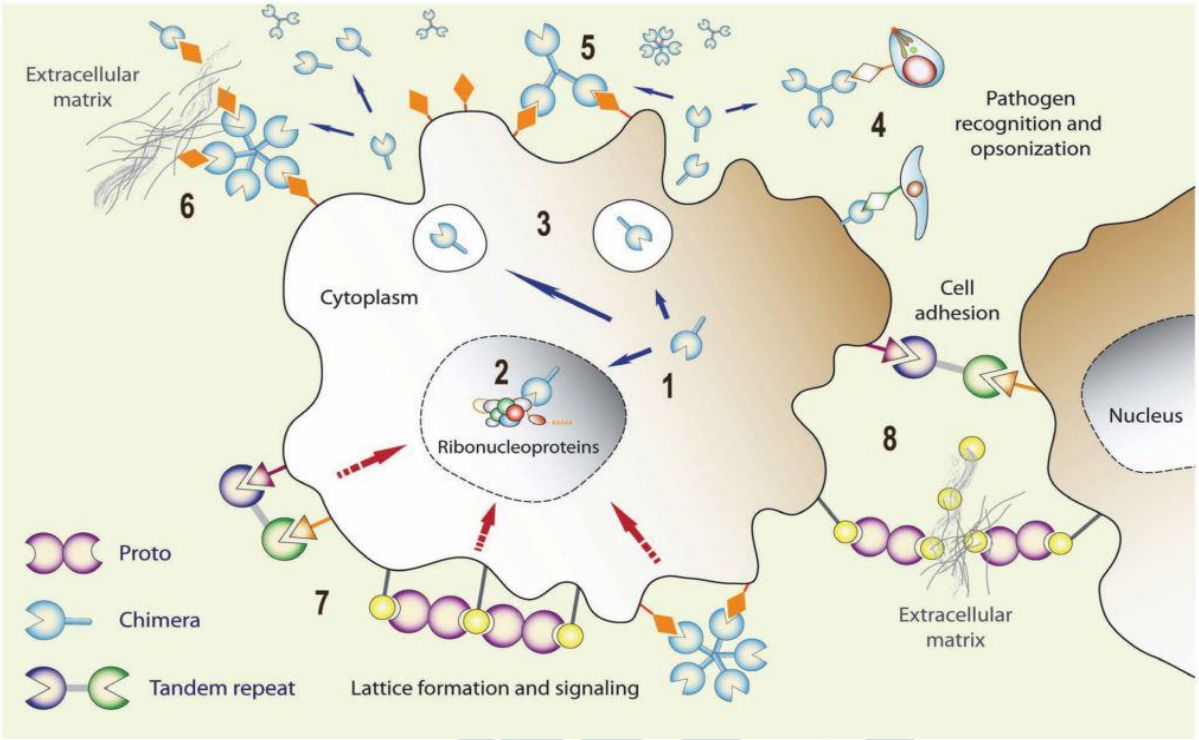

Figure 3. Intra- and extracellular located galectins and their functions. Proto-type: Galectin-1, -2, -5, -7, -10, -11, -13, -14, and -15; chimera-type: Galectin-3; tandem-repeat type: Galectin-4, -6, -8, -9, and -12. Functional diversification of galectins: (**1**) Galectin transcripts are translated in the cytoplasm, and the proteins can be translocated into the nucleus (**2**) where they can associate with ribonucleoproteins. Via unconventional mechanism(s), galectins can be secreted to the extracellular space (**3**) where they can function as pattern recognition receptors for microbial glycans (**4**), bind to the host cell surface glycans (**5**), and cross-link them with ECM glycans (**6**) thereby, for example, promoting cell migration. Galectins can also cross-link cell surface glycans and induce clustering of microdomains and lattice formation at the cell surface (**7**) that can trigger signaling cascades, or cross-link neighbouring cells (**8**) and promote cell–cell interactions/adhesion. Reproduced with permission from,[228] Copyright © 2012, Vasta et al., Creative Commons Attribution License.

3.1. Galectin-3 intracellular functions

Multiple functions of Gal-3 greatly comply with the noticeable phenomenon of dual localization.[213] Intracellularly, at the nucleus compartment, Gal-3 regulates pre-mRNA-splicing[213] and stabilizes protein-DNA interactions facilitating transcription,[207] contributing to gene expression and regulation.[229] But shuttling across nuclear pores to the cytoplasm Gal-3 has a post-transcriptional role in the stabilization of mature mucin 4 mRNAs,[230]

controls cell growth and has anti-apoptotic activity by the interaction with the apoptosis repressor Bcl-2.[196,231] Besides, Gal-3 inhibits the apoptosis by preventing the mitochondrial cytochrome C release.[207] Other Gal-3 functions were described in different stages of the cell cycle: cell differentiation,[208] intracellular trafficking,[225,232] and cell proliferation[233] (**Figure 4**).

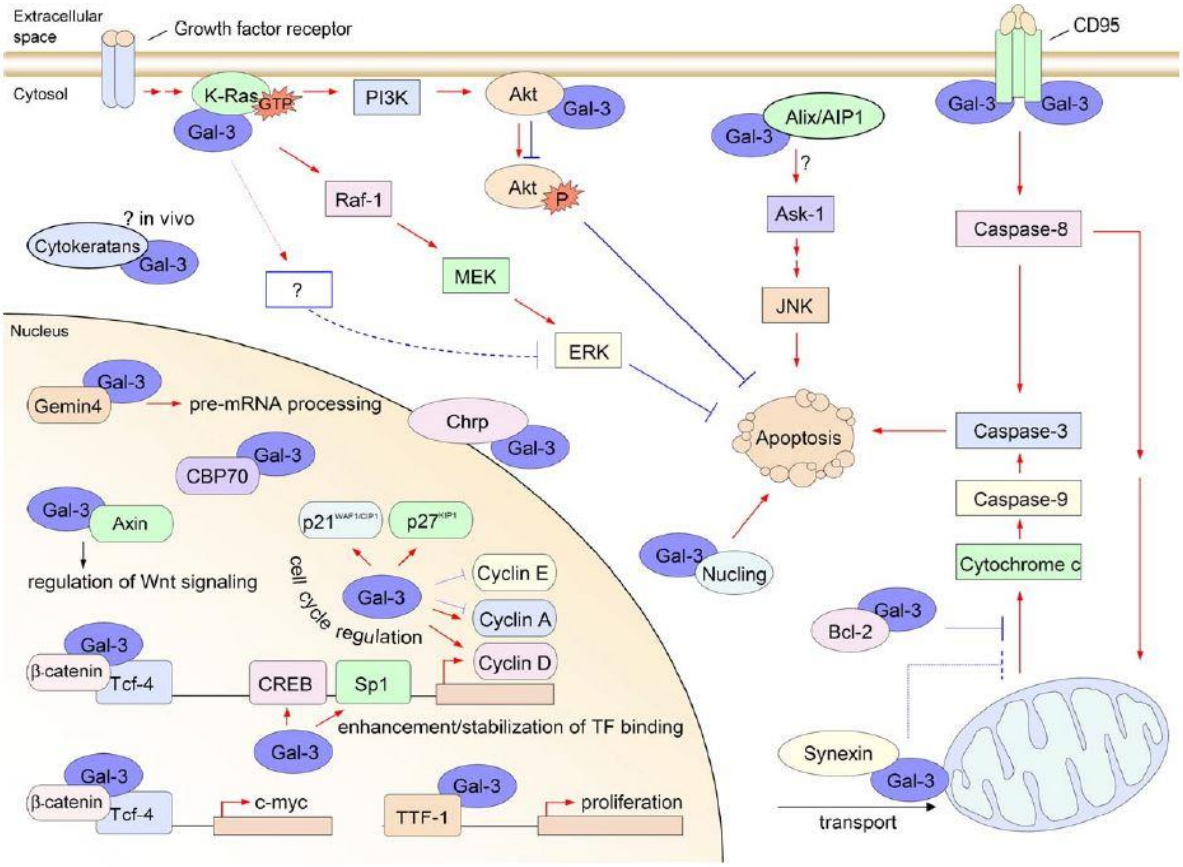

Figure 4. The intracellular functions of galectin-3. Red arrows indicate positive effects, blue lines – negative effects. Akt – the serine/threonine kinase Akt, Ask-1 – apoptosis signal-regulating kinase 1, CBP70 – carbohydrate binding protein 70, Chrp – cysteine- and histidine-rich protein, CREB – cAMP-response element-binding protein, ERK – extracellular signal-regulated kinase, Gal-3 – galectin-3, GTP – guanosine triphosphate, JNK – c-Jun NH2-terminal kinase, MEK – mitogen-activated protein/ERK kinase, P – phosphate, PI3K – phosphatidylinositol 3-kinase, Raf-1 – the serine/threonine kinase Raf-1, Tcf-4 – T cell factor 4, TF – transcription factor, TTF-1 – thyroid-specific transcription factor. Reprinted with permission from,[234] Copyright © 2006, Elsevier.

3.2. Galectin-3 extracellular functions

Extracellularly Gal-3 releases in vesicles, likely through exosomes or by direct translocation and stays on the cell membrane, in the vicinity of the cell or bounds to the

extracellular matrix.[207] Being abundantly expressed in different tissues, Gal-3 modulates distinct cellular processes such as cell-cell and cell-matrix interactions through specific binding to extracellular sugar ligands.[208] In such a manner, this protein takes part in multiple biological processes: cell adhesion,[226,235] cell migration,[200,236] transmembrane signalling,[237,238] immune response and inflammation[204,212,239,240] (**Figure 5**).

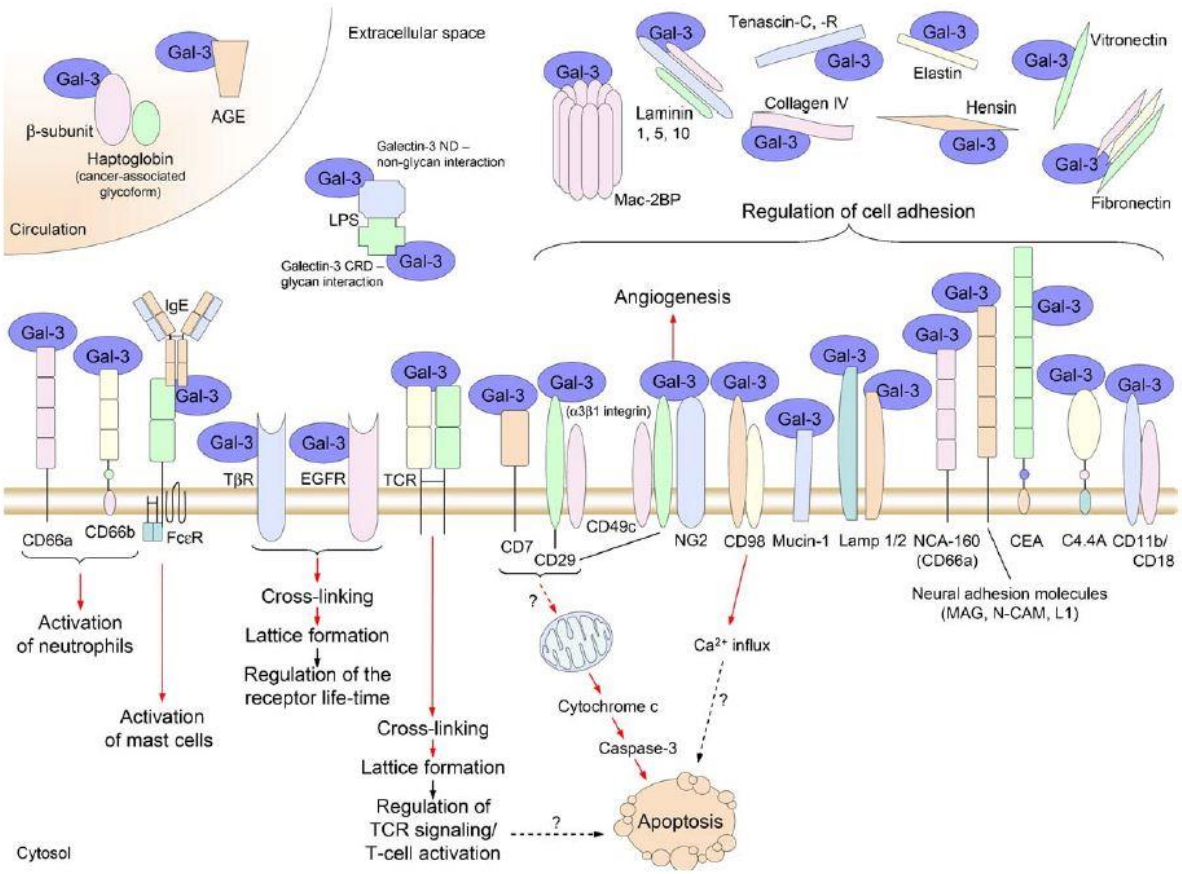

Figure 5. The extracellular functions of galectin-3. Red arrows indicate positive effects. AGE – advanced glycation end products, C4.4A – the GPI-anchoredglycoprotein C4.4A, CEA – carcinoembryonic antigen, CRD – carbohydrate-recognition domain, EGFR – epidermal growth factor receptor, FcεR – Fcε receptor, Gal-3 – galectin-3, IgE – immunoglobulin E, L1 – neural adhesion molecule L1, Lamp 1/2 – lysosome associated membrane protein 1/2, LPS – lipopolysaccharide, Mac-2BP – Mac-2 binding protein, MAG – myelin associated glycoprotein, N-CAM – neural cell adhesion molecule, NCA-160 – non-specific cross-reacting antigen 160, ND – N-terminal domain, NG2 – the transmembrane chondroitin sulfate proteoglycan NG2, TβR – transforming growth factor β receptor, TCR – T cell receptor. Reprinted with permission from,[234] Copyright © 2006, Elsevier.

One of the most important extracellular functions of Gal-3 is supporting the control of immune and inflammatory response.[207,212,241] The immune system cells are Gal-3 rich and

involved basically in each process: from controlling the B cells maturation in the bone marrow to activation or inhibition of B and T cells apoptosis.[207] Although resting B and T cells do not express it.[213] Gal-3 is expressed in neutrophils, basophils, eosinophils, macrophages (at all the stages from monocytes differentiation to macrophages and dendritic cells),[220,242–244] mast cells,[213] and has also considerable effects on both innate and adaptive immunity.[207] Innate immune functions of Gal-3 are cell activation, adhesion, migration, and promotion of pathogens phagocytosis (including mycobacteria, fungi, and parasites)[207] as well as autophagy.[245] It is both pro-inflammatory and anti-inflammatory mediator, working as a chemoattractant for monocytes, macrophages, followed by macrophages polarization,[246] and increasing the amount of neutrophils.[207] In adaptive immune system Gal-3 exposes immunosuppressive effect, restricting T cell receptor recruitment into immune synapses, prevents T cell proliferation, differentiation, and directly promotes T cell apoptosis,[207] resulting to prolonged inflammation.[247] On the other hand, Gal-3 anti-inflammatory activity includes phagocytosis of dead cells and stimulation of wound healing.[207]

3.3. Galetin-3 deregulation in RA

Noticeably, Gal-3 expression is up-regulated in synovial tissues in RA,[213] its concentration in SF increases from about 50 ng/mL up to 130-300 ng/mL[212] and being a pro-inflammatory regulator, it amplifies the inflammation.[247] As reported, Gal-3 stimulates synovial fibroblasts as well as infiltrated immune cells to release the pro-inflammatory cytokines (TNF-α, IL-6, IL-17) and chemokines (CCL2, CCL3, CCL5, CXCL8),[212] the expression of matrix metalloproteinases MMP-3,[248] MMP-9[249] and A Disintegrin And Metalloproteinase with Thrombospondin Motifs 5 (ADAMTS5).[212] These enzymes are involved in the degradation of the ECM[248] and type I-III collagen and tissue remodeling.[30,250] They also inhibit the osteocalcin production[220] leading to bone demineralization,[212] and, eventually, causing joint degradation.[19,251] In addition, IA injection of recombinant galectin-3 in mice induced cartilage and subchondral bone lesions.[220,247] Taking into account the involvement of Gal-3 into the pathophysiology of RA this protein appears as a novel potential immunotherapeutic target.

3.4. Galectin-3 structure

Human Gal-3 is a 30-35 kDa protein coded by the *LGALS3* gene,[234] composed by 250 amino acids (aa) organized into a secondary structure, mostly forming anti-parallel β-sheets and only in few regions assemble into α-helixes.[213,252,253] The protein is divided into 3 regions: N-terminal peptide (1-18 aa) with two phosphorylation sites involved in Gal-3

secretion;[254–256] a lateral collagen-like sequence (19-111 aa), which includes consensus sequence of nine PGAYP repeats,[213,254] which can give rise to multimerization; and the carbohydrate recognition domain – CRD (112-250 aa) that includes highly conserved amino acids, termed the carbohydrate-binding cassette, critical for glycan recognition and complexation.[207,252,257,258]

Gal-3 CRD domain has a structure typical for galectin family members with a canonical amino acid sequence,[259] suggesting that all the Gal-CRDs are able to bind β-galactoside motifs with similar K_d values for these ligands.[190,256,260] It is composed of two antiparallel β-sheets of six (S1-S6) and five (F1-F5) strands (**Figure 6A**) and includes highly conserved residues (*e.g.* His158, Asn160, Arg162, Glu165, Asn174, Trp181, Glu184) responsible for complexation with carbohydrate ligands and salt-bridge network (Arg162-Glu165-Glu184-Arg186), determining LN2 binding preference over LN1 core (**Figure 6B**).[190,252,259,261] Structural alignments and superimposition of CRD domains fragments (S4-S6) of human Gal-3 CRD (hGal-3-CRD), Gal-1 (hGal-1) and Gal-7 (hGal-7) CRDs are shown in **Figure 6C** and **D.**[190] These similarities explain the low specificity of some synthetic Gal-3 inhibitors that have dissociation constants of the same order for these three galectins.[262] It is important to emphasize that two arginine residues (Arg144 and Arg186), adjacent to the binding site of Gal-3 CRD, do not participate in natural ligands complexation,[259,263] but offer an opportunity to establish new binding contacts for selective targeting of Gal-3[190,252] (**Figure 7A**). Thus, one strategy to obtain more affine and specific Gal-3 inhibitors consists in the introduction of aromatic substituents to LN2 core to gain cation-π interactions between arenes and guanidinium ions of Arg144 and Arg186.

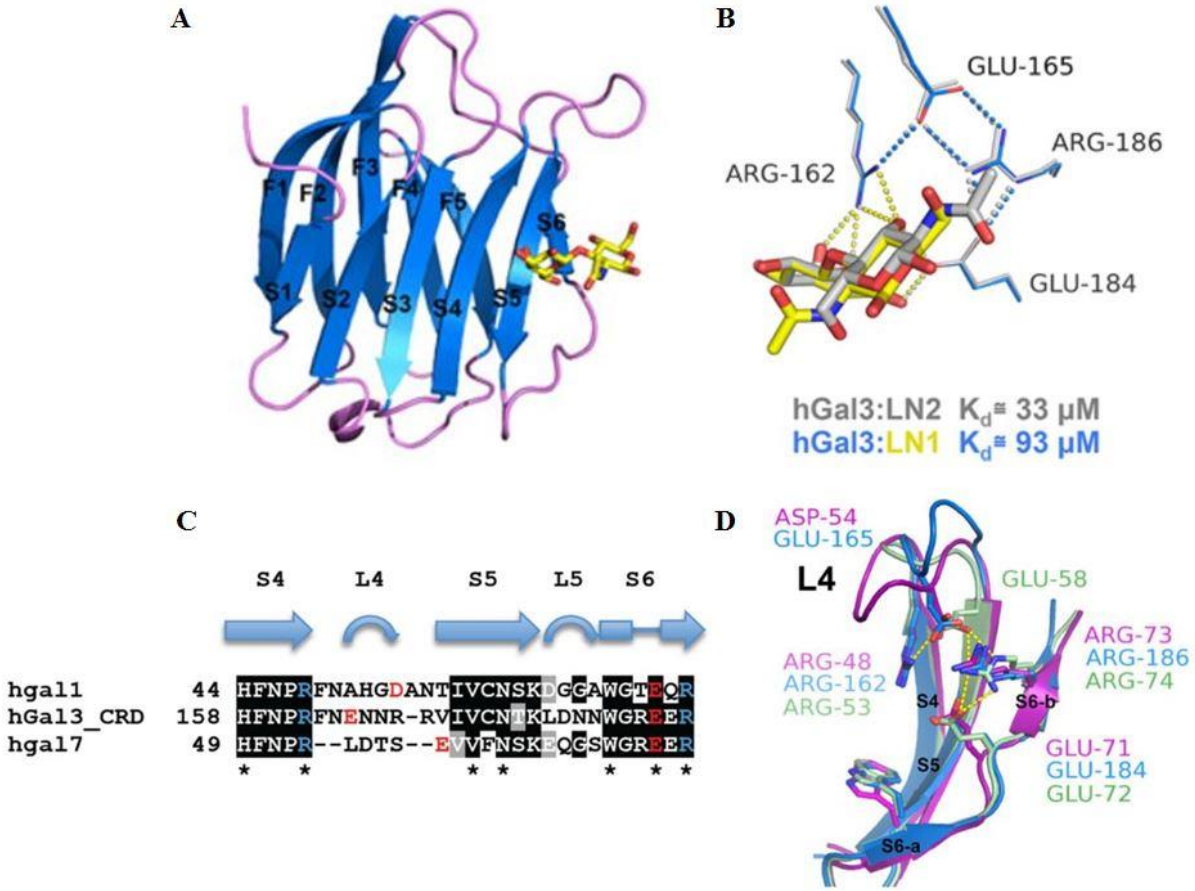

Figure 6. (A) 3-D structure of human Galectin-3 (hGal-3) CRD complexed with LN1; **(B)** Close-up view of the unique salt bridge networks in hGal-3-CRD and its affinity to LN1 and LN2; **(C)** Structure-based sequence alignment of S4-S6 β-strands of hGal-3-CRD and hGal-7. Secondary structures were designated according to the resolved X-ray structures. The highly conserved LNs-interacting residues among hGal-1, hGal-3-CRD and hGal-7 are indicated by asterisks. Residues involved in unique salt bridge network of hGal-1, hGal-3-CRD and hGal-7 are coloured in either red (Glu/Asp) or blue (Arg); **(D)** S4-S6 β-strands of hGal-1 (pink), hGal-3-CRD (blue) and hGal-7 (green) are superimposed. The unique salt bridge network of hGal-1 (R48-D54-E71-R73), hGal-3-CRD (R162-E165-E184-R186) and hGal-7 (R53-E58-E72-R74) are shown in stick models. Reproduced with permission from,[190] Copyright © 2015 Hsieh et al., Creative Commons Attribution License.

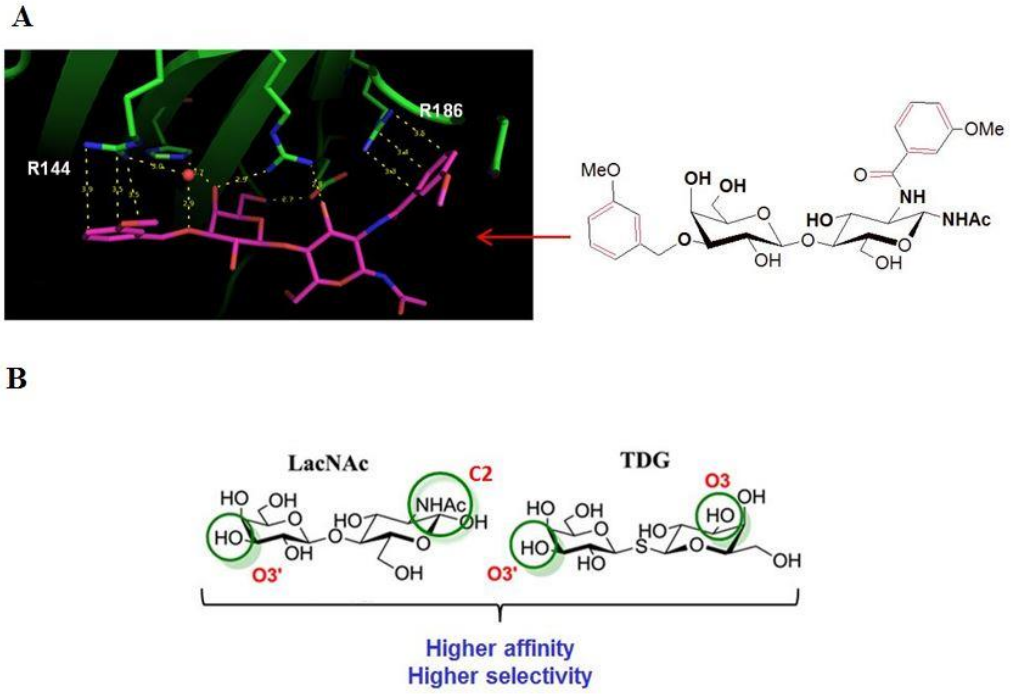

Figure 7. (A) A close-up view of the X-ray structure of Gal-3 CRD complexed with di-arylated Gal-3 inhibitor by cation-π interactions of aromatic substituents with guanidinium ions of highly conserved Arg144 and Arg186 residues. Reprinted with permission from[264], Copyright © 2017, Elsevier. **(B)** Structures of disaccharides *N*-acetyllactosamine (LacNAc) and thio-digalactoside (TDG), as the scaffolds to design galectin inhibitors. Green circles denote critical modified positions in search for high-binding affinity and selective galectin inhibitors. Modified with permission from[265] Copyright © 2016 Cagnoni et al., Creative Commons Attribution License.

3.5. Galectin-3 synthetic antagonists

Currently, only three Gal-3 antagonists among the reported inhibitors have entered clinical trials. One, designed against colon cancer, named DAVANAT® (GM-CT-01),[208,266] undergone phase II clinical trials.[267] DAVANAT® is obtained from guar gum natural galactomannan polysaccharide, where galactose residues are branched to a poly-mannopyranoside backbone (**Figure 8**). Initially, K_d of this derivative to Gal-3 was found to be 60-70 nM[268] at 4 °C, but the last findings of the collaborative research, published by Klyosov *et al.* contradicts this, showing no inhibition of Gal-3 (1-5 μM) at the tested concentrations of DAVANAT® (1-5 mg/mL). The inhibitor seems to complex with another non-canonical binding site/s and has higher affinity to galectin-1 (K_d ~ 10 μM).[269] Another drug candidate for the treatment of non-alcoholic steatohepatitis with advanced fibrosis/cirrhosis and plaque psoriasis, named GR-MD-02,[270] entered phase II clinical trials

for both diseases.[271,272] This inhibitor, in combination with Keytruda® and Yervoy®, is in Phase I for melanoma cancer immunotherapy.[270,273,274] GR-MD-02 is a complex carbohydrate molecule (galactoarabino-rhamnogalacturonan) (**Figure 8**), with MW 2-80 kDa, derived from a plant,[275] and binds Gal-3 with K_d 2.9 μM.[276] Lastly, a very potent Gal-3 inhibitor bis-{3-deoxy-3-[(3-fluorophenyl)-1H-1,2,3-triazol-1-yl]-β-D-galacto-pyranosyl}sulfane, usually referred to as TD139, was efficiently tested in idiopathic pulmonary fibrosis treatment,[215,237,261] and currently finished phase IIb clinical trials.[237,277] It is a small sugar-derived molecule inhibitor, based on a C2-symmetrical thio-digalactoside core identified from screenings of aromatic substituent libraries[263,278] (**Figure 8**). TD139 interacts with Gal-3 with K_d 14 nM at 4 °C.[215]

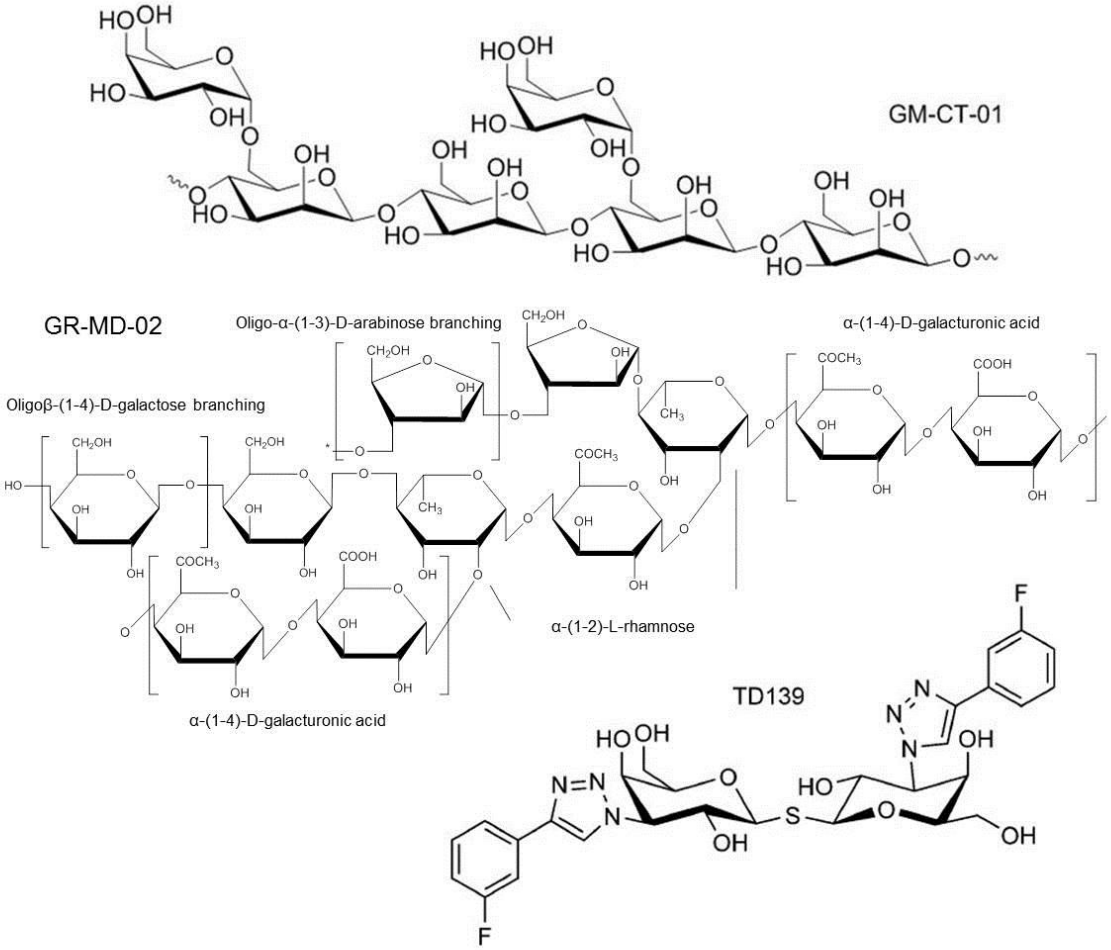

Figure 8. Structures of different commercial Gal-3 inhibitors: DAVANAT® (GM-CT-01), GR-MD-02, and TD139.

According to Nilsson and Leffler's approach,[260,278] the increase of the selectivity and binding affinity of inhibitors to Gal-3 could be achieved by establishing of cation-π interactions between aromatic substituents at positions 3'-C of galactose (Gal) and 2-C of glucosamine (GlcN) of type II N-acetyllactosamine (LacNAc) [Galβ(1→4)-GlcN] (**Figure 7B**) and guanidinium ions of two Gal-3 CRD Arg144 and Arg186 residues (**Figure 7A**).[264] Following this approach, we report herein the design, synthesis, characterization and *in vivo* activity evaluation of a highly selective and affine Gal-3 inhibitor derived from its natural ligand type II LacNAc with aromatic substituents at positions 3'-C of Gal and 2-C of GlcN.

4. Conclusions and perspectives

Important progress has been made in the treatment of arthropathies (mainly in osteoarthritis and rheumatoid arthritis) thanks to the development of controlled drug delivery systems and nano/microcarriers. Recently, a few liposome-based formulations have been approved for the treatment of joints diseases, although their IA residence time can be further improved. The development of biodegradable drug delivery systems with a prolonged drug release and an adequate IA retention is nowadays conceived as a promising approach to improve joints therapies. Besides, the limited ability of the articular cartilage for self-healing and the loss of synovial fluid functions requires a versatile carrier, which, apart from a controlled drug release, can act as a viscosupplement and an *in situ* cell scaffold for cartilage tissue regeneration. At the same time, the discovery of novel immunotherapeutic targets is triggering intensive efforts towards the development of highly specific small molecules-antagonists for inflammatory diseases therapies. Combination of the innovative approaches in both fields might lead to the development of advanced nanotechnological platforms for the treatment of joints pathologies headed by rheumatoid arthritis.

REFERENCES

1. Edwards, S. H. R., Cake, M. a, Spoelstra, G. & Read, R. a. Biodistribution and clearance of intra-articular liposomes in a large animal model using a radiographic marker. *J. Liposome Res.* **17,** 249–261 (2007).

2. Evans, C. H., Kraus, V. B. & Setton., L. A. Progress in intra-articular therapy. *Nat. Rev. Rheumatol.* **10,** 11–22 (2015).

3. Gerwin, N., Hops, C. & Lucke, A. Intraarticular drug delivery in osteoarthritis. *Adv. Drug Deliv. Rev.* **58,** 226–242 (2006).

4. Bajpayee, A. G. & Grodzinsky, A. J. Cartilage-targeting drug delivery: can electrostatic interactions help? *Nat. Rev. Rheumatol.* **13,** 183–193 (2017).

5. Fernández-Carballido, A., Herrero-Vanrell, R., Molina-Martínez, I. T. & Pastoriza, P. Biodegradable ibuprofen-loaded PLGA microspheres for intraarticular administration: Effect of Labrafil addition on release in vitro. *Int. J. Pharm.* **279,** 33–41 (2004).

6. Wernecke, C., Braun, H. J. & Dragoo, J. L. The Effect of Intra-articular Corticosteroids on Articular Cartilage: A Systematic Review. *Orthop. J. Sport. Med.* **3,** 1–7 (2015).

7. Brown, P. M., Pratt, A. G. & Isaacs, J. D. Mechanism of action of methotrexate in rheumatoid arthritis, and the search for biomarkers. *Nat. Rev. Rheumatol.* **12,** 731–742 (2016).

8. Takeuchi, T. & Kameda, H. The Japanese experience with biologic therapies for rheumatoid arthritis. *Nat. Rev. Rheumatol.* **6,** 644–652 (2010).

9. Soini, E. J., Leussu, M. & Hallinen, T. Administration costs of intravenous biologic drugs for rheumatoid arthritis. *Springerplus* **2,** 531 (2013).

10. Maroon, J. C., Bost, J. W. & Maroon, A. Natural anti-inflammatory agents for pain relief. *Surg. Neurol. Int.* **1,** 80 (2010).

11. Cecerale, S. in *Olive oil - Constituents, Health Properties and Bioconversions* (INTECH, 2011).

12. Kapoor, B., Singh, S. K., Gulati, M., Gupta, R. & Vaidya, Y. Application of liposomes in treatment of rheumatoid arthritis: Quo vadis. *Sci. World J.* **2014,** (2014).

13. Cheung, P. & March, L. Y. N. Treatment of established rheumatoid arthritis. *Med. Today* **11,** 18–34 (2010).

14. Mitragotri, S. & Yoo, J. W. Designing micro- and nano-particles for treating rheumatoid arthritis. *Arch. Pharm. Res.* **34,** 1887–1897 (2011).

15. Van Den Hoven, J. M. *et al.* Liposomal drug formulations in the treatment of rheumatoid arthritis. *Mol. Pharm.* **8,** 1002–1015 (2011).

16. Kang, M. L. & Im, G.-I. Drug delivery systems for intra-articular treatment of osteoarthritis. *Expert Opin. Drug Deliv.* **11,** 269–82 (2014).

17. Van den Hoven, J. M. *et al.* Liposomal drug formulations in the treatment of rheumatoid arthritis. *Mol Pharm* **8,** 1002–1015 (2011).

18. Butoescu, N., Jordan, O. & Doelker, E. Intra-articular drug delivery systems for the treatment of rheumatic diseases: A review of the factors influencing their performance. *Eur. J. Pharm. Biopharm.* **73,** 205–218 (2009).

19. Quan, L.-D., Thiele, G. M., Tian, J. & Wang, D. The Development of Novel Therapies for Rheumatoid Arthritis. *Expert Opin. Ther. Pat.* **18,** 723–738 (2008).

20. Albert, C., Brocq, O., Gerard, D., Roux, C. & Euller-Ziegler, L. Septic knee arthritis after intra-articular hyaluronate injection: Two case reports. *Jt. Bone Spine* **73,** 205–207 (2006).

21. Charalambous, C. P., Tryfonidis, M., Sadiq, S., Hirst, P. & Paul, a. Septic arthritis following intra-articular steroid injection of the knee - A survey of current practice regarding antiseptic technique used during intra-articular steroid injection of the knee. *Clin. Rheumatol.* **22,** 386–390 (2003).

22. Chen, Y. Intra-Articular Drug Delivery Systems for Arthritis Treatment. *Rheumatol. Curr. Res.* **02,** (2012).

23. Burt, H. M., Tsallas, A., Gilchrist, S. & Liang, L. S. Intra-articular drug delivery systems: Overcoming the shortcomings of joint disease therapy. *Expert Opin. Drug Deliv.* **6,** 17–26 (2009).

24. Iannitti, T., Lodi, D. & Palmieri, B. Intra-articular injections for the treatment of osteoarthritis: focus on the clinical use of several regimens. *Osteoarthritis-Diagnosis, Treat. …* **11,** 13–27 (2012).

25. Lipowitz, A. J. in *Textbook of Small Animal Orthopaedics* (1985).

26. Dahl, L. B., Dahl, I. M., Engström-Laurent, a & Granath, K. Concentration and molecular weight of sodium hyaluronate in synovial fluid from patients with rheumatoid arthritis and other arthropathies. *Ann. Rheum. Dis.* **44,** 817–822 (1985).

27. Castor, B. C. W. Hyaluronic Acid in Human Synovial Effusions; A Sensitive Indicator of Altered Connective Tissue Cell Function During Inflammation. *Arthritis Rheum.* **9,** 783–794 (1966).

28. Emry, P. *Atlas of Rheumatoid Arthritis*. 35–66 (2015).

29. Ekundi-Valentim, E. *et al.* Differing effects of exogenous and endogenous hydrogen sulphide in carrageenan-induced knee joint synovitis in the rat. *Br. J. Pharmacol.* **159,** 1463–1474 (2010).

30. Masuko, K., Murata, M., Yudoh, K., Kato, T. & Nakamura, H. Anti-inflammatory effects of hyaluronan in arthritis therapy: Not just for viscosity. *Int. J. Gen. Med.* **2,** 77–81 (2009).

31. Ghosh, P. & Guidolin, D. Potential mechanism of action of intra-articular hyaluronan therapy in osteoarthritis: Are the effects molecular weight dependent? *Semin. Arthritis Rheum.* **32,** 10–37 (2002).

32. Delmage, J. M., Powars, D. R., Jaynes, P. K. & Allerton, S. E. The selective suppression of immunogenicity by hyaluronic acid. *Ann. Clin. Lab. Sci.* **16,** 303–310 (1986).

33. Horvath, S. M. & Hollander, J. L. Intra-articular temperature as a measure of joint reaction. *J. Clin. Invest.* **28,** 469–473 (1949).

34. Journeau, P. *et al.* Hip septic arthritis in children: Assessment of treatment using needle aspiration/irrigation. *Orthop. Traumatol. Surg. Res.* **97,** 308–313 (2011).

35. Baker, K. & Orourke, K. S. Joint Aspiration and Injection : A Look at the Basics. *Rheumatol. Netw.* **28,** 216–222 (2011).

36. Zuber, T. J. Knee joint aspiration and injection. *Am. Fam. Physician* **66,** 1497–1500+1503 (2002).

37. Niiyama, S., Happle, R. & Hoffmann, R. Use of Intra-Articular Hyaluronic Acid in the Management of Knee Osteoarthritis in Clinical Practice. *Arthritis Care Res. (Hoboken).* **11,** 475–476 (2017).

38. Yang, W.-W. & Pierstorff, E. Reservoir-Based Polymer Drug Delivery Systems. *J. Lab. Autom.* **17,** 50–58 (2012).

39. Strauss, E. J., Hart, J., Miller, M. D., Altman, R. D. & Rosen, J. E. Hyaluronic Acid Viscosupplementation and Osteoarthritis. *Am. J. Sports Med.* **37,** 1636–1644 (2009).

40. Snyder, T. N., Madhavan, K., Intrator, M., Dregalla, R. C. & Park, D. A fibrin/hyaluronic acid hydrogel for the delivery of mesenchymal stem cells and potential for articular cartilage repair. *J. Biol. Eng.* **8,** 10 (2014).

41. Eymard F, Maillet B, Lellouche H, Mellac-Ducamp S, Brocq O, Loeuille D, Damien Loeuille D, Chevalier X & Conrozier T. Predictors of response to viscosupplementation in patients with hip osteoarthritis: results of a prospective, observational, multicentre, open-label, pilot study. *BMC Musculoskelet. Disord.* **18,** 1–8 (2017).

42. Blecher, A. M. Viscosupplementation: The Magic of Hyaluronic Acid Osteoarthritis of the knee. in *Southern California Orthopedic Institute* (2015).

43. Intra-articular MONOVISC^{TM}. Knee guru. 17–19 (2015).

44. Jamieson, E., Welch, E., Burke, R., Sakala, J. & Hrdy, M. *Cross-Linked Hyaluronate Monograph (Gel-One®)*. 1–10 (2013).

45. Goldberg, V. M. & Goldberg, L. Intra-articular hyaluronans: the treatment of knee pain in osteoarthritis. *J. Pain Res.* **3,** 51–56 (2010).

46. Gobbo, S. & Petrella, R. J. Hyaluronic acid binary mixtures and therapeutic use thereof. **1,** 1–20 (2009).

47. Bellamy, N. *et al.* Viscosupplementation for the treatment of osteoarthritis of the knee. *The Cochrane database of systematic reviews* **2,** CD005321 (2006).

48. Migliore, a., Giovannangeli, F., Granata, M. & Laganà, B. Hylan G-F 20: Review of its safety and efficacy in the management of joint pain in osteoarthritis. *Clin. Med. Insights Arthritis Musculoskelet. Disord.* **3,** 55–68 (2010).

49. Edsman, K. *et al.* Intra-articular Duration of DurolaneTM after Single Injection into the Rabbit Knee. *Cartilage* **2,** 384–388 (2011).

50. Anika Therapeutics. *Intra-articular Monovisc^{TM}, Sumary of safety and effectiveness data*. 1–36 (2014).

51. Bashaireh, K., Naser, Z., Hawadya, K. Al, Sorour, S. & Al-Khateeb, R. N. Efficacy and safety of cross-linked hyaluronic acid single injection on osteoarthritis of the knee: A post-marketing phase IV study. *Drug Des. Devel. Ther.* **9,** 2063–2072 (2015).

52. Smith, M. M., Russell, A. K., Schiavinato, A. & Little, C. B. Hymovis^{TM}, a hexadecylamide hyaluronan derivative (hyadd®4-g), inhibits gene expression changes induced by interleukin-1b in chondrocytes and synovial fibroblasts derived from osteoarthritis patients. *Osteoarthr. Cartil.* **19,** S234 (2011).

53. Fidia instruction to use. Hymovis ® High Molecular Weight Viscoelastic Hyaluronan. 3–4 (2016).

54. Benazzo, F. *et al.* A multi-centre, open label, long-term follow-up study to evaluate the benefits of a new viscoelastic hydrogel (Hymovis®) in the treatment of knee osteoarthritis. *Eur. Rev. Med. Pharmacol. Sci.* **20,** 959–68 (2016).

55. Wieland, H. a, Michaelis, M., Kirschbaum, B. J. & Rudolphi, K. a. Osteoarthritis - an untreatable disease? *Nat. Rev. Drug Discov.* **4,** 331–344 (2005).

56. Brown, T., Laurent, U. & Fraser. Turnover of hyaluronan in synovial joints: elimination of labelled hyaluronan from the knee joint of the rabbit. *Exp. Physiol.* **76,** 125–134 (1991).

57. Dagenais, S. Intra-articular hyaluronic acid (viscosupplementation) for hip osteoarthritis. *Issues Emerg. Health Technol.* 1–4 (2007).

58. *Monovisc Product Overview - Information Applies to Outside the US*. (2015).

59. Finelli, I., Chiessi, E., Galesso, D., Renier, D. & Paradossi, G. Gel-like structure of a hexadecyl derivative of hyaluronic acid for the treatment of osteoarthritis. *Macromol. Biosci.* **9,** 646–653 (2009).

60. Fidia Farmaceutici. *instructions for use Hymovis*. 1–15 (2016).

61. Saito, S., Momohara, S., Taniguchi, A. & Yamanaka, H. The intra-articular efficacy of hyaluronate injections in the treatment of rheumatoid arthritis. *Mod. Rheumatol.* **19,** 643–651 (2009).

62. Huang, T.-L. *et al.* Intra-articular injections of sodium hyaluronate (Hyalgan®) in osteoarthritis of the knee. a randomized, controlled, double-blind, multicenter trial in the asian population. *BMC Musculoskelet. Disord.* **12,** 221 (2011).

63. Miyamoto, K., Yasuda, Y. & Keiji Yoshioka. Hyaluronic acid derivative and drug containing the same. **2,** (2011).

64. Altman, R. D., Rosen, J. E., Bloch, D., Hatoum, H. T. & Korner, P. A Double-Blind, Randomized, Saline-Controlled Study of the Efficacy and Safety of EUFLEXXA for Treatment of Painful Osteoarthritis of the Knee, With an Open-Label Safety Extension (The FLEXX Trial). *Semin. Arthritis Rheum.* **39,** 1–9 (2009).

65. Anika, Therapeutics & Inc. FDA report. (2005).

66. Neustadt, D., Caldwell, J., Bell, M., Wade, J. & Gimbel, J. Clinical effects of intraarticular injection of high molecular weight hyaluronan (Orthovisc) in osteoarthritis of the knee: a randomized, controlled, multicenter trial. *J. Rheumatol.* **32,** 1928–1936 (2005).

67. Petrella, R. J., Cogliano, A. & Decaria, J. Combining two hyaluronic acids in osteoarthritis of the knee: A randomized, double-blind, placebo-controlled trial. *Clin. Rheumatol.* **27,** 975–981 (2008).

68. MDT Int'l s.a. RenehaVis instruction for use. (2011).

69. LSP Bio Ltd. RenehaVis broshure. (2013).

70. Petrella, R. J., Decaria, J. & Petrella, M. J. Long term efficacy and safety of a combined low and high molecular weight hyaluronic acid in the treatment of osteoarthritis of the knee. *Rheumatol. Reports* **3,** 16–21 (2011).

71. Chevalier, X. *et al.* Single, intra-articular treatment with 6 ml hylan G-F 20 in patients with symptomatic primary osteoarthritis of the knee: a randomised, multicentre, double-blind, placebo controlled trial. *Ann. Rheum. Dis.* **69,** 113–119 (2010).

72. Seikagaku Corporation & P80020/A014. Gel-One®. (2009).

73. Zimmer Biomet. *Gel-One Cross-Linked Hyaluronate*. (2017).

74. DUROLANE® & SingleInjection. *DUROLANE ® is stabilised and different from*. (2001).

75. Bioventus LLC. DUROLANE® Instructions for Use. 86 (2012).

76. Crespine® Gel Instruction for use. (2016).

77. Larsen, N. E. & Balazs, E. a. Drug delivery systems using hyaluronan and its derivatives. *Adv. Drug Deliv. Rev.* **7,** 279–293 (1991).

78. Spiller, K. L., Maher, S. a & Lowman, A. M. Hydrogels for the repair of articular cartilage defects. *Tissue Eng. Part B. Rev.* **17,** 281–99 (2011).

79. Lynn, K., Brooks, R., Bonfield, W. & Rushton, N. Repair of defects in articular joints. Prospects for material-based solutions in tissue engineering. *J. Bone Joint Surg. Br.* **86,** 1093–1099 (2004).

80. Liu, M. *et al.* Injectable hydrogels for cartilage and bone tissue engineering. *Bone Res.* **5,** 17014 (2017).

81. Vilela C, Correia C, Oliveira J M, Sousa R A, Espregueira-Mendes J, Reis R L. Cartilage repair using hydrogels: a critical review of in vivo experimental designs. *ACS Biomater. Sci. Eng.* 150813111234008 (2015).

82. Funayama, A. *et al.* Repair of full-thickness articular cartilage defects using injectable type II collagen gel embedded with cultured chondrocytes in a rabbit model. *J. Orthop. Sci.* **13,** 225–232 (2008).

83. Heiligenstein, S., Cucchiarini, M., Laschke, MW., Bohle, R.M., Kohn, D., Menger, MD., Madry, H. In vitro and in vivo characterization of nonbiomedical-and biomedical-grade alginates for articular chondrocyte transplantation. *Tissue Eng. Part C Methods* **17,** 829–842 (2011).

84. Dare, E., Griffith, M., Poitras, P., Wang, T., Dervin, G., F., Giulivi, A., Hincke, M. Fibrin sealants from fresh or fresh/frozen plasma as scaffolds for in vitro articular cartilage regeneration. *Tissue Eng. Part A* **15,** 2285–2297 (2009).

85. Silverman, R., Passaretti, D., Huang, W., Radolph, M. & Yaremchuk., M. J. Injectable tissue-engineered cartilage using a fibrin glue polymer. *Plast. Reconstr. Surg.* (1999).

86. Kayakabe, M., Tsutsumi, S., Watanabe, H., Kato, Y. & Takagishi, K. Transplantation of autologous rabbit BM-derived mesenchymal stromal cells embedded in hyaluronic acid gel sponge into osteochondral defects of the knee. *Cytotherapy* **8,** 343–353 (2006).

87. Lee, J. C. *et al.* Synovial membrane-derived mesenchymal stem cells supported by platelet-rich plasma can repair osteochondral defects in a rabbit model. *Arthrosc. - J. Arthrosc. Relat. Surg.* **29,** 1034–1046 (2013).

88. Oliveira, J. T. *et al.* Injectable gellan gum hydrogels with autologous cells for the treatment of rabbit articular cartilage defects. *J. Orthop. Res.* **28,** 1193–1199 (2010).

89. Douglas, T. E. L. *et al.* Injectable self-gelling composites for bone tissue engineering based on gellan gum hydrogel enriched with different bioglasses. *Biomed. Mater.* **9,** 045014 (2014).

90. Chenite, a *et al.* Novel injectable neutral solutions of chitosan form biodegradable gels in situ. *Biomaterials* **21,** 2155–2161 (2000).

91. Liu, Y., Shu, X. Z. & Prestwich, G. D. Osteochondral Defect Repair with Autologous Bone. *Tissue Eng.* **12,** (2006).

92. Holland, T. a. *et al.* Osteochondral repair in the rabbit model utilizing bilayered, degradable oligo(poly(ethylene glycol) fumarate) hydrogel scaffolds. *J. Biomed. Mater. Res. - Part A* **75,** 156–167 (2005).

93. Lim, C. T. *et al.* Repair of Osteochondral Defects with Rehydrated Freeze-Dried Oligo[Poly(Ethylene Glycol) Fumarate] Hydrogels Seeded with Bone Marrow Mesenchymal Stem Cells in a Porcine Model. *Tissue Eng. Part A* **19,** 1852–1861 (2013).

94. Park, J. S. *et al.* Chondrogenesis of human mesenchymal stem cells encapsulated in a hydrogel construct: Neocartilage formation in animal models as both mice and rabbits. *J. Biomed. Mater. Res. - Part A* **92,** 988–996 (2010).

95. Yan, S. *et al.* Injectable in situ forming poly(L -glutamic acid) hydrogels for cartilage tissue engineering. *J. Mater. Chem. B* **4,** 947–961 (2016).

96. Vinatier, C. *et al.* A silanized hydroxypropyl methylcellulose hydrogel for the three-dimensional culture of chondrocytes. *Biomaterials* **26,** 6643–6651 (2005).

97. Nettles, D. *et al.* NIH Public Access. *Tissue Eng. Part A* **14,** 1133–1140 (2012).

98. Degoricija, L. *et al.* Hydrogels for osteochondral repair based on photocrosslinkable carbamate dendrimers. *Biomacromolecules* **9,** 2863–2872 (2008).

99. De France, K. J., Chan, K. J. W., Cranston, E. D. & Hoare, T. Enhanced Mechanical Properties in Cellulose Nanocrystal-Poly(oligoethylene glycol methacrylate) Injectable Nanocomposite Hydrogels through Control of Physical and Chemical Cross-Linking. *Biomacromolecules* **17,** 649–660 (2016).

100. Zheng, Y. *et al.* Performance of novel bioactive hybrid hydrogels *in vitro* and *in vivo* used for artificial cartilage. *Biomed. Mater.* **4,** 015015 (2009).

101. Ibusuki, S., Fujii, Y., Iwamoto, Y. & Matsuda, T. Tissue-Engineered Cartilage Using an Injectable and *in Situ* Gelable Thermoresponsive Gelatin: Fabrication and *in Vitro* Performance. *Tissue Eng.* **9,** 371–384 (2003).

102. Ohya, S., Nakayama, Y. & Matsuda, T. In vivo evaluation of poly(N-isopropylacrylamide) (PNIPAM)-grafted gelatin as an in situ-formable scaffold. *J. Artif. Organs* **7,** 181–186 (2004).

103. Han, Y., Zeng, Q., Li, H. & Chang, J. The calcium silicate/alginate composite: Preparation and evaluation of its behavior as bioactive injectable hydrogels. *Acta Biomater.* **9,** 9107–9117 (2013).

104. Yan, S. *et al.* Injectable in situ self-cross-linking hydrogels based on poly(l -glutamic acid) and alginate for cartilage tissue engineering. *Biomacromolecules* **15,** 4495–4508 (2014).

105. Yu, F. *et al.* An injectable hyaluronic acid/PEG hydrogel for cartilage tissue engineering formed by integrating enzymatic crosslinking and Diels-Alder "click chemistry. *Optoelectron. Adv. Mater. Rapid Commun.* **4,** 1166–1169 (2010).

106. Fukuda, A. *et al.* Enhanced repair of large osteochondral defects using a combination of artificial cartilage and basic fibroblast growth factor. *Biomaterials* **26,** 4301–4308 (2005).

107. Park, H., Temenoff, J. S., Tabata, Y., Caplan, A. I. & Mikos, A. G. Injectable biodegradable hydrogel composites for rabbit marrow mesenchymal stem cell and growth factor delivery for cartilage tissue engineering. *Biomaterials* **28,** 3217–3227 (2007).

108. Yang, J., Shrike Zhang, Y., Yue, K. & Khademhosseini, A. Cell-Laden Hydrogels for Osteochondral and Cartilage Tissue Engineering. *Acta Biomater.* (2017).

109. Shive, M. S. *et al.* BST-CarGel: In Situ ChondroInduction for Cartilage Repair. *Oper. Tech. Orthop.* **16,** 271–278 (2006).

110. Piramal Healthcare Canada Ltd. BST-CarGel Trial Comparing BST-CarGel and Microfracture in Repair of Articular Cartilage Lesions in the Knee NCT00314236. 1–6 (2016).

111. Piramal Healthcare Canada Ltd. *BST-CarGel Randomized Evaluation of BST-CarGel Versus Microfracture Alone On Recovery From Distal Femoral Cartilage Lesions (RECORD) NCT02981355*. 1–7 (2016).

112. Janssen, M., Mihov, G., Welting, T., Thies, J. & Emans, P. Drugs and polymers for delivery systems in OA joints: Clinical needs and opportunities. *Polymers (Basel).* **6,** 799–819 (2014).

113. Wang, D. *et al.* Novel dexamethasone-HPMA copolymer conjugate and its potential application in treatment of rheumatoid arthritis. *Arthritis Res. Ther.* **9,** R2 (2007).

114. Mero, A. & Campisi, M. Hyaluronic acid bioconjugates for the delivery of bioactive molecules. *Polymers (Basel).* **6,** 346–369 (2014).

115. Homma, A. *et al.* Synthesis and optimization of hyaluronic acid-methotrexate conjugates to maximize benefit in the treatment of osteoarthritis. *Bioorganic Med. Chem.* **18,** 1062–1075 (2010).

116. Tamura, T. *et al.* Novel hyaluronic acid–methotrexate conjugate suppresses joint inflammation in the rat knee: efficacy and safety evaluation in two rat arthritis models. *Arthritis Res. Ther.* **18,** 79 (2016).

117. Chen, B., Miller, R. J. & Dhal, P. K. Hyaluronic acid-based drug conjugates: State-of-the-art and perspectives. *J. Biomed. Nanotechnol.* **10,** 4–16 (2014).

118. Rothenfluh, D. A., Bermudez, H., Neil, C. P. O. & Hubbell, J. A. Biofunctional polymer nanoparticles for intra-articular targeting and retention in cartilage. **7,** 1–7 (2008).

119. Horisawa, E. *et al.* Size-Dependency of DL-Lactide/\rGlycolide Copolymer Particulates for\rIntra-Articular Delivery System on\rPhagocytosis in Rat Synovium. *Pharm. Res.* **19,** 132–139 (2002).

120. Laura Brown, Cui, H. & Wu, Z. Method of treatment for osteoarthritis by local intra-articular injection of microparticles. (2007).

121. Larsen, C. *et al.* Intra-Articular Depot Formulation Principles : Role in the Management of Postoperative Pain and Arthritic Disorders. *J. Pharm. Sci.* **97,** (2008).

122. Haywood, L. & Walsh, D. a. Vasculature of the normal and arthritic synovial joint. *Histol. Histopathol.* **16,** 277–284 (2001).

123. Barrera, P. *et al.* Synovial macrophage depletion with clodronate-containing liposomes in rheumatoid arthritis. *Arthritis Rheum.* **43,** 1951–1959 (2000).

124. Morgen, M. *et al.* Nanoparticles for improved local retention after intra-articular injection into the knee joint. *Pharm. Res.* **30,** 257–268 (2013).

125. Hellmich, D. *et al.* Acute treatment of facet syndrome by CT-guided injection of dexamethasone-21-palmitate alone and in combination with mepivacaine. *Clin. Drug Investig.* **24,** 559–569 (2004).

126. Bellamy, N. *et al.* Intraarticular corticosteroid for treatment of osteoarthritis of the knee. *Cochrane Database Syst Rev* CD005328 (2006).

127. Annual Report RecordatiPharma. *Annual Report*. (2016).

128. Enceladus Pharmaceuticals B.V. WO2013066179A1 Liposomal corticosteroids for treatment of inflammatory disorders in humans. 1–13 (2013).

129. Aalbers, C. J. *et al.* Empty Capsids and Macrophage Inhibition / Depletion Increase rAAV Transgene Expression in Joints of Both Healthy and Arthritic Mice. **00,** 1–11 (2016).

130. Valleala, H., Laitinen, K., Pylkkänen, L., Konttinen, Y. T. & Friman, C. Clinical and biochemical response to single infusion of clodronate in active rheumatoid arthritis--a double blind placebo controlled study. *Inflamm. Res.* **50,** 598–601 (2001).

131. Conaghan, P. G. *et al. In Pivotal Clinical Trials , FX006 Produces Sustained and Profound Analgesic Benefits in People With Osteoarthritis of the Knee*. (2017).

132. Flexion Therapeutics Inc. Clinical Trials. Study of FX006 for the Treatment of Pain in Patients With Osteoarthritis of the Knee NCT02357459, 4–7 (2017).

133. Bodick, N. *et al.* FX006 prolongs the residency of triamcinolone acetonide in the synovial tissues of patients with knee osteoarthritis. *Osteoarthr. Cartil.* **21,** S144–S145 (2013).

134. Ho, M. J., Kim, S. R., Choi, Y. W. & Kang, M. J. A Novel Stable Crystalline Triamcinolone Acetonide-loaded PLGA Microsphere for Prolonged Release After Intra-Articular Injection. *Bull. Korean Chem. Soc.* **37,** 1496–1500 (2016).

135. Flexion Therapeutics Inc. ZILRETTA Prescribing Information. (2017).

136. Gierut, A., Perlman, H. & Pope, R. M. Innate Immunity and Rheumatoid Arthritis. *Rheum Dis Clin North Am.* **36,** 1–24 (2011).

137. Huang, G. & Zhang, Z. Micro- and nano-carrier mediated intra-articular drug delivery systems for the treatment of osteoarthritis. *J. Nanotechnol.* **2012,** (2012).

138. Vanniasinghe, A. S., Bender, V. & Manolios, N. The Potential of Liposomal Drug Delivery for the Treatment of Inflammatory Arthritis. *Semin. Arthritis Rheum.* **39,** 182–196 (2009).

139. Yang, M., Feng, X., Ding, J., Chang, F. & Chen, X. Nanotherapeutics relieve rheumatoid arthritis. *J. Control. Release* **252,** 108–124 (2017).

140. Dyondi, D., Lakhawat, R. & Banerjee, R. Biodegradable Nanoparticles for Intra-articular Therapy. (2009).

141. Danhier, F. *et al.* PLGA-based nanoparticles: An overview of biomedical applications. *J. Control. Release* **161,** 505–522 (2012).

142. Bartneck, M. *et al.* Liposomal encapsulation of dexamethasone modulates cytotoxicity, inflammatory cytokine response, and migratory properties of primary human macrophages. *Nanomedicine Nanotechnology, Biol. Med.* **10,** 1209–1220 (2014).

143. Bonanomi, M. H., Velvart, M., Stimpel, M., Fehr, K. & Weder, H. G. Studies of pharmacokinetics and therapeutic effects of glucocorticoids entrapped in liposomes

after intraarticular application in healthy rabbits and in rabbits with antigen-induced arthritis. *Reumatol. Int. Clin. Exp. Investig.* 203–212 (1987).

144. Hofkens, W., Schelbergen, R., Storm, G., Berg, W. B. van den & Lent, P. L. van. Liposomal targeting of prednisolone phosphate to synovial lining macrophages during experimental arthritis inhibits M1 activation but does not favor M2 differentiation. *PLoS One* e54016 (2013).

145. Turker, S. *et al.* Gamma-irradiated liposome/noisome and lipogelosome/niogelosome formulations for the treatment of rheumatoid arthritis. *Interv. Med. Appl. Sci.* **5,** 60–69 (2013).

146. Srinath, P., Vyas, S. P. & Diwan, P. V. Preparation and pharmacodynamic evaluation of liposomes of indomethacin. *Drug Dev. Ind. Pharm.* **26,** 313–321 (2000).

147. Foong, W. C. & Green, K. L. Retention and Distribution of Liposome-entrapped [3H]Methotrexate Injected into Normal or Arthritic Rabbit Joints. *J. Pharm. Pharmacol.* **40,** 464–468 (1988).

148. Williams, a S., Camilleri, J. P., Goodfellow, R. M. & Williams, B. D. A single intra-articular injection of liposomally conjugated methotrexate suppresses joint inflammation in rat antigen-induced arthritis. *Br. J. Rheumatol.* **35,** 719–24 (1996).

149. Čeponis, A. *et al.* Effects of low-dose, noncytotoxic, intraarticular liposomal clodronate on development of erosions and proteoglycan loss in established antigen-induced arthritis in rabbits. *Arthritis Rheum.* **44,** 1908–1916 (2001).

150. Phillips, N. C., Thomas, D. P. P., Knight, C. G. & Dingle, J. T. Therapeutic activity in experimental arthritis. 553–557 (1979).

151. Horisawa, E. *et al.* Prolonged anti-inflammatory action of DL-lactide/glycolide copolymer nanospheres containing betamethasone sodium phosphate for an intra-articular delivery system in antigen-induced arthritic rabbit. *Pharm. Res.* **19,** 403–410 (2002).

152. Higaki, M., Ishihara, T., Izumo, N., Takatsu, M. & Mizushima, Y. Treatment of experimental arthritis with poly(D, L-lactic/glycolic acid) nanoparticles encapsulating betamethasone sodium phosphate. *Ann. Rheum. Dis.* **64,** 1132–1136 (2005).

153. Butoescu, N., Seemayer, C. a., Foti, M., Jordan, O. & Doelker, E. Dexamethasone-containing PLGA superparamagnetic microparticles as carriers for the local treatment of arthritis. *Biomaterials* **30,** 1772–1780 (2009).

154. Gómez-Gaete, C., Fattal, E., Silva, L., Besnard, M. & Tsapis, N. Dexamethasone acetate encapsulation into Trojan particles. *J. Control. Release* **128,** 41–49 (2008).

155. Liang, L. S., Wong, W. & Burt, H. M. Pharmacokinetic study of methotrexate following intra-articular injection of methotrexate loaded poly(L-lactic acid) microspheres in rabbits. *J. Pharm. Sci.* **94,** 1204–1215 (2005).

156. Liggins, R. T. *et al.* Intra-articular treatment of arthritis with microsphere formulations of paclitaxel: biocompatibility and efficacy determinations in rabbits. *Inflamm. Res.* **53,** 363–372 (2004).

157. Kawadkar, J. & Chauhan, M. K. Intra-articular delivery of genipin cross-linked chitosan microspheres of flurbiprofen: Preparation, characterization, in vitro and in vivo studies. *Eur. J. Pharm. Biopharm.* **81,** 563–572 (2012).

158. Zhang, J. X. *et al.* Local delivery of indomethacin to arthritis-bearing rats through polymeric micelles based on amphiphilic polyphosphazenes. *Pharm. Res.* **24,** 1944–1953 (2007).

159. Kang, M. L., Kim, J. E. & Im, G. Il. Thermoresponsive nanospheres with independent dual drug release profiles for the treatment of osteoarthritis. *Acta Biomater.* **39,** 65–78 (2016).

160. Kang, M. L., Kim, J. E., Ko, J.-Y. & Im., G.-I. Intra-articular delivery of kartogenin-conjugated chitosan nano/microparticles for cartilage retention. *Ann. Rheum. Dis.* **74,** 366.3–367 (2015).

161. Kim, S. R. *et al.* Cationic PLGA/eudragit RL nanoparticles for increasing retention time in synovial cavity after intra-articular injection in knee joint. *Int. J. Nanomedicine* **10,** 5263–5271 (2015).

162. Butoescu, N. *et al.* Dexamethasone-containing biodegradable superparamagnetic microparticles for intra-articular administration: Physicochemical and magnetic properties, in vitro and in vivo drug release. *Eur. J. Pharm. Biopharm.* **72,** 529–538 (2009).

163. Türker, S. *et al.* Scintigraphic imaging of radiolabelled drug delivery systems in rabbits with arthritis. *Int. J. Pharm.* **296,** 34–43 (2005).

164. Tuncay *et al.* In vitro and in vivo evuluation of diclofenac sodium loaded albumin microspheres. *J. Microencapsul.* **16,** 625–637 (1999).

165. Arora, R., Kuhad, a., Kaur, I. P. & Chopra, K. Curcumin loaded solid lipid nanoparticles ameliorate adjuvant-induced arthritis in rats. *Eur. J. Pain* n/a–n/a (2014). doi:10.1002/ejp.620

166. Ye, J., Wang, Q., Zhou, X. & Zhang, N. Injectable actarit-loaded solid lipid nanoparticles as passive targeting therapeutic agents for rheumatoid arthritis. *Int. J. Pharm.* **352,** 273–279 (2008).

167. Cai, L. *et al.* A slow release formulation of insulin as a treatment for osteoarthritis. *Osteoarthr. Cartil.* **10,** 692–706 (2002).

168. Schmitt, F. *et al.* Chitosan-based nanogels for selective delivery of photosensitizers to macrophages and improved retention in and therapy of articular joints. *J. Control. Release* **144,** 242–250 (2010).

169. Park SH, Park SR, Chung SI, Pai KS, M. B. Tissue-engineered Cartilage Using Fibrin/Hyaluronan Composite Gel and Its In Vivo Implantation. **29,** 838–860 (2005).

170. Zhang, Y., Heher, P., Hilborn, J., Redl, H. & Ossipov, D. a. Hyaluronic acid-fibrin interpenetrating double network hydrogel prepared in situ by orthogonal disulfide cross-linking reaction for biomedical applications. *Acta Biomater.* **38,** 23–32 (2016).

171. Barbucci, R. *Hydrogels Biological Properties andApplications*. (2009).

172. Hillel, A. et al. in *Ch.3* 2007 (2007).

173. Zhang, Z. *et al.* Intra-articular injection of cross-linked hyaluronic acid-dexamethasone hydrogel attenuates osteoarthritis: An experimental study in a rat model of osteoarthritis. *Int. J. Mol. Sci.* **17,** (2016).

174. Petit, A. In situ forming hydrogels for intra-articular delivery of celecoxib : from polymer design to in vivo studies. (2014).

175. Webber, M. J., Matson, J. B., Tamboli, V. K. & Stupp, S. I. Controlled release of dexamethasone from peptide nanofiber gels to modulate inflammatory response. *Biomaterials* **33,** 6823–6832 (2012).

176. Song, J. *et al.* A phase I/IIa study on intra-articular injection of holmium-166-chitosan complex for the treatment of knee synovitis of rheumatoid arthritis. *Eur. J. Nucl. Med.* **28,** 489–497 (2001).

177. Cho, Y. J. *et al.* Radioisotope synoviorthesis with Holmium-166-chitosan complex in haemophilic arthropathy. *Haemophilia* **16,** 640–646 (2010).

178. Bolong Miao, Cunxian Song, G. M. Injectable Thermosensitive Hydrogels for Intra-Articular Delivery of Methotrexate. *J. Appl. Polym. Sci.* **21,** 449–456 (2011).

179. Appel, E. a *et al.* Self-assembled hydrogels utilizing polymer–nanoparticle interactions. *Nat. Commun.* **6,** 1–9 (2015).

180. Lei, Y., Rahim, M., Ng, Q. & Segura, T. Hyaluronic acid and fibrin hydrogels with concentrated DNA/PEI polyplexes for local gene delivery. *J. Control. Release* **153,** 255–261 (2011).

181. Sandker, M. J. *et al.* In situ forming acyl-capped PCLA-PEG-PCLA triblock copolymer based hydrogels. *Biomaterials* **34,** 8002–8011 (2013).

182. Bédouet, L. *et al.* Intra-articular fate of degradable poly(ethyleneglycol)-hydrogel microspheres as carriers for sustained drug delivery. *Int. J. Pharm.* **456,** 536–544 (2013).

183. Shan-Bin, G., Yue, T. & Ling-Yan, J. Long-term sustained-released in situ gels of a water-insoluble drug amphotericin B for mycotic arthritis intra-articular

administration: preparation, in vitro and in vivo . *Drug Dev. Ind. Pharm.* **9045,** 1–10 (2014).

184. Wu, Q. *et al.* Thermosensitive hydrogel containing dexamethasone micelles for preventing postsurgical adhesion in a repeated-injury model. *Sci. Rep.* **5,** 13553 (2015).

185. Liechty, W. B., Kryscio, D. R., Slaughter, B. V. & Peppas, N. a. Polymers for Drug Delivery Systems. *Annu. Rev. Chem. Biomol. Eng.* **1,** 149–173 (2010).

186. Suchaoin, W. *et al.* Novel bioadhesive polymers as intra-articular agents: Chondroitin sulfate-cysteine conjugates. *Eur. J. Pharm. Biopharm.* **101,** 25–32 (2016).

187. Bédouet, L. *et al.* Synthesis of hydrophilic intra-articular microspheres conjugated to ibuprofen and evaluation of anti-inflammatory activity on articular explants. *Int. J. Pharm.* **459,** 51–61 (2014).

188. Cooper, D. N. W. & Barondes, S. H. God must love galectins; he made so many of them. *Glycobiology* **9,** 979–984 (1999).

189. Klyosov, A. a., Witczak, Z. J. & Platt, D. *Galectins*. 1–288 (2008).

190. Hsieh, T. J. *et al.* Structural basis underlying the binding preference of human galectins-1, -3 and -7 for Galβ1-3/4GlcNAc. *PLoS One* **10,** 1–19 (2015).

191. Barondes, S. H. & Vincent Castronovo, Douglas N. W. Cooper, R. D. C. Galectins: A Family of Animal p-GalactosideBinding Lectins. *Cell Biochem. Funct.* **76,** 597–598 (1994).

192. Di Lella, S. *et al.* When galectins recognize glycans: From biochemistry to physiology and back again. *Biochemistry* **50,** 7842–7857 (2011).

193. Hughes, R. C. Galectins. *Encycl. Biol. Chem.* **2,** 171–174 (2004).

194. Yang, R. Y., Hsu, D. K., Yu, L., Ni, J. & Liu, F. T. Cell Cycle Regulation by Galectin-12, a New Member of the Galectin Superfamily. *J. Biol. Chem.* **276,** 20252–20260 (2001).

195. Ahmed, H. & Alsadek, D. M. M. Galectin-3 as a potential target to prevent cancer metastasis. *Clin. Med. Insights Oncol.* **9,** 113–121 (2015).

196. Haudek, K. C. *et al.* Dynamics of galectin-3 in the nucleus and cytoplasm. *Biochim. Biophys. Acta - Gen. Subj.* **1800,** 181–189 (2010).

197. Hsu, D. K., Yang, R., Saegusa, J. & Liu, F. Analysis of the Intracellular Role of Galectins in Cell Growth and Apoptosis. **1207,** 451–463 (2015).

198. Hsu, D. K. *et al.* Endogenous galectin-3 is localized in membrane lipid rafts and regulates migration of dendritic cells. *J. Invest. Dermatol.* **129,** 573–583 (2009).

199. Le Mercier, M., Fortin, S., Mathieu, V., Kiss, R. & Lefranc, F. Galectins and gliomas. *Brain Pathol.* **20,** 17–27 (2010).

200. Panjwani, N. Role of galectins in re-epithelialization of wounds. *Ann. Transl. Med.* **2,** 89 (2014).

201. Gaelle Gendronneau, Sukhvinder S. Sidhu, Delphine Delacour, Tien Dang, Chloe Calonne, Denis Houzelstein, Thierry Magnaldo, F. P. Galectin-7 in the Control of Epidermal Homeostasis after Injury. *Mol. Biol. Cell* **82,** 327–331 (2008).

202. Hokama, A., Mizoguchi, E. & Mizoguchi, A. Roles of galectins in inflammatory bowel disease. *World J. Gastroenterol.* **14,** 5133–5137 (2008).

203. Chen, H. Y., Weng, I. C., Hong, M. H. & Liu, F. T. Galectins as bacterial sensors in the host innate response. *Curr. Opin. Microbiol.* **17,** 75–81 (2014).

204. Rabinovich, G. A., van Kooyk, Y. & Cobb, B. A. Glycobiology of immune responses. *Ann. N. Y. Acad. Sci.* **1253,** 1–15 (2012).

205. Kaltner, H. *et al.* Galectins: their network and roles in immunity/tumor growth control. *Histochem. Cell Biol.* **147,** 239–256 (2017).

206. De Oliveira, F. L. *et al.* Galectin-3 in autoimmunity and autoimmune diseases. *Exp. Biol. Med.* (2015).

207. Thiemann, S. & Baum, L. G. Galectins and Immune Responses—Just How Do They Do Those Things They Do? *Annu. Rev. Immunol* **34,** 243–64 (2016).

208. Klyosov, A. a. Galectins as New Therapeutic Targets for Galactose-Containing Polysaccharides. *Bull. Georg. Natl. Acad. Sci.* **8,** 5–17 (2014).

209. Elola, M. T., Wolfenstein-Todel, C., Troncoso, M. F., Vasta, G. R. & Rabinovich, G. a. Galectins: Matricellular glycan-binding proteins linking cell adhesion, migration, and survival. *Cell. Mol. Life Sci.* **64,** 1679–1700 (2007).

210. Rabinovich, G. a. & Croci, D. O. Regulatory Circuits Mediated by Lectin-Glycan Interactions in Autoimmunity and Cancer. *Immunity* **36,** 322–335 (2012).

211. Vasta, G. R., Ahmed, H., Bianchet, M. a, Fernández-Robledo, J. a & Amzel, L. M. Diversity in recognition of glycans by F-type lectins and galectins: molecular, structural, and biophysical aspects. *Ann. N. Y. Acad. Sci.* **1253,** E14–26 (2012).

212. Hu, Y., Yéléhé-Okouma, M., Ea, H. K., Jouzeau, J. Y. & Reboul, P. Galectin-3: A key player in arthritis. *Jt. Bone Spine* **84,** 15–20 (2017).

213. Chen, H. Y., Liu, F.-T. & Yang, R.-Y. Roles of galectin-3 in immune responses. *Arch. Immunol. Ther. Exp. (Warsz).* **53,** 497–504 (2005).

214. Nio-Kobayashi, J., Takahashi-Iwanaga, H. & Iwanaga, T. Immunohistochemical Localization of Six Galectin Subtypes in the Mouse Digestive Tract. *J. Histochem. Cytochem.* **57,** 41–50 (2008).

215. Mackinnon, A. C. *et al.* Regulation of transforming growth factor-β1-driven lung fibrosis by galectin-3. *Am. J. Respir. Crit. Care Med.* **185,** 537–546 (2012).

216. Melorose, J., Perroy, R. & Careas, S. Dynamics of Galectin-3 in the Nucleus and Cytoplasm. *Statew. Agric. L. Use Baseline 2015* **1,** (2015).

217. Chen, S. C. & Kuo, P. L. The role of galectin-3 in the kidneys. *Int. J. Mol. Sci.* **17,** 1–10 (2016).

218. Le Mercier, M., Fortin, S., Mathieu, V., Kiss, R. & Lefranc, F. Galectins and gliomas. *Brain Pathol.* **20,** 17–27 (2010).

219. Cant, S. H. & Pitcher, J. a. G Protein-coupled Receptor Kinase 2–mediated Phosphorylation of Ezrin Is Required for G Protein- coupled Receptor–dependent Reorganization of the Actin Cytoskeleton. *Mol. Biol. Cell* **16,** 1–13 (2005).

220. Janelle-Montcalm, A. *et al.* Extracellular localization of galectin-3 has a deleterious role in joint tissues. *Arthritis Res. Ther.* **9,** R20 (2007).

221. Guévremont, M. *et al.* Galectin-3 surface expression on human adult chondrocytes: a potential substrate for collagenase-3. *Ann. Rheum. Dis.* **63,** 636–643 (2004).

222. Aubin, J. E., Liu, F., Malaval, L. & Gupta, a. K. Osteoblast and chondroblast differentiation. *Bone* **17,** (1995).

223. Henderson, N. C. *et al.* Galectin-3 expression and secretion links macrophages to the promotion of renal fibrosis. *Am. J. Pathol.* **172,** 288–298 (2008).

224. Delacour, D. *et al.* Loss of galectin-3 impairs membrane polarisation of mouse enterocytes in vivo. *J. Cell Sci.* **121,** 458–65 (2008).

225. Delacour, D. *et al.* Apical sorting by galectin-3-dependent glycoprotein clustering. *Traffic* **8,** 379–388 (2007).

226. Yabuta, C., Yano, F., Fujii, A., Shearer, T. R. & Azuma, M. Galectin-3 enhances epithelial cell adhesion and wound healing in rat cornea. *Ophthalmic Res.* **51,** 96–103 (2014).

227. Baldenhofer, G. *et al.* Galectin-3 predicts short- and long-term outcome in patients undergoing transcatheter aortic valve implantation (TAVI). *Int. J. Cardiol.* **177,** 912–917 (2014).

228. Vasta, G. R. *et al.* Galectins as self/non-self recognition receptors in innate and adaptive immunity: An unresolved paradox. *Front. Immunol.* **3,** 1–14 (2012).

229. Patterson, R. J., Wang, W. & Wang, J. L. Understanding the biochemical activities of galectin-1 and galectin-3 in the nucleus. *Glycoconj. J.* **19,** 499–506 (2004).

230. Coppin, L. *et al.* Galectin-3 is a non-classic RNA binding protein that stabilizes the mucin MUC4 mRNA in the cytoplasm of cancer cells. *Sci. Rep.* **7,** 43927 (2017).

231. Ahmed, H. & AlSadek, D. M. M. Galectin-3 as a Potential Target to Prevent Cancer Metastasis. *Clin. Med. Insights. Oncol.* **9,** 113–121 (2015).

232. Schneider, D. *et al.* Trafficking of galectin-3 through endosomal organelles of polarized and non-polarized cells. *Eur. J. Cell Biol.* **89,** 788–798 (2010).

233. Gendronneau, G. *et al.* Galectin-7 in the control of epidermal homeostasis after injury. *Mol. Biol. Cell* **19,** 5541–5549 (2008).

234. Dumic, J., Dabelic, S. & Flögel, M. Galectin-3: An open-ended story. *Biochim. Biophys. Acta - Gen. Subj.* **1760,** 616–635 (2006).

235. Boscher, C. *et al.* Galectin-3 protein regulates mobility of N-cadherin and GM1 ganglioside at cell-cell junctions of mammary carcinoma cells. *J. Biol. Chem.* **287,** 32940–32952 (2012).

236. Liu, W. *et al.* Galectin-3 regulates intracellular trafficking of EGFR through Alix and promotes keratinocyte migration. *J. Invest. Dermatol.* **132,** 2828–2837 (2012).

237. Hsieh, T. *et al.* Dual thio-digalactoside-binding modes of human galectins as the structural basis for the design of potent and selective inhibitors. *Sci. Rep.* **6,** 29457 (2016).

238. Rabinovich, G. A. & Toscano, M. A. Turning 'sweet' on immunity: galectin-glycan interactions in immune tolerance and inflammation. *Nat. Rev. Immunol.* **9,** 338–352 (2009).

239. Chen, H.-Y., Weng, I.-C., Hong, M.-H. & Liu, F.-T. Galectins as bacterial sensors in the host innate response. *Curr. Opin. Microbiol.* **17,** 75–81 (2014).

240. De Oliveira, F. L. *et al.* Galectin-3 in autoimmunity and autoimmune diseases. *Exp. Biol. Med. (Maywood).* **240,** 1019–1028 (2015).

241. Lepur, A. Functional properties of Galectin-3. Beyond the sugar binding. *Lund University, University of Zagreb* (2012).

242. Than, N. G. *et al.* A primate subfamily of galectins expressed at the maternal-fetal interface that promote immune cell death. *Proc. Natl. Acad. Sci. U. S. A.* **106,** 9731–9736 (2009).

243. Joo, H. G. *et al.* Expression and function of galectin-3, a beta-galactoside-binding protein in activated T lymphocytes. *J. Leukoc. Biol.* **69,** 555–64 (2001).

244. Ohshima, S. *et al.* Galectin 3 and Its Binding Protein in Rheumatoid Arthritis. *Arthritis Rheum.* **48,** 2788–2795 (2003).

245. Kimura, T. *et al.* Dedicated SNAREs and specialized TRIM cargo receptors mediate secretory autophagy. 1–19 (2016).

246. Mantovani, A., Sozzani, S., Locati, M., Allavena, P. & Sica, A. Macrophage polarization: Tumor-associated macrophages as a paradigm for polarized M2 mononuclear phagocytes. *Trends Immunol.* **23,** 549–555 (2002).

247. Forsman, H. *et al.* Galectin 3 aggravates joint inflammation and destruction in antigen-induced arthritis. *Arthritis Rheum.* **63,** 445–454 (2011).

248. Palmer, M., Stanford, E. & Murray, M. M. The effect of synovial fluid enzymes on the biodegradability of collagen and fibrin clots. *Materials (Basel).* **4,** 1469–1482 (2011).

249. Ortega, N., Behonick, D. J., Colnot, C., Douglas N.W. Cooper & Werb, and Z. Galectin-3 Is a Downstream Regulator of Matrix Metalloproteinase-9 Function during Endochondral Bone Formation. *Mol. Biol. Cell* **16,** 1–13 (2005).

250. Lee, F. & Kurisawa, M. Formation and stability of interpenetrating polymer network hydrogels consisting of fibrin and hyaluronic acid for tissue engineering. *Acta Biomater.* **9,** 5143–5152 (2013).

251. Page-McCaw, A., Ewald, A. J. & Werb, Z. Matrix metalloproteinases and the regulation of tissue. *Nat Rev Mol Cell Biol.* **8,** 221–233 (2007).

252. Seetharaman, J. *et al.* X-ray crystal structure of the human galectin-3 carbohydrate recognition domain at 2.1-A resolution. *J. Biol. Chem.* **273,** 13047–13052 (1998).

253. Jones, J. L. *et al.* Galectin-3 is associated with prostasomes in human semen. 227–236 (2010).

254. Ippel, H. *et al.* Intra- and intermolecular interactions of human galectin-3: Assessment by full-assignment-based NMR. *Glycobiology* **26,** 888–903 (2016).

255. Berbís, M. Á. *et al.* Peptides derived from human galectin-3 N-terminal tail interact with its carbohydrate recognition domain in a phosphorylation-dependent manner. *Biochem. Biophys. Res. Commun.* **443,** 126–131 (2013).

256. Cooper, D. N. W. Galectinomics: Finding themes in complexity. *Biochim. Biophys. Acta - Gen. Subj.* **1572,** 209–231 (2002).

257. Barboni, E. a. M., Bawumia, S., Henrick, K. & Hughes, R. C. Molecular modeling and mutagenesis studies of the N-terminal domains of galectin-3: evidence for participation with the C-terminal carbohydrate recognition domain in oligosaccharide binding. *Glycobiology* **10,** 1201–1208 (2000).

258. Hill, M. *et al.* A novel clinically relevant animal model for studying galectin-3 and its ligands during colon carcinogenesis. *J. Histochem. Cytochem.* **58,** 553–65 (2010).

259. Blanchard, H., Yu, X., Collins, P. M. & Bum-erdene, K. Galectin-3 inhibitors : a patent review (2008 -- present). *Expert Opin. Ther. Patents* 1–13 (2014).

260. Cumpstey, I., Salomonsson, E., Sundin, A., Leffler, H. & Nilsson, U. J. Studies of arginine-arene interactions through synthesis and evaluation of a series of galectin-binding aromatic lactose esters. *ChemBioChem* **8,** 1389–1398 (2007).

261. Delaine, T. *et al.* Galectin-3-Binding Glycomimetics that Strongly Reduce Bleomycin-Induced Lung Fibrosis and Modulate Intracellular Glycan Recognition. *ChemBioChem* **17,** 1759–1770 (2016).

262. Dion, J. *et al.* Lactosamine-Based Derivatives as Tools to Delineate the Biological Functions of Galectins: Application to Skin Tissue Repair. *ChemBioChem* **18,** 782–789 (2017).

263. Cumpstey, I., Salomonsson, E., Sundin, A., Leffler, H. & Nilsson, U. J. Double affinity amplification of galectin-ligand interactions through arginine-arene interactions: synthetic, thermodynamic, and computational studies with aromatic diamido thiodigalactosides. *Chemistry* **14,** 4233–4245 (2008).

264. Atmanene, C. *et al.* Biophysical and structural characterization of mono/di-arylated lactosamine derivatives interaction with human galectin-3. *Biochem. Biophys. Res. Commun.* (2017).

265. Cagnoni, A. J., Perez Saez, J. M., Rabinovich, G. a & Marino, K. V. Turning-Off Signaling by Siglecs, Selectins, and Galectins: Chemical Inhibition of Glycan-Dependent Interactions in Cancer. *Front. Oncol.* **6,** 109 (2016).

266. Klyosov, A., Zomer, E. & Platt, D. in *Glycobiology and Drug Design* **1102,** 89–130 (American Chemical Society, 2012).

267. ClinicalTrials. A New Agent GM-CT-01 in Combination With 5-FU, Avastin and Leucovorin in Subjects With Colorectal A New. 10–12 (2016).

268. Klyosov, A. A. *Galectin Therapeutics* (2012).

269. Stegmayr, J. *et al.* Low or No Inhibitory Potency of the Canonical Galectin Carbohydrate-binding Site by Pectins and Galactomannans. *J. Biol. Chem.* **291,** 13318–13334 (2016).

270. Harrison, S. a. *et al.* Randomised clinical study: GR-MD-02, a galectin-3 inhibitor, vs. placebo in patients having non-alcoholic steatohepatitis with advanced fibrosis. *Aliment. Pharmacol. Ther.* **44,** 1183–1198 (2016).

271. ClinicalTrials. An Open-Label , Phase 2a Study to Evaluate Safety and Efficacy of GR-MD-02 for Treatment of Psoriasis An Open-Label, 12–14 (2017).

272. ClinicalTrials. Clinical Trial to Evaluation the Safety and Efficacy of GR-MD-02 for the Treatment of Liver Fibrosis and Resultant Portal Hypertension in Patients With Nash Cirrhosis (NASH-CX), 4–7 (2017).

273. ClinicalTrials. Galectin Inhibitor (GR-MD-02) and Ipilimumab in Patients With Metastatic Melanoma. 2–5 (2017).

274. ClinicalTrials. GR-MD-02 Plus Pembrolizumab in Melanoma Patients GR-MD-02 Plus Pembrolizumab in Melanoma Patients - 2–5 (2017).

275. Eliezer Zomer, Traber, P. G., Klyosov, A. A. & Chekhova, E. (19) United States. **1,** (2013).

276. Traber, P. G. & Zomer, E. Therapy of experimental NASH and fibrosis with galectin inhibitors. *PLoS One* **8,** (2013).

277. ClinicalTrials. RCT (Randomized Control Trial) of TD139 vs Placebo in HV's (Human Volunteers) and IPF Patients Purpose. 10–12 (2016).

278. Sörme, P., Arnoux, P., Kahl-Knutsson, B. & Leffler, H. Structural and Thermodynamic Studies on Cation − Π Interactions in Lectin− Ligand Complexes: High-Affinity Galectin-3 Inhibitors through Fine-Tuning of an Arginine− *J Am Chem* 543–549 (2005).

USC
UNIVERSIDADE
DE SANTIAGO
DE COMPOSTELA

Chapter

Background, Hypothesis and Objectives

> Science never solves a problem without creating ten more.
>
> *George Bernard Shaw*

Background

1. Most diarthrodial joints, due to their anatomical features, are well suited and studied for intra-articular (IA) injections. The main benefit of IA administration over oral or intravenous drug delivery is related to the increased drug concentration at the target place and, a consequent reduction of its systemic toxicity.[1–4] The main drugs used for the treatment of arthropathies and improvement of knee homeostasis that are currently available on the market are COX-2, TNF-α, IL-1 and IL-6 antagonists administrated systematically. Only very few products are available for local delivery.
2. The advances in the biopharmaceutical field along the past decades have led to the development of drug delivery systems (DDSs) that release the drug in a controlled manner in the articular cavity, thereby improving the efficacy/toxicity balance of the drug.[3,5] Nevertheless, IA drug delivery remains challenging mainly due to the premature elimination of the DDS from the synovial cavity along with fast synovial fluid (SF) turnover.[3] Among the DDSs developed for the local treatment of arthropathies are nano-/microcarriers and hydrogels,[2,3,5,6] being the most promising and advanced formulations a combination of both systems.[7–12] Such DDSs allow increased retention and prolonged release of the drugs in the joints compared with the same drugs administered in solution.[3,13]
3. Articular cartilage has a limited ability for self-regeneration.[14–16] Besides, SF greatly loses its intrinsic functions at pathological joints conditions.[17] Having this in mind, multifunctional drug delivery carriers should contribute to diarthrosis healing. They should not only provide a controlled and prolonged drug release, but also be composed of deformation-resistant materials that may have a prolonged retention in the articulation. Simultaneously, such a nanotechnology-based platform should ideally work as a viscosupplementation agent for improving the knee homeostasis, and as an *in situ* cell scaffold for cartilage tissue regeneration.
4. The discovery of novel immune targets is driving research towards the development of highly specific antagonists for more effective therapies.[18–21] This is the case of the extracellular protein galectin-3 (Gal-3), which was recently identified as a primer trigger of inflammation.[22,23] Moreover, this protein favors the secretion of macrophage pro-inflammatory cytokines, chemokines,[22] and matrix metalloproteinases,[24] which are involved in cartilage remodeling and bone demineralization.[1,25]

Hypothesis

1. The use of drug-loaded nanocapsules (NCs) dispersed in *in situ* hydrogels, composed by hyaluronic acid (HA) and fibrin, can substantially increase intra-articular drug retention time. NCs can act as multireservoirs for lipophilic drugs, and will allow controlled release, while *in situ* hydrogel might protect NCs from the fast decomposition, endocytosis and efflux from the synovial cavity contribution to the modulation of drug release as well. Such an injectable composition of NCs combined with *in situ* hydrogel could also have a role in maintaining the knee hemostasis. This is supported by the fact that both, olive oil core and 700 kDa HA coating of the NCs that have anti-inflammatory properties.[26–29] Besides, HA-fortified fibrin 3D hydrogel should serve as a viscosupplement with elastic properties for IA persistence and a support for cartilage regeneration.[30–32]

2. Since blocking of traditional COX-2 and pro-inflammatory cytokines TNF-α, IL-1, IL-6 has not led to the adequate alleviation of the inflammatory joint diseases,[3,5,33–35] we hypothesize that targeting to the novel immune target galectin-3,[22] could help to block more efficiently the inflammatory cascade and prevent further joints degradation.

Objectives

Based on the background information and outlined hypothesis, the objective of this thesis has been double, on the one hand, to develop a new injectable hydrogel containingnano-reservoirs for the prolong release of lipophilic drugs to the intra-articular cavity; on the other hand, to synthesize a new galactin-3 antagonist and its incorporation in the before-mentioned hydrogel for *in vivo* evaluation.

For this purpose overall aims have been aligned with the following experimental activities:

1) Development and *in vitro* assessment of a new DDS intended for intra-articular administration

1. To develop new dexamethasone (as a model drug)-loaded NCs and to characterize them with regard to their physicochemical properties, stability in simulated synovial fluid and stability upon storage.
2. To design and develop a novel injectable intra-articular hydrogel, and study the influence of its composition on the gelation time as well as on its rheological and mechanical properties.
3. To study the hydrogel formation in the presence of the NCs and the modification of its rheological properties and its microscopic architecture.
4. To optimize and characterize two DDS made of NCs combined with *in situ* hydrogels designed for acute- and chronic-joint inflammatory rat models differed by additional fortification of the interpenetrating network.
5. To test the *in vitro* release profile of dexamethasone from the NCs loaded in the gel.

The results corresponding to these objectives are presented in **Chapter 1:**
"An injectable, *in situ* hyaluronic acid-fibrin hydrogel containing nanocapsules for prolonged intra-articular drug delivery".

2) Anti-inflammatory drug synthesis, incorporation into the developed DDS and *in vivo* activity assessment

6. To design and synthesise a small-molecule-antagonist of extracellular galectin-3 (Gal-3), using its natural ligand type II lactosamine [Galβ(1→4)-GlcN] core, modified with aromatic substituents to greatly amplify its affinity and specificity.
7. To characterise the obtained Gal-3 inhibitor, test its affinity and selectivity among Gal-1/Gal-3/Gal-7, compare with the first commercial low MW Gal-3 inhibitor (TD139) and select the most potent synthetic inhibitor for *in vivo* evaluation.
8. To incorporate Gal-3 inhibitor in the developed DDS, characterise its physicochemical properties, and test the *in vivo* anti-inflammatory activity in a carrageenan-induced acute knee joint synovitis rat model.

The results related to this work are presented in **Chapter 2:**
"New galectin-3 inhibitor as a lead compound for anti-inflammatory drug candidates".

References:

1. Quan, L.-D., Thiele, G. M., Tian, J. & Wang, D. The Development of Novel Therapies for Rheumatoid Arthritis. *Expert Opin. Ther. Pat.* **18,** 723–738 (2008).

2. Kapoor, B., Singh, S. K., Gulati, M., Gupta, R. & Vaidya, Y. Application of liposomes in treatment of rheumatoid arthritis: Quo vadis. *Sci. World J.* **2014,** (2014).

3. Evans, C. H., Kraus, V. B. & Setton., L. A. Progress in intra-articular therapy. *Nat. Rev. Rheumatol.* **10,** 11–22 (2015).

4. Butoescu, N., Jordan, O. & Doelker, E. Intra-articular drug delivery systems for the treatment of rheumatic diseases: A review of the factors influencing their performance. *Eur. J. Pharm. Biopharm.* **73,** 205–218 (2009).

5. Kang, M. L. & Im, G.-I. Drug delivery systems for intra-articular treatment of osteoarthritis. *Expert Opin. Drug Deliv.* **11,** 269–82 (2014).

6. Evans, C. H., Kraus, V. B. & Setton, L. a. Progress in intra-articular therapy. *Nat. Rev. Rheumatol.* **10,** 11–22 (2014).

7. Vorvolakos, K., Isayeva, I. S., do Luu, H. M., Patwardhan, D. V. & Pollack, S. K. Ionically cross-linked hyaluronic acid: Wetting, lubrication, and viscoelasticity of a modified adhesion barrier gel. *Med. Devices Evid. Res.* **4,** 1–10 (2011).

8. Turker, S. *et al.* Gamma-irradiated liposome/noisome and lipogelosome/niogelosome formulations for the treatment of rheumatoid arthritis. *Interv. Med. Appl. Sci.* **5,** 60–69 (2013).

9. Morgen, M. *et al.* Nanoparticles for improved local retention after intra-articular injection into the knee joint. *Pharm. Res.* **30,** 257–268 (2013).

10. Kim, S. R. *et al.* Cationic PLGA/eudragit RL nanoparticles for increasing retention time in synovial cavity after intra-articular injection in knee joint. *Int. J. Nanomedicine* **10,** 5263–5271 (2015).

11. Wu, Q. *et al.* Thermosensitive hydrogel containing dexamethasone micelles for preventing postsurgical adhesion in a repeated-injury model. *Sci. Rep.* **5,** 13553 (2015).

12. Webber, M. J., Matson, J. B., Tamboli, V. K. & Stupp, S. I. Controlled release of dexamethasone from peptide nanofiber gels to modulate inflammatory response. *Biomaterials* **33,** 6823–6832 (2012).

13. Burt, H. M., Tsallas, A., Gilchrist, S. & Liang, L. S. Intra-articular drug delivery systems: Overcoming the shortcomings of joint disease therapy. *Expert Opin. Drug Deliv.* **6,** 17–26 (2009).

14. Spiller, K. L., Maher, S. a & Lowman, A. M. Hydrogels for the repair of articular cartilage defects. *Tissue Eng. Part B. Rev.* **17,** 281–99 (2011).

15. Ahearne, M., Buckley, C. T. & Kelly, D. J. A growth factor delivery system for chondrogenic induction of infrapatellar fat pad-derived stem cells in fibrin hydrogels. *Biotechnol. Appl. Biochem.* **58,** 345–352 (2011).

16. Jiang, Y., Chen, J., Deng, C., Suuronen, E. J. & Zhong, Z. Click hydrogels, microgels and nanogels: Emerging platforms for drug delivery and tissue engineering. *Biomaterials* **35,** 4969–4985 (2014).

17. Lipowitz, A. J. in *Textbook of Small Animal Orthopaedics* (1985).

18. Klyosov, A. A. in *Galectin Therapeutics* (2012).

19. Roy, R., Murphy, P. V. & Gabius, H. J. Multivalent carbohydrate-lectin interactions: How synthetic chemistry enables insights into nanometric recognition. *Molecules* **21,** (2016).

20. Oberg, C. T., Leffler, H. & Nilsson, U. J. Inhibition of galectins with small molecules. *Chimia (Aarau).* **65,** 18–23 (2011).

21. St-Pierre, C. *et al.* Galectin-1-specific inhibitors as a new class of compounds to treat HIV-1 infection. *Antimicrob. Agents Chemother.* **56,** 154–162 (2012).

22. Hu, Y., Yéléhé-Okouma, M., Ea, H. K., Jouzeau, J. Y. & Reboul, P. Galectin-3: A key player in arthritis. *Jt. Bone Spine* **84,** 15–20 (2017).

23. Janelle-Montcalm, A. *et al.* Extracellular localization of galectin-3 has a deleterious role in joint tissues. *Arthritis Res. Ther.* **9,** R20 (2007).

24. Palmer, M., Stanford, E. & Murray, M. M. The effect of synovial fluid enzymes on the biodegradability of collagen and fibrin clots. *Materials (Basel).* **4,** 1469–1482 (2011).

25. Page-McCaw, A., Ewald, A. J. & Werb, Z. Matrix metalloproteinases and the regulation of tissue. *Nat Rev Mol Cell Biol.* **8,** 221–233 (2007).

26. Fezai, M., Senovilla, L., Jemaà, M., Ben-Attia, M. & Ben-Attia, M. Analgesic, Anti-Inflammatory and Anticancer Activities of Extra Virgin Olive Oil. *J. Lipids* **2013,** 1–7 (2013).

27. Ghosh, P. & Guidolin, D. Potential mechanism of action of intra-articular hyaluronan therapy in osteoarthritis: Are the effects molecular weight dependent? *Semin. Arthritis Rheum.* **32,** 10–37 (2002).

28. Aly, M. N. S. Intra-articular drug delivery: a fast growing approach. *Recent Pat. Drug Deliv. Formul.* **2,** 231–7 (2008).

29. Mehta, D. P., Shodhan, K., Modi, R. I. & Ghosh, P. K. Sodium hyaluronate of defined molecular size for treating osteoarthritis. *Curr. Sci.* **92,** 209–213 (2007).

30. LeBoeuf, R. D., Raja, R. H., Fuller, G. M. & Weigel, P. H. Human fibrinogen specifically binds hyaluronic acid. *J. Biol. Chem.* **261,** 12586–12592 (1986).

31. Zhang, Y., Heher, P., Hilborn, J., Redl, H. & Ossipov, D. a. Hyaluronic acid-fibrin interpenetrating double network hydrogel prepared in situ by orthogonal disulfide cross-linking reaction for biomedical applications. *Acta Biomater.* **38,** 23–32 (2016).

32. Snyder, T. N., Madhavan, K., Intrator, M., Dregalla, R. C. & Park, D. A fibrin/hyaluronic acid hydrogel for the delivery of mesenchymal stem cells and potential for articular cartilage repair. *J. Biol. Eng.* **8,** 10 (2014).

33. Li, S., Yu, Y., Koehn, C. D., Zhang, Z. & Su, K. Galectins in the pathogenesis of rheumatoid arthritis. *J Clin Cell Immunol* **4,** 164 (2013).

34. De Oliveira, F. L. *et al.* Galectin-3 in autoimmunity and autoimmune diseases. *Exp. Biol. Med.* (2015). doi:10.1177/1535370215593826

35. Chen, H. Y., Liu, F.-T. & Yang, R.-Y. Roles of galectin-3 in immune responses. *Arch. Immunol. Ther. Exp. (Warsz).* **53,** 497–504 (2005).

USC
UNIVERSIDADE
DE SANTIAGO
DE COMPOSTELA

Chapter 1

An injectable, *in situ* forming hydrogel containing nanocapsules for intra-articular drug delivery

> The science of today is the technology of tomorrow.
>
> *Edward Teller*

This work was done in collaboration with Dr. David Cabaleiro and Dr. Luis Lugo

Department of Applied Physics, Faculty of Science, University of Vigo, 36310 Vigo, Spain

USC
UNIVERSIDADE
DE SANTIAGO
DE COMPOSTELA

ABSTRACT

Controlled release drug delivery systems (DDSs) that can be easily injectable into the intra-articular cavity are appealing for the treatment of joints pathologies. In this work, we present a novel intra-articular DDS consisting of nanocapsules (NCs), composed of an oil core and a hyaluronic acid (HA) shell, dispersed in an *in-situ* forming hydrogel. The NCs, with a mean particle size of 135 nm and a negative surface charge (−31 ± 5 mV), were loaded with the anti-inflammatory drug dexamethasone (DXM) and, subsequently, dispersed in a hydrogel consisting of a HA-fibrin interpenetrating network, fortified with factor XIII and α-2 antiplasmin. The gelation time and microarchitecture of the hydrogel could be controlled by adjusting the concentration of thrombin, HA, factor XIII and the MW of HA. Hydrogel samples loaded with up to 30% (v/v) of NCs, showed adequate rheological properties for intra-articular application. Microscopy studies revealed random distribution of NCs within the hydrogels. The morphology and porosity of the hydrogels showed a regular structure with a narrow pore size distribution and mean pore diameter of 4.88 ± 1.12 μm. The release studies from non-fortified HA-fibrin hydrogels with 30% (v/v) NCs loading showed a controlled release of DXM to simulated synovial fluid for 72 hours. In conclusion, this intra-articular DDS, which has been designed to resist the fast degradation by rheumatic synovial fluid enzymes and to serve as a viscosupplement, might be of interest for the treatment of rheumatoid arthritis and other athropathies.

GRAPHICAL ABSTRACT

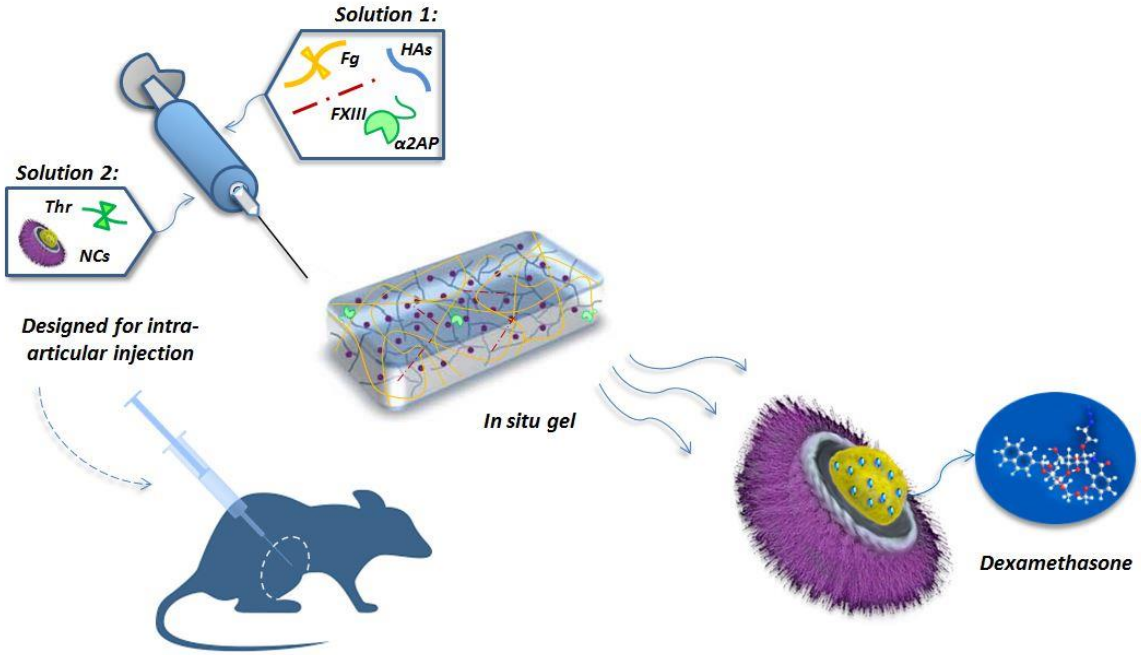

α2-AP - α2-antiplasmin, Fg- Fibrinogen, FXIII -Factor XIII, HAs - Hyaluronic acids, NCs – Nanocapsules, Thr – Thrombin.

1. INTRODUCTION

Despite the interest of the intra-articular (IA) administration of drugs for the treatment of joint diseases, this type of therapies remain challenging due to the rapid elimination from the articular cavity of the injected drugs through the synovial capillaries (for low molecular weight drugs) or the lymphatic vessels (for high molecular weight drugs).[1–5] Intra-articular (IA) drug delivery systems (DDSs) have been developed with the objective of improving the treatment of arthropathies[3,5] by reducing systemic exposure and, hence, off-target effects.[3,4,6,7] The work in this area, aiming at prolonging drug release in the joint cavity, has been so far oriented towards the development of two types of DDSs: nano-/microsystems and hydrogels.

1.1. Nano- and microsystems for IA delivery

Nanoparticles (NPs) injected into the joint cavity may penetrate into the cartilage extracellular matrix (ECM) and interact with collagen fibers particularly when their particle size is < 100 nm. For larger sizes, nanoparticles can be internalized by macrophages, synovial macrophages-like cells or dendritic cells. Similarly, microparticles are also prone to be either phagocytized (< 20 μm) or remain in the synovial fluid (SF), adhere to the cartilage and synovium or become entrapped within synovial folds (> 20 μm).[5,8–10]

At present, only one liposomal formulation for IA application is available for the treatment of inflammatory osteoarthritis (OA) (**Table 1**). The liposomal formulation, (Lipotalon®), which contains dexamethasone 21-palmitate,[11–13] has shown a maximal therapeutic effect on day 4 and the lowest disease activity index score at 16 days post injection.[12,14,15] Another liposomal formulation, Clodrosome® (Encapsula NanoSciences LLC, USA), loaded with clodronate (antiosteoporotic cytotoxic drug), has been found to be effective in a preliminary clinical trial (7 days study) on patients with RA and has been marketed for non-human RA model studies (**Table 1**).[16–18] On the other hand, a new product PLGA microspheres (MS), namely Zilretta™/FX006 (Flexion Therapeutics, USA), containing corticosteroid drug triamcinolone acetonide, has recently been approved by FDA and reached the market for OA treatment (**Table 1**).[19,20] The therapeutic effect of this formulation was maintained for up to 12 weeks.[19–22] Overall, these formulations have been shown to reduce the systemic drug toxicity thanks to the improvement of its retention in the synovial cavity.

Table 1. Marketed formulations or in clinical trials based on nano-/microsystems for joints pathologies treatment by IA route.

Product name	Drug	Drug delivery system	Indication	Phase of development	Ref.
Lipotalon®	Dexamethasone 21-palmitate (Corticosteroid anti-inflammatory)	Liposomes, ~200 nm	Inflammatory OA	Market, 2004	11–13
Zilretta™ (FX006)	Triamcinolone acetonide (Corticosteroid anti-inflammatory)	poly(D,L-lactic/glycolic acid) (PLGA) microspheres 9.7–10.3 μm	OA	Market, 2017	19–23
Clodrosome®	Clodronate disodium salt (Antiosteoporotic cytotoxic)	Liposomes, ~200 nm	RA, osteoporosis	Preliminary clinical trial on patients. Marketed for non-human RA model studies	16,18,24

The commercialization of these products has encompassed a quite active research activity in the field of liposomes and nano-/microparticles for intra-articular application made of a variety of biomaterials.[25–30] The most important recent advances with these formulations *in vivo* are summarized in **Chapter Introduction**, **Table 3**. Overall, these liposomal or polymeric formulations containing anti-inflammatory or disease-modifying anti-rheumatic drugs have shown expected PK/PD changes and increased drug residence time and, consequently, an enhancement of their efficacy and a reduction of their systemic toxicity.

The drugs that have been more extensively studied are corticosteroids (i.e dexamethasone (DXM), betamethasone, prednisolone), NSAIDs (i.e. diclofenac, indomethacin), DMARDs cytotoxic drugs (i.e. methotrexate, paclitaxel, clodronate), and others, such as kartogenin and actarit.[9,31–48] With regard to the composition of the nanosystems, in most cases they have been made of lipids (liposomes), polyesters (e.g. PLGA, PLA nanoparticles) and polysaccahrides (e.g. chitosan nanoparticles). Despite of the positive initial *in vivo* data obtained with these formulations, their therapeutic responses have not been as long-lasting as expected. In fact, the longest response has been reported for the thermo-responsive Pluronic® F127/chitosan nanospheres for co-delivery of kartogenin and diclofenac (to achieve a dual chondroprotective and anti-inflammatory effect), and showed a-

2 week retention time in joints.[48,49] A strategy to prolong the dwelling time of the nanoparticulate systems has relied on making them interactive with the surrounding environment. For example, cationic (Eudragit RL100 or PLGA/Eudragit RL) NPs, with the capacity to interact with endogenous HA, formed an *in situ* gel once injected to the rat joint cavity.[50,51] As a consequence, the NPs remained in the articular joints up to 28 days after the injection.[51]

1.2. Hydrogels

Due to their rheological properties hydrogels have received significant attention as IA drug delivery systems. As a result of the intense research in that field some formulations has already reached the market. This is the case of viscosupplementation agents, consisting of crosslinked high MW HA[52–63] or HA derivatives, an example of which is Hymovis® that contains a hexadecylamide derivative of HA.[64–66] The prolonged residence time of these hydrogels in the articular cavity[5,60,67] has resulted in a long-lasting effect on OA patients (up to 26 weeks),[60,66] and RA animal models (up to 8 weeks).[67] The longest therapeutic effect for a HA-based hydrogel has been reported for Crespine® (6-8 months), which is indicated for the treatment of OA. However, a limitation of these hydrogel therapies is related to their high viscosity, which often leads to an increase of the IA pressure and causes pain in the knee joint.[70]

In addition to the viscosupplementation properties, these hydrogels have also been used for the controlled delivery of drugs. For example, a crosslinked HA gel with pre-mixed DXM has been shown to significantly extend the drug release in an OA rat model. As a consequence, the gel significantly reduced the inherent DXM toxicity providing an anti-inflammatory and chondroprotective effect at 12 weeks after the injection.[71]

A different strategy has relied on the design of *in situ* forming hydrogels that are easy to inject and exhibit a prolonged residence time in the articular cavity. Among them, it is worth mentioning a radiopharmaceutical pH responsive Holmium-166-chitosan hydrogel[72] tested in Phase II clinical trials for the treatment of knee synovitis in RA.[73] Another example, so far only tested in rats, is a thermosensitive triblock poly(ε-caprolactone)-poly(ethylene glycol)-poly(ε-caprolactone) copolymer hydrogel, which has been proposed for the controlled delivery of methotrexate. However, the drug release from this hydrogel could only be controlled *in vivo* for up to 24 h.[74]

1.3. Nano-/microsystems-loaded hydrogels

Recent attention has also been paid to the combination of drug loaded nano-/microsystems with hydrogels aiming at improving the residence time in the synovial cavity and the drug release profile.[75–77] These nano-/microcarrier-containing hydrogels were reported to control the delivery of the associated drugs for about a month[78–80] or even longer.[81] Nevertheless, overall, the work of *in situ*-forming hydrogels containing drug-loaded nano-/microparticles is at a very early stage and only a few of these formulations have been tested *in vivo* (**Table 2**).[78,79,81,82]

In most of the cases these combined systems were tested in healthy animals and their residence time and prolonged release at inflamed joints remains unknown. An exception is represented by the radio-labelled liposomes (235 nm) incorporated into a Carbopol® 940/carboxymethylcellulose gel, which was evaluated in a rabbit induced arthritis model, and was shown to be 67% retained in the articular cavity at 24 h after injection.[34,83] In healthy rat joints the maximal sustained-released reached 42 days post IA injection by using amphotericin B precipitates/crystals suspended in glyceryl monooleate-HA hydrogel.[81]

Table 2. Nano-/microsystems loaded into hydrogels for IA applications tested *in vivo.*

Drug	Drug delivery system	*In vivo* model	Key observation	Ref.
Celecoxib (NSAID)	Precipitates/crystals (size non defined) dispersed in a poly(ε-caprolactone-co-lactide)-b-poly(ethylene glycol)-b-poly(ε-caprolactone-co-lactide) (PCLA-PEG-PCLA) gel network (*in situ*)	Healthy rat	The degradation and the release profiles were tested by different routes of administration: 3) In the articular cavity the DDS degraded between week 3 and 4. Release was not evaluated. 4) At subcutaneous injection in rats gel degradation happened in ~12 weeks, ~30 % celecoxib released during the first 3 days followed by a sustained release up to 4-8 weeks	78,79
Ibuprofen (NSAID)	Polyethylene glycol (PEG)-microspheres (40–100 μm) crosslinked by short PLGA chains to a hydrogel. Two populations: slow degradable and non-degradable	Healthy sheep shoulder joint	At 4 weeks non-degradable MS and not completely degraded MS were found, in synovial fluid and in the synovium. Degradable MS caused low inflammation compared to the non-degradable ones	80,84
Amphotericin B (Antifungal)	Precipitates/crystals (size non defined) suspended in glyceryl monooleate-HA hydrogel (*in situ*)	Healthy rat	This formulation showed sustained-released during 42 days after IA injection	81
Dexamethasone (Corticosteroid)	Monomethyl poly(ethylene glycol)-poly(ε -caprolactone) (MPEG-PCL) micelles (25 nm) incorporated into thermosensitive *in situ* PEG-PCL-PEG hydrogel (*in situ*)	Rat repeated-injury adhesion model	The gel biodegradation was evaluated upon subcutaneous injection and degraded in ~20 days	82
Diclofenac Sodium (Corticosteroid)	Lipogelosomes: Radio-labelled liposomes DMPC–CHOL–DCP (235 nm) incorporated into Carbopol® 940/carboxymethylcellulose gel	Rabbit antigen-induced arthritis	Scintigraphic imaging showed 67% retention of the formulations in the articular cavity at 24 h after injection	34,83

1.4. Rational design and selection of the DDS components

An intra-articular DDS should fulfil a number of properties, such as biocompatibility, and biodegradability, in addition to an effective and prolonged disease improvement.[85] Another distinctive feature is bioadhesiveness,[86] which allows to increase the residence time of DDS in the synovial cavity and impart the chondroprotective effect.[87]

Taking these criteria into account, we have developed a novel *in situ* HA-fibrin hydrogel containing HA nanocapsules (NCs). NCs serve as multireservoirs for lipophilic drugs, i.e. DXM, used as a model anti-inflammatory drug in this study. The hydrogel prevents the fast and uncontrolled biodistribution of the NCs, thereby extending the effect of the encapsulated drug (**Figure 1**).

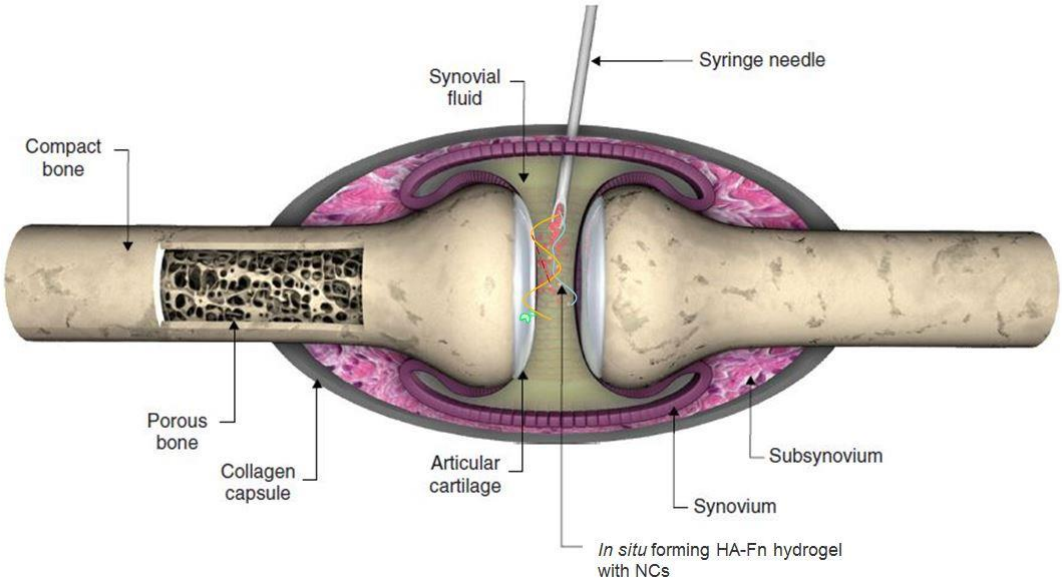

Figure 1. Schematic illustration showing the intra-articular injection of an *in situ* forming hydrogel. Adapted and modified from[8] with permission, Copyright© 2009, Taylor & Francis.

HA was selected as a biomaterial to form the hydrogel due to it essential role in diarthrodial joints homeostasis.[55,88–91] High MW HA is a key component of articular cartilage[92,93] and SF,[94] working as a physical barrier, providing the joint with adequate lubrication in addition to a chondroprotective effect.[3,89,90] Furthermore, HA provides viscoelasticity of SF and viscoinduction (promoting the endogenous HA synthesis); it also has anti-inflammatory and antinociceptive properties.[88,90,95]

The other key component of the hydrogel, fibrin, is a biomaterial derived from human blood plasma, marketed and widely used as a glue sealant Tisseel® (Baxter Healthcare

corporation, USA) for postsurgical tissue healing.[96–98] It has been used to prepare different hydrogels, in combination with other polymers,[86,99–103] noteworthy, with HA that has received major breakthrough for testing at different biomedical application for tissue engineering.[99,101,104–107]

Hence, we exploited the affinity of high MW HA to fibrin[108–110] and their capacity to form interpenetrating 3D networks (IPN),[99,101,104] through covalent and ionic interactions.[108,110] The synergistic effect of HA and fibrin is expected to provide the resulting hydrogel with improved mechanical properties and resistance against intra-articular deformations.[101,111] Aiming at extending the residence time in the articular cavity, fibrin was fortified by factor XIII (FXIII),[112,113] its natural covalent crosslinker,[96,114] and α2-antiplasmin (α2AP) in order to reduce the degradation by enzymes of pathological synovial fluid.[115–118] Additionally, HA, as the main component of hyaline cartilage, together with fibrin are essential for chondrocytes-ECM interactions, migration, proliferation, and differentiation what can be an advantage for regeneration of the damaged tissue if they are included in a DDS.[105,106] Besides, the biodegradability,[97,99,119] bioadhesiveness[103,120,121] and cytocompatibility[97,99,105] of the components could contribute to an adequate joint healing. In order to validate the potential of our *in situ*-forming hydrogel we selected DXM, a potent synthetic anti-inflammatory corticosteroid,[122] widely used for the treatment of arthropathies.[71]

Within the context of this work it is important to mention that RegenoGel™, composed of fibrinogen chemically linked to a high molecular weight HA, has been recently approved as a medical device of next generation by the Israeli Ministry of Health for degenerative joint diseases, primary for OA.[123] Moreover, its modified form (RegenoGel-OSP™ that uses autologous patient's plasma, instead of fibrinogen) now in Phase I/II clinical trials, has also shown an unprecedented response in long pain relief, superior stability and mechanical integrity, along with a strong chondrogenic effect. No adverse effects, neither local nor systemic were observed for both products.[123–125]

2. MATERIALS AND METHODS

2.1. Materials

Fibrinogen and thrombin, both from human blood plasma (premium quality grade) were purchased from Sigma-Aldrich, Germany. Sodium hyaluronate (research grade) of different average molecular weights 51 kDa, 752 kDa and 1.38 MDa, with trade names 40 kDa, 700 kDa, 1.5 MDa, correspondingly, were acquired from Lifecore Biomedical, USA. Factor XIII (FXIII) from the human blood plasma (>95% pure) was obtained from Haematologic Technologies, Inc, USA. Alpha-2 antiplasmin (α2AP) from human blood plasma (>95% pure) was bought from Lee Biosolutions, USA. Dexamethasone (97.2%) was purchased from Acofarma, Spain. The stabilizing surfactants, phosphatidylcholine enriched soy lecithin (EPIKURON® 145 V) was a kind gift from Cargill, Spain, and oleylamine and Tween 80 were bought from Sigma-Aldrich, Germany, all of high-purity grade. Labrafac™ Lipophile WL1349 was acquired from Gattefossé, France, Poloxamer-407 (Kolliphor® P 407) was obtained from Basf, Germany, Lipoid PEG-2000 was purchased from Lipoid, Germany, all of pharmaceutical grade. Virgin olive oil (extra pure) was purchased from Acros Organics, Belgium. Nile red (technical grade), HEPES, BSA (≥98%), sodium chloride, calcium chloride dihydrate, potassium chloride, sodium phosphate dibasic and potassium phosphate monobasic of ≥99% purity, were acquired from Sigma-Aldrich, Germany. Human synovial fluid (rheumatoid arthritis) was purchased from SeraLab, UK. Ultrapure (Milli-Q) or endotoxin-free water was used throughout the experiments and organic solvents were of HPLC grade.

2.2. Preparation and characterization of HA NCs

2.2.1. Preparation of HA NCs

HA NCs were produced by the solvent displacement technique, adapting the procedure earlier described by our group.[126] Briefly, lecithin (Lec, 5.625 mg), oleylamine (OAm, 1.125 mg) and olive oil (OO, 30 mg) were dissolved in 5 mL of ethanol. In the case of drug loaded NCs, DXM (8.1 mg or 2.5 mg) was incorporated to the ethanol, and for labeled NCs, Nile Red (0.125 mg) was also included to this phase. Then, the organic phase was

injected under pressure through a needle (23G) to 10 mL of aqueous phase containing 2.5 mg of HA 700 kDa, and kept under magnetic stirring at 900 rpm during 10 minutes at room temperature. The elimination of organic solvent was performed by evaporation under vacuum (Rotavapor Heidolph, Germany) and the final volume was adjusted to 5 mL with ultrapure water. Thereafter, the NCs were isolated by ultracentrifugation (Avanti® J-E, Ultracentrifuge, Beckman Coulter, USA) at 30,000×*g* for 1 h at 15 °C.

2.2.2. Physicochemical and morphological properties of HA NCs

The mean size and polydispersity index (PDI) of the HA NCs were measured after dilution (100×) with ultrapure water by dynamic light scattering (DLS) at 25 °C with an angle detection of 173°. The zeta potential (ζ) was measured by laser Doppler anemometry (LDA) after diluting the samples (100×) with ultrapure water. Both DLS and LDA analysis were performed in a Zetasizer®, NanoZS, Malvern Instruments, Malvern, UK. Particle size distribution and morphology were evaluated by transmission electron microscopy (TEM) using a JEOL JEM-2010 microscope, 200 kV, resolution: 0.23 nm (Tokyo, Japan). Samples for TEM analysis were diluted (20×), deposited on a copper grid, stained with a phosphotungstic acid solution (2% w/v) and allowed to dry overnight prior to analysis. The pH of nanoformulations was measured at Sartorius Basic Meter PB-11, Sartorius AG, Germany.

2.2.3. Determination of dexamethasone concentration in the formulation

The dexamethasone (DXM) concentration was determined after the isolation of the NCs by ultracentrifugation at 30,000×*g* for 1 h at 15 °C (Avanti® J-E, Ultracentrifuge, Beckman Coulter, USA). The amount of the free drug in the undernatant was quantified by high-performance liquid chromatography (HPLC), described below. For the extraction of DXM 0.1 mL of sample were mixed with 0.9 mL ethanol/acetonitrile (ACN) and kept under magnetic stirring at a high speed overnight to obtain a clear solution. The samples were analyzed by HPLC, using a method adapted from the literature.[127–129] The HPLC system consisted of a VWR-Hitachi LaChrom Elite® system equipped with a UV detector L-2400 set at 239 nm and a reverse phase SunFire column 186002560, 100Å, C18 (4.6 ID × 250 mm, pore size 5 μm), Waters, USA. The mobile phase was a mixture of methanol and ultrapure water (65 % : 35 % v/v), isocratic, and the flow rate was 1 mL/min. The column was set at

30 °C and the injection volume was 20 μL. The standard calibration curves of DXM were linear in the range of 1-1000 μg/mL (r^2 = 0.999). Samples were transferred into auto-sampler vials, capped and placed in the HPLC auto-sampler. The concentration of DXM in the aliquots was used to calculate the free amount of DXM and, indirectly, its concentration in the final system.

2.3. Preparation of blank and NCs-loaded HA-fibrin in situ forming hydrogels

2.3.1. Preparation of HA-fibrin in situ forming hydrogels

The HA-fibrin *in situ* hydrogels matrixes were obtained by thrombin (Thr)-activated enzymatic polymerization. For this purpose the following stock solutions were prepared.

Lyophilized powder of fibrinogen (Fg) from human blood plasma was dissolved in 0.15 M solution of NaCl at 37 °C to a final concentration of 25 mg/mL, aliquoted and stored at -20 °C. Before each experiment, an aliquot was thawed at 37 °C for 30 min and was maintained at 37 °C no more than 2 hours.[130]

Lyophilized powder of thrombin from human blood plasma was dissolved in cooled to 4 °C PBS buffer (0.01 M Na_2HPO_4, 0.0018 M KH_2PO_4, 0.137 M NaCl, and 0.0027 M KCl, pH 7.2) to a final concentration of 100 NIH-U/mL. Thrombin activity is usually expressed in NIH-U/mL, established by National Institute of Health standard for the calibration of commercial thrombin reagents,[131] taken 1 NIH-U = 0.324 ± 0.073 μg (9.0 nM). Additionally, 1% (w/v) solution of BSA was added as stabilizing agent. Thrombin was aliquoted and stored at -20 °C. Before each experiment the aliquot was thawed on an ice plate.

Sodium hyaluronate (HA) of different MW 40 kDa, 700 kDa and 1.5 MDa was diluted in warmed to 37 °C "polymerization buffer 10^{-4} M Ca^{2+}" (0.02 M HEPES, 0.1 M NaCl, 10^{-4} M $CaCl_2$, pH 7.4) or "polymerization buffer 10^{-3} M Ca^{2+}" (0.02 M HEPES, 0.1 M NaCl, 10^{-3} M $CaCl_2$, pH 7.4) to 0.1%, 0.25%, 0.5% and 0.65% (w/v) solutions. The solutions were incubated at 37 °C under shaking during 2 hours to dissolve HA and were stored at 4 °C. Additionally, HA mixed solutions 0.5% and 0.65% (w/v) made from HA 700 kDa : HA 1.5 MDa = 1:1 were prepared.

Factor XIII from human blood plasma was aliquoted and kept in 50% glycerol, 0.5 mM EDTA at concentration 5.1 mg/mL at -80 °C.

Lyophilized powder of α2-antiplasmin (α2AP) from human blood plasma was dissolved in PBS buffer (0.01 M Na_2HPO_4, 0.0018 M KH_2PO_4, 0.137 M NaCl, and 0.0027 M KCl, pH 7.2) + 1% (w/v) BSA as carrier and stored at concentration 0.1 mg/mL at -20 °C.

The hydrogel preparation was started with testing the gelation time of Fg by the action of Thr. For that purpose, stock solution of Fg was added to the "polymerization buffer 10^{-4} M Ca^{2+}" to final concentration 1 mg/mL and by the action of Thr in the range of concentrations 0.1-2 NIH-U/mL was converted to the gel.

Later, we tested the influence of HA on fibrin gelation and obtained so-called HA-fibrin hydrogel. Fg at a fixed concentration of 1 mg/mL was mixed with HA solutions of 40 kDa, 700 kDa and 1.5 MDa and theirs mixtures at concentrations of 0.1%, 0.25%, 0.5% (w/v) in "polymerization buffer 10^{-4} M Ca^{2+}" gelated upon addition of Thr in the range of concentrations 0.1-1 NIH-U/mL. Finally, 0.5% (w/v) mixture of HA 700 kDa : HA 1.5 MDa = 1:1 was selected at the optimized third component to enable syringeability due to moderate viscosity and postponed gelation time.

To formulate fortified HA-fibrin hydrogel FXIII at final concentration 10 µg/mL and α2AP at final concentration 0.14 µg/mL were added to the Fg (1 mg/mL) and HAs 0.5% (w/v) mixture 700 kDa : 1.5 MDa = 1:1 in "polymerization buffer 10^{-4} M Ca^{2+}". Thr was added as the last component at 0.75-1 NIH-U/mL to initiate the polymerization.

2.3.2. Loading of HA NCs into the hydrogel

The maximum loading of isolated HA NCs to *in situ* hydrogels was performed for non-fortified and fortified HA-fibrin hydrogels. Prior the experiments Fg samples, 0.5% (w/v) HAs Mix 1:1 = 700 kDa : 1.5 MDa solutions in "polymerization buffer 10^{-4} M Ca^{2+}", 0.5% (w/v) HAs Mix 1:1 = 700 kDa : 1.5 MDa solutions in "polymerization buffer 10^{-3} M Ca^{2+}" and blank or drug loaded HA NCs were warmed up at 37 °C for 30 minutes. For the samples preparation, we used fibrin at concentration 1 mg/mL and 1.5 mg/mL, 0.5% (w/v, final concentration) mixture of HA 700 kDa : HA 1.5 MDa in = 1:1 in "polymerization buffer 10^{-4} M Ca^{2+}" or in "polymerization buffer 10^{-3} M Ca^{2+}", and FXIII 10 µg/mL, α2AP 0.14 µg/mL (in case of fortified HA-fibrin hydrogels), as summarized in **Table 3**. The reaction was initiated by Thr (1-2 NIH-U/mL). *In situ* hydrogel NCs loading capacity in the range of 10 - 50% was tested.

Table 3. Composition of fortified HA-fibrin hydrogel with 30% loaded NCs.

Composition	Final concentration
Fg	1-1.5 mg/mL
Thr (added as a last component)	1-2 NIH-U/mL
HAs mix 1:1 (1.5 MDa : 700 kDa) in HEPES buffer, 10^{-3} M Ca^{2+}, pH 7.4	0.5%
DXM NCs	30%
FXIII	10 µg/mL
α2AP	0.14 µg/mL

2.3.3. Determination of the hydrogel gelation time

Determination of the lag-time and the gelation point was performed by turbidity analysis using UV-Vis scanning spectrophotometry (Manual Beckman-Coulter DU®730 spectrophotometer, USA). The device was set up at the mode, allowing the measurement of the absorbance at 350 nm each 10 s within 20 min, recording the kinetics of the polymerization.

The gelation point of blank and NCs loaded hydrogels was additionally measured in rheology studies, described in *Section 2.4.5.*

2.4. Physical characterization of the hydrogels containing NCs

2.4.1. Syringeability studies

For this analysis, samples of HA-fibrin and fortified HA-fibrin gels with blank HA NCs were prepared as described in *Section 2.3.1* and *Section 2.2.1*, correspondingly. Components mentioned in *Section 2.3.3* and PBS buffer (0.01 M Na_2HPO_4, 0.0018 M KH_2PO_4, 0.137 M NaCl, and 0.0027 M KCl, pH 7.2) were warmed up at 37 °C 30 min before the experiments. All the components, including 30% NCs, were mixed and transferred to the syringe Terumo Myjector U-100 Insulin with superfine 29G needle, as usual Thr was added as the last component and mixed again before injection to the vial filled with warmed up to 37 °C PBS buffer (1:1).

Hydrogel samples were prepared in the same way, although were injected to the cuvettes with no PBS buffer and were analyzed by UV-spectrophotometry as described in *Section 2.3.2*, to verify whether the value of absorbance correlates with the UV spectrophotometry data of gels formed without injection.

2.4.2. Porosity and surface morphology

The samples for SEM were prepared as described in *Section 2.3.3.* by the injection of blank and 30% NCs loaded non-fortified and fortified HA-fibrin *in situ* hydrogels to PBS buffer 1:1 and 1:1.73. Samples were shaken for 20 hours at 37 °C, then, the gels were rinsed with ultrapure H_2O to extract the salt excess. The samples were frozen at -80 °C and lyophilized during 48 hours to preserve the structure. Afterwards, samples were transferred to the metal supports and coated with gold nanolayer and additionally sputtered with 5-nm-thick layer of Ti with an SPI sputter coater. All SEM images were obtained on SEM EVO LS15 with EDX, Resolution: 1kv SE e W (Zeiss) and FESEM ULTRA-Plus, Resolution: 1 kV e WD (Zeiss).

2.4.3. Distribution of NCs within the hydrogel

Nile Red labeled NCs were prepared according to the procedure described in *Section 2.2.1.* The NCs distribution in the gels was analyzed by confocal laser scanning microscopy (SP5 Leica AOBS-SP5) without any additional processing. A lamp ion laser operated at 530 nm wavelengths (corresponding to Nile Red maximum wavelength emission) was used as an excitation source. The images were taken at 50 μm and 490 μm the sample depth.

2.4.4. 3D surface and porosity

Non-fortified and fortified HA-fibrin hydrogels without and with NCs were prepared as described in *Section 2.3.2.* and were analyzed by a Wyko-NT1100 microscope (Bruker) that enables topographic sample characterization using non-contact White Light Optical Interferometry (WLOI) with the Vertical Scanning Interferometry (VSI) method. The images were analyzed by WycoVision 32 analytical Software package. The hydrogel hydrated and semi-hydrated images were obtained by Optical Microscope DMS 300, at 50× objective lens

and an intermediate ×0.5 to obtain a magnification of 25.6×, with a field of view of 241×183 μm^2 of the samples. At least three zoomed areas from these topographic images were analyzed.

Three-dimensional parameters of surface texture and roughness: arithmetic mean height (S_a), root mean squared height (S_q), maximum height (S_z), skewness (S_{sk}), and kurtosis (S_{ku}) represent the statistical distribution of height values and were calculated by standard equations according to International Standard ISO 25178-2. The contribution due to dominant geometric shape and plane inclination were eliminated in these calculations. S_{sk} represents the degree of symmetry of the surface heights about the mean plane. The sign of S_{sk} indicates the preponderance of peaks (that is $S_{sk} > 0$) or valley structures ($S_{sk} < 0$) that the surface contains. S_{ku} reflects the nature of the height distribution and, therefore it is useful for indicating the presence of either peak or valley defects such as scratches. If the surface heights are normally distributed (a bell curve) then S_{ku} is equal 3.00. Surfaces composed of inordinately high peaks/deep valleys have $S_{ku} > 3.00$. $S_{ku} < 3.00$ indicates gradually varying surfaces.

2.4.5. Rheological behavior of hydrogels

A Discovery Hybrid Rheometer (DHR-2 from TA Instruments) with a standard steel parallel-plate geometry of 20 mm diameter together with a Physica MCR 101 rheometer (Anton Paar, Graz) working with a plate-plate geometry with a diameter of 25 mm and a constant gap of 0.5 mm were employed for the rheological measurements of hydrogel samples. The agreement between the results in the two devices was checked and achieved in both non-linear viscoelastic tests and oscillatory shear mode. Firstly, flow curves for HA-fibrin hydrogel were carried out with the aim to obtain the initial viscosities. Then, the methods employed were oscillatory time sweeps, strain sweeps, and frequency sweeps. Time sweep experiments were performed to monitor, into a time frame, the *in situ* gelation of the blank and NCs loaded hydrogel samples. During these time sweeps, a torque of 0.9 μN·m and a frequency of 0.5 Hz were maintained for a maximum time of 30 min to account for the temporal evolution of the elastic or storage modulus G' and the viscous or shear loss modulus, G''. Strain sweeps were carried out to characterize and compare G'/G'' ratios under the same physical conditions identifying the linear viscoelastic region (LVR) in the strain range from 0.1% to 1,000% or until structure breakdown. These tests were set up holding the frequency at 0.1 Hz or 1 Hz to ensure the best measuring conditions of the rheometer.

Moreover, hydrogels were also subjected to oscillatory frequency sweep experiments, which were performed at frequencies from 0.01 to 100 Hz taking into account the obtained LVR profiles. As it is well known, frequency sweep tests are widely used to obtain information about the stability of three-dimensional crosslinked networks.[133]

The measurements were taken at 20 °C and/or 37 °C and all samples were reproduced three times with good accuracy. The results were analyzed directly from the software controlling the experimental devices (Trios Software for DHR-2 rheometer and Rheoplus Software for Physica MRC 101) and the polymerization reactions of hydrogels were studied by recording both elastic and viscous modulus.

2.5. In vitro release studies

2.5.1. Simulated synovial fluid (SSF) preparation

SSF was reproduced following the protocol described by Margareth and Raimar[132] and contained 0.017 M NaCl, 0.0027 M KCl, 0.01 M Na_2HPO_4, 0.00176 M KH_2PO_4, 3 mg/mL HA (non-specified MW), pH 7.4. We used 1.5 MDa HA as one of the high MW HA presented in the normal human SF able to maintain predetermined viscosity.

SSF was applied to test stability of NCs in the hydrogel, the drug release from this system and measurements of refractive index (RI).

2.5.2. SSF refractive index

The measurements of RI values of SSF were performed for further NCs stability studies by DLS. SSF sample was prepared as described in *Section 2.3.5* and analyzed by using an automatic Abbemat-WR refractometer (Dr Kernchen), which has an uncertainty of 4×10^{-5} and control of temperature with 0.01 °C resolution. The apparatus was calibrated by measuring Millipore quality water and pure solvents before the sample analysis. The RI values were recorded in the range of the temperatures 20 - 50 °C.

2.5.3. In vitro DXM release studies from the gel to SSF

To study the release of DXM from the NCs loaded hydrogels to SSF, the samples were prepared as described in *Section 2.3.2. In situ* HA-fibrin hydrogel with 30% DXM loaded NCs was formed in SSF, pH 7.4 (a ratio 1:1.3 was selected to comply with *in vivo* model), **Table 4**.

Table 4. The preparation of HA-fibrin/fortified HA-fibrin hydrogel with 30% loaded DXM NCs for release studies.

Composition	Volume (µL)
Non-fortified/fortified HA-fibrin hydrogel	213.8
30% DXM NCs	91.2
Total gel system	**305**
SSF	395
Total composition	**700**

Briefly, each vial correspondent to specific time point withdrawal, contained SSF were placed in an incubator at 37 °C with horizontal shaking for 20 minutes before warmed to 37 °C gel components with and DXM NCs were added to SSF and well-mixed. Hydrogels were let 30 minutes to be completely formed at 37 °C with horizontal shaking (300 rpm) and maintained at these conditions along the experiment. Once formed, at different time intervals (from 0 to 72 h), until the complete gel degradation, 100 µL of the medium surrounding the gel were withdrawn and mixed with 300 µl EtOH (1:3) to extract the released DXM. The amount of released DXM was determined by HPLC as described in Section *2.2.3.*

2.6. Statistical analysis

All the measurements at each experimental condition were carried out in triplicates and were expressed as mean ± standard deviation (SD). Statistical analysis of the data was performed using a one-way ANOVA and Student's t test using Microsoft® Excel software; a value of $p < 0.05$ was considered significant.

3. RESULTS AND DISCUSSION

In this work, we designed, developed and characterized an injectable *in situ* forming HA-fibrin crosslinked hydrogel loaded with HA NCs. This formulation is intended to extend the retention of the NCs in the intra-articular cavity and to control the delivery of the associated drug (DMX). This hydrogel is supposed to act as a reservoir for controlled release of hydrophobic drugs and a viscosupplement with viscoinductive properties.

3.1. Preparation and characterization of DXM-loaded HA NCs

Although a number of authors have described the potential use of nanosystems for the IA drug delivery of drugs, the success of these DDSs relies on their final fate. Indeed, nanosystems may suffer from a rapid efflux from the articular cavity[4,5] and they may also be taken-up by synovial macrophages, dendritic cells and chondrocytes.[8,134] In this regard, it has been shown that particles with sizes below 100 nm[135–137] and above 20 µm are not prone to be endocytosed by macrophages and chondrocytes.[8,9,138,139] On the other hand, the diameter of blood capillaries (2-3 µm) and the lymph vessels (8-30 µm),[5,16,140] prevent the elimination of large particles,[5,50,141] whereas very small NPs may drain to the blood or the lymphatic circulation and even diffuse across the cartilage ECM.[8] An additional advantage of NPs vs. large particles relies in the small size of the needle required for the injection and the fact that smaller particles were expected to cause no mechanical cartilage damage in the joint.[50]

Taking this information into account, our objective was to obtain HA NCs with a size close to 100 nm and to load them with the model drug DXM prior to their incorporation into a hydrogel. The purpose behind this system is to avoid the drainage to the systemic circulation and, at the same time reduce the macrophages up-take.

Prior to the NCs formulation, we performed a thoughtful selection of their components. Among the different oils tested (caprilic/capric acid triglicerides and olive oil (OO)), we selected extra pure virgin OO due to its anti-inflammatory properties[142,143] and because of its capacity to dissolve DXM.[144] Soy lecithin (Lec) and oleylamine (OAm) were selected in order to produce cationic nanoemulsions to which the HA molecules to be attached.[145,146] HA (700 kDa) was selected as a shell polymer as this molecular weight was found to exhibit anti-inflammatory responses.[90]

HA NCs were prepared by the solvent displacement technique, a mild and easily scalable preparation method, previously described in our laboratory.[147] The ratio oil/neutral

surfactant/cationic surfactant/shell polymer 4:1:0.2:0.5 yielded stable 100 – 200 nm NCs. The injection under pressure of the organic phase over the aqueous phase was applied in order to decrease the NCs size. The particle size, zeta potential and encapsulation efficiency of two different formulations are summarized in **Table 5**. The first prototype with encapsulated DXM was prepared with a ratio slightly modified of DXM/OO/Lec/OAm/HA = 1:6:1.5:0.3:1 (prototype 1) to better control the NCs physicochemical properties, however, the DXM EE% was low (**Table 5**). On the other hand, in order to increase the DXM loading a new prototype of NCs (prototype 2) with a ratio DXM/OO/Lec/OAm/HA = 3.2:8.8:2.3:0.45:1 was prepared, with higher amount of oil and surfactants in an attempt to increase the drug content in the suspension (**Figure 2**).

Table 5. Physicochemical characteristics of the nanocapsules (NCs) prepared with 700 kDa HA (mean ± SD; n = 6). PDI: polydispersity index.

Type of NCs		OO (mg)	Lec (mg)	OAm (mg)	Particle size (nm)	PDI	ζ-potential (mV)	Drug concentration (mg/mL)
Blank	prototype 1	15	3.75	0.75	128 ± 13	0.2	−27 ± 3	n/a
	prototype 2	22	5.625	1.125	121 ± 10	0.2	−30 ± 3	n/a
DXM - loaded	prototype 1	15	3.75	0.75	160 ± 12	0.2	−20 ± 4	0.75 ± 0.125
	prototype 2	22	5.625	1.125	135 ± 9	0.2	−31 ± 5	5.6 ± 0.4

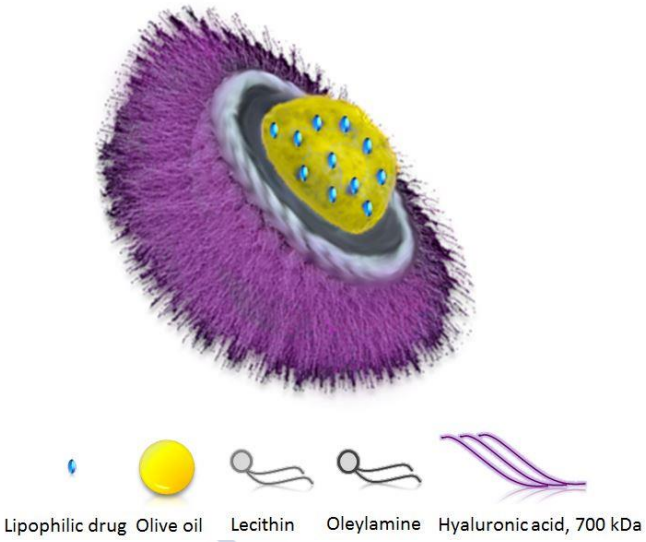

Figure 2. Representation of the structure of HA nanocapsule.

The size of the NCs, obtained by DLS, was compared with TEM data. Images from electronic microscopy (**Figure 3**) revealed the spherical shape of NCs with considerably smaller particle size values compared to DLS data (**Figure 3B and C**). These results can be explained considering that TEM requires detection of NCs in a dry state, whereas DLS analyzes NCs in aqueous suspension, measuring the hydrodynamic diameter.[148]

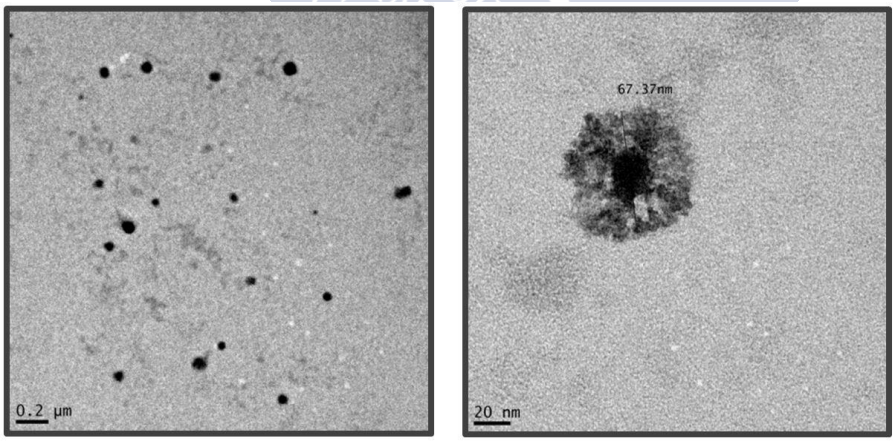

A **B**

Figure 3. TEM images of HA blank nanocapsules: (**A**) at magnification 50,000×; (**B**) and (**C**) at 500,000×.

3.2. Preparation and characterization of in situ forming hydrogels

In order to increase the residence time of NCs in the articular cavity, we developed an *in situ* forming hydrogel, which in addition to having good rheological properties and high resistance to deformation after IA injection, would serve as a reservoir for the NCs. For its preparation we used a combination of HA and fibrin with crosslinking agents, i.e. factor XIII (FXIII) and α2-antiplasmin (α2AP).

For the production of fibrin gel, we started with the precursor fibrinogen (Fg), at a concentration of 1 mg/mL, and investigated the time required for its polymerization by the action of different concentrations of thrombin (Thr, 0.1-2 NIH-U/mL) (**Figure 4A and B**). The optimal gelation speed at physiological conditions was achieved at 1-5 NIH-U/mL.[149]

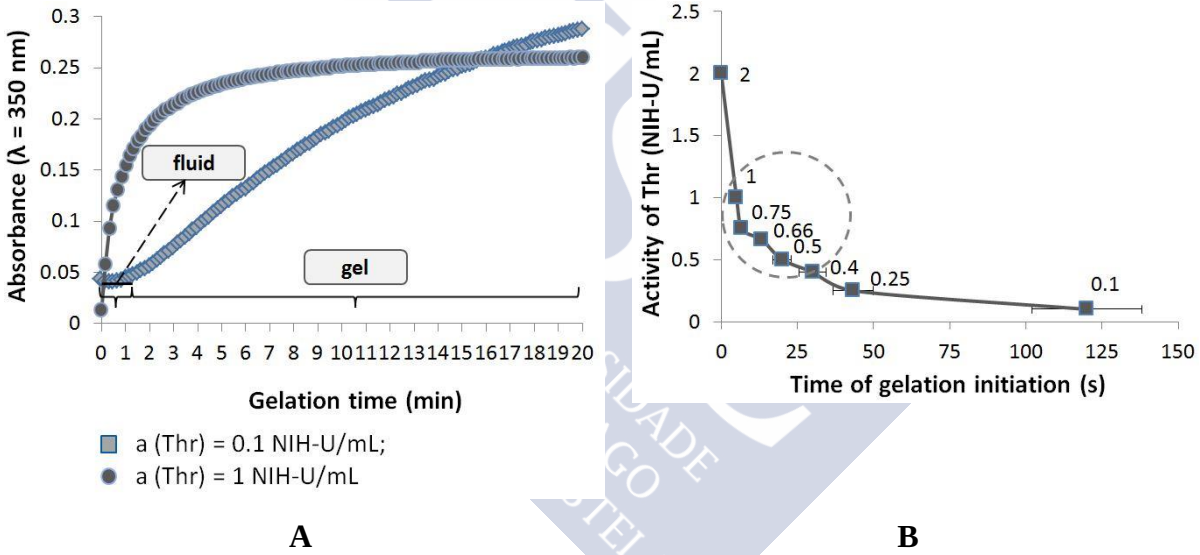

A **B**

Figure 4. (A) Influence of thrombin (0.1 or 1 NIH-U/mL) on the fibrin gelation time. **(B)** Fibrin gelation points by the action of thrombin (0.1 - 2 NIH-U/mL) on fibrinogen. The range marked by dot-dash line represents the thrombin activity at which the hydrogels revealed the best stability profiles. The polymerization kinetics was determined by turbidity analysis during 20 minutes at λ = 350 nm.
Fibrinogen was always taken at concentration 1 mg/mL. For thrombin (Thr), 1 NIH-U = 0.324 ± 0.073 μg (9.0 nM). Expressed as mean ± SD; n = 3.

In the first stage of polymerization, shown as the "fluid" phase in **Figure 4A**, fibrin is presented in the form of soluble fibrin-monomers. The second stage of polymerization[130] is characterized by the lateral association of protofibrils to fibrils and their subsequente organization in the form of a 3D-network hydrogel.[150,151] As shown in **Figure 4A** this process is characterized by a constant increase of the absorbance until the gel is completely formed

and, hence is named as "gel" phase. The times at which fibrin starts to polymerize (gelation points) were calculated from the kinetics curves of polymerization by the method described by Chernysh *et al.*[152] (**Figure 4B**).

Ca^{2+} ions are among the key factors controlling the speed of polymerization and final gel rheology, rigidity and porosity. Based on this, the buffer for hydrogel formation was made with a Ca^{2+} concentration that was one order of magnitude lower to the one found in plasma ($1\text{-}1.1\times10^{-3}$ M),[130] with a composition of 0.02 M HEPES, 0.1 M NaCl, 10^{-4} M $CaCl_2$, pH 7.4.

Taking advantage of the affinity between HA and fibrin's positively charged E-domain and αC-domains[150,151] ($K_d \sim 45 \times 10^{-9}$ M),[108,109] we explored the formation of HA-fibrin hydrogels. We used HA polymers of different MW to study the influence of the macromolecule length in the polymerization process. We tested HA of three MW (40 kDa, 700 kDa, 1.5 MDa) in different concentrations. The gelation point of the HA-fibrin system was calculated from the kinetics curves of polymerization, as described earlier for fibrin kinetics. For these experiments, 0.1%, 0.25%, and 0.5% (w/v) solutions of HA of each MW (40 kDa, 700 kDa and 1.5 MDa) and a mixture of 700 kDa and 1.5 MDa were used (**Table 6**).

Table 6. Screening of compositions to optimize HA-fibrin gel formation. Fg: fibrinogen, Thr: Thrombin, HA: hyaluronic acid, FXIII: factor XIII, α2AP: α2-antiplasmin.

System	Components concentrations					
	Fg (mg/mL)	Thr (NIH-U/mL)	HA		FXIII (µg/mL)	α2AP (µg/mL)
			w/v	MW		
Fibrin gel	1	0.1 - 2	-	-	-	-
HA-fibrin gel	1	0.5 - 1	0.1 - 0.5%	40 kDa	-	-
			0.1 - 0.5%	700 kDa		
			0.1 - 0.5%	1.5 MDa		
			0.5%	Mix 1:1 of 700 kDa : 1.5 MDa		
Fortified HA-fibrin gel	1	0.75 - 1	0.5%	Mix 1:1 of 700 kDa : 1.5 MDa	10	0.14

As shown in **Figure 5**, in general, the higher the concentration of HA the higher the inhibition of the gelation process is. Namely, in the case of 700 kDa and 1.5 MDa HA, an

increase in HA concentration from 0.1% to 0.5% led to a significant increase in the gelation time. However, in the case of 40 kDa HA, the influence of the HA concentration had only a minor impact on the gelation process. On the other hand, 0.5% 1.5 MDa HA solution was highly viscous and, thus, difficult to inject. For that reason, a mixture of HAs (700 kDa : HA 1.5 MDa = 1:1, 0.5%), with moderate viscosity, was selected to enable proper injection into the knee. In addition, the use of a mixture of HA of different molecular weights allowed us to modulate the gelation time to the one required for the adequate syringeability. This composition was also found to be good for viscosupplementations purposes.[153–155] In this regard, it is worth noting that the marketed product RenehaVis®, which involves a combination of 1 MDa (2.2%, w/v) and 2 MDa (1%, w/v) HAs, is highly used for the long term treatment (12 months) of OA.[156–159] Furthermore, HA with a MW of 0.5-1 MDa has been found to be effective in reducing synovial inflammation,[55,90,160] while 1.3-1.7 MDa HAs are able to restore the rheological properties of arthritic synovial fluid.[55,89,90]

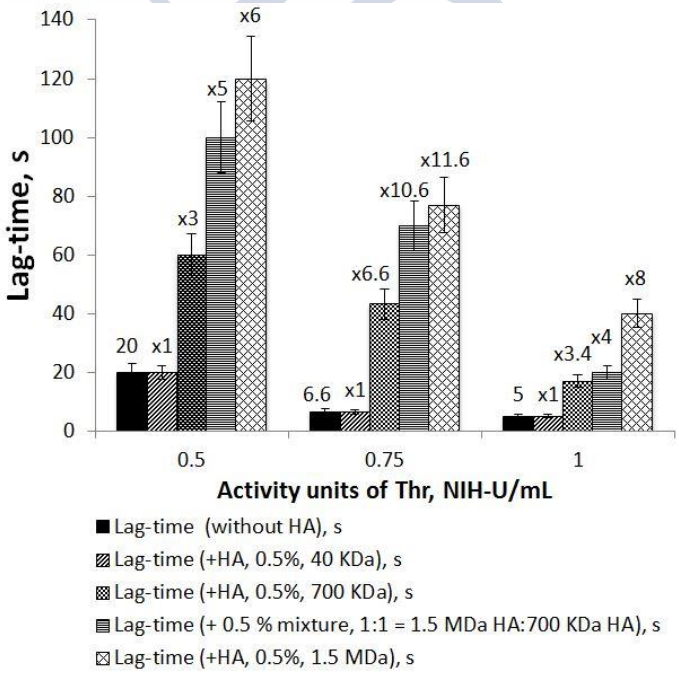

Figure 5. Comparative studies of the influence of different hyaluronic acid (HA) on fibrin polymerization kinetics (indicated as "without HA"). HA, 0.5% (w/v) of 40 kDa, 700 kDa, 1.5 MDa and HA mix solution of 700 kDa : 1.5 MDa = 1:1 were added to the "polymerization buffer 10^{-4} M Ca^{2+}". The polymerization kinetics was recorded by turbidity analysis during 20 minutes at λ = 350 nm. Fibrinogen was always taken at 1 mg/mL concentration, activity of thrombin (Thr) = 0.5 - 1 NIH-U/mL. The gelation point was calculated from the kinetics curves of polymerization. The numbers above the bars represent in how many times the gelation is inhibited compared to fibrin polymerization alone. Expressed as mean ± SD; n = 3.

To increase the *in vivo* half-life of the developed HA-fibrin hydrogel we incorporated FXIII and α2AP as fortifying components of the gel. FXIII is a natural fibrin covalent crosslinker that fortifies and stabilizes fibrin mesh increasing the resistance against the gel degradation by 5 times.[112,113] Whereas, α2AP, incorporated into fibrin network, greatly reduces the degradation of crosslinked fibrin gels by plasmin, normally found in rheumatic SF.[115,117,118] Hence, by adding FXIII and α2AP to *in situ* HA-fibrin hydrogel a fortified HA-fibrin IPN was engineered (**Figure 6**). This combination of materials is expected to resist the action of hyaluronidase, which degrades non-crosslinked HA at RA condition.[161,162]

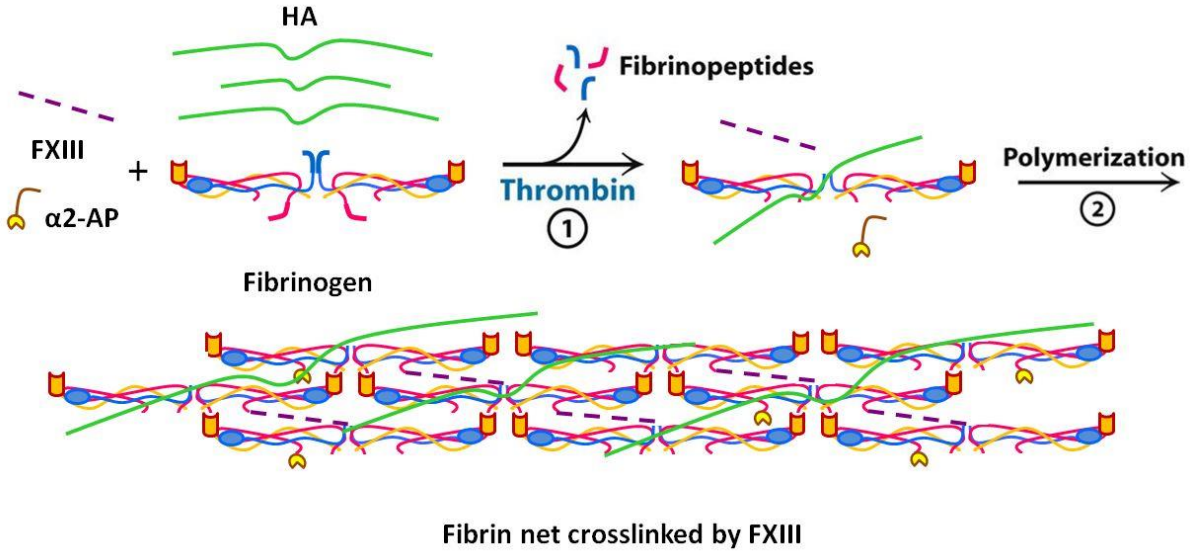

Figure 6. The schematic illustration of the fortified HA-fibrin gel formation, activated by thrombin. HA: hyaluronic acid, FXIII: factor XIII, α2AP: α2-antiplasmin.

We investigated the influence of FXIII and α2AP on the hydrogel formation by turbidity analysis. The results gathered in **Figure 7** indicate that, as expected, the gelation time is reduced upon addition of FXIII. Overall, we could control the polymerization speed and the rheological properties of the developed hydrogel by adjusting different parameters, namely the temperature, the amount of thrombin, the MW and concentration of HA, Ca^{2+} and FXIII.

3.3. Loading of NCs into the in situ forming hydrogel

We investigated the capacity of the hydrogel to load NCs in the range of 10 – 50% (v/v) (blank or drug-loaded NCs concentrated to 1 mL) in HA-fibrin and fortified HA-fibrin systems at the concentrations gathered in **Table 3**. NCs showed a significant inhibition of the

gel formation process (> 20 min) and even no gelation was observed when the NCs/hydrogel v/v ratio was higher than 30% (fibrinogen 1 mg/mL, thrombin 1 NIH-U/mL and HAs 0.5% (w/v) mixture 700 kDa : 1.5 MDa = 1:1 in a "polymerization buffer 10^{-4} M Ca^{2+}"). Thus, the next step was the adjustment of the hydrogel formation conditions (fibrin, thrombin, Ca^{2+} and HAs concentrations) for 30% NCs loaded gels. The optimal time for the formation of a HA-fibrin gel with adequate rheological properties was achieved at a concentration of 1.5 mg/mL of fibrinogen, 2 NIH-U/mL of thrombin, 0.5% (w/v) mixture 700 kDa : 1.5 MDa HAs and 10^{-3} M Ca^{2+}. In the case of the fortified HA-fibrin hydrogel, 10 µg/mL of FXIII and 0.14 µg/mL α2AP were additionally used. **Figure 7** shows the summary of polymerization kinetics observed by turbidity analysis, the lag time was calculated based on spectrophotometric determinations, as described in *Section 3.2*.

The amount of HA in the gel was envisaged to be ~3 mg/mL, bearing in mind that this is the HA physiological concentration found in healthy SF.[94]

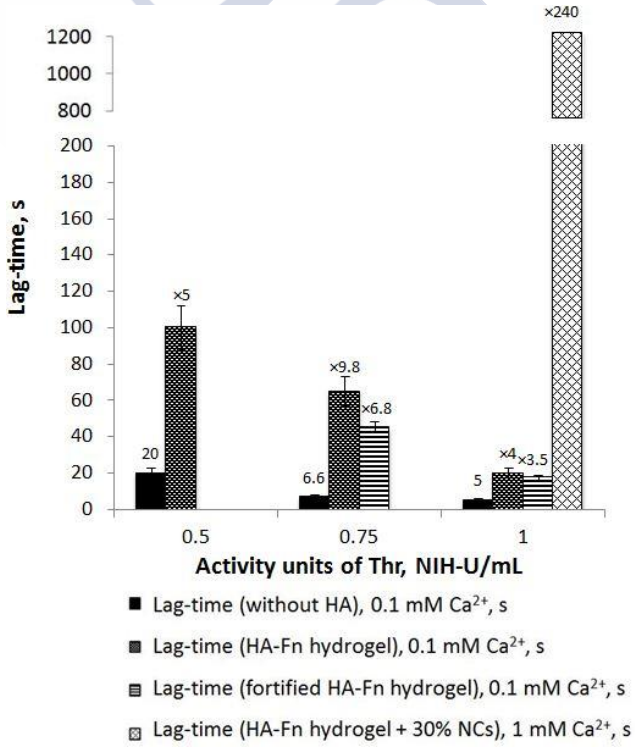

Figure 7. Comparative studies for the gelation of fibrin (Fn) (without HA), HA-fibrin, and fortified HA-fibrin systems, driven by different Ca^{2+} ions concentration in blank and 30% NCs loaded gels. The polymerization kinetics was recorded by turbidity analysis during 20 minutes at λ = 350 nm. Fibrinogen was always taken at 1 mg/mL concentration, activity of thrombin (Thr) = 0.5 - 1 NIH-U/mL for blank gels and NCs loaded gels. The gelation point was calculated from the kinetics curves of polymerization. The numbers above the bars represent in how many times the gelation is inhibited compared to Fn polymerization alone. Expressed as mean ± SD; n = 3.

3.4. Rheological behavior of in situ forming the hydrogels

A basic principle for the development of an *in situ* gelling system is to have a low vicosity of the components mixture in order to ensure its good syringeability. The viscosity of the HA-fibrin mixture (with no thrombin addition) at 20 °C and 37 °C is 118.9 mPa·s and 81.3 mPa·s, respectively. As these values are much lower than those of commercial viscosupplements,[59,154] the mixed solutions necessary to form the *in situ* hydrogel are expected to be easily injected intra-articularly *in vivo*.

Oscillatory rheological experiments are known to be a useful tool to determine the macro- and micro-structural rearrangements that influence the rheological behavior of gels with time.[163,164] The gelling point can be detected by monitoring the gelation process with an oscillatory time sweep. The temporal evolution of the elastic or storage modulus (G'), which measures the elastic nature of the material, and the viscous or shear loss modulus (G"), which measures the viscous nature of the material was monitored upon the tests.

As an example, **Figure 8A** and **B** gathers the gelation process of HA-fibrin and fortified HA-fibrin hydrogels with 30% loaded NCs. It can be observed thatthe viscous/shear loss modulus (G") is higher than the elastic/storage modulus (G'). This is logical if we take into account that the gel samples are in liquid state, where the viscous properties predominate. As soon as the blank or NCs-loaded gels begin to form a crosslinked network the two indicated moduli rise. Nevertheless, the increase of G' is faster than that of G", because the elastic nature of the gelling hydrogel starts to dominate. Hence, a crossover point appears in the curves is the gelation time of the sample. These gelling times are compared with those obtained for HA-fibrin and fortified HA-fibrin blank gels (**Figure 9**). The results of the rheology studies allowed us to detect the starting gelation point, by observing the gel evolution in time and the endpoint at which the gel is completely formed.

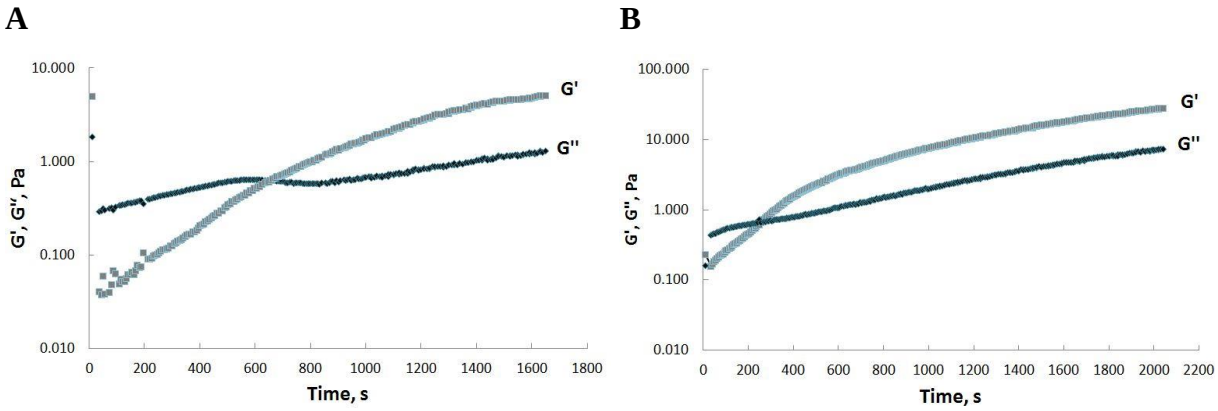

Figure 8. Gelation point detection by the response of elastic (G') and viscous (G") moduli in HA-fibrin with 30% loaded NCs **(A)** and fortified HA-fibrin hydrogels with 30% loaded NCs **(B)**. Fibrinogen was always taken at 1.5 mg/mL concentration, activity of thrombin (Thr) = 2 NIH-U/mL, 0.5% HAs mix solution 1:1 (1.5 MDa : 700 kDa), 10^{-3} M Ca^{2+}, 10 µg/mL of factor XIII and 0.14 µg/mL α2-antiplasmin at 37 °C. Expressed as mean ± SD; n = 3.

To provide an adequate syringeability of *in situ* hydrogel for *in vivo* experiments, our approach was to delay the gel formation for at least a 2 min (lag-time) after mixing the gel components in non- and fortified HA-fibrin blank and 30% NCs loaded gels. The resulting gelation times are shown in **Figure 9**.

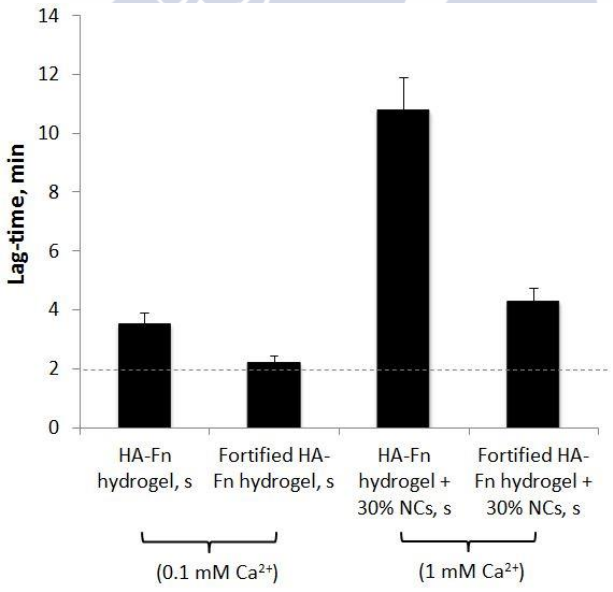

Figure 9. Summary of gelation time point determination by rheological measurements in different systems: HA-fibrin (HA-Fn) and fortified HA-Fn blank and 30% NCs loaded gels. For blank gels fibrinogen was always taken at 1 mg/mL concentration, activity of thrombin (Thr) = 1 NIH-U/mL. For 30% NCs loaded gels fibrinogen was always taken at 1.5 mg/mL concentration, activity of Thr = 2 NIH-U/mL. The dash-and-dot line reflects the 2 minutes lag-phase requirements. The measurements were carried out at 37 °C. Expressed as mean ± SD; n = 3.

To evaluate the deformation profiles we measured the behavior of the G' and G'' moduli of the formed blank and NCs-loaded HA-fibrin and fortified HA-fibrin gels by oscillatory strain and frequency sweeps.

As an example, **Figure 10** shows the elastic and viscous moduli of the non- and fortified HA-fibrin hydrogel loaded with 30% NCs as a function of the deformation. Initially, the linear viscoelastic region, i.e. the region in which deformations are not large enough to destroy material structure, was identified through strain sweeps ranging from 0.1% to 1,000 or 10,000% depending on the parameters of the crossover point. At strains lower than 10-15% (critical strain), the value of elastic and viscous moduli is constant and independent of the deformation, G'>G". In this linear viscoelastic region the deformation is completely recoverable and the material exhibits an elastic "solid-like" behavior. As mentioned earlier, HA and fibrin significantly contribute to rheological properties of each other: *e.g.* high hydrophilicity of HA prevents the compression of the fibrin network and improves it mechanical properties,[101] while fibrin provides desired elasticity and resistance to stretching for HA gels.[96] The crossover point of G' and G" modulus, indicating a sample deformation point in this experiment, for NCs loaded fortified HA-fibrin gels was observed at a strain of 630%, while the NCs loaded non-fortified HA-fibrin gels destroyed at a strain of 100%. Thus, fortified NCs loaded gels reveled 6.3 times higher resistance to deformations compared to non-fortified loaded gels. Other authors also showed that fibrin hydrogels crosslinked by FXIII under physiological conditions are more stable and shows 8 times higher Young's (elastic) modulus values than non-crosslinked one.[96] Furthermore, FXIII increases the rigidity and strength of the fibrin hydrogel and protects it against shear stress in the physiological environment.[112,113,165] Under larger deformations an overshoot phenomenon can be observed in the G' and G" moduli of the fortified HA-fibrin hydrogel loaded with 30% NCs (**Figure 10B**). This response is typical for materials with resistance to a permanent deformation, which is the evidence of FXIII contribution to the stability profile. Lorand and Muszbek *et al.* have also observed increase in viscous and elastic moduli of fibrin gel crosslinked by FXIII as a measure of clot stability against shear stress.[113,114] At the higher strains applied the values of two moduli decreased as the strain increases corresponding to thinning behavior until the breakdown of the material structure.

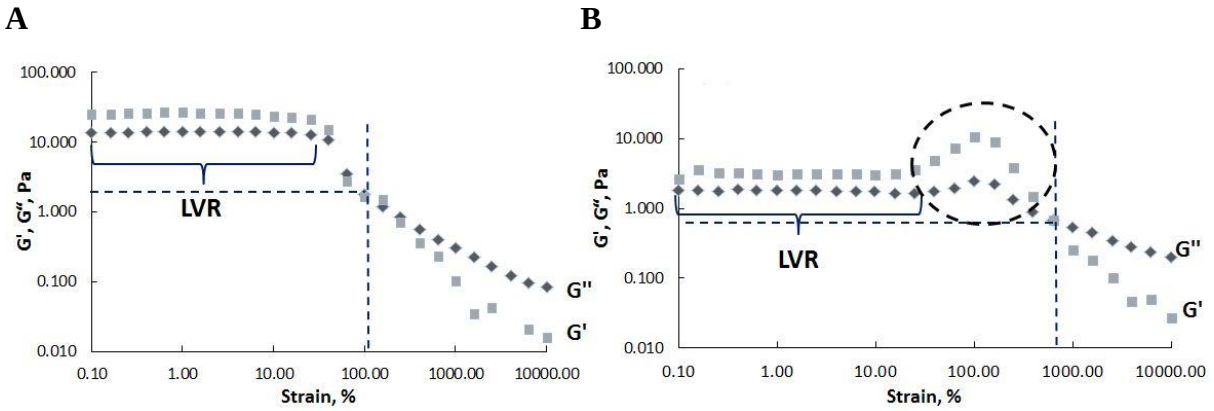

Figure 10. Deformation point detection by the response of elastic (G') and viscous (G") moduli in HA-fibrin **(A)** and fortified HA-fibrin systems **(B)** with 30% loaded NCs as a function of strain at 1 Hz. The range marked by dot-dash line represents an overshoot phenomenon. Fibrinogen was always taken at 1.5 mg/mL concentration, activity of Thr = 2 NIH-U/mL. The measurements were carried out at 37 °C. Expressed as mean ± SD; n = 3.

The oscillatory frequency sweeps exhibited a plateau-type behavior of the G' and G" modulus in the range 0.01-1 Hz for 30% NCs loaded non- and fortified HA-fibrin gels (*Supplementary materials*, **Figure S1**), which is indicative of a stable crosslinked network. In all the cases the hydrogel samples showed an increase in G' at higher frequencies assuming "solid-like" behavior characterized by an increase of the elastic modulus, moreover, the rate of increase being highest for 30% NCs loaded hydrogels. Interestingly, gels with incorporated 30% of NCs showed higher stability to deformations than blank gels and, thus, longer persistence, which could be explained by additional crosslinking of IPN by NCs, due to covalent and ionic interactions between shell polymer of NCs and fibrin network of the hydrogel.

These results indicate that the hydrogels composed of HA and fibrin, crosslinked with FXIII, and combined with NCs can be modulated with regard to their mechanical and elastic properties, in order to obtain a system that resists potential deformations in the articular cavity.

3.5. Surface morphology and porosity of in situ forming hydrogels

Topographic characterization of HA-fibrin and fortified HA-fibrin loaded with 30% of NCs was performed (*Supplementary materials*, **Table S1**). As an example, the topography of the blank HA-fibrin hydrogel (entry 1, **Table S1**) is shown in **Figure 11**. As it can be

observed, this hydrogel has a homogenous structure with normally distributed surface heights and valleys.

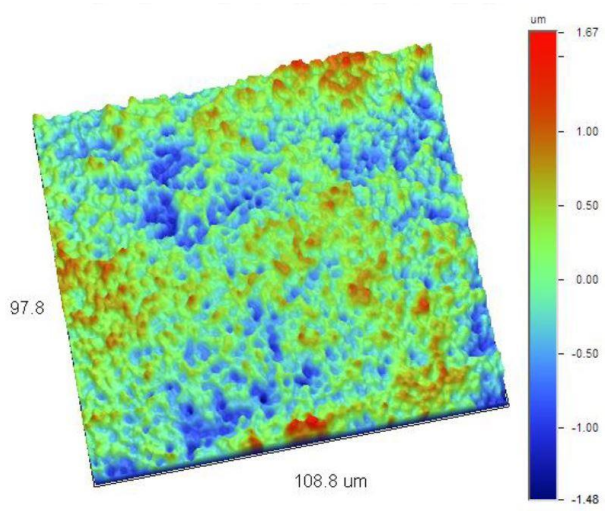

Figure 11. 3D topographical image of HA-fibrin hydrogel, obtained with the spatial resolution of the optical profiler at the field of view 97×108 μm^2. HA-fibrin hydrogel was prepared from 1 mg/mL fibrinogen, thrombin activity = 1 NIH-U/mL, 0.5% HAs mix solution of 1:1 (1.5 MDa : 700 kDa),10^{-4} M Ca^{2+} at 37 °C.

On the other hand, the average pore sizes for HA-fibrin and fortified HA-fibrin gels are summarized in **Table 7**. All the gel samples presented homogenous and well-determined pores with a low value of pore size distribution, which is the evidence of well-organized architecture. These data correlate well with the data obtained from SEM (*Section 3.8*).

Table 7. Mean pore size and depth of the different hydrogel compositions.

Sample	Mean pore diameter (μm)	Depth (μm)
HA-fibrin hydrogel	4.23 ± 0.89	1.07 ± 0.18
HA-fibrin hydrogel + 30% NCs	7.29 ± 1.23	0.7 ± 0.17
Fortified HA-fibrin hydrogel	3.26 ± 1.01	1.07 ± 0.41
Fortified HA-fibrin hydrogel + 30% NCs	4.88 ± 1.12	0.98 ± 0.12

According to these data, blank fortified HA-fibrin gels appeared to be more crosslinked with mean pore diameter 3.26 ± 1.01 μm compared to non-fortified HA-fibrin gels with mean value 4.23 ± 0.89 μm. The same tendency was observed for 30% NCs loaded fortified HA-fibrin, which is in agreement with the rheological results described above, and,

thus, have smaller pore size (4.88 ± 1.12 μm) than 30% NCs loaded HA-fibrin gels (7.29 ± 1.23 μm). The average pore diameter of fortified HA-fibrin NCs loaded gels (4.88 μm) only slightly exceeds the one of blank fortified HA-fibrin gels (3.26 μm), which is a good indication, meaning that FXIII provides sufficient crosslinking canvas and, thus, improves and maintains the structural rheology of the NCs-loaded gels.

At the next stage, NCs-loaded HA-fibrin hydrogels were formed upon mixing all components and extrusion by an ultra-fine insulin needle (29G) simulating conditions used for *in vivo* administration. Samples were incubated for 20 h at 37 ºC in order to form mature hydrogels, which were, then, lyophilized and analysed by SEM and FESEM (**Figure 12A, B, C,** and **D**).

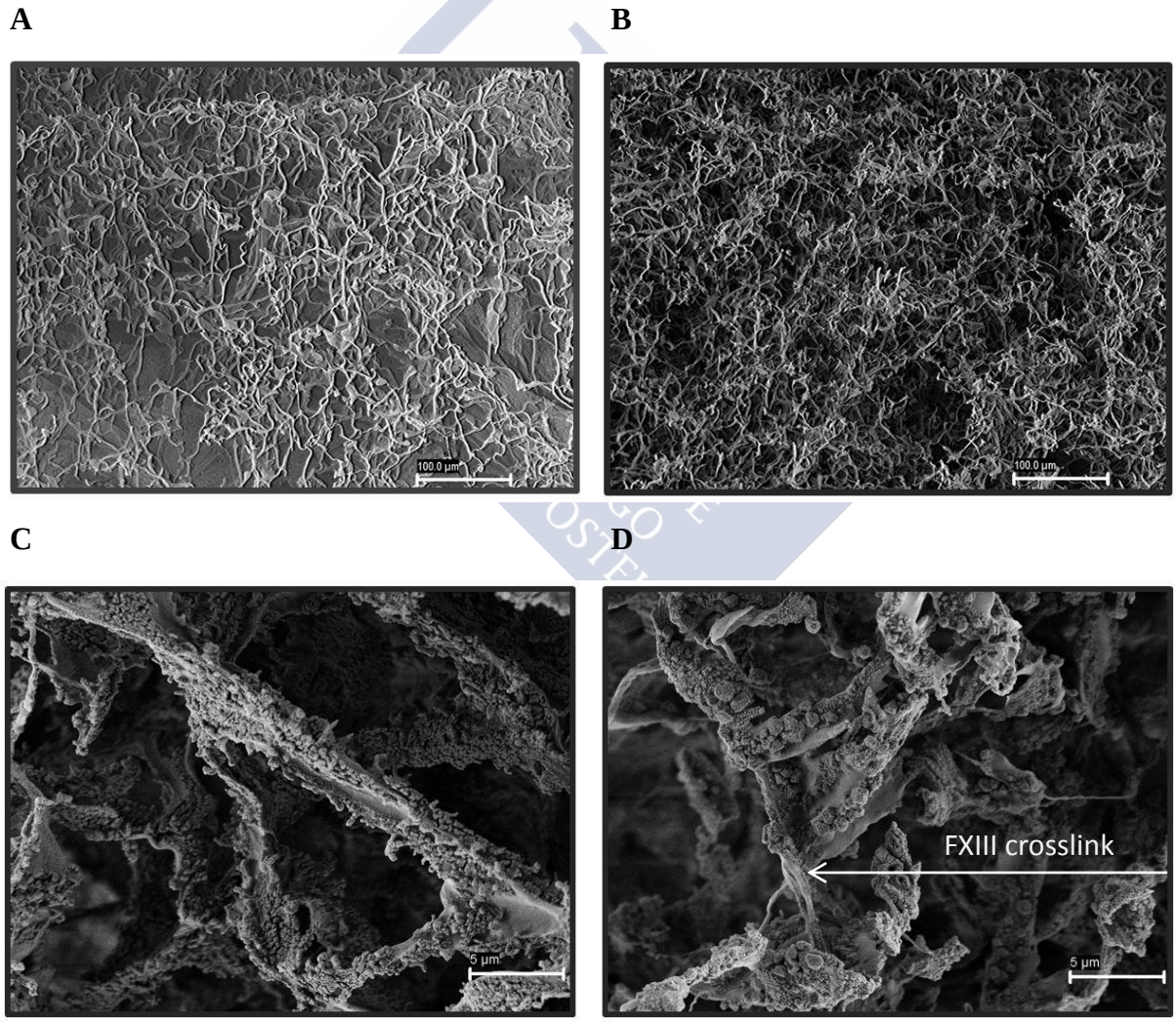

Figure 12. SEM images of the blank HA-fibrin (**A**) and blank fortified HA-fibrin hydrogels (**B**) at magnification is 500×. FESEM images of the blank HA-fibrin (**C**) and blank fortified HA-fibrin hydrogels (**D**) at magnification is 10,000×.

Analysis of the SEM images allowed us to visually evaluate the differences in non- and fortified HA-fibrin gels structure. As previously shown in the topography study, fortified HA-fibrin hydrogels have smaller pores compared to HA-fibrin hydrogels for both, blank and NCs loaded systems. Thus, SEM/FESEM studies confirmed that fortified HA-fibrin gel has more compact structure of the network, as porosity data indicated. We hypothesize, that possibly, one of the crosslinks of fibrin chains by FXIII was detected in **Figure 12D**. Microscopy images revealed fibrin gel fibrils with the diameter of 1-2 μm, such fibril thickness is an indication of stable fibrin hydrogels was described by several authors.[121,130]

Microscopy images of NCs-loaded hydrogels are shown at **Figure 13A** and **B**. HA NCs were found bound to fibrin fibrils. The crystals observed in the images of the gel fibrils are probably inorganic salts of $CaCl_2$, which are present in the polymerization buffer, that have high affinity to fibrin and are responsible for formation and stabilization of polymerization sites during the gelation process.[130,166]

A **B**

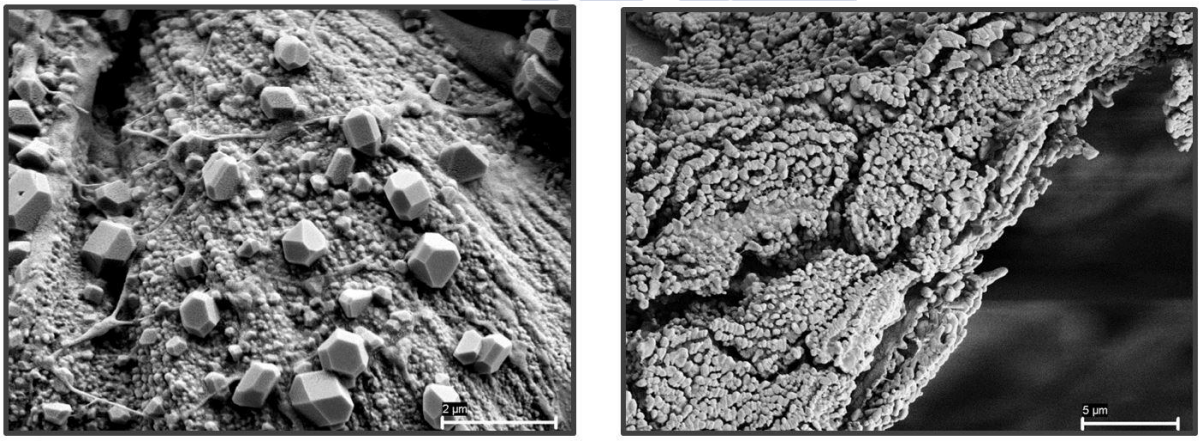

Figure 13. FESEM images of the HA-fibrin hydrogel with 30% of blank NCs (A) and fortified HA-fibrin hydrogel with 30% blank NCs (B) prepared by injection through the needle to PBS buffer (1:1.73). NCs appeared in the images as little round-shape particles bound to gel fibrils.

Section 3.6. Distribution of NCs within the in situ forming hydrogel

The distribution of Nile Red labeled NCs within the HA-fibrin hydrogel (30% loading) was observed by confocal electron microscopy. The images in **Figure 14A and B**

indicate that HA NCs are randomly dispersed in the hydrogel network. Possibly, HA NCs interact with the positively charged regions of fibrin and stay adhered to fibrin fibrils.

A **B**

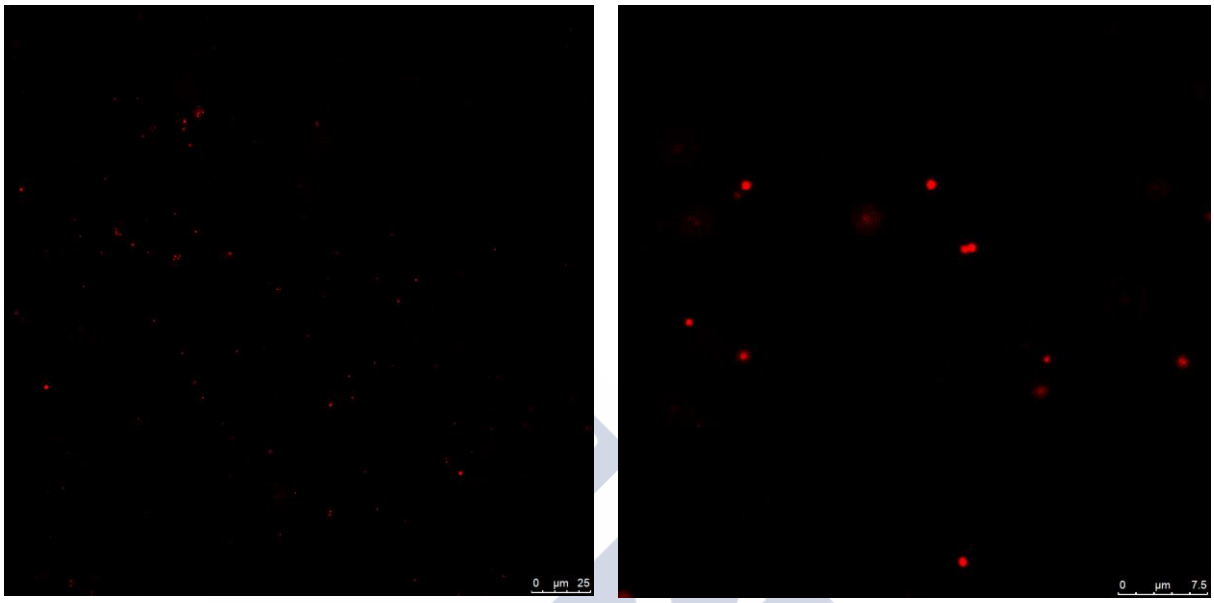

Figure 14. Confocal microscopy images of Nile Red-labeled HA NCs dispersed in the HA-Fibrin hydrogel (30% loading) (**A**). HA-fibrin hydrogel was prepared from 1.5 mg/mL fibrinogen, a (Thr) = 2 NIH-U/mL, 0.5% HAs mix solution 1:1 (1.5 MDa : 700 kDa), 10^{-3} M Ca^{2+} at 37 °C. Magnification is 320× (A), 1600× (**B**).

Section 3.7. In vitro DXM release from NCs containing hydrogels

The release studies of DXM were carried out under sink conditions for both, NCs and 30% NCs-loaded hydrogel, in SSF (RI = 1.334) at 37 °C.

In the case of the free NCs, a burst of approximately 70% DXM release was observed in the first hour of incubation in SSF, reaching 100% after 24 hours *(data not shown)*. In contrast, in the case of NCs loaded into the non-fortified HA-fibrin hydrogel (prepared as explained in **Table 3**) a slow release was observed in SSF (**Figure 15**). In this system, we have observed ~30% DXM release in the first time point, and then a slow release up to ~50% within 24 hours. In the next phase 24-60 h the drug was released gradually till 60%, between 60-72 h the gel started to slowly degrade and 100% of DXM release was reached at 72 h. Overall, the results underline the importance of the hydrogel in controlling the release of the drug that was incorporated within the NCs. Hence, both, the NCs and the hydrogel have a role in terms of controlling the release of DMX.

It is expected that the release from the fortified HA-fibrin hydrogel might be more prolonged due to slower rate of degradation. In this case, FXIII and α2-antiplasmin enzyme should retard the gel decomposition[167] at simulated and physiological environments.

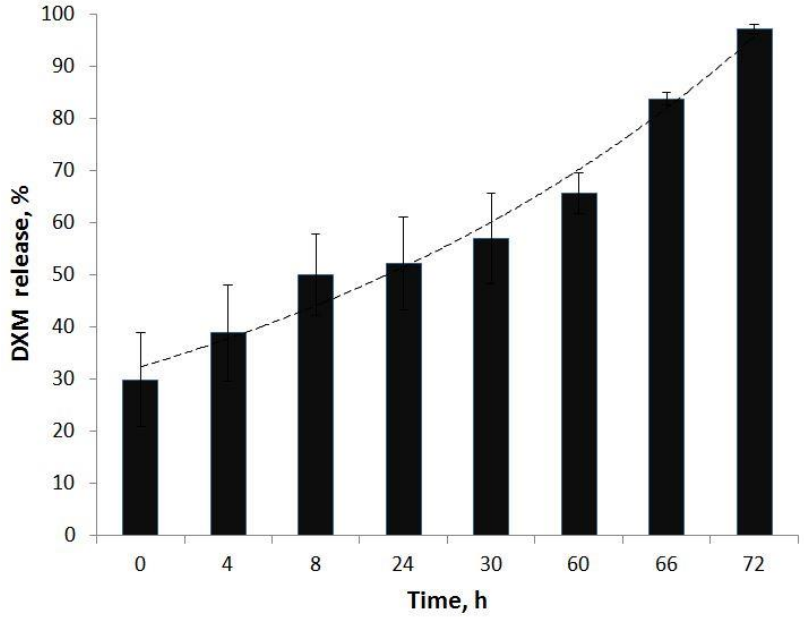

Figure 15. DXM release from HA-fibrin hydrogel with 30% loaded NCs to SSF incubated at 37 °C during 72 h. HA-fibrin hydrogel was prepared from: fibrinogen 1.5 mg/mL, thrombin 2 NIH-U/mL, 0.5% HAs mix solution 1:1 (1.5 MDa : 700 kDa), 10^{-3} M Ca^{2+}, 30% NCs.

These *in vitro* release results are in line with other previously reported in the literature. For example, Ranch *et al.* described a fast release of DMX from Carbopol® 940-gellan gum gels,[168] whereas Borden *et al.* reported a 72 h *in vitro* release profile.[169] On the other hand, Webber *et al.* reported the longest *in vitro* controlled release of DXM conjugated to a peptide-based nanofiber gels during 32 days.[170] Wu *et al.* have shown similar 1 month long *in vitro* release profile of DXM from micelles loaded into a PEG-PCL-PEG hydrogel.[82]

CONCLUSIONS

A novel *in situ* hydrogel that involves the mixture of gelling agents (HA, fibrin, thrombin and fortifying agents) with a suspension of HA nanocapsules has been developed and characterized. The gel is intended for the IA delivery of anti-inflammatory drugs, such as DXM. HA nanocapsules with mean particle size of 135 nm and negative surface charge, served as multi-reservoirs for DXM. The NCs were dispersed in the gel depot, in order to prevent their fast drainage from the articular cavity. The gel provided a controlled DXM release in simulated synovial fluid, for 72 h. NCs-loaded hydrogels have a well-organized structure with narrow pores sizes distribution and rheological behavior similar to the blank hydrogels, exhibiting high resistance to deformation, being suitable for intra-articular application. The developed hydrogel might also have self-healing properties, behaving as a viscosupplement and could work as an *in situ* cell scaffold, all these properties being of interest for the treatment of the degenerative joint diseases.

REFERENCES

1. Shi, J. *et al.* Distribution and alteration of lymphatic vessels in knee joints of normal and osteoarthritic mice. *Arthritis Rheumatol.* **66,** 657–666 (2014).

2. Chen, Y. Intra-Articular Drug Delivery Systems for Arthritis Treatment. *Rheumatol. Curr. Res.* **02,** (2012).

3. Gerwin, N., Hops, C. & Lucke, A. Intraarticular drug delivery in osteoarthritis. *Adv. Drug Deliv. Rev.* **58,** 226–242 (2006).

4. Kang, M. L. & Im, G.-I. Drug delivery systems for intra-articular treatment of osteoarthritis. *Expert Opin. Drug Deliv.* **11,** 269–82 (2014).

5. Evans, C. H., Kraus, V. B. & Setton., L. A. Progress in intra-articular therapy. *Nat. Rev. Rheumatol.* **10,** 11–22 (2015).

6. Edwards, S. H. R., Cake, M. a, Spoelstra, G. & Read, R. a. Biodistribution and clearance of intra-articular liposomes in a large animal model using a radiographic marker. *J. Liposome Res.* **17,** 249–261 (2007).

7. Cheung, P. & March, L. Y. N. Treatment of established rheumatoid arthritis. *Med. Today* **11,** 18–34 (2010).

8. Burt, H. M., Tsallas, A., Gilchrist, S. & Liang, L. S. Intra-articular drug delivery systems: Overcoming the shortcomings of joint disease therapy. *Expert Opin. Drug Deliv.* **6,** 17–26 (2009).

9. Larsen, C. *et al.* Intra-Articular Depot Formulation Principles : Role in the Management of Postoperative Pain and Arthritic Disorders. *J. Pharm. Sci.* **97,** (2008).

10. Bajpayee, A. G. & Grodzinsky, A. J. Cartilage-targeting drug delivery: can electrostatic interactions help? *Nat. Rev. Rheumatol.* **13,** 183–193 (2017).

11. Hellmich, D. *et al.* Acute treatment of facet syndrome by CT-guided injection of dexamethasone-21-palmitate alone and in combination with mepivacaine. *Clin. Drug Investig.* **24,** 559–569 (2004).

12. Bellamy, N. *et al.* Intraarticular corticosteroid for treatment of osteoarthritis of the knee. *Cochrane Database Syst Rev* CD005328 (2006). doi:10.1002/14651858.CD005328.pub2

13. Annual Report RecordatiPharma. *Annual Report*. (2016).

14. Enceladus Pharmaceuticals B.V. WO2013066179A1 Liposomal corticosteroids for treatment of inflammatory disorders in humans. 1–13 (2013).

15. Kapoor, B., Singh, S. K., Gulati, M., Gupta, R. & Vaidya, Y. Application of liposomes in treatment of rheumatoid arthritis: Quo vadis. *Sci. World J.* **2014,** (2014).

16. Barrera, P. *et al.* Synovial macrophage depletion with clodronate-containing liposomes in rheumatoid arthritis. *Arthritis Rheum.* **43,** 1951–1959 (2000).

17. Aalbers, C. J. *et al.* Empty Capsids and Macrophage Inhibition / Depletion Increase rAAV Transgene Expression in Joints of Both Healthy and Arthritic Mice. **00,** 1–11 (2016).

18. Valleala, H., Laitinen, K., Pylkkänen, L., Konttinen, Y. T. & Friman, C. Clinical and biochemical response to single infusion of clodronate in active rheumatoid arthritis--a double blind placebo controlled study. *Inflamm. Res.* **50,** 598–601 (2001).

19. Conaghan, P. G. *et al. In Pivotal Clinical Trials , FX006 Produces Sustained and Profound Analgesic Benefits in People With Osteoarthritis of the Knee*. (2017).

20. Flexion Therapeutics Inc. Clinical Trials. Study of FX006 for the Treatment of Pain in Patients With Osteoarthritis of the Knee NCT02357459,. 4–7 (2017).

21. Bodick, N. *et al.* FX006 prolongs the residency of triamcinolone acetonide in the synovial tissues of patients with knee osteoarthritis. *Osteoarthr. Cartil.* **21,** S144–S145 (2013).

22. Ho, M. J., Kim, S. R., Choi, Y. W. & Kang, M. J. A Novel Stable Crystalline Triamcinolone Acetonide-loaded PLGA Microsphere for Prolonged Release After Intra-Articular Injection. *Bull. Korean Chem. Soc.* **37,** 1496–1500 (2016).

23. Flexion Therapeutics Inc. ZILRETTA Prescribing Information. (2017).

24. Gierut, A., Perlman, H. & Pope, R. M. Innate Immunity and Rheumatoid Arthritis. *Rheum Dis Clin North Am.* **36,** 1–24 (2011).

25. Huang, G. & Zhang, Z. Micro- and nano-carrier mediated intra-articular drug delivery systems for the treatment of osteoarthritis. *J. Nanotechnol.* **2012,** (2012).

26. Vanniasinghe, A. S., Bender, V. & Manolios, N. The Potential of Liposomal Drug Delivery for the Treatment of Inflammatory Arthritis. *Semin. Arthritis Rheum.* **39,** 182–196 (2009).

27. Van Den Hoven, J. M. *et al.* Liposomal drug formulations in the treatment of rheumatoid arthritis. *Mol. Pharm.* **8,** 1002–1015 (2011).

28. Yang, M., Feng, X., Ding, J., Chang, F. & Chen, X. Nanotherapeutics relieve rheumatoid arthritis. *J. Control. Release* **252,** 108–124 (2017).

29. Dyondi, D., Lakhawat, R. & Banerjee, R. Biodegradable Nanoparticles for Intra-articular Therapy. (2009).

30. Danhier, F. *et al.* PLGA-based nanoparticles: An overview of biomedical applications. *J. Control. Release* **161,** 505–522 (2012).

31. Bartneck, M. *et al.* Liposomal encapsulation of dexamethasone modulates cytotoxicity, inflammatory cytokine response, and migratory properties of primary human macrophages. *Nanomedicine Nanotechnology, Biol. Med.* **10,** 1209–1220 (2014).

32. Bonanomi, M. H., Velvart, M., Stimpel, M., Fehr, K. & Weder, H. G. Studies of pharmacokinetics and therapeutic effects of glucocorticoids entrapped in liposomes after intraarticular application in healthy rabbits and in rabbits with antigen-induced arthritis. *Reumatol. Int. Clin. Exp. Investig.* 203–212 (1987).

33. Hofkens, W., Schelbergen, R., Storm, G., Berg, W. B. van den & Lent, P. L. van. Liposomal targeting of prednisolone phosphate to synovial lining macrophages during experimental arthritis inhibits M1 activation but does not favor M2 differentiation. *PLoS One* e54016 (2013).

34. Turker, S. *et al.* Gamma-irradiated liposome/noisome and lipogelosome/niogelosome formulations for the treatment of rheumatoid arthritis. *Interv. Med. Appl. Sci.* **5,** 60–69 (2013).

35. Srinath, P., Vyas, S. P. & Diwan, P. V. Preparation and pharmacodynamic evaluation of liposomes of indomethacin. *Drug Dev. Ind. Pharm.* **26,** 313–321 (2000).

36. Foong, W. C. & Green, K. L. Retention and Distribution of Liposome-entrapped [3H]Methotrexate Injected into Normal or Arthritic Rabbit Joints. *J. Pharm. Pharmacol.* **40,** 464–468 (1988).

37. Williams, a S., Camilleri, J. P., Goodfellow, R. M. & Williams, B. D. A single intra-articular injection of liposomally conjugated methotrexate suppresses joint inflammation in rat antigen-induced arthritis. *Br. J. Rheumatol.* **35,** 719–24 (1996).

38. Čeponis, A. *et al.* Effects of low-dose, noncytotoxic, intraarticular liposomal clodronate on development of erosions and proteoglycan loss in established antigen-induced arthritis in rabbits. *Arthritis Rheum.* **44,** 1908–1916 (2001).

39. Phillips, N. C., Thomas, D. P. P., Knight, C. G. & Dingle, J. T. Therapeutic activity in experimental arthritis. 553–557 (1979).

40. Horisawa, E. *et al.* Prolonged anti-inflammatory action of DL-lactide/glycolide copolymer nanospheres containing betamethasone sodium phosphate for an intra-articular delivery system in antigen-induced arthritic rabbit. *Pharm. Res.* **19,** 403–410 (2002).

41. Higaki, M., Ishihara, T., Izumo, N., Takatsu, M. & Mizushima, Y. Treatment of experimental arthritis with poly(D, L-lactic/glycolic acid) nanoparticles encapsulating betamethasone sodium phosphate. *Ann. Rheum. Dis.* **64,** 1132–1136 (2005).

42. Butoescu, N., Seemayer, C. a., Foti, M., Jordan, O. & Doelker, E. Dexamethasone-containing PLGA superparamagnetic microparticles as carriers for the local treatment of arthritis. *Biomaterials* **30,** 1772–1780 (2009).

43. Gómez-Gaete, C., Fattal, E., Silva, L., Besnard, M. & Tsapis, N. Dexamethasone acetate encapsulation into Trojan particles. *J. Control. Release* **128,** 41–49 (2008).

44. Liang, L. S., Wong, W. & Burt, H. M. Pharmacokinetic study of methotrexate following intra-articular injection of methotrexate loaded poly(L-lactic acid) microspheres in rabbits. *J. Pharm. Sci.* **94,** 1204–1215 (2005).

45. Liggins, R. T. *et al.* Intra-articular treatment of arthritis with microsphere formulations of paclitaxel: biocompatibility and efficacy determinations in rabbits. *Inflamm. Res.* **53,** 363–372 (2004).

46. Kawadkar, J. & Chauhan, M. K. Intra-articular delivery of genipin cross-linked chitosan microspheres of flurbiprofen: Preparation, characterization, in vitro and in vivo studies. *Eur. J. Pharm. Biopharm.* **81,** 563–572 (2012).

47. Zhang, J. X. *et al.* Local delivery of indomethacin to arthritis-bearing rats through polymeric micelles based on amphiphilic polyphosphazenes. *Pharm. Res.* **24,** 1944–1953 (2007).

48. Kang, M. L., Kim, J. E. & Im, G. Il. Thermoresponsive nanospheres with independent dual drug release profiles for the treatment of osteoarthritis. *Acta Biomater.* **39,** 65–78 (2016).

49. Kang, M. L., Kim, J. E., Ko, J.-Y. & Im., G.-I. Intra-articular delivery of kartogenin-conjugated chitosan nano/microparticles for cartilage retention. *Ann. Rheum. Dis.* **74,** 366.3–367 (2015).

50. Morgen, M. *et al.* Nanoparticles for improved local retention after intra-articular injection into the knee joint. *Pharm. Res.* **30,** 257–268 (2013).

51. Kim, S. R. *et al.* Cationic PLGA/eudragit RL nanoparticles for increasing retention time in synovial cavity after intra-articular injection in knee joint. *Int. J. Nanomedicine* **10,** 5263–5271 (2015).

52. Jamieson, E., Welch, E., Burke, R., Sakala, J. & Hrdy, M. *Cross-Linked Hyaluronate Monograph (Gel-One®).* 1–10 (2013).

53. Seikagaku Corporation & P80020/A014. Gel-One®. (2009).

54. Bellamy, N. *et al.* Viscosupplementation for the treatment of osteoarthritis of the knee. *The Cochrane database of systematic reviews* **2,** CD005321 (2006).

55. Goldberg, V. M. & Goldberg, L. Intra-articular hyaluronans: the treatment of knee pain in osteoarthritis. *J. Pain Res.* **3,** 51–56 (2010).

56. Strauss, E. J., Hart, J. a, Miller, M. D., Altman, R. D. & Rosen, J. E. Hyaluronic Acid Viscosupplementation and Osteoarthritis. *Am. J. Sports Med.* **37,** 1636–1644 (2009).

57. Dagenais, S. Intra-articular hyaluronic acid (viscosupplementation) for hip osteoarthritis. *Issues Emerg. Health Technol.* 1–4 (2007).

58. Blecher, A. M. Viscosupplementation: The Magic of Hyaluronic Acid Osteoarthritis of the knee. in *Southern California Orthopedic Institute* (2015).

59. *Instruction For Use Synvisc® (hylan G-F 20).* 1–6 (2014).

60. Migliore, a., Giovannangeli, F., Granata, M. & Laganà, B. Hylan G-F 20: Review of its safety and efficacy in the management of joint pain in osteoarthritis. *Clin. Med. Insights Arthritis Musculoskelet. Disord.* **3,** 55–68 (2010).

61. Edsman, K. *et al.* Intra-articular Duration of DurolaneTM after Single Injection into the Rabbit Knee. *Cartilage* **2,** 384–388 (2011).

62. Anika Therapeutics. *Intra-articular Monovisc™, Sumary of safety and effectiveness data*. 1–36 (2014).

63. Bashaireh, K., Naser, Z., Hawadya, K. Al, Sorour, S. & Al-Khateeb, R. N. Efficacy and safety of cross-linked hyaluronic acid single injection on osteoarthritis of the knee: A post-marketing phase IV study. *Drug Des. Devel. Ther.* **9,** 2063–2072 (2015).

64. Smith, M. M., Russell, A. K., Schiavinato, A. & Little, C. B. Hymovis™, a hexadecylamide hyaluronan derivative (hyadd®4-g), inhibits gene expression changes induced by interleukin-1b in chondrocytes and synovial fibroblasts derived from osteoarthritis patients. *Osteoarthr. Cartil.* **19,** S234 (2011).

65. Fidia instruction to use. Hymovis ® High Molecular Weight Viscoelastic Hyaluronan. 3–4 (2016).

66. Benazzo, F. *et al.* A multi-centre, open label, long-term follow-up study to evaluate the benefits of a new viscoelastic hydrogel (Hymovis®) in the treatment of knee osteoarthritis. *Eur. Rev. Med. Pharmacol. Sci.* **20,** 959–68 (2016).

67. Brown, T., Laurent, U. & Fraser. Turnover of hyaluronan in synovial joints: elimination of labelled hyaluronan from the knee joint of the rabbit. *Exp. Physiol.* **76,** 125–134 (1991).

68. *Monovisc Product Overview - Information Applies to Outside the US*. (2015).

69. Saito, S., Momohara, S., Taniguchi, A. & Yamanaka, H. The intra-articular efficacy of hyaluronate injections in the treatment of rheumatoid arthritis. *Mod. Rheumatol.* **19,** 643–651 (2009).

70. Intra-articular MONOVISC™. Knee guru. 17–19 (2015).

71. Zhang, Z. *et al.* Intra-articular injection of cross-linked hyaluronic acid-dexamethasone hydrogel attenuates osteoarthritis: An experimental study in a rat model of osteoarthritis. *Int. J. Mol. Sci.* **17,** (2016).

72. Song, J. *et al.* A phase I/IIa study on intra-articular injection of holmium-166-chitosan complex for the treatment of knee synovitis of rheumatoid arthritis. *Eur. J. Nucl. Med.* **28,** 489–497 (2001).

73. Cho, Y. J. *et al.* Radioisotope synoviorthesis with Holmium-166-chitosan complex in haemophilic arthropathy. *Haemophilia* **16,** 640–646 (2010).

74. Bolong Miao, Cunxian Song, G. M. Injectable Thermosensitive Hydrogels for Intra-Articular Delivery of Methotrexate. *J. Appl. Polym. Sci.* **21,** 449–456 (2011).

75. Appel, E. a *et al.* Self-assembled hydrogels utilizing polymer–nanoparticle interactions. *Nat. Commun.* **6,** 1–9 (2015).

76. Lei, Y., Rahim, M., Ng, Q. & Segura, T. Hyaluronic acid and fibrin hydrogels with concentrated DNA/PEI polyplexes for local gene delivery. *J. Control. Release* **153,** 255–261 (2011).

77. Liu, M. *et al.* Injectable hydrogels for cartilage and bone tissue engineering. *Bone Res.* **5,** 17014 (2017).

78. Petit, A. In situ forming hydrogels for intra-articular delivery of celecoxib : from polymer design to in vivo studies. (2014).

79. Sandker, M. J. *et al.* In situ forming acyl-capped PCLA-PEG-PCLA triblock copolymer based hydrogels. *Biomaterials* **34,** 8002–8011 (2013).

80. Bédouet, L. *et al.* Intra-articular fate of degradable poly(ethyleneglycol)-hydrogel microspheres as carriers for sustained drug delivery. *Int. J. Pharm.* **456,** 536–544 (2013).

81. Shan-Bin, G., Yue, T. & Ling-Yan, J. Long-term sustained-released in situ gels of a water-insoluble drug amphotericin B for mycotic arthritis intra-articular administration: preparation, in vitro and in vivo . *Drug Dev. Ind. Pharm.* **9045,** 1–10 (2014).

82. Wu, Q. *et al.* Thermosensitive hydrogel containing dexamethasone micelles for preventing postsurgical adhesion in a repeated-injury model. *Sci. Rep.* **5,** 13553 (2015).

83. Türker, S. *et al.* Scintigraphic imaging of radiolabelled drug delivery systems in rabbits with arthritis. *Int. J. Pharm.* **296,** 34–43 (2005).

84. Bédouet, L. *et al.* Synthesis of hydrophilic intra-articular microspheres conjugated to ibuprofen and evaluation of anti-inflammatory activity on articular explants. *Int. J. Pharm.* **459,** 51–61 (2014).

85. Liechty, W. B., Kryscio, D. R., Slaughter, B. V. & Peppas, N. a. Polymers for Drug Delivery Systems. *Annu. Rev. Chem. Biomol. Eng.* **1,** 149–173 (2010).

86. Vilela, C. *et al.* Cartilage repair using hydrogels: a critical review of in vivo experimental designs. *ACS Biomater. Sci. Eng.* 150813111234008 (2015). doi:10.1021/acsbiomaterials.5b00245

87. Suchaoin, W. *et al.* Novel bioadhesive polymers as intra-articular agents: Chondroitin sulfate-cysteine conjugates. *Eur. J. Pharm. Biopharm.* **101,** 25–32 (2016).

88. Masuko, K., Murata, M., Yudoh, K., Kato, T. & Nakamura, H. Anti-inflammatory effects of hyaluronan in arthritis therapy: Not just for viscosity. *Int. J. Gen. Med.* **2,** 77–81 (2009).

89. Mehta, D. P., Shodhan, K., Modi, R. I. & Ghosh, P. K. Sodium hyaluronate of defined molecular size for treating osteoarthritis. *Curr. Sci.* **92,** 209–213 (2007).

90. Ghosh, P. & Guidolin, D. Potential mechanism of action of intra-articular hyaluronan therapy in osteoarthritis: Are the effects molecular weight dependent? *Semin. Arthritis Rheum.* **32,** 10–37 (2002).

91. Niiyama, S., Happle, R. & Hoffmann, R. Use of Intra Articular Hyaluronic Acid in the Management of Knee Osteoarthritis in Clinical Practice. *Arthritis Care Res. (Hoboken).* **11,** 475–476 (2017).

92. Hari G. Garg, C. A. H. *Chemistry and Biology Hyaluronan*. (2004).

93. Wang, C. T., Lin, Y. T., Chiang, B. L., Lin, Y. H. & Hou, S. M. High molecular weight hyaluronic acid down-regulates the gene expression of osteoarthritis-associated cytokines and enzymes in fibroblast-like synoviocytes from patients with early osteoarthritis. *Osteoarthr. Cartil.* **14,** 1237–1247 (2006).

94. Castor, B. C. W. Hyaluronic Acid in Human Synovial Effusions; A Sensitive Indicator of Altered Connective Tissue Cell Function During Inflammation. *Arthritis Rheum.* **9,** 783–794 (1966).

95. Delmage, J. M., Powars, D. R., Jaynes, P. K. & Allerton, S. E. The selective suppression of immunogenicity by hyaluronic acid. *Ann. Clin. Lab. Sci.* **16,** 303–310 (1986).

96. Janmey, P. a, Winer, J. P. & Weisel, J. W. Fibrin gels and their clinical and bioengineering applications. *J. R. Soc. Interface* **6,** 1–10 (2009).

97. Li, Y., Meng, H., Liu, Y. & Lee, B. P. Fibrin Gel as an Injectable Biodegradable Scaffold and Cell Carrier for Tissue Engineering. **2015,** (2015).

98. Kirilak, Y. *et al.* Fibrin sealant promotes migration and proliferation of human articular chondrocytes : Possible involvement of thrombin and protease-activated receptors. 551–558 (2006).

99. Lee, F. & Kurisawa, M. Formation and stability of interpenetrating polymer network hydrogels consisting of fibrin and hyaluronic acid for tissue engineering. *Acta Biomater.* **9,** 5143–5152 (2013).

100. Rampichová, M. *et al.* Fibrin/hyaluronic acid composite hydrogels as appropriate scaffolds for in vivo artificial cartilage implantation. *ASAIO J.* **56,** 563–568 (2010).

101. Zhang, Y., Heher, P., Hilborn, J., Redl, H. & Ossipov, D. a. Hyaluronic acid-fibrin interpenetrating double network hydrogel prepared in situ by orthogonal disulfide cross-linking reaction for biomedical applications. *Acta Biomater.* **38,** 23–32 (2016).

102. Myers, K. R., Sgaglione, N. a & Grande, D. a. Trends in biological joint resurfacing. *Bone Joint Res.* **2,** 193–9 (2013).

103. Karp, J. M., Sarraf, F., Shoichet, M. S. & Davies, J. E. Fibrin-filled scaffolds for bone-tissue engineering: An in vivo study. *J. Biomed. Mater. Res. - Part A* **71,** 162–171 (2004).

104. Snyder, T. N., Madhavan, K., Intrator, M., Dregalla, R. C. & Park, D. A fibrin/hyaluronic acid hydrogel for the delivery of mesenchymal stem cells and potential for articular cartilage repair. *J. Biol. Eng.* **8,** 10 (2014).

105. Kim, D. Y. *et al.* Tissue-engineered allograft tracheal cartilage using fibrin/hyaluronan composite gel and its in vivo implantation. *Laryngoscope* **120,** 30–38 (2010).

106. Park SH, Park SR, Chung SI, Pai KS, M. B. Tissue-engineered Cartilage Using Fibrin/Hyaluronan Composite Gel and Its In Vivo Implantation. **29,** 838–860 (2005).

107. Park, S.-H. *et al.* Silk-Fibrin/Hyaluronic Acid Composite Gels for Nucleus Pulposus Tissue Regeneration. *Tissue Eng. Part A* **17,** 2999–3009 (2011).

108. LeBoeuf, R. D., Raja, R. H., Fuller, G. M. & Weigel, P. H. Human fibrinogen specifically binds hyaluronic acid. *J. Biol. Chem.* **261,** 12586–12592 (1986).

109. Weigel, P. H., Fuller, G. M. & LeBoeuf, R. D. A model for the role of hyaluronic acid and fibrin in the early events during the inflammatory response and wound healing. *J. Theor. Biol.* **119,** 219–234 (1986).

110. Frost, S. J. & Weigel, P. H. Binding of hyaluronic acid to mammalian fibrinogens. *BBA - Gen. Subj.* **1034,** 39–45 (1990).

111. Park, S. H., Cui, J. H., Park, S. R. & Min, B. H. Potential of fortified fibrin/hyaluronic acid composite gel as a cell delivery vehicle for chondrocytes. *Artif. Organs* **33,** 439–447 (2009).

112. Francis W and Marder, J. Increased resistance to plasmic degradation of fibrin with highly crosslinked alpha-polymer chains formed at high factor XIII concentrations. *Blood* **71,** (1988).

113. Muszbek, L., Bereczky, Z., Bagoly, Z., Komáromi, I. & Katona, É. Factor XIII: a coagulation factor with multiple plasmatic and cellular functions. *Physiol. Rev.* **91,** 931–972 (2011).

114. Lorand, L. Factor XIII: structure, activation, and interactions with fibrinogen and fibrin. *Ann. N. Y. Acad. Sci.* **936,** 291–311 (2001).

115. Tsurupa, G., Yakovlev, S., McKee, P. & Medved, L. Noncovalent interaction of alpha(2)-antiplasmin with fibrin(ogen): localization of alpha(2)-antiplasmin-binding sites. *Biochemistry* **49,** 7643–7651 (2010).

116. Carpenter, S. L. & Mathew, P. α2-antiplasmin and its deficiency: Fibrinolysis out of balance. *Haemophilia* **14,** 1250–1254 (2008).

117. Lee, K. N. *et al.* Antiplasmin-cleaving enzyme is a soluble form of fibroblast activation protein. *Blood* **107,** 1397–1404 (2006).

118. Palmer, M., Stanford, E. & Murray, M. M. The effect of synovial fluid enzymes on the biodegradability of collagen and fibrin clots. *Materials (Basel).* **4,** 1469–1482 (2011).

119. Lorentz, K. M., Kontos, S., Frey, P. & Hubbell, J. a. Engineered aprotinin for improved stability of fibrin biomaterials. *Biomaterials* **32,** 430–438 (2011).

120. Alves, C. S., Yakovlev, S., Medved, L. & Konstantopoulos, K. Biomolecular characterization of CD44-fibrin(ogen) binding distinct molecular requirements mediate binding of standard and variant isoforms of CD44 to immobilized fibrin(ogen). *J. Biol. Chem.* **284,** 1177–1189 (2009).

121. Chiu, C. L., Hecht, V., Duong, H., Wu, B. & Tawil, B. Permeability of Three-Dimensional Fibrin Constructs Corresponds to Fibrinogen and Thrombin Concentrations. *Biores. Open Access* **1,** 34–40 (2012).

122. Lasa, M., Brook, M., Saklatvala, J. & Clark, A. R. Dexamethasone Destabilizes Cyclooxygenase 2 mRNA by Inhibiting Mitogen-Activated Protein Kinase p38 Dexamethasone Destabilizes Cyclooxygenase 2 mRNA by Inhibiting Mitogen-Activated Protein Kinase p38. *Mol. Cell. Biol. Biol.* **21,** 771–780 (2001).

123. ProCore BioMed LTD. RegenoGel™ and RegenoGel™-OSP - Next Generation product for Degenerative Joint Diseases. 1–3 (2017).

124. Study, N., View, F. T., View, T., Study, N. & Posted, R. Trial record 9 of 10 for : intra-articular gels drugs A Phase I , Prospective , Randomized , Open-label , Active-Controlled Clinical Trial for Safety Evaluation of Intra-articular Injection of RegenoGel-SP for the Treatment of Moderate to Severe Osteoarth. 1–6 (2017).

125. Avner Yayon, Meital Ben-Dayan Bloch, Ezequiel Wexselblatt, Ron Arbel, G. A. A Chondrogenic Fibrin-HA Hybrid Proteoglycan for OA Pain Relief and Cartilage Preservation from Bench to Clinics. 1–106 (2017).

126. Prego, C., Fabre, M., Torres, D. & Alonso, M. J. Efficacy and mechanism of action of chitosan nanocapsules for oral peptide delivery. *Pharm. Res.* **23,** 549–556 (2006).

127. Iqbal, M. S., Shad, M. a., Ashraf, M. W., Bilal, M. & Saeed, M. Development and Validation of an HPLC Method for the Determination of Dexamethasone, Dexamethasone Sodium Phosphate and Chloramphenicol in Presence of Each Other in Pharmaceutical Preparations. *Chromatographia* **64,** 219–222 (2006).

128. Samtani, M. N. & Jusko., W. J. Quantification of dexamethasone and corticosterone in rat biofluids and fetal tissue using highly sensitive analytical methods: assay validation and application to a pharmacokinetic study. **48,** 1–6 (2010).

129. Cristina, M., Urban, C., Mainardes, R. M., Palmira, M. & Gremião, D. Development and validation of HPLC method for analysis of dexamethasone acetate in microemulsions. **45,** (2009).

130. Lugovskoy, E.V., Makogonenko, E.M., Komisarenko, S. *Molecular Mechanisms of formation and degradation of fibrin* (2013).

131. Gaffney, P. & Edgell, T. The International and NIH units for thrombin--how do they compare. *Thromb Haemost.* **74,** 900–3. (1995).

132. Margareth RC & Raimar L. Simulated biologic fluids with possible application in dissolution testing. *Dissolutio Technol.* 15–28 (2011).

133. Lutolf, M. P. & Hubbell, J. a. Synthesis and physicochemical characterization of end-linked poly(ethylene glycol)-co-peptide hydrogels formed by Michael-type addition. *Biomacromolecules* **4,** 713–722 (2003).

134. Butoescu, N., Jordan, O. & Doelker, E. Intra-articular drug delivery systems for the treatment of rheumatic diseases: A review of the factors influencing their performance. *Eur. J. Pharm. Biopharm.* **73,** 205–218 (2009).

135. Alonso, M. J. & Garcia-Fuentes, M. *Nano-Oncologicals: New Targeting and Delivery Approaches*. (2014).

136. Hillaireau, H. & Couvreur, P. Nanocarriers' entry into the cell: Relevance to drug delivery. *Cell. Mol. Life Sci.* **66,** 2873–2896 (2009).

137. Clemons, T. D., Viola, H. M., House, M. J., Hool, L. C. & Iyer, K. S. *The Design and Testing of Multifunctional Nanoparticles for Drug Delivery Applications*. **6,** 978–981 (2016).

138. Horisawa, E. *et al.* Size-Dependency of DL-Lactide Glycolide Copolymer Particulates for\rIntra-Articular Delivery System on Phagocytosis in Rat Synovium. *Pharm. Res.* **19,** 132–139 (2002).

139. Laura Brown, Cui, H. & Wu, Z. Method of treatment for osteoarthritis by local intra-articular injection of microparticles. (2007).

140. Haywood, L. & Walsh, D. a. Vasculature of the normal and arthritic synovial joint. *Histol. Histopathol.* **16,** 277–284 (2001).

141. Janssen, M., Mihov, G., Welting, T., Thies, J. & Emans, P. Drugs and polymers for delivery systems in OA joints: Clinical needs and opportunities. *Polymers (Basel).* **6,** 799–819 (2014).

142. Fezai, M., Senovilla, L., Jemaà, M., Ben-Attia, M. & Ben-Attia, M. Analgesic, Anti-Inflammatory and Anticancer Activities of Extra Virgin Olive Oil. *J. Lipids* **2013,** 1–7 (2013).

143. Cecerale, S. in *Olive oil - Constituents, Health Properties and Bioconversions* (INTECH, 2011).

144. Moghimipour, E., Salimi, A., Karami, M. & Isazadeh, S. Preparation and characterization of dexamethasone microemulsion based on pseudoternary phase diagram. *Jundishapur J. Nat. Pharm. Prod.* **8,** 105–112 (2013).

145. Chime, S. a, Kenechukwu, F. C. & Attama, a a. Nanoemulsions — Advances in Formulation , Characterization and Applications in Drug Delivery. (2014).

146. Mourdikoudis, S. & Liz-Marzán, L. M. Oleyamine in Nanoparticle Synthesis. *Chem. Mater.* **25,** 1465 (2013).

147. Oyarzun-Ampuero, F., Rivera-Rodriguez, G. R., Alonso, M. J. & Torres, D. Hyaluronan nanocapsules as a new vehicle for intracellular drug delivery. *Eur. J. Pharm. Sci.* **49,** 483–490 (2013).

148. Chernyshev, V. S. *et al.* Size and shape characterization of hydrated and desiccated exosomes. *Anal. Bioanal. Chem.* **407,** 3285–3301 (2015).

149. Lugovskoy, E. V. Molecular background of fibrin clotting. *Monograph* 2009 (2009).

150. Averett, L. E. & Schoenfisch, M. H. Atomic force microscope studies of fibrinogen adsorption. *Analyst* **135,** 1201–1209 (2010).

151. Weisel, J. W. & Medved, L. The structure and function of the alpha C domains of fibrinogen. *Ann. N. Y. Acad. Sci.* **936,** 312–327 (2001).

152. Chernysh, I. N., Nagaswami, C. & Weisel, J. W. Visualization and identification of the structures formed during early stages of fibrin polymerization Visualization and identification of the structures formed during early stages of fibrin polymerization. **117,** 4609–4614 (2011).

153. Piccirilli, E. *et al.* Viscosupplementation with intra-articular hyaluronic acid for hip disorders. A systematic review and meta-analysis. (3) *Muscles, Ligaments and Tendons Journal*. **6** (3), 293–299 (2016).

154. Eymard, F. *et al.* Predictors of response to viscosupplementation in patients with hip osteoarthritis: results of a prospective, observational, multicentre, open-label, pilot study. *BMC Musculoskelet. Disord.* **18,** 1–8 (2017).

155. Leboeuf, R. D., Gregg, R. R., Weigel, P. H. & Fuller, G. M. Effects of Hyaluronic Acid and Other Glycosaminoglycans on Fibrin Polymer Formation. 6052–6057 (1987).

156. Gobbo, S. & Petrella, R. J. Hyaluronic acid binary mixtures and therapeutic use thereof. **1,** 1–20 (2009).

157. Petrella, R. J., Cogliano, A. & Decaria, J. Combining two hyaluronic acids in osteoarthritis of the knee: A randomized, double-blind, placebo-controlled trial. *Clin. Rheumatol.* **27,** 975–981 (2008).

158. MDT Int'l s.a. RenehaVis instruction for use. (2011).

159. LSP Bio Ltd. RenehaVis broshure. (2013).

160. Moreland, L. W. Intra-articular hyaluronan (hyaluronic acid) and hylans for the treatment of osteoarthritis: mechanisms of action. *Arthritis Res. Ther.* **5,** 54–67 (2003).

161. Aya, K. L. & Stern, R. Hyaluronan in wound healing: Rediscovering a major player. *Wound Repair Regen.* **22,** 579–593 (2014).

162. Berg, J., Tymoczko, J. & Strye, L. *Biochemistry 7th Edition*. 1–1224 (2011).

163. Choi, B., Loh, X. J., Tan, A., Loh, C. K. & Ye, E. *Introduction to In Situ Forming Hydrogels for Biomedical Applications*. (2015). doi:10.1007/978-981-287-152-7

164. Nesrinne, S. & Djamel, A. Synthesis, characterization and rheological behavior of pH sensitive poly(acrylamide-co-acrylic acid) hydrogels. *Arab. J. Chem.* **10,** 539–547 (2017).

165. Lovejoy, A. E. *et al.* Safety and pharmacokinetics of recombinant factor XIII-A 2 administration in patients with congenital factor XIII deficiency. *Hematology* **108,** 57–62 (2006).

166. Dang, C. V., Ebert, R. F. & Bell, W. R. Localization of a fibrinogen calcium binding site between γ-subunit positions 311 and 336 by terbium fluorescence. *J. Biol. Chem.* **260,** 9713–9719 (1985).

167. Mosesson, M. W. *et al.* Evidence that a2-antiplasmin becomes covalently ligated to plasma fibrinogen in the circulation: A new role for plasma factor XIII in fibrinolysis regulation. *J. Thromb. Haemost.* **6,** 1565–1570 (2008).

168. Ranch, K. *et al.* Development of in situ ophthalmic gel of dexamethasone sodium phosphate and chloramphenicol: A viable alternative to conventional eye drops. *J. Appl. Pharm. Sci.* **7,** 101–108 (2017).

169. Borden, R. C. *et al.* Hyaluronic acid hydrogel sustains the delivery of dexamethasone across the round window membrane. *Audiol. Neurotol.* **16,** 1–11 (2010).

170. Webber, M. J., Matson, J. B., Tamboli, V. K. & Stupp, S. I. Controlled release of dexamethasone from peptide nanofiber gels to modulate inflammatory response. *Biomaterials* **33,** 6823–6832 (2012).

171. Leach, R. *Optical Measurement of Surface Topography*. (2012).

Supplementary materials

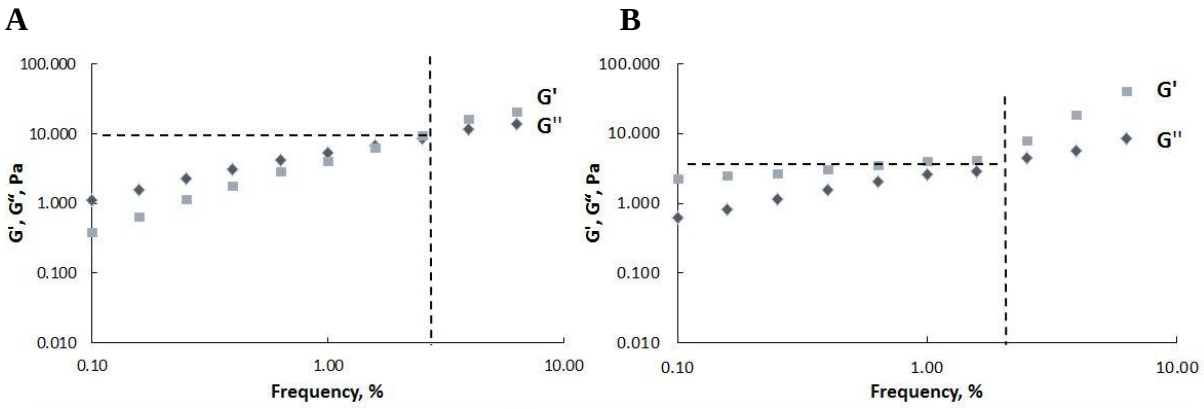

Figure S1. Deformation point detection by the response of elastic (G') and viscous (G") moduli in HA-fibrin **(A)** and fortified HA-fibrin systems **(B)** with 30% loaded NCs as a function of frequency at torque 0.5 μN·m. Fibrinogen was always taken at 1.5 mg/mL concentration, activity of Thr = 2 NIH-U/mL. The measurements were carried out at 37 °C. Expressed as mean ± SD; n = 3.

Hydrogels 3D roughness parameters (S_{sk}, which represents the degree of symmetry of the surface heights distribution about the mean plane, and S_{ku}, which indicates the nature of the height distribution)[171] are gathered in **Table S1**.

Table S1. Experimental roughness results from different zoomed areas of hydrogel samples. S_{sk} = 0: Symmetrical about the average line (normal distribution), S_{sk} > 0: skewed downward relative to the average line S_{sk} < 0: skewed upward relative to the average line. S_{ku} = 3: normal distribution, S_{ku} > 3: the height distribution is spiked. S_{ku} < 3: the form of the surface roughness height distribution is squashed.

Sample	3D Roughness Parameters	
	S_{sk}	S_{ku}
HA-fibrin hydrogel		
Area 1 (Field of View 97×108 μm^2)	0.01	3.00
Area 2 (Field of View 63×73 μm^2)	0.19	3.42
Area 3 (Field of View 53×61 μm^2)	-0.09	3.00
HA-fibrin hydrogel + 30% NCs		
Area 1 (Field of View 98×124 μm^2)	-0.17	3.08
Area 2 (Field of View 103×129 μm^2)	-0.30	3.17
Area 3 (Field of View 87×109 μm^2)	-0.61	3.23
Fortified HA-fibrin hydrogel		
Area 1 (Field of View 84×108 μm^2)	0.25	3.11
Area 2 (Field of View 90×110 μm^2)	0.62	7.21
Area 3 (Field of View 74×94 μm^2)	0.36	3.51
Fortified HA-fibrin hydrogel + 30% NCs		
Area 1 (Field of View 97×136 μm^2)	0.34	7.28
Area 2 (Field of View 101×131μm^2)	-0.03	2.67
Area 3 (Field of View 91×110 μm^2)	0.39	4.47

USC
UNIVERSIDADE
DE SANTIAGO
DE COMPOSTELA

Chapter 2

New galectin-3 inhibitor as a lead compound for anti-inflammatory drug candidate

> All the truths are easy to understand once they are discovered; the point is to discover them.
>
> *Galileo Galilei*

This work was done in collaboration with Dr. Sandra Isabel Dias Simões[1] and Dr. Madalena Monteiro[2]

[1]*Faculdade de Farmácia, Universidade de Lisboa, 1649-003 Lisboa, Portugal*

[2]*Laboratório de Patologia, Instituto Nacional de Investigação Agrária e Veterinária, 2780-157 Oeiras – Portugal*

USC
UNIVERSIDADE
DE SANTIAGO
DE COMPOSTELA

ABSTRACT

Rheumatoid arthritis (RA) is a chronic autoimmune disorder that primarily affects the joints. This disease is characterized by synovial inflammation and swelling, finally leading to joints cartilage and bone destruction. Nowadays RA is a non-curable disease guiding to the lethal outcome. The etiology of this disease is vague and remains the subject of intense research. Current therapies for RA include antagonists of COX-2 and pro-inflammatory cytokines TNF-α, IL-1, IL-6, however do not lead to the adequate alleviation of the inflammatory joint diseases.

The extracellular protein galectin-3 (Gal-3) has recently found to be a primer trigger of inflammation in autoimmune diseases, in particular in RA, attracting attention as a new potential immunotherapeutic target. The inhibition of Gal-3 by high-affine compounds based on β-galactoside motifs has recently seen major breakthrough. The design, synthesis and characterization of a highly selective and potent Gal-3 antagonist are reported in this chapter. To this aim, aromatic substituents have been introduced at positions 3'-C of the galactose and 2-C of the glucosamine residues of type II lactosamine core [Galβ(1→4)-GlcN], used as the starting material. Such modifications resulted in considerably enhanced affinity, K_d = 590 nM (4 °C), due to the establishment of cation-π interactions between the arene substituents with guanidinium ions of two key arginine residues (Arg144 and Arg186) of the Gal-3 carbohydrate recognition domain. Subsequently, the inhibitor was encapsulated in an *in situ* hydrogel developed for intra-articular administration (described in **Chapter 1**, *Section 2.3*). First, the inhibitor was encapsulated in hyaluronic acid (HA) nanocapsules (NCs) that act as lipophilic reservoirs for the drug, and later, the NCs were included in a HA-fibrin hydrogel. Anti-inflammatory properties of Gal-3 inhibitor were evaluated in a rat carrageenan-induced knee joint synovitis model. The inhibitor incorporated in the hydrogel and administered intra-articularly at microgram scale doses, showed a remarkable suppression of inflammation, being a potential drug candidate for RA treatment.

1. INTRODUCTION

Rheumatoid arthritis (RA) is a chronic autoimmune disorder that primarily affects diartroidal joints causing synovial inflammation and swelling.[1–3] Besides, the disease is characterized by the production of autoantibodies and, at advanced stages, cartilage and bone destruction.[4] The etiology of this disease is vague and remains the subject of intense research.[1,5,6] So far, RA is a non-curable disease, affecting about 1% of globe population and guiding to the lethal outcome.[1,7] Over the last decades, the pace of development of RA significantly increased with a tendency ~4.1% for USA inhabitants per year.[3,7,8]

RA affects mostly small joints, leading to their deformation and affecting theirs performance. As the disease progresses, symptoms often spread to the wrists, knees, ankles, elbows, hips and shoulders. In most of the cases, symptoms occur in the same joints on both sides of the body representing bilateral symmetry.[3,9] In addition, RA may produce extra-articular manifestations, affecting other organs of the body, *e.g*. skin, eyes, lungs and blood vessels.[10] The factors amplifying the risk of RA development include non-modifiable: i) gender (women are more predisposed to develop RA than men, 4:1, respectively)[11]; ii) age (RA typically occurs between the ages of 40 and 60); iii) genetics (it can be inherited due to the family history)[7] and modifiable: overweight and obesity, joint injuries, infection, and occupation.[12]

As an autoimmune disorder, RA occurs when the immune system mistakenly attacks the synovial membrane. Among the immune cells involved in this disease are leukocytes (neutrophils), lymphocytes (memory $CD4^+$, $CD8^+$ T cells and B-cells), monocytes, synovial macrophages, dendritic cells and mast cells.[6] These cells play important roles in the autoimmune process, releasing pro-inflammatory cytokines (TNF-α, IL-1, IL-6, and TGF-β), chemokines, matrix metalloproteinases (MMPs), cathepsins, vasoactive amines and proteases.[1,13,14] These molecules lead to hyperplasia of synovial tissues,[7] synovial fluid (SF) accumulation,[15] followed by joint inflammation,[7] pain, stiffness, swelling[16] and subsequent degradation of articular cartilage,[2] bone and ligaments[1,17] (**Figure 1**).

Current therapies for RA include antagonists of COX-2 and pro-inflammatory cytokines TNF-α, IL-1, IL-6, like ibuprofen,[18] dexamethasone,[19] methotrexate,[20,21] infliximab,[22] etc. However these treatments do not lead to the adequate alleviation of the inflammatory joint diseases, as far as none of drugs exhibit joints specificity.[2,23–26]

Protein galectin-3 (Gal-3), once shuttled to the extracellular space, has recently been found to be a primer trigger of inflammation that favours the secretion of macrophage pro-inflammatory cytokines.[27–32,13] Gal-3 is expressed in neutrophils, basophils, eosinophils, macrophages, dendritic,[33–37] and mast cells,[24] and has considerable effects on both innate and adaptive immunity.[30] Innate immune functions of Gal-3 are cell activation, adhesion, migration, and promotion of pathogens phagocytosis (including mycobacteria, fungi, and parasites)[30] as well as autophagy.[38] It is both pro-inflammatory and anti-inflammatory mediator, working as a chemoattractant for monocytes, macrophages, followed by macrophages polarization,[39] and increasing the amount of neutrophils.[30]

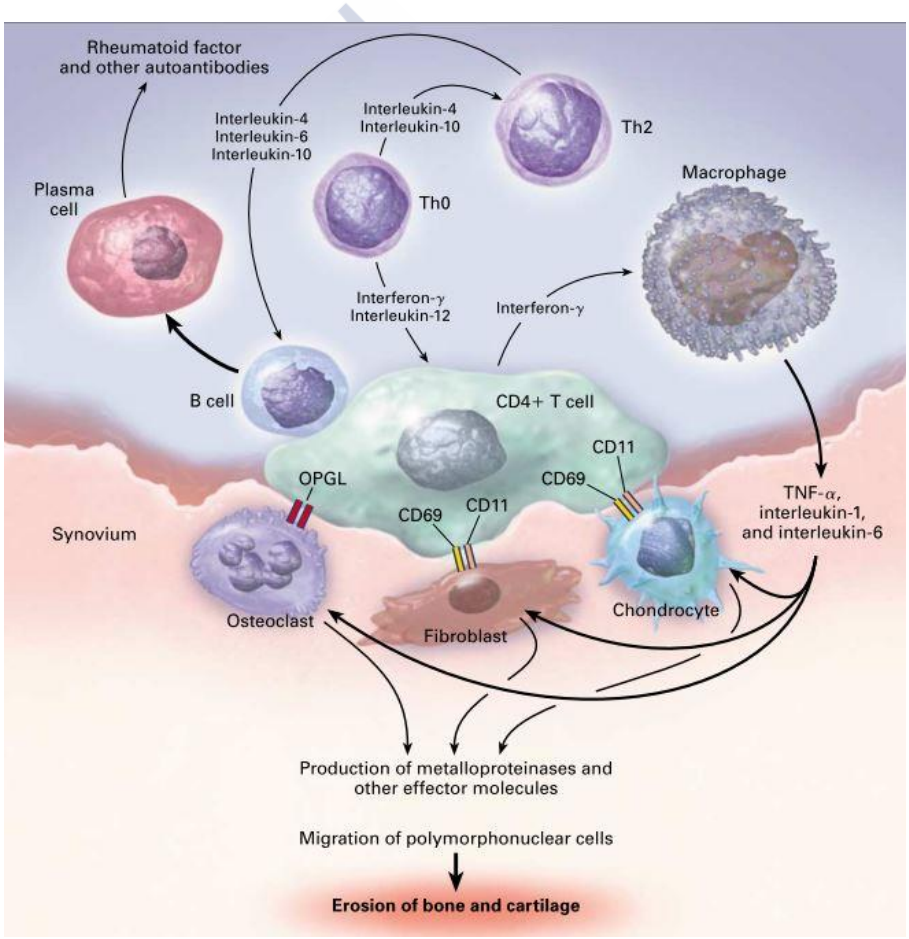

Figure 1. Pro-inflammatory cytokines signaling pathways involved in rheumatoid arthritis. Reproduced with permission from,[17] Copyright © 2001 Massachusetts Medical Society.

In adaptive immune system, Gal-3 exhibits immunosuppressive effect, restricting T cell receptor recruitment into immune synapses, prevents T cell proliferation, differentiation, and directly promotes T cell apoptosis,[30] resulting in prolonged inflammation.[40] On the other

hand, Gal-3 anti-inflammatory activity includes phagocytosis of dead cells and stimulation of wound healing.[30]

As reported, Gal-3 expression is up-regulated in synovial tissues in RA,[24] reaching a concentration in SF of 130-300 ng/mL (once about 50 ng/mL found at normal state)[13] and being a pro-inflammatory regulator and presenting immunosuppressive effect, it amplifies and prolong the inflammation.[30,40] Noticeably, Gal-3 stimulates synovial fibroblasts and immune cells to release pro-inflammatory cytokines (TNF-α, IL-6, IL-17), chemokines (CCL2, CCL3, CCL5, CXCL8)[13] and the expression of different matrix metalloproteinases.[41,42] These enzymes are involved in the degradation of the extracellular matrix (ECM)[41] and destroy specifically type I-III collagen, leading to tissue remodelling.[43,44] Besides, they inhibit the osteocalcin production,[36] leading to bone demineralization,[13] and, finally, causing joint degradation.[6,45] In addition, IA injection of recombinant galectin-3 in mice induced cartilage and subchondral bone lesions.[36,40] Taking into account such involvement into pathophysiology of RA, Gal-3 appears as a novel potential immunotherapeutic target.

Currently, three Gal-3 antagonists have entered clinical trials for the treatment of different pathologies: DAVANAT® (GM-CT-01), GR-MD-02, and TD139.[46–54] However, none of them was tested for RA treatment. Taking into account their success in clinical trials, it could be extremely useful to synthetize novel Gal-3 inhibitor and prolong its action administering it in a drug delivery system (DDS) to the articular cavity. Gal-3 inhibitors based on the lactosamine (LacNAc) core to mimic Gal-3 natural ligand complexation might represent an adequate strategy. However, to enhance its affinity and selectivity and facilitate its binding with highly conserved amino acids of Gal-3 carbohydrate-recognition domain (CRD), specific modifications have to be introduced to establish the complexation in multiple points (**Figure 2**).

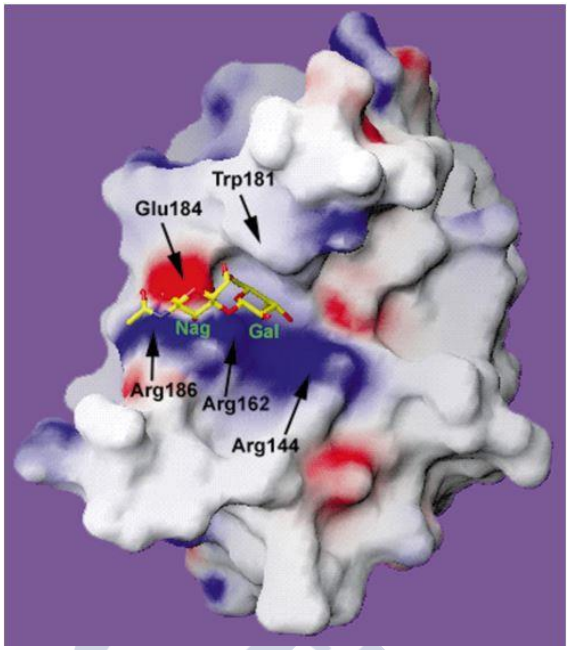

Figure 2. X-ray crystal structure of human galectin-3 carbohydrate-recognition domain with bound lactosamine moiety representation in yellow. The molecular surface was generated using GRASP with a probe radius of 1.4 Å. Blue and red regions indicate positive and negative electrostatic potentials, respectively. Reproduced with permission from,[55] Copyright © 1998 by The American Society for Biochemistry and Molecular Biology, Inc.

2. MATERIALS AND METHODS

2.1. Materials and animals

All the reagents for the organic synthesis were acquired from commercial sources and used without further purification. Fibrinogen from human blood plasma (premium quality grade) and thrombin from human blood plasma (premium quality grade) were purchased from Sigma-Aldrich, Germany. Sodium hyaluronate (HA, research grade) of different average molecular weight 51 kDa, 752 kDa and 1.38 MDa, with trade names 40 kDa, 700 kDa, 1.5 MDa, correspondingly, were acquired from Lifecore Biomedical, USA. Factor XIII (FXIII) from the blood plasma (>95% pure) was obtained from Haematologic Technologies, Inc, USA. Alpha-2 antiplasmin (α2AP) from human blood plasma (>95% pure) was bought from Lee Biosolutions, USA. Dexamethasone (97.2%) was purchased from Acofarma, Spain. The stabilizing surfactants, phosphatidylcholine enriched soy lecithin (EPIKURON® 145 V) was a kind gift from Cargill, Spain and oleylamine was bought from Sigma-Aldrich, Germany all of high-purity grade. Virgin olive oil (extra pure) was purchased from Acros Organics, Belgium. HEPES, BSA (≥98%), sodium chloride, calcium chloride dihydrate, potassium chloride, sodium phosphate dibasic and potassium phosphate monobasic of ≥99% purity, were acquired from Sigma-Aldrich, Germany. Carrageenan was purchased from Sigma Aldrich (St. Louis, MO). ELISA kit for IL-6 determination in rat plasma was purchased from Sigma. All the testing materials were obtained in sterile conditions using of endotoxin-free water and all other ingredients were of analytical grade. Ultrapure (Milli-Q) or endotoxin-free water was used throughout the experiments and organic solvents were of HPLC grade. The laboratory glassware used for *in vivo* formulations preparation was previously sterilized by autoclave (Systec, Wettenberg, Germany).

Animals

18 male Sprague-Dawley rats (200/225 g), were acquired from Charles River, Germany. They were used after 1-week acclimatization to the laboratory environment and housed in polypropylene cages (maximum five per cage) under standard controlled conditions (24 ± 1 °C, 12 h light/dark cycle), were fed commercial chow and acidified drinking water *ad libitum*.

All animal experiments were carried out in accordance with the EU Directive (2010/63/EU), Portuguese law (DL 113/2013) and all relevant legislations. The experimental protocol was approved by Direcção Geral de Alimentação e Veterinária (DGAV).

2.2. Gal-3 inhibitors preparation, purification and control

Gal-3 inhibitors were synthesized according to the designed protocols; each reaction step was controlled by thin-layer chromatography (TLC) on 0.25 nm silica gel plates with fluorescent indicator (GF254) and visualized under UV light. Detection was further achieved by charring with vanillin in sulfuric acid/ethanol (1.5:95 v/v). Flash chromatography purifications were made on silica gel columns (4 to 80 g, 240-400 mesh) using an automated Reveleris® Flash Chromatography system (Grace Alltech) equipped with both Evaporative Light Scattering (ELS) and UV/diode array allowing the simultaneous use of two customizable wavelengths detectors.

All NMR experiments were performed at 400.13 MHz using Bruker Avance 400 MHz spectrometer equipped with DUAL+ $^{1}H/^{13}C$ ATMA grad 5 mm probe. Assignments were performed be stepwise identification using COSY and HSQC experiments using standard pulse programs from the Bruker library. Chemical shifts are given to external TMS with calibration involving the residual signals.

High-resolution mass spectra were recorded in positive mode on Waters SYNAPT G2-Si HDMS with detection by a hybrid quadripole time of flight (Q-TOF) detector. The compounds were individually dissolved in MeOH at a concentration 1 mg/mL and then infused into the electrospray ion source at a flow rate of 10 µL/min at 100 °C. The mass spectrometer was operated at 3kV whilst scanning the magnet at a typical range of 4000-100 Da. The mass spectra were collected as continuum profile data. Accurate mass measurement was achieved based on every five second auto-calibration using leucine-enkephalin (m/z = 556.2771 $[M+H]^+$) as internal standard.

2.2.1. Experimental procedures for the synthesis of compounds 1-8. Approach A, using iodosulfonamidation as a key reaction

D-Lactal/1,5-Anhydro-2-deoxy-4-*O*-β-D-galactopyranosyl-D-arabinohex-1-enitol (4)

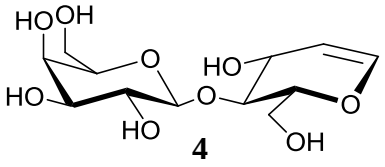

4

This step included 4 reactions. Lactose (20.0 g, 58.4 mmol, 1 eq.) was dissolved in AcOH (107 mL) and Ac_2O (53 mL, 560 mmol; 8.4 eq), $HClO_4$ (few drops) was added to initiate the reaction. After 1 hour of strong stirring at room temperature (RT) TLC monitoring showed that the reaction was complete and peracetylated lactose was obtained (**1**). TLC R_f = 0.5 (cyclohexane/ethyl acetate 1:1).

Reaction mixture containing intermediate **1**, was next cooled to 0 °C, before the addition of HBr (60 mL) via a dropping funnel. After 1 hour of strong stirring at 0 °C the reaction was complete (confirmed by TLC). The reaction mixture was diluted upon addition of CH_2Cl_2 (150 mL) and washed with H_2O (50 mL). Organic layer was separated and extracted with saturated $NaHCO_3$ (2 × 50 mL) and brine (50 mL). The organic layers were collected, dried over Na_2SO_4, filtrated, concentrated under reduced pressure and recrystallized in EtOAc (30 mL) at 4 °C, overnight. The derivative acetobromo-α-D-lactose **2** was further filtrated and washed with cyclohexane giving a pure white compound (38.5 g, 94%). TLC R_f = 0.44 (cyclohexane/EtOAc 1:1).

Zn powder (20.00 g, 330 mmol; 6 eq.) was activated by 1N HCl (a volume to cover Zn layer) with strong stirring during 10 min and washed with AcOH. A solution of AcOH/H_2O 1:1 (80 mL) was added to the flask with Zn and cooled to 0 °C. Meanwhile compound **2** (38.5 g, 55 mmol; 1 eq.) was dissolved in EtOAc (50 mL) and was added via a dropping funnel to the cold flask under strong stirring. The reaction was carried 48 h at 4 °C. The solution of intermediate peracetylated lactal **3** was filtrated and washed with small portions of EtOAc and H_2O. The filtrate was diluted with CH_2Cl_2 (100 mL) and H_2O (50 mL). The organic layer was recovered and further extracted with saturated $NaHCO_3$ (2 × 50 mL) and brine (50 mL). The organic layers were collected, dried over Na_2SO_4, filtrated, concentrated under reduced pressure and dried under vacuum, giving a compound **3** (22.92 g, 72%). TLC R_f = 0.5 (cyclohexane/ethyl acetate 1:1).

To a solution of derivative **3** (22.92 g, 39.6 mmol; 1 eq.) in MeOH (325 mL) was added solid Na_2CO_3 (119.6 mmol, 6.5 eq.). The reaction mixture was stirred at RT for 7 h. The crude mixture was filtered over a pad of Celite® 535 and the filtrate concentrated under

reduced pressure, to give compound **4** (9.64 g, 79%). TLC R_f = 0.05 (CH_2Cl_2/MeOH 9:1).

[3-*O*-(3,5-dimethoxybenzyl)-*O*-β-D-galactopyranosyl]-D-arabinohex-1-enitol (6a)

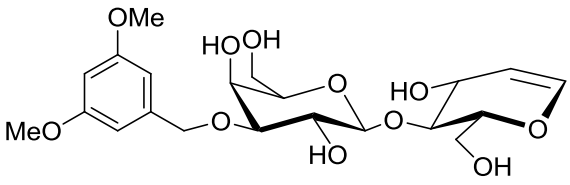

6a

At the step 1 compound **4** (2.0 g, 6.5 mmol; 1 eq.) and Bu_2SnO (1.78 g, 7.15 mmol; 1.1 eq.) were dried under vacuum overnight. Later they were dissolved in dry MeOH (distilled over Mg pellets) (57 mL) and refluxed during 5 hours under argon. The solvent was evaporated to dryness under reduced pressure to give stannylidene intermediate **5**. At the step 2 the residue **5** was dissolved in CH_2Cl_2 (11.5 mL) in the presence of 3,5-dimethoxybenzyl bromide (1.8 g, 7.8 mmol; 1.2 eq.) and stirred under argon at RT. After 48 h of TLC showed the reaction was completed. The solvent was reduce under reduced pressure and the title compound **6a** was purified by flash chromatography on silica column (eluent: CH_2Cl_2/MeOH to 100:0 CH_2Cl_2/MeOH 70:30) giving (1.86 g, yield 63%), TLC R_f = 0.65 (CH_2Cl_2/MeOH 9:1). ^{1}H NMR (400 MHz, $CDCl_3$) δ 6.66 (2 H, t, *J* = 2.3 Hz, 2 H arom), 6.40 (1 H, t, *J* = 2.3 Hz, 1 H arom), 6.39 (1 H, dd, *J* = 1.9 and 5.8 Hz, H-1), 4.74 (1 H, br d, *J* = 12.2 Hz, C*H*H), 4.72 (1 H, dd, *J* = 2.1 and 5.8 Hz, H-2), 4.63 (1 H, d, *J* = 12.2 Hz, CH*H*), 4.47 (1 H, d, *J* = 7.8 Hz, H-1'), 4.34 (1 H, dt, *J* = 2.1 and 6.8 Hz, H-3), 4.04 (1 H, dd, *J* = 1.0 and 3.2 Hz, H-4'), 3.97 (1 H, dd, J = 3.9 and 10.4 Hz, H-6), 3.91 (1 H, dd, J = 2.5 and 10.4 Hz, H-6), 3.87-3.73 (4 H, m, H-4, H-5, H-2' and H-6'), 3.80 (6 H, s, 2 CH_3), 3.71 (1 H, dd, J = 4.4 and 8.7 Hz, H-6'), 3.57 (1 H, ddd, J = 1.0, 3.8 and 8.0 Hz, H-5'), 3.48 (1 H, dd, J = 3.2 and 9.6 Hz, H-3'); ^{13}C NMR (75 MHz, CD_3OD) δ 160.2 (C arom), 143.7 (C-1), 140.8 (C arom), 105.3 (C arom), 103.8 (C-1'), 102.1 (C-2), 99.3 (C arom), 80.7 (C-3'(C-4), 77.4 (C-5), 75.5 (C-5'), 70.9 (CH_2), 70.5 (C-2'), 68.2 (C-3), 65.7 (C-4'), 61.2 (C-6'), 60.2 (C-6), 54.4 (2 CH_3); HR-ESI-MS: *m/z* calculated for $C_{21}H_{30}O_{11}$ $[M+Na]^+$ 481.1686, found 481.1682.

[3-*O*-(2-naphthyl)methyl-*O*-β-D-galactopyranosyl]-D-arabinohex-1-enitol (6b)

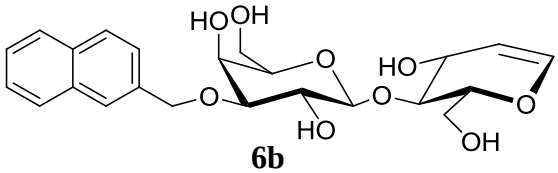

6b

The procedure was reproduced using (2-naphthyl)methyl bromide (1.55 g; 7 mmol; 1.2 eq.) and catalytic amount of Bu_4NI as electrophile agent at the step 2, to give a derivative **6b** (1.08 g, 42% yield). TLC R_f = 0.65 (CH_2Cl_2/MeOH 9:1). ^{1}H NMR (400 MHz, $CDCl_3$) δ 7.94 (1 H, br s, H arom), 7.88-7.82 (3 H,

m, 3 H arom), 7.61 (1 H, dd, *J* = 1.6 and 8.4 Hz, 1 H arom), 7.51-7.44 (2 H, m, 2 H-arom), 6.38 (1 H, dd, *J* = 1.8 and 6.0 Hz, H-1), 4.95 (1 H, d AB system, *J* = 12.1 Hz, C*H*H), 4.85 (1 H, AB system, *J* = 12.1 Hz, CH*H*), 4.71 (1 H, dd, *J* = 1.3 and 6.0 Hz, H-2), 4.48 (1 H, d, *J* = 7.8 Hz, H-1'), 4.37 (1 H, dt, *J* = 1.3 and 6.9 Hz, H-3), 4.06 (1 H, d, *J* = 3.2 Hz, H-4'), (1 H, dd, *J* = 3.9 and 10.4 Hz, H-6), 3.91 (1 H, dd, *J* = 2.5 and 10.4 Hz, H-6), 3.87-3.73 (4 H, m, H-4, H-5, H-2' and H-6'), 3.72 (1 H, dd, *J* = 4.4 and 11.4 Hz, H-6'), 3.57 (1 H, dd, *J* = 4.4 and 7.7 Hz, H-5'), 3.48 (1 H, dd, *J* = 3.2 and 9.7 Hz, H-3'); ^{13}C NMR (100 MHz, CD_3OD) δ 143.7 (C-1), 136.9, 133.4, 133.1, 127.6, 127.5, 127.3, 126.3, 125.8, 125.7 and 125.5 (10 C arom), 103.8 (C-1'), 102.1 (C-2), 80.9 (C-3'), 78.6 (C-4), 77.4 (C-5), 75.5 (C-5'), 71.3 (CH_2), 70.6 (C-2'), 68.3 (C-3), 65.8 (C-4'), 61.1 (C-6'), 60.2 (C-6); HR-ESI-MS: *m/z* calculated for $C_{23}H_{28}O_9$ $[M+Na]^+$ 471.1631, found 471.1628.

1,5-Anhydro-2-deoxy-[3-*O*-(3,5-dimethoxybenzyl)methyl-2,4,6-tri-*O*-triethylsilyl-β-D-galactopyranosyl]-(1-4)-3,6-di-*O*-triethylsilyl-D-arabinohex-1-enitol (7a)

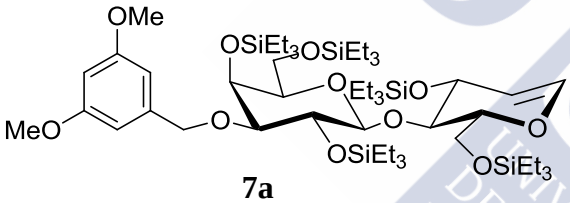

7a

Chlorotriethylsilane (TES-Cl, Et_3Si-Cl) (11.8 mL, 70.5 mmol; 9 eq.) and imidazole (9.6 g, 140.94 mmol; 18 eq.) were dissolved in DMF (28 mL) and activated during 20 min under argon, before the addition of compound **6a** (2.415 g, 7.83 mmol). After 12 h stirring at RT TLC showed the reaction was completed. The crude mixture was poured into the beaker with H_2O (50 mL) and after extracted with diethyl ether (3 × 20 mL). The organic layers were collected, dried over $MgSO_4$, filtrated, concentrated under reduced pressure and dried under vacuum to give a compound **7a** (7.39 g, 95%) which was used in the next step without further purification. TLC R_f = 0.71 (cyclohexane/ethyl acetate 9.5:0.5).

1,5-Anhydro-2-deoxy-[3-*O*-(2-naphthyl)methyl-2,4,6-tri-*O*-triethylsilyl-β-D-galactopyranosyl]-(1-4)-3,6-di-*O*-triethylsilyl-D-arabinohex-1-enitol (7b)

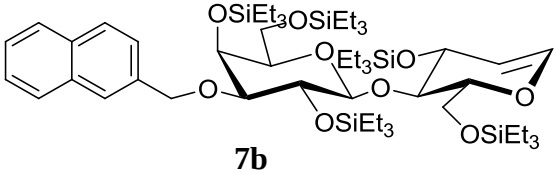

7b

The same reaction was reproduced to compound **6b** to obtain derivative **7b** (2.97 mg, yield 95%) which was used in the next step without further purification. TLC R_f = 0.71 (cyclohexane/ethyl acetate 9.5:0.5).

2.2.2. Experimental procedures for the synthesis of compounds 9-16. Approach B, using azidophenylselenation as a key reaction

Similar to the previous synthetic pathway, it is started from the D-lactose modification to obtain D-lactal. First 4 reactions of the sequence were performed by the protocols described at the Approach A (*Section 2.2.1.*).

1,5-Anhydro-2-deoxy-[2,3,4,6-tetra-*O*-triethylsilyl-β-D-galactopyranosyl]-(1-4)-3,6-di-*O*-triethylsilyl-D-arabinohex-1-enitol (9)

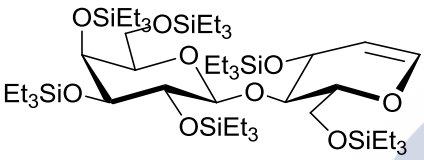

9

A persilylation reaction was held (by previously described protocol as for compound **7** in iodosulfonamidation approach) to give compound **9** (11.52 g, yield 95%) which was used in the next step without further purification, TLC R_f = 0.86 (cyclohexane/ethyl acetate 9.8:0.2).

Phenyl 2-azido-1,2-dideoxy-3,6-di-*O*-triethylsilyl-4-*O*-(2,3,4,6-tetra-*O*-triethylsilyl-β-D-galactopyranosyl)-1-seleno-β-D-glucopyranoside (10)

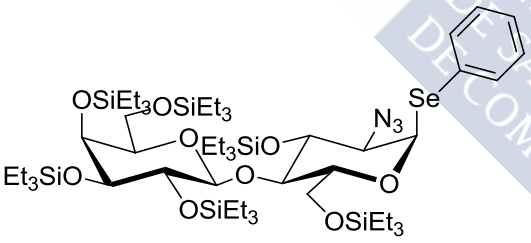

10

A compound **9** (11.52 g, 11.297 mmol; 1 eq.) was dissolved in CH_2Cl_2 (30 mL) and cooled to -20 °C before the addition of diphenyl diselenide (Ph_2Se_2) (3.53 g, 11.30 mmol; 1 eq.), followed by azidotrimethylsilane (1.49 mL, 11.30 mmol; 1 eq.) and iodobenzene diacetate $PhI(AcO)_2$ (3.64 g, 11.297 mmol; 1 eq.) of. The temperature -20 °C was kept 10 min, after the reaction mixture was allowed to warm to -10 °C during next 1-2 h under argon before TLC showed the reaction was complete. The title compound was extracted in with diethyl ether (30 mL) and H_2O (2 × 60 mL) and brine (60 mL). The organic layers were collected, dried over Na_2SO_4, filtrated, concentrated under reduced pressure, to provide known compound **10** (5.61 g, 40.5%) after flash-chromatography on silica gel (eluent: gradient of cyclohexane/ cyclohexane:ethyl acetate 95:5). TLC R_f = 0.78 (cyclohexane/EtOAc 9.8:0.2).

Phenyl 2-azido-2-deoxy-4-*O*-(β-D-galactopyranosyl)-1-seleno-β-D-glucopyranoside (11)

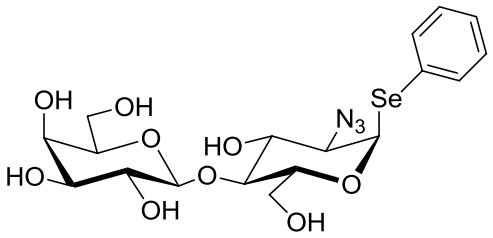

11

To persilylated derivative **10** (4.75 g, 4.42 mmol) in solution in DMF (20 mL) was added CsF (4.03 g, 26.55 mmol). The reaction mixture was stirred at RT under argon for 4 h and then concentrated to dryness under reduced pressure. The crude residue was purified by flash chromatography on the silica column (eluent: CH_2Cl_2/MeOH) to give compound **11** (2.13 g, 93%). TLC R_f = 0.08 (CH_2Cl_2/MeOH 9:1); ^{1}H RMN (400 MHz, CD_3OD) δ 7.63-7.60 (m, 2H, Ar-H), 7.33-7.28 (m, 3H, Ar-H), 5.90 (d, *J* = 4.3 Hz, 1H, H-1), 4.44 (d, *J* = 7.6 Hz, 1H, H-1'), 4.12 (br dt, *J* = 3.2, 9.2 Hz 1H, H-5), 3.94 (dd, *J* = 3.4, 12.3 Hz, 1H, H-6), 3.91 (d, *J* = 3.3 Hz, 1H, H-4'), 3.83-3.76 (m, 4H, H-2, H-3, 2 H-6'), 3.75 (dd, *J* = 3.4, 12.3 Hz, 1H, H-4) 3.69 (dd, *J* = 2.4, 12.3 Hz, 1H, H-6), 3.65-3.57 (m, 2H, H-2', H-5'), 3.52 (dd, *J* = 3.2, 9.7 Hz, 1H, H-3'); ^{13}C RMN (100 MHz, CD_3OD) δ 134.4 (2 C-Ar), 128.8 (2 C-Ar), 128.6 (C-Ar), 127.5 (C-Ar), 103.7 (C-1'), 87.1 (C-1), 78.8 (C-4), 75.7 (C-5'), 73.6 (C-3'), 73.4 (C-5), 72.9 (C-3), 71.3 (C-2'), 69.0 (C-4'), 64.3 (C-2), 61.2 (C-6'), 59.8 (C-6); HR-ESI-MS: *m/z* calculated for $C_{18}H_{25}N_3O_9Se$ $[M+Na]^+$ 530.0654, found 530.0653.

Phenyl 2-azido-2-deoxy-4-*O*-[3-*O*-(3,5-dimethoxybenzyl]-β-D-galactopyranosyl)-1-seleno-β-D-glucopyranoside (12)

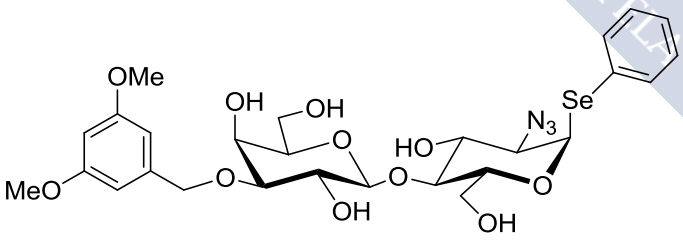

12

Derivative **11** (2.01 g, 4 mmol) and dibutyltin oxide (Bu_2SnO, 1.09 g, 4.4 mmol) in dry MeOH (57 mL) was refluxed for 5 h. Then the crude mixture was evaporated to dryness under reduced pressure. The residue was dissolved in DMF (11.5 mL) in the presence of 3,5-dimethoxybenzyl bromide (1.10 g, 4.8 mmol) and Bu_4NI (147 mg, 0.4 mmol) and stirred under argon at RT for 48 h. The reaction mixture was concentrated under reduced pressure and the crude residue purified by flash chromatography on silica gel column (eluent: CH_2Cl_2/MeOH) to give compound **12** (1.09 g, 48%); TLC R_f = 0.52 (CH_2Cl_2/MeOH 9:1); ^{1}H RMN (400 MHz, CD_3OD) δ 7.52 (d, *J* = 7.7 Hz, 2H, Ar-H), 7.28-

7.18 (m, 3H, Ar-H), 6.56 (d, *J* = 2.2 Hz, 2H, Ar-H), 6.37 (t, *J* = 2.2 Hz, 1H, Ar-H), 5.70 (d, *J* = 4.7 Hz, 1H, H-1), 4.65 (d, *J* = 11.0 Hz, 1H, C*H*H), 4.57 (d, *J* = 11.0 Hz, 1H, CH*H*) 4.45 (d, *J* = 7.5 Hz, 1H, H-1'), 4.12 (d, *J* = 9.6 Hz 1H, H-5), 4.02-3.65 (m, 9H, H-2, H-3, 2 H-6, H-2', H-3', H-4', 2 H-6'), 3.73 (s, 6H, 2 OMe), 3.59-3.57 (m, 1H, H-5'), 3.40 (m, 1H, H-4); ^{13}C RMN (100 MHz, CD_3OD) δ 160.9 (2 C-Ar), 140.1 (C-Ar), 134.7 (2 C-Ar), 129.2 (2 C-Ar), 128.3 (C-Ar), 128.0 (C-Ar), 105.9 (2 C-Ar), 103.3 (C-1'), 99.6 (C-Ar), 85.1 (C-1), 80.8 (C-4), 78.9 (C-3'), 75.0 (C-5'), 73.1 (C-3 and C-5), 71.7 (CH_2), 70.3 (C-2'), 66.6 (C-4'), 63.8 (C-2), 62.0 (C-6'), 60.8 (C-6), 55.4 (2 CH_3); HR-ESI-MS: *m/z* Calculated for $C_{27}H_{35}N_3O_{11}Se$ $[M+Na]^+$ 680.1335, found 680.1298.

Phenyl 3,6-di-*O*-acetyl-2-azido-2-deoxy-4-*O*-[2,4,6-tri-*O*-acetyl-3-*O*-(3,5-dimethoxybenzyl]-β-D-galactopyranosyl)-1-seleno-β-D-glucopyranoside (13)

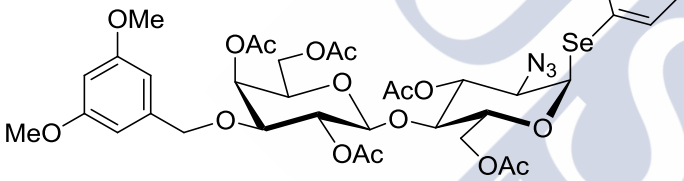

13

To a solution of compound **12** (0.96 g, 1.47 mmol) in CH_2Cl_2 (25 mL) cooled at 0 °C were successively added Ac_2O (0.83 mL, 8.09 mmol) and DIPEA (1.54 mL, 8.09 mmol) and a catalytic amount of DMAP (17.9 mg, 0.15 mmol). The reaction mixture was allowed to warm to RT and stirred during next 12 h. The crude reaction mixture was diluted with CH_2Cl_2 (30 mL) and extracted with H_2O (60 mL), saturated aqueous $NaHCO_3$ (2×30 mL), and brine (30 mL). The organic layers were collected, dried (Na_2SO_4), filtered and concentrated under reduced pressure. The crude residue was purified by flash chromatography on silica gel (eluent: cyclohexane/ethyl acetate) to give compound **13** (1.3 g, 97%); TLC R_f = 0.64 (cyclohexane/ethyl acetate 1:1); ^{1}H RMN (400 MHz, $CDCl_3$) δ 7.60 (br d, *J* = 5.7 Hz, 2H, Ar-H), 7.33-7.28 (m, 3H, Ar-H), 6.44-6.38 (m, 3H, Ar-H), 5.89 (d, *J* = 5.3 Hz, 1H, H-1), 5.48 (dd, *J* = 1.1, 3.4 Hz 1H, H-4'), 5.27 (dd, *J* = 9.4, 10.3 Hz, 1H, H-3), 5.08 (dd, *J* = 7.9, 10.0 Hz, 1H, H-2'), 4.62 (d, *J* = 12.4 Hz, 1H, C*H*H), 4.46-4.40 (m, 1H, H-5), 4.42 (d, *J* = 8.1 Hz, 1H, H-1'), 4.35 (d, *J* = 12.4 Hz, 1H, CH*H*), 4.32 (dd, *J* = 2.1, 10.0 Hz, 1H, H-6), 4.22-4.12 (m, 3H, H-6, 2 H-6'), 3.96 (dd, *J* = 5.3, 10.3 Hz, 1H, H-2), 3.82-3.72 (m, 2H, H-4, H-5'), 3.80 (s, 6H, 2×OMe), 3.51 (dd, *J* = 3.4, 10.0 Hz, 1H, H-3'), 2.19 (s, 3H, CH_3), 2.14 (s, 3H, CH_3), 2.10 (s, 3H, CH_3), 2.06 (s, 6H, 2×CH_3), 2.04 (s, 3H, CH_3); ^{13}C NMR (75 MHz, $CDCl_3$) δ 170.4 (C=O), 170.3 (C=O), 170.2 (C=O), 169.2 (C=O), 169.0 (C=O),

160.9 (2 C-Ar), 139.7 (C-Ar), 134.4 (2 C-Ar), 129.2 (2 C-Ar), 128.1 (C-Ar), 105.6 (2 C-Ar), 101.0 (C-1'), 99.7 (C-Ar), 84.0 (C-1), 76.9 (C-3'), 76.2 (C-4), 72.1 (C-3), 71.4 (C-5), 71.2 (CH_2), 71.0 and 70.7 (C-2'and C-5'), 65.6 (C-4'), 62.7 (C2), 62.2 (C-6), 61.5 (C-6'), 55.3 (2 OMe), 20.8, 20.8, 20.7 and 20.7 (5 CH_3); HR-ESI-MS *m/z* Calcd for $C_{37}H_{45}N_3O_{16}Se$ $[M+Na]^+$ 890.1863, found 890.1848.

Phenyl 3,6-di-*O*-acetyl-2-amino-2-deoxy-4-*O*-[2,4,6-tri-*O*-acetyl-3-*O*-(3,5-dimethoxybenzyl]-β-D-galactopyranosyl)-1-seleno-β-D-glucopyranoside (14)

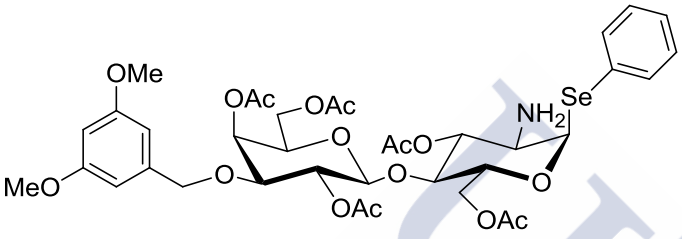

14

To a solution of compound **13** (1.18 g, 1.26 mmol) in THF (3.5 mL) was added PMe_3 (1 M Solution in THF) (1.3 mL, 1.50 mmol) and stirred 1 h at RT under argon. H_20 (25 µL, 1.36 mmol) was then added and the reaction mixture and further stirred at 50 °C for 5 h. The crude reaction mixture was concentrated under reduced pressure and purified by flash chromatography on silica gel (eluent: cyclohexane/ethyl acetate) to give compound **14** (1.06 g, 93%); TLC R_f = 0.11 (cyclohexane/ethyl acetate 1:1); ^{1}H RMN (400 MHz, CD_3OD) δ 7.65-7.62 (m, 2H, Ar-H), 7.33-7.28 (m, 3H, Ar-H), 6.47-6.38 (m, 3H, Ar-H), 5.84 (d, *J* = 4.9 Hz, 1H, H-1), 5.54 (dd, *J* = 1.1, 3.4 Hz 1H, H-4'), 4.98 (dd, *J* = 8.0, 10.3 Hz, 1H, H-2'), 5.08 (dd, *J* = 9.0, 9.6 Hz, 1H, H-3), 4.58 (d, *J* = 8.0 Hz, 1H, H-1'), 4.62 (d, *J* = 12.1 Hz, 1H, C*H*H), 4.43-4.38 (m, 1H, H-5), 4.36 (d, *J* = 12.1 Hz, 1H, CH*H*), 4.32 (dd, *J* = 2.1, 10.0 Hz, 1H, H-6), 4.24-4.13 (m, 3H, H-6, 2 H-6'), 4.00 (dt, *J* = 1.2, 6.5 Hz, 1H, H-5'), 3.79 (s, 6H, 2×OMe), 3.80-3.72 (m, 2H, H-4, H-3'), 3.14 (dd, *J* = 4.9, 10.6 Hz, 1H, H-2), 2.16 (s, 3H, CH_3), 2.14 (s, 3H, CH_3), 2.07 (s, 3H, CH_3), 2.04 (s, 6H, 2×CH_3), 2.02 (s, 3H, CH_3); ^{13}C NMR (75 MHz, CD_3OD) δ 171.3 (C=O), 170.9 (C=O), 170.7 (C=O), 170.6 (C=O), 170.0 (C=O), 161.0 (2 C-Ar), 140.1 (C-Ar), 133.8 (2 C-Ar), 128.9 (2 C-Ar), 127.5 (C-Ar), 105.3 (2 C-Ar), 100.8 (C-1'), 99.2 (C-Ar), 90.4 (C-1), 77.2 and 76.3 (C-3' and C-4), 74.4 (C-3), 71.8 (CH_2), 71.3 (C-5), 71.0 (C-2'), 70.7 (C-5'), 66.5 (C-4'), 62.5 (C-6), 61.5 (C-6'), 55.3 (C2), 54.4 (2 OMe), 20.1, 20.0, 19.4, 19.3 and 19.3 (5 CH_3); HR-ESI-MS *m/z* Calculated for $C_{37}H_{47}NO_{16}Se$ $[M+H]^+$ 842.2138, found 842.2149.

Phenyl 3,6-di-*O*-acetyl-2-deoxy-2-(3,5-dimethoxybenzamido)-4-*O*-[2,4,6-tri-*O*-acetyl-3-*O*-(3,5-dimethoxybenzyl]-β-D-galactopyranosyl)-1-seleno-β-D-glucopyranoside (15)

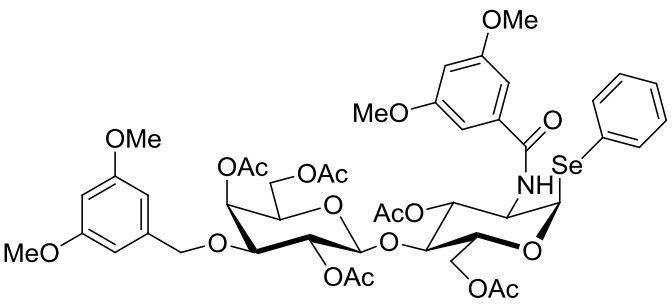

15

To a solution of compound **14** (1.06 g, 1.25 mmol) in CH_2Cl_2 (15 mL) were successively added 3,5-dimethoxybenzoyl choride (0.76 mL, 3.75 mmol), DIPEA (0.44 mL, 2.5 mmol) and DMAP (15.5 mg, 0.13 mmol) at 0 °C. The reaction mixture was then stirred at reflux for 14 h under argon. After cooling, the crude reaction mixture was diluted with CH_2Cl_2 (50 mL) and extracted with H_2O (2 × 50 mL) and brine (50 mL). The organic layers were collected, dried (Na_2SO_4), filtered and concentrated under reduced pressure. The crude residue was purified by flash chromatography on silica gel (eluent: cyclohexane/ethyl acetate) to give compound **15** (941 mg, 76%); R_f = 0.20 (ethyl acetate/cyclohexane 1:1); ^{1}H RMN (400 MHz, CD_3OD) δ 7.58-7.56 (m, 2H, Ar-H), 7.30-7.25 (m, 3H, Ar-H), 6.93 (d, *J* = 2.3 Hz, 2H, Ar-H), 6.68 (t, *J* = 2.3 Hz, 1H, Ar-H), 6.45 (d, *J* = 2.3 Hz, 2H, Ar-H), 6.41 (t, *J* = 2.3 Hz, 1H, Ar-H), 6.07 (d, *J* = 5.0 Hz, 1H, H-1), 5.54 (dd, *J* = 1.1, 3.3 Hz 1H, H-4'), 5.22 (dd, *J* = 8.6, 11.1 Hz, 1H, H-3), 5.00 (dd, *J* = 8.0, 10.1 Hz, 1H, H-2'), 4.65 (d, *J* = 8.0 Hz, 1H, H-1'), 4.60 (d, *J* = 11.7 Hz, 1H, C*H*H), 4.61-4.55 (m, 1H, H-2), 4.47-4.40 (m, 2H, H-5, H-6), 4.37 (d, *J* = 11.7 Hz, 1H, CH*H*), 4.22 (dd, *J* = 6.4, 11.8 Hz, 1H, H-6), 4.19-4.14 (m, 2H, 2 H-6'), 4.03 (t, *J* = 6.6 Hz, 1H, H-5'), 3.95 (br t, *J* = 9.2 Hz, 1H, H-4), 3.83 (s, 6H, 2×OMe), 3.80-3.75 (m, 1H, H-3'), 2.14 (s, 3H, CH_3), 2.12 (s, 3H, CH_3), 2.10 (s, 3H, CH_3), 2.08 (s, 6H, 2×CH_3), 2.05 (s, 3H, CH_3); ^{13}C NMR (75 MHz, CD_3OD) δ 171.6 (C=O), 171.3 (C=O), 170.8 (C=O), 170.7 (C=O), 170.6 (C=O), 170.1 (C=O), 161.1 (2 C-Ar), 161.0 (2 C-Ar), 140.0 (C-Ar), 135.5 (C-Ar), 133.8 (2 C-Ar), 128.9 (2 C-Ar), 128.5 (C-Ar), 127.5 (C-Ar), 105.3 (2 C-Ar), 105.0 (2 C-Ar), 103.6 (C-Ar), 100.9 (C-1'), 99.2 (C-Ar), 86.0 (C-1), 77.1 and 76.2 (C-3' and C-4), 71.7, 71.7, 71.4, 71.0 and 70.7 (C-3, C-5, C-2', C-5' and CH_2), 66.5 (C-4'), 62.3 (C-6), 61.4 (C-6'), 54.7 (2 OMe), 54.4 (2 OMe), 53.9 (C-2), 19.9, 19.7, 19.4, 19.4, 19.3 and 19.3 (5 CH_3); HR-ESI-MS *m/z* Calculated for $C_{46}H_{55}NO_{19}Se$ $[M+Na]^+$ 1028.2439, found 1028.2431.

2-(3,5-dimethoxyphenyl)-{2,6-Di-*O*-acetyl-1,2-dideoxy-4-*O*-[2,4,6-tri-*O*-acetyl-3-*O*-(3,5-dimethoxybenzyl)-β-D-galactopyranosyl]-β-D-glucopyrano}-[2,1,d]-oxazoline (16)

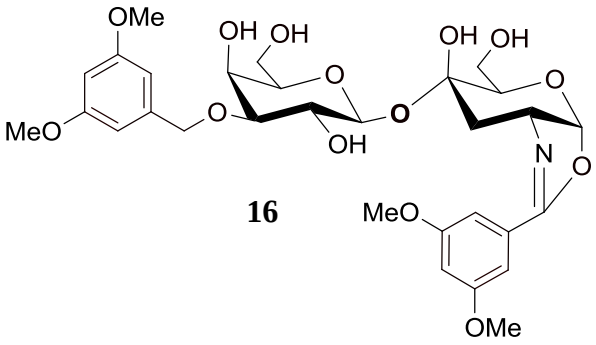

16

A solution of compound **15** (420 mg, 0.42 mmol) in CH_2Cl_2 (5 mL) and cooled to -20 °C before the addition of 24 µL (0.46 mmol) of Br_2. The reaction was stirred 1 h under argon and then quenched upon addition of Et_3N. The solvent was evaporated and the crude residue purified by flash-chromatography (eluent: cyclohexane/ethyl acetate) to give oxazoline **16** (216 mg, yield 61%) as a foam. R_f = 0.23 (ethyl acetate/cyclohexane 1:1); ^{1}H RMN (400 MHz, CD_3OD) δ 7.18 (d, *J* = 2.0 Hz, 2H, Ar-H), 6.68 (br s, 1H, Ar-H), 6.42 (br s, 2H, Ar-H), 6.40 (br s, 1H, Ar-H), 611 (d, *J* = 7.0 Hz, 1H, H-1), 5.75 (br s, 1H, H-3), 5.45 (br d, *J* = 3.3 Hz 1H, H-4'), 5.08 (t, *J* = 8.4 Hz, 1H, H-2'), 4.65-4.59 (m, *2*H, H-1', C*H*H), 4.37-4.33 (m, 2H, H-2, CH*H*), 4.27-4.22 (m, 1H, H-6), 4.16-4.05 (m, 2H, H-6, H-6'), 4.02-3.95 (m, 1H, H-6'), 3.85 (s, 6H, 2×OMe), 3.80 (s, 6H, 2×OMe), 3.90-3.80 (m, 1H, H-4), 3.69 (t, *J* = 6.0 Hz, 1H, H-5), 3.63-3.57 (m, 1H, H-5'), 3.52 (dd, *J* = 3.1, 9.6 Hz 1H, H-3), 2.18 (s, 3H, CH_3), 2.15 (s, 3H, CH_3), 2.10 (s, 3H, CH_3), 2.03 (s, 3H, CH_3), 2.01 (s, 3H, CH_3); ^{13}C NMR (75 MHz, CD_3OD) δ 170.5, 170.4, 170.3, 169.4 and 169.2 (5 C=O and C=N), 160.9 (2 C-Ar), 160.8 (2 C-Ar), 139.8 (C-Ar), 127.4 (C-Ar), 106.2 (2 C-Ar), 105.7 (2 C-Ar), 105.2 (C-1), 105.0 (C-Ar), 101.5 (C-1'), 99.6 (C-Ar), 77.4 and 77.2 (C-4 and C-3'), 71.3, 71.1, 71.0, 70.3 and 67.7 (C-3, C-5, C-2', C-5' and CH_2), 65.7 (C-4'), 65.6 (C-2), 63.4 (C-6), 61.5 (C-6'), 55.6 (2 OMe), 55.3 (2 OMe), 21.0, 20.8, 20.8, 20.7, 20.6 (4 CH_3); HR-ESI-MS *m/z* Calculated for $C_{40}H_{49}NO_{19}$ $[M+Na]^+$ 870.2821, found 870.2812.

2.2.3. Experimental procedures for the synthesis of compounds 18-28. Approach C, using "1+1" donor-acceptor glycosylation as a key reaction (The synthesis has been carried out in collaboration with a post-doctoral fellow from the lab – Dr. Christophe Dussouy)

Methyl 3-*O*-(2-naphthyl)methyl-β-D-galactopyranoside (18)

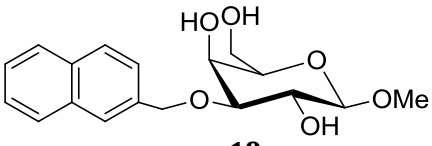

18

A mixture of methyl β-D-galactopyranoside **17** (1.84 g, 9.48 mmol) and dibutyltin oxide (2.6 g, 1.04 mmol) in dry MeOH (55 mL) was refluxed for 5 h. Then the solvent was distilled to give a syrup, which was evaporated to dryness under reduced pressure. The residue was dissolved in DMF (10 mL) in the presence of (2-naphthyl)methyl bromide (2.52 mg, 11.38 mmol) and a catalytic amount of Bu_4NI and stirred under argon at 40 °C overnight. The reaction mixture was concentrated under reduced pressure and the crude residue purified by flash chromatography on silica gel (eluent: CH_2Cl_2/MeOH 100:0, CH_2Cl_2/MeOH 90:10) to give compound **18** (1.63 g, 50%); TLC R_f = 0.63 (CH_2Cl_2/MeOH 9:1); ^{1}H NMR (400 MHz, CD_3OD) δ 7.96 (1 H, br s, 1 H arom), 7.85-7.81 (3 H, m, 3 H arom), 7.67-7.58 (3 H, m, 3 H arom), 4.93 (1 H, AB system, *J* = 11.1 Hz, C*H*H), 4.83 (1 H, AB system, *J* = 11.1 Hz, CH*H*), 4.17 (1 H, d, *J* = 7.7 Hz, H-1), 4.10 (1 H, br d, *J* = 3.2 Hz, H-4), 3.79-3.74 (2 H, m, 2 H-6), 3.73 (1 H, dd, *J* = 7.7 and 9.6 Hz, H-2), 3.54 (1 H, s, CH_3), 3.47 (1 H, br t, *J* = 6.4 Hz, H-5), 3.44 (1 H, dd, *J* = 3.2 and 9.6 Hz, H-3); ^{13}C NMR (100 MHz, CD_3OD) δ 136.0, 135.5, 133.3, 128.1, 127.6, 127.5, 126.2, 125.8, 125.7 and 125.5(10 C arom), 100.0 (C-1), 81.0 (C-3), 75.1 (C-5), 71.2 and 70.4 (CH_2 and C-2), 65.7 (C-4), 61.1 (C-6), 55.9 (CH_3); HR-ESI-MS *m/z* calculated for $C_{18}H_{22}O_6$ $(M + Na)^+$ 357.1315, found 357.1314.

Methyl 2,4,6-tri-*O*-acetyl-3-*O*-(2-naphthyl)methyl-β-D-galactopyranoside (19)

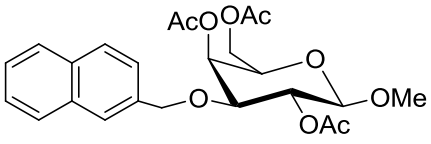

19

To a suspension of triol **18** (2.45 g, 6.34 mmol) in dry CH_2Cl_2 (10 mL) at 0°C were successively added Ac_2O (2.7 mL, 28.5 mmol), Et_3N (3.42 mL, 22.2 mmol) and DMAP (77 mg, 0.63 mmol). The reaction mixture was reacted at RT for 24 h. The crude reaction mixture was then diluted with CH_2Cl_2 and successively washed with 0.1 N aqueous HCl, aqueous saturated $NaHCO_3$ and brine. The extract was dried over Na_2SO_4, filtered and concentrated under reduced pressure. Flash chromatography (eluent: cyclohexane/ethyl acetate 100:0 to

cyclohexane/ethyl acetate 50:50) of the resulting residue provided the peracetylated derivative **19** (2.45 g, 85%); TLC R_f = 0.29 (ethyl acetate/cyclohexane 3:7); ^{1}H NMR (400 MHz, $CDCl_3$) δ 7.80-7.75 (3 H, m, 3 H-arom), 7.69 (1 H, br s, 1 H-arom), 7.46-7.33 (3 H, m, 3 H-arom), 5.53 (1 H, br d, *J* = 3.5 Hz, H-4), 5.14 (1 H, dd, *J* = 8.0 and 9.8 Hz, H-2), 4.82 (1 H, AB system, *J* = 12.4 Hz, C*H*H), 4.53 (1 H, AB system, *J* = 12.4 Hz, CH*H*), 4.24 (1 H, d, *J* = 8.0 Hz, H-1), 4.20-4.11 (2 H, m, 2 H-6), 3.76 (1 H, br t, *J* = 6.6 Hz, H-5), 3.57 (1 H, dd, *J* = 3.5 and 9.8 Hz, H-3); 3.43 (1 H, s, CH_3), 2.08, 2.03 and 2.0 (3 x 3 H, 3 s, 3 CH_3); ^{13}C NMR (100 MHz, CD_3OD) δ 170.3, 170.2 and 169.4 (3 CO), 135.0, 133.2, 133.0, 128.1, 127.8, 127.7, 126.5, 126.2, 126.0 and 125.7 (10 C-arom), 102.0 (C-1), 76.6 (C-3), 71.3, 70.8 and 70.4 (CH2, C-2 and C-5), 66.0 (C-4), 61.9 (C-6), 56.6 (CH_3), 20.9, 20.7 and 20.6 (3 CH_3); HR-ESI-MS *m/z* calculated for $C_{24}H_{28}O_9$ $(M + Na)^+$ 483.1631, found 483.1638.

2,4,6-Tri-*O*-acetyl-3-*O*-(2-naphthyl)methyl-D-galactopyranoside trichloroacetimidate (21)

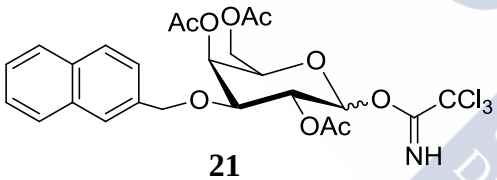

21

A stirred solution of methyl glycoside **19** (2.4 g, 5.3 mmol) in $Ac_2O/H_2SO_4/CH_2Cl_2$ (1.97:0.055:24 mL) was warmed from -15 °C to 4 °C overnight and then was neutralized upon addition of $NaHCO_3$ at 0 °C. The reaction mixture was diluted with ethyl acetate and washed with water and brine. The organic layer was dried (Na_2SO_4), filtered and purified by flash chromatography (eluent: cyclohexane/ethyl acetate 100:0 to cyclohexane/ethyl acetate 40:60) to give tetra-acetylated intermediate **20** (2.4 g, 95%). TLC R_f = 0.55 (cyclohexane/ethyl acetate 6:4). Peracetylated derivative **20** (2.4 g, 4.92 mmol) was further reacted with piperidine (583 µL, 5.9 mmol) in dry THF (10 mL) at RT under inert atmosphere overnight and then quenched with aq. HCl 1N. The solvent was evaporated under reduced pressure and the crude residue was purified by flash chromatography (eluent: cyclohexane/ethyl acetate 100:0 to cyclohexane/ethyl acetate 80:20) to provide 2,4,6-tri-*O*-acetyl-3-*O*-(2-naphthyl)methyl-D-glucopyranose (2.12 g, 95%) as an colorless oil. TLC R_f = 0.56 (cyclohexane/ethyl acetate 1:1). To a solution of this intermediate (2.12 g, 4.75 mmol) in CH_2Cl_2 (15 mL) were added trichloroacetonitrile (4.76 mL, 47.5 mmol) and 1,8-diazabicyclo(5.4.0)undec-7-ene (DBU, 355 µL, 2.38 mmol) dropwise at 0 °C. The mixture was then stirred at RT for 2 h and then concentrated *in vacuo*. The residue was purified by flash chromatography on silica gel (eluent: 0.1 % Et_3N in cyclohexane/ethyl acetate 100:0 to

0.1 % Et_3N in cyclohexane/ethyl acetate 80:20) to give glycoside donor **21** (2.03 g, 73%) as a pale yellow oil as a mixture of α/β (85/15) anomers. R_f = 0.84 (cyclohexane/ethyl acetate 1:1); ^{1}H NMR (300 MHz, $CDCl_3$) (α anomer) δ 8.61 (1 H, s, NH), 7.88-7.80 (3 H, m, 3 H-arom), 7.78 (1 H, br s, 1 H-arom), 7.50-7.41 (3 H, m, 3 H-arom), 6.60 (1 H, d, *J* = 3.5 Hz, H-1), 5.72 (1 H, d, *J* = 2.8 Hz, H-4), 5.33 (1 H, dd, *J* = 3.5 Hz and *J* = 10.5 Hz, H-2), 4.91 (1 H, AB system, *J* = 12.1 Hz, C*H*H), 4.68 (1 H, AB system, *J* = 12.1 Hz, CH*H*), 4.37 (1 H, br t, *J* = 6.2 Hz, H-5), 4.24 (1 H, dd, *J* = 6.1 Hz, *J* = 11.4 Hz, H-6), 4.14-4.07 (2 H, m, H-3 and H-6), 2.19, 2.05 and 2.01 (3 x 3 H, 3 s, 3 CH_3); ^{13}C NMR (100 MHz, $CDCl_3$) δ 170.4 (COα), 170.2 (COα), 170.0 (COα), 160.7 (C=NH), 134.8, 133.2, 133.1, 128.1, 127.8, 127.7, 126.8, 126.2, 126.1 and 125.9 (10 C-arom), 94.0 (C-1α), 90.9 (CCl_3), 72.4 (C-3), 71.7 (CH_2), 69.6 (C-5), 68.9 (C-2), 66.7 (C-4), 61.9 (C-6), 20.7, 20.6 and 20.5 (3 CH_3); HR-ESIMS: *m/z* Calculated for $C_{25}H_{26}Cl_3NO_9$ $[M + Na]^+$: 612.0571. Found 612.0577.

2-Azidoethyl 3-*O*-acetyl-6-*O*-*tert*-butyldimethylsilyl-2-deoxy-2-(3-methoxybenzamido)-β-D-glucopyranoside (24)

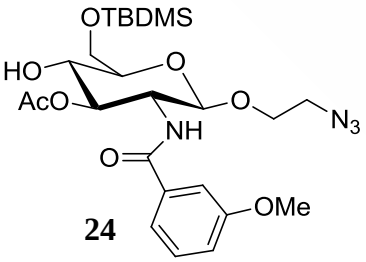

24

A stirred solution of known compound **22**[56] (2.23 g, 4.53 mmol) in 0.8 M ethylenediamine in MeOH (9.6 mL) was warmed at 50 °C for 5 h. Then the solvent was evaporated under reduced pressure and the crude residue was purified by flash chromatography (eluent: CH_2Cl_2/MeOH 100:0 to CH_2Cl_2/MeOH 90:10) to give the free amine intermediate (1.6 g, 97%). TLC R_f = 0.46 (CH_2Cl_2/MeOH 9:1). To a solution of this free amine intermediate (770 mg, 2.12 mmol) in dry CH_2Cl_2 (15 mL) at 0 °C were successively added triethylamine (311 µL, 2.23 mmol) and 3-methoxybenzoyl chloride (313 µL, 2.23 mmol). The reaction mixture was reacted from 0 °C to RT under inert atmosphere for 6 h. The crude reaction mixture was then diluted with CH_2Cl_2 and successively washed with 0.2 N aqueous HCl, aqueous saturated $NaHCO_3$ and brine. The extract was dried over Na_2SO_4, filtered and concentrated under reduced pressure. The residue was purified by flash chromatography on silica gel (eluent: cyclohexane/ethyl acetate 100:0 to cyclohexane/ethyl acetate 50:50) to give 2-azidoethyl 6-*O*-*tert*-butyldimethylsilyl-2-deoxy-2-(3-methoxybenzamido)-β-D-glucopyranoside, compound **23** (840 mg, 80%). TLC R_f = 0.23 (cyclohexane/ethyl acetate 1:1); HR-ESIMS: *m/z* Calculated for $C_{22}H_{36}N_4O_7Si$ $[M + Na]^+$: 519.2251. Found 519.2258.

This intermediate (830 mg, 1.67 mmol) was further reacted with pyridine (270 µL, 3.34 mmol) and acetyl chloride (131 µL, 1.84 mmol) in dry THF (15 mL) at -20 °C to RT under inert atmosphere for 5 h. The solvent was evaporated under reduced pressure and the crude residue was then solubilized with ethyl acetate and successively washed with 0.2 N aqueous HCl, aqueous saturated $NaHCO_3$ and brine. The extract was dried over Na_2SO_4, filtered and concentrated under reduced pressure and then purified by flash chromatography (eluent: cyclohexane/ethyl acetate 100:0 to cyclohexane/ethyl acetate 65:25) to provide glycosamine acceptor **24** (679 mg, 76%). TLC R_f = 0.42 (cyclohexane/ethyl acetate 1:1); ^{1}H NMR (400 MHz, $CDCl_3$) δ 7.34 (1 H, br s, 1 H-arom), 7.30-7.24 (2 H, m, 2 H-arom), 7.00 (1 H, dt, *J* = 2.1 and 7.4 Hz, 1 H-arom), 6.79 (1 H, d, *J* = 9.2 Hz, NH), 5.35 (1 H, dd, *J* = 9.4 and 10.2 Hz, H-3), 4.75 (1 H, d, *J* = 8.3 Hz, H-1), 4.20 (1 H, q, *J* = 9.1 Hz, H-2), 4.02-3.88 (3 H, m, 2 H-6 and 1 OCH*H*), 3.81 (1 H, t, *J* = 9.3 Hz, H-4), 3.78 (3 H, s, OCH_3), 3.71-3.64 (1 H, m, OC*H*H), 3.57-3.51 (1 H, m, H-5), 3.47-3.38 (1 H, m, C*H*H), 3.29 (1 H, dt, *J* = 4.2 and 13.2 Hz, CH*H*), 2.07 (3H, s, CH_3), 0.92 (3 × 3 H, s, SiC(CH_3)$_3$), 0.13 (3 H, s, SiCH_3), 0.12 (3 H, s, SiCH_3); ^{13}C NMR (100 MHz, $CDCl_3$) δ 172.3 and 167.9 (2 CO), 159.8, 135.8, 129.6, 118.9, 117.8 and 112.5 (6 C-arom), 101.0 (C-1), 75.58 (C-3), 74.8, (C-5), 71.3 (C-4), 67.6 (OCH_2), 64.4 (C-6), 55.40 (OCH_3), 54.3 (C-2), 50.8 (CH_2), 25.9 (3 SiC(CH_3)), 21.09 (CH_3), 18.34 (SiC(CH_3)$_3$), - 5.35 and - 5.37 (2 $SiCH_3$); HR-ESIMS: *m/z* Calculated for $C_{24}H_{38}N_4O_8Si$ [M + Na]$^+$: 561.2357. Found 561.2371.

2-Azidoethyl [2,4,6-Tri-*O*-acetyl-3-*O*-(2-naphthyl)methyl-β-D-galactopyranosyl]-(1-4)-3-*O*-acetyl-2-deoxy-2-(3-methoxybenzamido)-β-D-glucopyranoside (25)

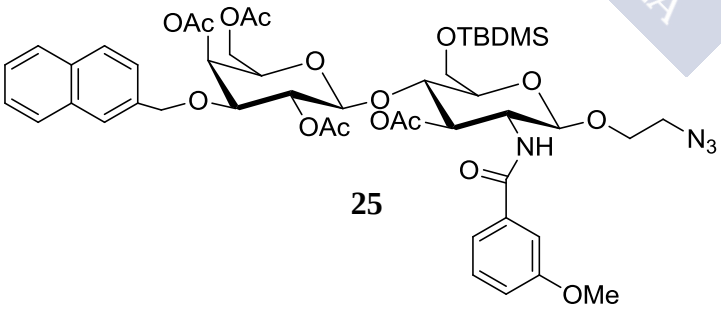

25

A solution of TBSOTf (1 M in CH_2Cl_2; 70 mL, 0.070 mmol) was added to a mixture of acceptor **24** (200 mg, 0.37 mmol) and donor **21** (273 mg, 0.46 mmol) in anhydrous dichloromethane at -20 °C under argon and further stirred at this temperature, followed by TLC (cylohexane/ethyl acetate 6:4). After 1 h, **21** was entirely consumed, as monitored by TLC (cyclohexane/ethylacetate 6:4), and DiPEA (14 mL, 0.08 mmol) was added. The solvent was evaporated under reduced pressure, and the crude residue was purified by flash chromatography (eluent: cyclohexane/ethyl acetate 100:0 to 80:20) to give an inseparable mixture of disaccharide,

hydrolyzed donor, and acceptor. Then the mixture was treated with HF-pyridine (2 mL) in CH_3CN (2 mL) at 0 °C for 2 h. The crude reaction mixture was then diluted wit ethyl acetate and washed with aqueous saturated $NaHCO_3$ (2 × 20 mL), and brine. The extract was dried over Na_2SO_4, filtered, and concentrated under reduced pressure. Flash chromatography (eluent : cyclohexane/ethyl acetate 100:0 to 40:60) of the resulting residue provided disaccharide **25** (100 mg, yield 32%); TLC R_f = 0.49 (cyclohexane/ethyl acetate 0:1); ^{1}H NMR (400 MHz, CDCl3): δ = 7.85–7.78 (m, 3H), 7.69 (br s, 1H), 7.51–7.45 (m, 2H), 7.37–7.32 (m, 2H), 7.28–7.23 (m, 1H), 7.19 (t, *J* = 7.9 Hz, 1H), 7.00–6.93 (m, 2H), 5.52 (d, *J* = 3.5 Hz, 1H), 5.27 (dd, *J* = 9.0, 10.7 Hz, 1H), 5.02 (dd, *J* = 8.0, 10.0 Hz, 1H), 4.81 (AB system, *J* = 12.3 Hz, 1H), 4.66 (d, *J* = 8.3 Hz, 1H), 4.53 (AB system, *J* = 12.3 Hz, 1H), 4.49 (d, *J* = 8.0 Hz, 1H), 4.40–4.30 (m, 1H), 4.14 (dd, *J* =6.9, 11.0 Hz, 1H), 4.06 (dd, *J* = 6.9, 11.6 Hz, 1H), 3.98 (ddd, *J* = 3.6, 5.6, 11.1 Hz, 1H), 3.94–3.87 (m, 2H), 3.84–3.78 (m, 1H), 3.77–3.70 (m, 2H), 3.57 (dd, *J* = 3.5, 10 Hz, 1H), 3.43–3.33 (m, 1H, H-5), 3.29 (ddd, *J* =3.6, 5.6, 13.3 Hz, 1H), 2.11, 2.07. 2.00 and 1.99 ppm (4 s, 4V3H); ^{13}C NMR (100 MHz, CDCl3): δ = 171.6, 170.6, 170.3, 169.5, 167.7, 159.8, 135.8, 134.8, 133.2, 133.2, 129.5, 128.3, 127.9, 127.8, 126.8, 126.3, 126.2 and 125.7, 119.0, 117.6, 112.8, 101.5, 101.4, 76.6, 75.6, 75.5, 73.5, 71.6, 71.0, 70.9, 68.1, 65.7, 61.6, 60.7, 55.4, 53.9, 50.6, 20.9, 20.8, 20.7 ppm; HR-ESIMS: *m/z* Calculated for $C_{41}H_{48}N_4O_{16}$: 875.2963 $[M+Na]^+$; found: 875.2993.

2-Azidoethyl [3-*O*-(2-naphthyl)methyl-β-D-galactopyranosyl]-(1-4)-2-deoxy-2-(3-methoxybenzamido)-β-D-glucopyranoside (26)

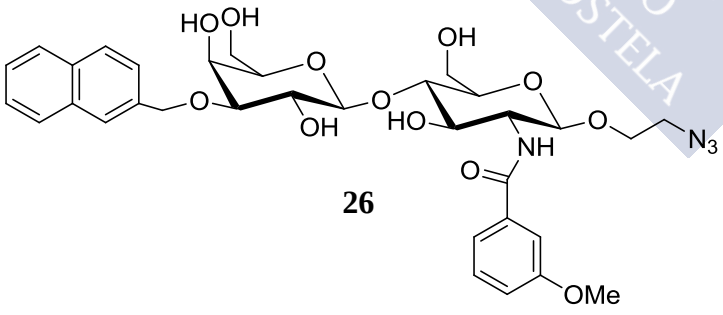

26

Disaccharide **25** (99 mg, 0.12 mmol) was dissolved in MeOH (2 mL) and treated with sodium methoxide (10 µL of a 25% w/v solution in MeOH) at RT for 2 h. The reaction mixture was then neutralized with IR 120 (H^+) resin, filtered, and concentrated under vacuum. The crude mixture was purified by flash chromatography on silica gel (eluent: CH_2Cl_2/MeOH 100:0 to 90:10) to give compound **26** (60 mg, 75%); TLC R_f = 0.34 (CH_2Cl_2/MeOH 95:5); ^{1}H NMR (400 MHz, DMSO-d_6) δ 8.26 (1 H, d, *J* = 8.9 Hz, NH), 7.94 (1 H, s, H arom naphthyl), 7.93-7.85 (3 H, m, 3 H arom naphthyl), 7.60 (1 H, dd, *J* = 1.6 and 8.4 Hz, 1 H arom naphthyl), 7.54-7.46 (2 H, m, 2 H-arom naphthyl), 7.42 (1 H, dd, *J* = 1.6 and 7.6 Hz, 1 H-arom MeOBz),

7.39-7.34 (2 H, m, 2 H-arom MeOBz), 7.12-7.04 (1 H, m, 1 H-arom MeOBz), 5.34 (1 H, d, *J* = 5.2 Hz, OH), 4.87 (1 H, AB system, *J* = 12.4 Hz, C*H*H), 4.74 (1 H, AB system, *J* = 12.4 Hz, C*H*H), 4.71-4.63 (4 H, m, 4 OH), 4.61 (1 H, d, *J* = 8.7 Hz, H-1), 4.31 (1 H, d, *J* = 7.8 Hz, H-1'), 3.99-3.94 (1 H, m, H-4'), 3.92-3.81 (3 H, m, OC*H*H, H-6a', H-2), 3.80 (3 H, s, CH_3), 3.75-3.51 (6 H, m, H-3, H-6b', OC*H*H, H-2', H-6a, H-6b), 3.50-3.34 (6 H, m, H-5', H-4, 2 C*H*HN_3, H-5, H-3'); ^{13}C NMR (100 MHz, DMSO-d_6) δ 165.8 (CONH), 159.0 (C arom MeOBz), 136.6 and 136.5 (C arom naphthyl and C arom MeOBz), 132.8 and 132.4 (2 C arom naphthyl), 129.2 (C arom MeOBz), 127.6, 127.5, 126.0, 125.8 and 125.7 (7 C arom naphthyl), 119.4, 116.6 and 112.6 (3 C-arom MeOBz), 103.9 (C-1'), 100.7 (C-1), 81.4 and 81.2 (C-4 and C-3'), 75.5 and 75.3 (C-5 and C-5'), 72.2 (C-3), 70.4 (CH_2), 69.7 (C-2'), 67.1 (CH_2), 64.7 (C-4'), 60.7 and 60.5 (C-6' and C-6), 55.2 (CH_3), 55.1 (C-2), 50.2 (CH_2); HR-ESIMS: *m/z* Calculated for $C_{33}H_{40}N_4O_{12}$ $[M + Na]^+$: 707.2540. Found 707.2534.

2-Aminoethyl [3-*O*-(2-naphthyl)methyl-β-D-galactopyranosyl]-(1-4)-2-deoxy-2-(3-methoxybenzamido)-β-D-glucopyranoside (27)

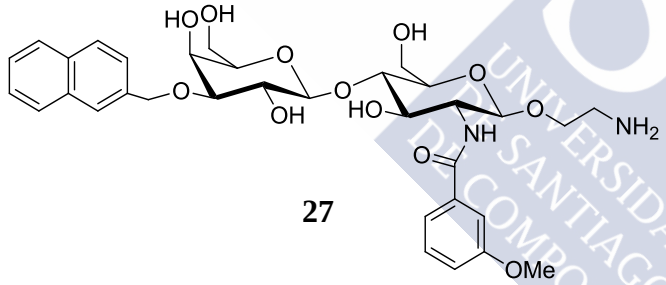

27

To a solution of azido derivative **26** (55 mg, 80.3 μmol) in THF (2 mL) were added PMe_3 (1 M in THF) (120 μL, 1.5 eq.) under argon and further stirred one day at RT. H_2O was then added to the mixture, which was further heated at 50 °C overnight. The crude mixture was then evaporated to dryness under reduced pressure and the residue purified by flash chromatography on silica gel (eluent: CH_2Cl_2/MeOH 100:0 CH_2Cl_2/MeOH 50:50) to give compound **27** (53 mg, 80%); TLC R_f = 0.05 (CH_2Cl_2/MeOH 90:10); ^{1}H NMR (400 MHz, CD_3OD) δ 7.93 (1 H, br s, 1 H arom naphthyl), 7.87-7.83 (3 H, m, 3 H-arom naphthyl), 7.60 (1 H, dd, *J* = 1.4 Hz and 8.5 Hz, 1 H-arom naphthyl), 7.50-7.44 (2 H, m, 2 H-arom naphthyl), 7.46-7.34 (3 H, m, 3 H arom MeOBz), 7.12-7.08 (1 H, m, 1 H arom MeOBz), 4.96 (1 H, AB system, *J* = 12.1 Hz, C*H*H), 4.84 (1 H, AB system, *J* = 12.1 Hz, CH*H*), 4.62 (1 H, d, *J* = 8.3 Hz, H-1), 4.45 (1 H, d, *J* = 7.8 Hz, H-1'), 4.08 (1 H, d, *J* = 3.0 Hz, H-4'), 4.01 (1 H, dd, *J* = 8.3 and 9.5 Hz, H-2), 4.00-3.82 (4 H, m, 2 H-6', OC*H*H and H-3), 3.85 (3 H, s, CH_3), 3.84-3.73 (1 H, m, H-6), 3.73 (1 H, br t, *J* = 7.8 Hz, H-2'), 3.74-3.48 (5 H, m, H-6, H-4, CH*H*, H-5 and H-5'), 3.47 (1 H, dd, *J* = 3.0 and 9.4 Hz, H-3'), 2.80 (2 H, br s, CH_2); ^{13}C NMR (100 MHz, CD_3OD) δ 169.2 (CONH),

159.8 (C arom MeOBz), 136.0 and 135.9 (C arom naphthyl and C arom MeOBz), 133.3 and 133.1 (2 C arom naphthyl), 129.2 (C arom MeOBz), 127.6, 127.5, 127.3, 126.3, 125.8, 125.7 and 125.5 (7 C arom naphthyl), 119.0, 117.0 and 112.4 (3 C-arom MeOBz), 103.8 (C-1), 101.6 (C-1'), 80.9 (C-3'), 80.0 (C-4), 75.6 (C-5), 75.3 (C-5'), 72.6 (C-3), 71.3 (CH_2), 70.6 (C-2'), 70.0 (CH_2), 65.8 (C-4'), 61.1 (C-6), 60.6 (C-6'), 55.8 (C-2), 54.5 (CH_3), 40.6 (CH_2); HR-ESIMS: *m/z* Calculated for $C_{33}H_{43}N_2O_{12}$ $[M + Na]^+$: 659.2816. Found 659.2813.

2-(Fluorescein-5-thiourea)ethyl [3-*O*-(2-naphthyl)methyl-β-D-galactopyranosyl]-(1-4)-2-deoxy-2-(3-methoxybenzamido)-β-D-glucopyranoside (28)

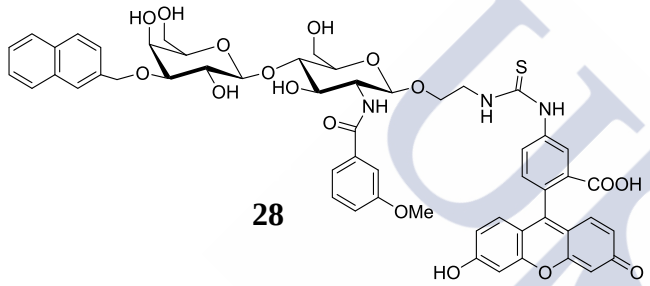

28

To a solution of azido derivative **27** (20 mg, 0.030 mmol) in THF (2 mL) were added PMe_3 (1 M in THF, 60 µL) under argon and further stirred one day at RT. H_2O was then added to the mixture which was further heated at 50 °C overnight. The crude mixture was evaporated to dryness under reduced pressure then diluted with DMF (2 mL). To this solution *N*,*N*-diisopropylethylamine (7.6 mL, 0.044 mmol) and fluorescein isothiocyanate (14.8 mg, 0.038 mmol) were added under argon and stirred overnight at RT. The mixture was concentrated under reduced pressure and then purified by flash chromatography (eluent: CH_2Cl_2/MeOH 100:0 to CH_2Cl_2/MeOH 95:5) to provide the flurescent compound **28** (16.1 mg, 55%). TLC R_f = 0.26 (CH_2Cl_2/MeOH 9:1); ESIMS: *m/z* Calculated for $C_{54}H_{52}N_3O_{17}S$ $[M - H]^-$: 1046.3017. Found 1046.3059.

2.3. Affinity studies (Experiments have been carried out by the lab technician Dr. Annie Lambert)

Fluorescence polarization (direct assay) was used to evaluate the affinity of an inhibitor coupled with a fluorescent tag towards human recombinant Gal-1, Gal-3 and Gal-7, expressed in *E. coli*. Fluorescence anisotropy was measured on a Tecan infinite M1000 plate reader with an excitation at 470 nm and emission at 525 nm, using Greiner 96 flat bottom black plate. Fixed probe concentration (0.1 µM) is added to an increasing concentration of galectin (0.001 to 200 µM) in a final sample volume of 200 µL (PBS containing 5% DMSO). Each measurement is realized after 1 hour incubation at room temperature or at 4 °C under 100 rpm (in duplicate).

K_d, A_{max} and A_0 were characterized for every galectin/labeled inhibitor pair tested using PRISM 7 software (GraphPad, USA).

K_d values for **28** were determined by fitting anisotropy data using non-linear least square method according to the following quadratic equation:

$$Y = A0 + ((Amax \times ((Cl + X + Kd - \sqrt[2]{(Cl + X + Kd)^2 - (4 \times Cl \times X)}/((2 \times Cl))$$

Whereby, Y = fluorescence anisotropy (A or mA); X = galectin concentration (µM); $A0$ = Ymin; A_{max} = Ymax Ymin; Cl = labeled inhibitor concentration (µM); K_d = labeled inhibitor dissociation constant (µM).

For competitive fluorescence anisotropy assays, each inhibitor was incubated at a 0.2 to 180 µM concentrations with a mixture of compound **26** (at a 0.1 µM concentration) and galectin-1 C3S, galectin-3 or galectin-7 (at a 1 µM concentration). Measurements were undertaken according to the same procedure reported for saturation polarization experiments.

Ki values were calculated using following equations:

$$logEC50 = \log(10^{logKi} \times \left(1 + \frac{Cl}{Kd}\right));$$

$$Y = \frac{Amax}{1 + 10^{X - LogEC50}} + A0$$

EC50 = Half maximal effective concentration (µM); Ki = Inhibitor dissociation constant (µM).

2.4. Preparation and characterization of HA NCs

2.4.1. Preparation of HA NCs

HA NCs were prepared by the solvent displacement technique, adapting the procedure earlier described by our group.[57] Briefly, lecithin (Lec, 5.625 mg), oleylamine (OAm, 1.125 mg) and olive oil (OO, 30 mg) were dissolved in 5 mL of ethanol. In the case of drug loaded NCs, Gal-3 inhibitor (2.5-5 mg) was incorporated to this phase. Then, the organic phase was injected through a needle (23G) to 10 mL of aqueous phase containing 2.5 mg of HA 700 kDa, and kept under magnetic stirring at 900 rpm during 10 minutes at room temperature. The elimination of organic solvent was performed by evaporation under vacuum (Rotavapor Heidolph, Germany) and the final volume adjusted to 5 mL with ultrapure water. Thereafter, the NCs were isolated by ultracentrifugation (Avanti® J-E, Ultracentrifuge, Beckman Coulter, USA) at 30,000×*g* for 1 h at 15 °C.

2.4.2. Physicochemical and morphological properties of HA NCs

The mean size and polydispersity index (PDI) of the HA NCs were measured after dilution (100×) with ultrapure water by dynamic light scattering (DLS) at 25 °C with an angle detection of 173°. The zeta potential (ζ) was measured by laser Doppler anemometry (LDA) after diluting the samples (100×) with ultrapure water. Both DLS and LDA analysis were performed in a Zetasizer®, NanoZS, Malvern Instruments, Malvern, UK. Particle size distribution and morphology were evaluated by transmission electron microscopy (TEM) using a JEOL JEM-2010 microscope, 200 KV, resolution: 0.23 nm (Tokyo, Japan). Samples for TEM analysis were diluted (20×), deposited on a copper grid, stained with a phosphotungstic acid solution (2% w/v) and allowed to dry overnight prior to analysis. The pH of formulations was measured at Sartorius Basic Meter PB-11, Sartorius AG, Germany.

2.4.3. Gal-3 inhibitor encapsulation efficiency of the NCs

The encapsulation efficiency (EE%) of Gal-3 inhibitor was determined after the isolation of the NCs by ultracentrifugation at 30,000×*g* for 1 h at 15 °C (Avanti® J-E, Ultracentrifuge, Beckman Coulter, USA). The amount of the drug encapsulated into the NCs

(EE% by direct method), the free drug in the undernatant (EE% by indirect method) and the total drug in the non-isolated NCs were quantified by high-performance liquid chromatography (HPLC), described below. For the extraction of Gal-3 inhibitor from the non-isolated, isolated NCs and undernatant, 0.1 mL of each sample were mixed with 0.9 mL ethanol/acetonitrile (ACN) and kept under magnetic stirring at a high speed overnight to obtain a clear solution. The samples were analyzed by HPLC method, developed specifically for this molecule based on the methods described for saccharides.[58–60] The HPLC system consisted of a VWR-Hitachi LaChrom Elite® system equipped with a UV detector L-2400 set at 254 nm and a reverse phase SunFire column 186002560, 100Å, C18 (4.6 ID × 250 mm, pore size 5 μm), Waters, USA. The mobile phase was a mixture of ACN and ultrapure water (60:40% v/v), isocratic, and the flow rate was 1 mL/min. The column was set at 30 °C and the injection volume was 20 μL. The standard calibration curves of Gal-3 inhibitor were linear in the range of 1-1000 μg/mL (r^2 = 0.999). Samples were transferred into auto-sampler vials, capped and placed in the HPLC auto-sampler. The concentration of Gal-3 inhibitor in the aliquots was used to calculate the encapsulation efficiency (EE%) by direct method as follows:

$$EE\% = \frac{Amount\ of\ \ DXM\ \ in\ isolated\ \ destructed\ \ NCs}{Total\ \ DXM} \times 100$$

2.5. NCs loaded HA-fibrin in situ hydrogels

Non-fortified HA-fibrin hydrogel samples with 30% of blank or Gal-3 inhibitor loaded NCs were prepared and characterized as described in **Chapter 1** (*Section 2.1*). Briefly, fibrinogen (Fg), HAs, NCs were mixed in polymerization buffer and the gelation process was initiated by thrombin (Thr).

2.6. In vivo studies

2.6.1. Carrageenan-induced acute knee joint inflammation (synovitis) model

At the day of experiment, animals were randomly separated into three groups (of at least 5 animals per group) and two reference animals (one was used for a carrageenan test and another for a gel syringeability test). Animals average body weight (BW) was 281 ± 9 g. Rats

were anesthetized by intra-peritoneal injection (300 µL) of a solution containing ketamine (75 mg/kg) and medetomidine (0.50 mg/kg) and thereafter the skin around the knee joints was shaved.

Carrageenan-induced knee joint inflammation model (synovitis) was used to evaluate the anti-inflammatory effect of the selected formulations. The acute synovial inflammation of the rat knee was induced 1 hour after the treatment by intra-articular (IA) injection of a freshly prepared solution of carrageenan (50 µL, 3% w/v) in physiological saline (0.9% w/v NaCl), using 27G needles, into the right knee of rats according to the technique described elsewhere.[61,62]

2.6.2. In vivo treatment

Before distributing the animals according to the tested treatments, one animal was induced with carrageenan (identified I, **Table 1**), acting as a disease control and one animal served as reference for gel syringeability test (identified II, **Table 1**), receiving 100 µL of HA-fibrin *in situ* gel with 30% blank NCs and without further inflammation induction.

First group of animals was treated with blank NCs, used as vehicle control (group 1). Second group received Gal-3 inhibitor loaded NCs administered at the dose of 200 µg/kg (group 2). The third group was treated with HA-fibrin *in situ* gel with 30% Gal-3 inhibitor loaded NCs at the dose of 55 µg/kg (group 3). Groups 1-3 received an IA injection (100 µL) of the formulations using low dead *space* 30G × 1/2" Omnican 50 (BBraun) syringes 1 hour prior the injection of carrageenan. All the components were mixed in the syringe and immediately injected into the right knee. The left knee without injection was used as a control. **Table 1** summarizes the animal distribution to the certain groups according to the tested materials and Gal-3 inhibitor doses.

Samples for animal II and group 3, consisted of HA-fibrin hydrogel with 30% of blank or Gal-3 inhibitor loaded NCs, respectively, were prepared as the presented in **Table 2**.

Table 1. Experimental animal groups.

Group	Rat number	Carrageenan 3%, (µL)	Gal-3i dose (µg/kg)	Tested materials	Injected volume (µL)
I	1	50	-	-	-
1	2		-	Blank NCs	100
	3		-		
	4		-		
	5		-		
	6		-		
2	7		200	Gal-3i NCs	
	8				
	9				
	10				
	11				
	12				
II	13	-	-	Gel + 30% blank NCs (Gel syringeability test)	
3	14	50	55	Gel + 30% Gal-3i NCs	
	15				
	16				
	17				
	18				

Table 2. The samples "HA-fibrin hydrogel + 30% NCs" composition.

Composition	Final concentration	Volume (µL)
Fg in 0.15 M NaCl	1.5 mg/mL	6
HAs mix 1:1 (1.5 MDa : 700 kDa) in HEPES buffer, 10^{-3} M Ca^{2+}, pH 7.4	0.5%	62
Blank or Gal-3i NCs	30%	30
Thr in PBS + 1% BSA (added as a last component)	2 NIH-U/mL	2
Total volume		**100**

At time 4 hours after carrageenan injection (the peak of inflammation) 3 animals of each group were sacrificed by isoflurane inhalation and blood was collected by cardiac puncture. The other animals were kept for measurements at 6 and 24 hours.

2.6.3. Knee swelling measurement

The diameter of each rat shaved knee (in mm) was measured by digital calliper (150 mm / 6" - 0.01 mm, Perel Tools), before treatment and 2, 4, 6 and 24 hours after carrageenan injection. Before measurements, rats were additionally anaesthetized (if it was necessary) with inhaled isoflurane. Knee swelling was expressed as the change (Δ) in the knee diameter before and after the induction of inflammation:

$$\text{Knee swelling } \Delta = A - B,$$

where A represents the knee diameter at different time points after injection, and B represents the knee diameter before injection.

While, the percentage of increase in knee diameter (knee edema) of the right knee of each rat at each time point was calculated by the following equation:

$$\text{Percentage of increase} = (A - B)/B \times 100,$$

where A represents the knee diameter at different time points after injection, and B represents the in knee diameter before injection.

2.6.4. Whole blood, plasma tests and histopathology studies

Blood was collected into heparinized tubes and was used for whole blood analysis immediately.

The animal paws were surgically cut at the level above the patella. All the paws were fixed in 10% buffered formalin and decalcified with 10% formic acid before histopathological analysis. In order to evaluate the surroundings of the site of application, decalcified paws were processed for embedding in paraffin wax by using routine protocol. Sections (5 µm thick) were stained with haematoxylin and eosin (H&E). The slides were examined using light microscopy at 40, 100, 400× magnification using an Olympus BX40 microscope coupled with an Olympus DP 10 camera (Olympus, Shinjuku, Tokyo, Japan). The images were obtained using the respective Olympus DP 10 camera software and edited with Microsoft Image Composite Editor. The histopathological appearance of tissues was compared for structure changes, edema and inflammatory cell infiltration (mononuclear and/or polymorphonuclear cells).

2.7. Statistical analysis

All the measurements at each experimental condition were carried out in triplicates and were expressed as mean ± standard deviation (SD). Statistical analysis of the data was performed using an one-way ANOVA and Student's t-test using Microsoft® Excel software; a value of $p < 0.05$ was considered significant.

Regarding the *in vivo* data, the mean ± standard error of mean (SEM) was determined for each treatment group (n = 5). The statistical analysis was carried out using a two-way ANOVA test followed by Bonferroni's post-hoc test. All other analyses were performed using a Student's t test. Differences were considered statistically significant at $p < 0.05$.

3. RESULTS AND DISCUSSION

3.1. Synthesis of galectin-3 inhibitors

The natural ligands for Gal-3 are polylactosamine and LacNAc of both types I and II.[63] Lactosamine type II core (Gal-β(1→4)GlcN) has been selected for the inhibitors preparation due to higher intrinsic affinity to Gal-3, K_d (LN2) = 33 μM versus K_d (LN1) = 93 μM[64]. Gal-3 sugar binding site comprises 7 highly conserved amino acid residues (His158, Asn160, Arg162, Glu165, Asn174, Trp181, Glu184.[55,65] Five of them (His158, Asn160, Arg162, Asn174 and Glu184) and highly conserved water molecules are involved in the tight cooperative hydrogen bonding with Gal O-5, OH-4 and OH-6 and GlcNAc OH-3, while Trp181 stabilizes the galactose residue through H-π stacking[55] (**Figure 3**). Other LacNAc positions do not contribute significantly to the binding.[28,55,63] Especially important are the residues Arg144 and Arg186, because their guanidinium ions can establish cation-π interactions with aromatic substituents at Gal 3'-C and GlcN 2-C positions, increasing compound affinities and selectivities[28,51,66–68] (**Figure 3** and **Figure 7, Chapter Introduction**). Indeed, amino acids residues Arg144, Ala146 and Asn160 from the CRD side chains form a polar pocket that due to Arg144 presence, binds strongly to introduced aromatic substituents at 3'-C position of Gal by cation-π interactions.[28] Similarly, Arg186 can bind introduced aromatic substituents at 2-C position of GlcN by mentioned interactions.[51,69] Additionally, aromatic substituents at both 3'-C and 2-C positions of the inhibitor are involved in intramolecular protein salt bridges and van der Waals contacts with Gal-3

CRD.[51,67] Combination of aromatic substitutations at 3'-C and 2-C positions can provide additive or even synergistic effect to the binding when carried out on lactosamine or thio-digalactoside scaffolds, respectively.[68,69] While both scaffolds are able to discriminate between different galectins,[70] the lactosamine one offers the unique advantage of further derivatization at its reducing end to obtain multivalent,[71,72] grafted or labelled derivatives (**Figure 4**). All these possibilities make inhibitors based on LacNAc attractive and well-established ligands for Gal-3.[28,51,66,67]

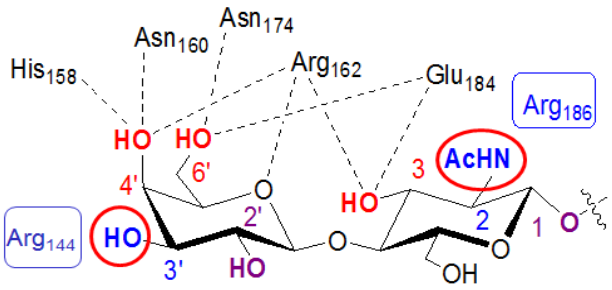

Figure 3. Scheme showing possible modification of LacNAc unit with aromatic substituents at Gal 3'-C position and *GlcN* 2-C positions (surrounded with red circles) to increase affinity to Gal-3 CRD.

We developed a first generation of inhibitors using 3-methoxyphenyl as the aromatic ring.[68,71] Based on Nilsson and coworkers' results, we hypothesized that 3-methoxyphenyl ring could be advantageously replaced by either a 2-naphthyl or a 3,5-dimethoxyphenyl at the Gal 3'-C position. In their hands, such substituents lead to 5× and 2× more affine inhibitors as well as considerably enhanced specificity towards Gal-7, respectively. It was also suggested that introduction of 3,5-dimethoxyphenyl, but not 2-naphthyl at GlcN 2-C position could provide more efficient stacking[69] (**Figure 4**).

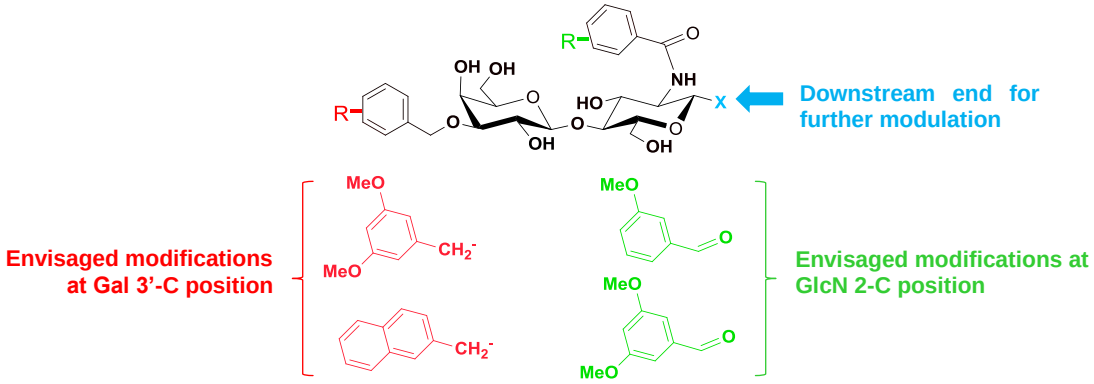

Figure 4. A schematic representation of the strategy selected for Gal-3 inhibitors synthesis.

Lactosamine is not commercially available at a reasonable price. Therefore access to the planned inhibitors could rely on amine functionalization at 2-C of D-lactal, in turn obtained from D-lactose in four steps or, alternatively, according to a glycosylation reaction between advanced galactose donor and glucosamine acceptor intermediates.

Synthesis of inhibitors had been initially envisaged according to strategies **(A)** and **(B)**, which differ from each other by the key reactions applied for lactal functionalization: **(A)** an iodosulfonamidation/azidation sequence, previously developed by our laboratory;[71,73] **(B)** an azidophenylselenation,[74,75] as presented in **Scheme 1**.

Synthetic pathways for both approaches started from D-lactal **4**, derived from commercially available D-lactose in four known steps comprising peracetylation, bromation, zinc-mediated reductive elimination and Zemplén deacetylation,[76,77] as detailed in **Scheme 2**. Subsequently regioselective arylation of the OH group at Gal-3 position of lactal **4** was envisaged using stannylene chemistry.[78] To this aim, D-lactal was treated with dibutyltin oxide in refluxing methanol and the resulting unstable intermediate further treated with either 3,5-dimethoxybenzyl bromide or (2-naphthyl)methyl bromide to provide derivatives **6** with 63% and 42% yields, respectively. These intermediates were treated with an excess of chlorotriethylsilane in the presence of imidazole for protection of free hydroxy groups resulting to 3'-C substituted persilylated lactal **7** in quantitative yields 95% for both. Iodosulfonamidation and azido-phenylselenation were attempted in parallel on both derivatives. However, both procedures led to complex mixtures (monitored by TLC) and low yield of expected products, probably due to partial iodine oxidation of the naphthyl and considerable oxidation of highly electrophilic, dimethoxy substituted phenyl rings.

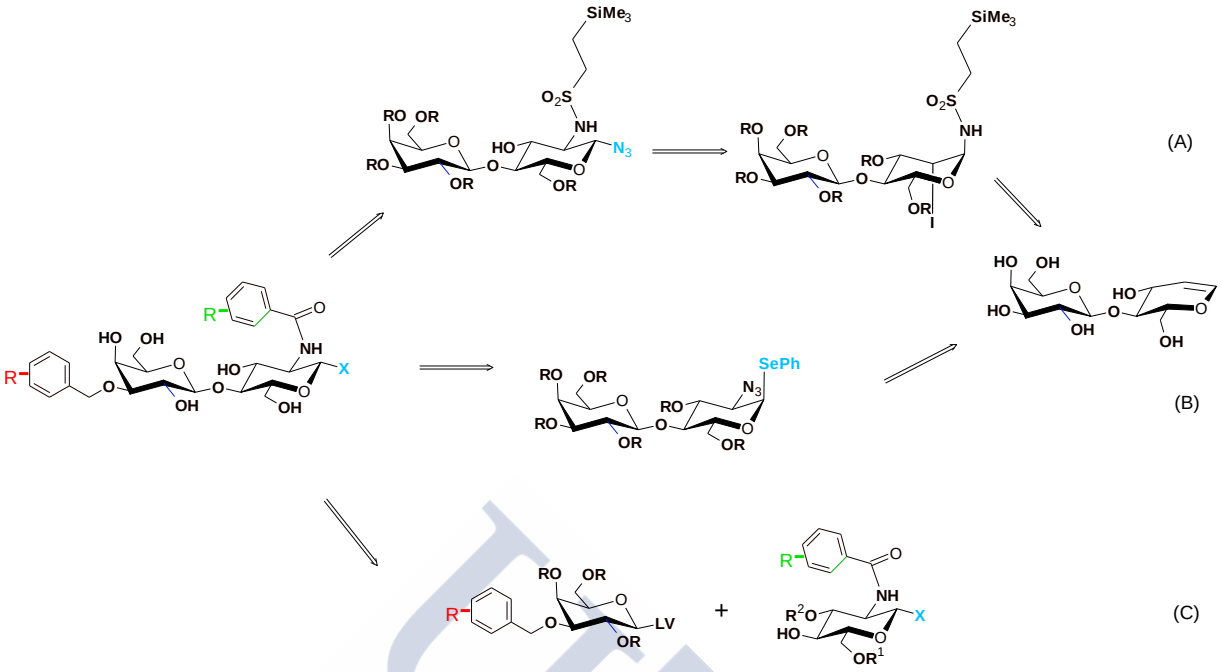

Scheme 1. A short scheme of derivatives preparation by 3 approaches: iodosulfonamidation (**A**), azidophenylselenation (**B**) and 1+1 glycosylation (a donor-acceptor coupling approach) (**C**).

We, thus, envisaged to modify the original strategy and to carry out the 1-C, 2-C lactal functionalization prior to the introduction of the 3'-C aromatic group to circumvent these side-reactions. This novel approach was, however, attempted only for the azidophenylselenation-based strategy, which appeared more promising (**Scheme 3**).

D-lactal **4,** was persilylated as described previously to give intermediate **9** (quantitative). Compound **9** was further treated with iodosylbenzene diacetate in the presence of diphenyl diselenide and trimethylsilyl azide to give 2-azido-1-phenylseleno disaccharide **10** in the expected "*gluco*" configuration. Key intermediate **10** was deprotected to give polyhydroxylated derivative **11**. Regioselective arylation of **11** using 3,5-dimethoxybenzyl bromide gave rise to intermediate **12**, which was further acetylated to furnish azide **13** (96% yield). Azido group in **13** was reduced using an excess of trimethylphosphine to give amine **14**, further acylated using 3,5-dimethoxybenzoyl chloride in 67% yield.

Approach **A**

(Iodosulfonamidation approach)

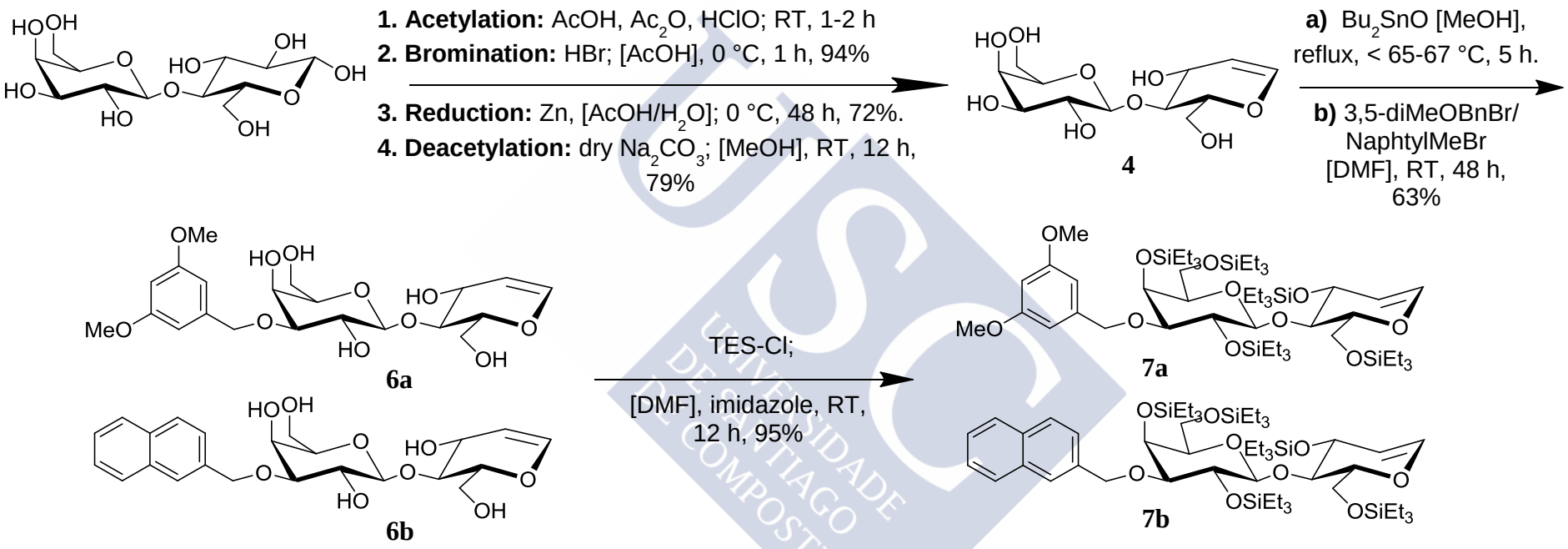

Scheme 2. The sequence of the reactions in iodosulfonamidation approach, reagents and compounds yields.

Approach **B**

(Azidophenylselenation approach, page 1)

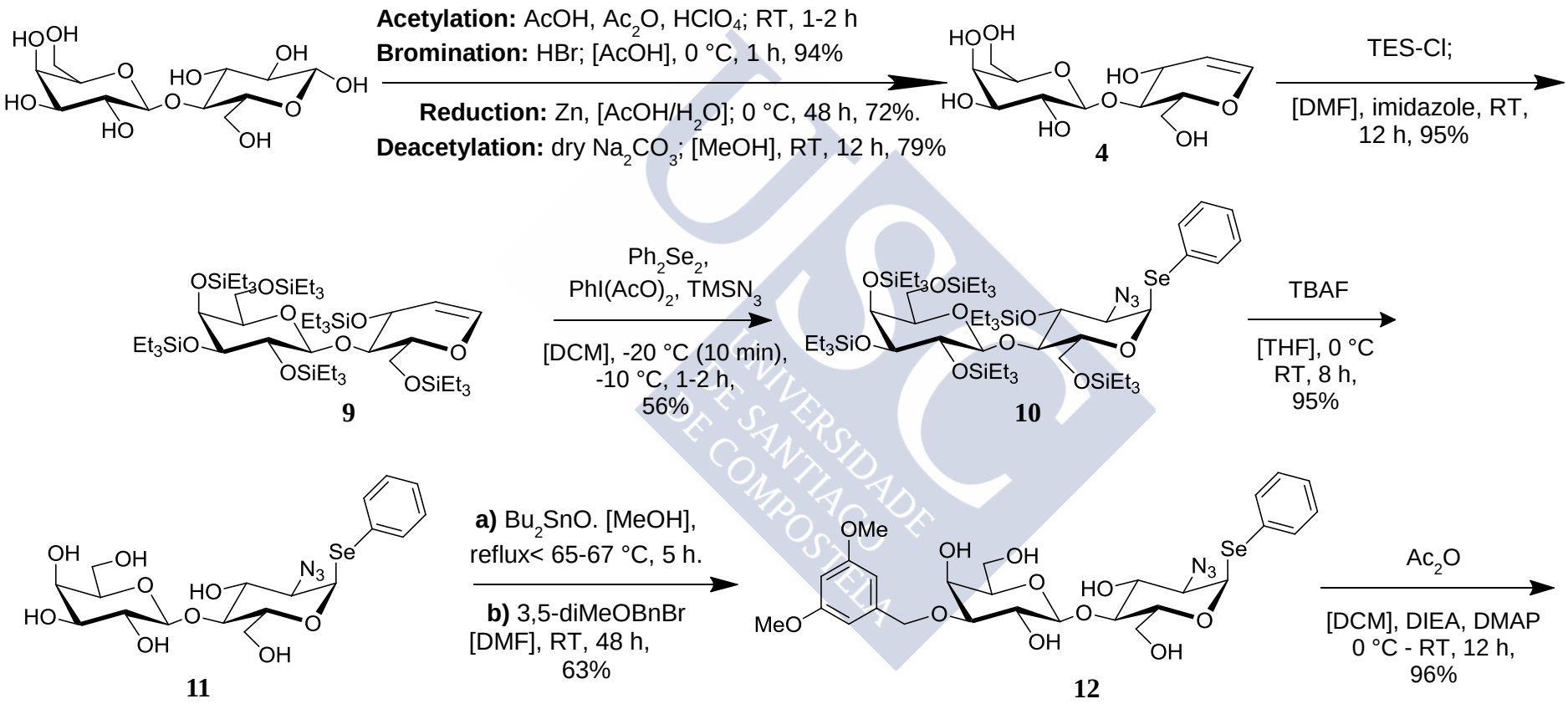

Scheme 3. The sequence of the reactions in azidophenylselenation approach, reagents and compounds yields (page 1 of 2).

Approach **B**

(Azidophenylselenation approach, page 2)

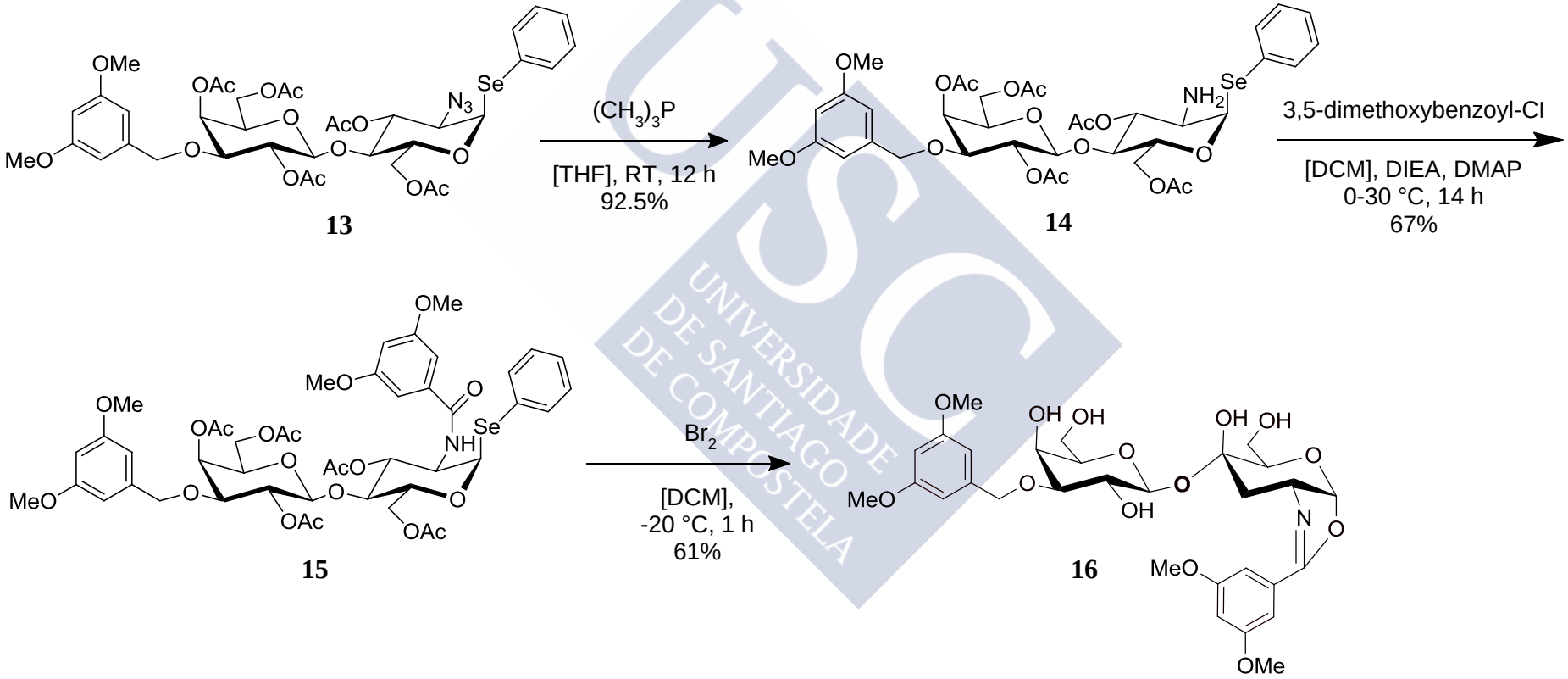

Scheme 3. The sequence of the reactions in azidophenylselenation approach, reagents and compounds yields (page 2 of 2).

Attempts to activate the phenylselenide at the anomeric position of the GlcN moiety *e.g.* using bromine to pursue the functionalization of this derivative led to the formation of unprecedented oxazoline **15**. This compound was finally deprotected under Zemplén conditions to provide a first potential inhibitor **16**.

Having a 3,5-dimethoxyphenyl derivative in hands, we decided to prepare an inhibitor with a (2-naphthyl)methyl substituent to give enhanced and more specific interaction with the Gal-3, since larger π-systems are more polarizable and form stronger interactions with Arg144 cation in the polar pocket.[67] This modification at the Gal 3'-C position is known to increase more than five times the affinity of the LacNAc to Gal-3 compared to a 3-methoxybenzyl substituent,[79] while conferring full and 22 times more selectivity for this galectin versus the galectin-7 and galectin-1, respectively.[69] Thus, we devised a new synthetic approach (**Scheme 1,** route **(C)**), named "1+1" glycosylation, relying on the glycosylation reaction between a galactosyl donor and a glucosamine acceptor for its assembly to a disaccharide. The latter was thought to be equipped with an azido spacer to afford further modulation of its properties.

This synthetic route started with regioselective alkylation of commercially available methyl β-D-galactopyranoside **17** using (2-naphtyl)methyl bromide as the electrophile. Resulting derivative **18** was acetylated to give **19,** which, in turn, was submitted to acetolysis. Maintaining the reaction temperature below 4 °C proved essential to prevent premature hydrolysis of the napthyl ether group as a side-reaction. Intermediate **20** was finally transformed into galactosyl trichloroacetimidate donor **21**. In parallel, removal of the phthaloyl protecting group of the known 2-azidoethyl glucosamine derivative **25**[56] with ethylenediamine followed by acylation (**23**) and selective acetylation of the 3-OH gave key acceptor **24**. Glycosylation of donor **21** with acceptor **24** followed by desilylation furnished the expected disaccharide **25** in a moderate yield, consequence of the disarming effect of both 3-methoxybenzamido and acetate on **24**, together with important amount of desilylated acceptor. Final step consisted in the deacetylation of **25** to give di-aromatic inhibitor **26** (2-azidoethyl [3-*O*-(2-naphtyl)methyl-β-D-galactopyranosyl]-(1-4)-2-deoxy-2-(3-methoxybezamido)-β-D-glucopyranoside). Azido group of **26** was next reduced in the presence of trimethylphosphine to give amino intermediate **27**. Compound **27** was reacted with fluorescein isothiocyanate to give a fluorescent probe **28** for further affinity evaluation by fluorescence polarization assay (**Scheme 4**).

Approach **C**

(1+1, donor-acceptor coupling approach)

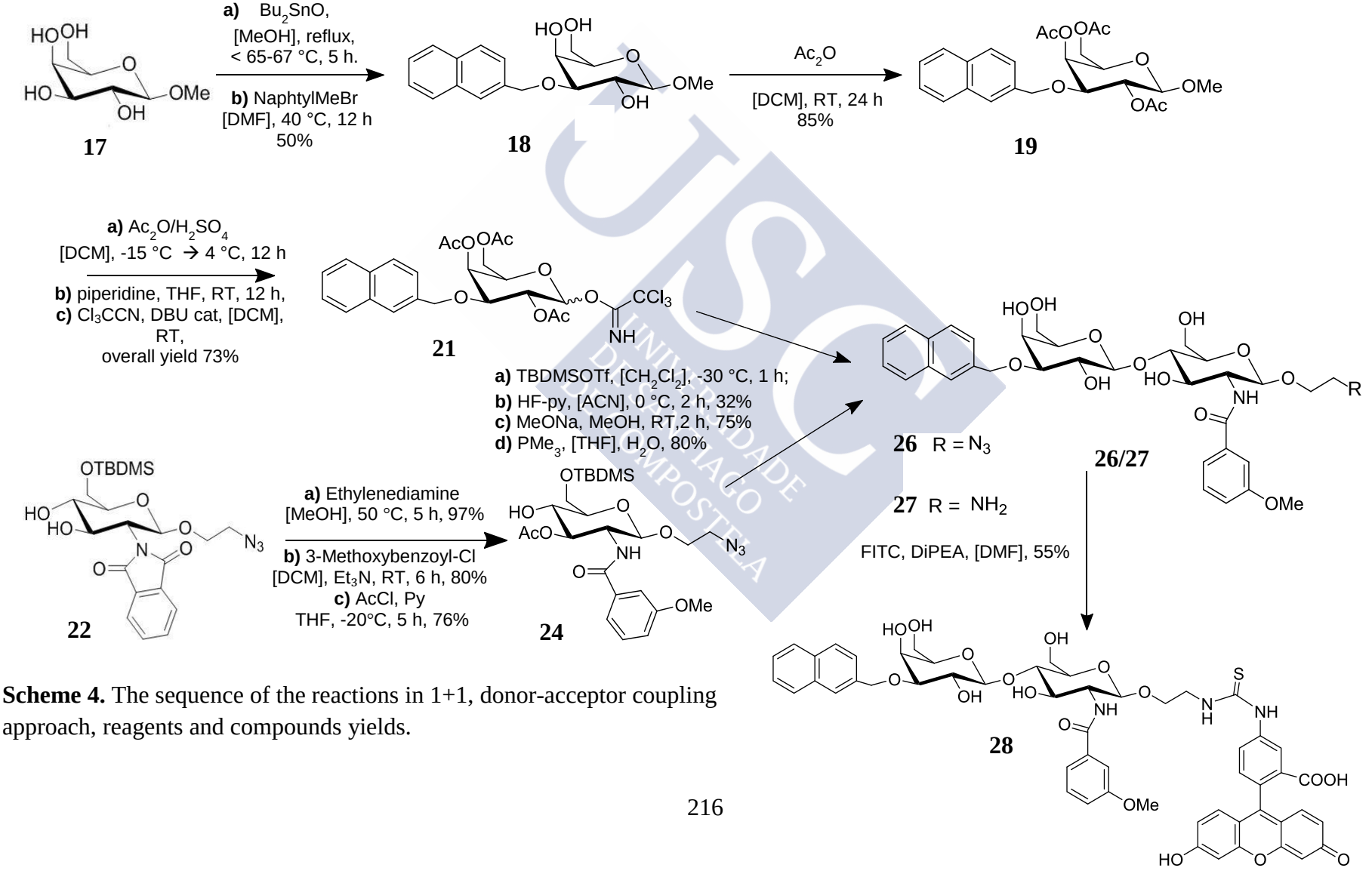

Scheme 4. The sequence of the reactions in 1+1, donor-acceptor coupling approach, reagents and compounds yields.

Finally, the introduction of a spacer arm at position 1-C of GlcN, initially envisaged for all the approaches, may be used to modulate the properties of the inhibitor: providing the hydrophobicity (for following encapsulation), grafting to the polymers or binding to the scaffolds for multivalent inhibitors preparation.

3.2. Affinity studies

An intact inhibitor **16**, **26**, fluorescein-labeled derivative **28,** an intact inhibitor and TD139 were selected for affinity studies by direct fluorescence polarization assay (**Table 3**).[80] *In vitro* evaluation of dissociation constants has been carried out at two different temperatures for the recombinant human galectin-1 C3S (a stable mutant in which Cys is substituted for oxidation-insensitive Ser),[81] galectin-3 and galectin-7.

Table 3. Dissociation constants of FITC-labeled compound **16,** compound **26**, compound **28** and **TD139** and galectin-1 C3S, galectin-3 and galectin-7.

	K_d (μM)[a]			
Compound	**Galectin-1[b]**	**Galectin-3**	**Galectin-7**	**Affinity**
	Temperature 4 °C			
LacNAc-β-OMe [c]	65 ± 28	n.d.	550 ± 98	+
16	112 ± 7	4.4 ± 0.25	249 ± 21	++
26	27 ± 5	0.59 ± 0.11	90 ± 35	+++
28	16 ± 1	0.014 ± 0.005	21 ± 1	++++
TD139	2.2 ± 1.4	0.036 ± 0.023	32 ± 17	++++
TD139[e]	0.012 ± 0.003	0.014 ± 0.003	1.9 ± 0.38	++++
	RT			
LacNAc-β-OMe [c]	n.d.	59 ± 12	n.d.	+
16	n.d.	23 ± 0.31	n.d.	++
26	n.d.[d]	2.99 ± 0.17	n.d.	+++
28	43 ± 4	0.082 ± 0.014	129 ± 18	++++
TD139	n.d.	0.166 ± 0.091	n.d.	++++
TD139 [f]	0.22 ± 0.05	0.068 ± 0.01	38 ± 0.71	++++

[a] Mean values from two assays; [b] Galectin-1: galectin-1 C3S (this study) or native galectin-1 (last two rows) [c] Determined by fluorescence polarization (from reference[67]); [d] n.d. = not determined; [e] Measured by fluorescence polarization at RT except for Gal-7 (from ref.[82]); [f] Determined by ITC at 24.8 °C (from ref.[51]).

Fluorescence polarization is sensitive to experimental temperature and higher affinity is observed at lower temperature in these studies. Moreover, the fluorescein tag has been shown to contribute galectins binding.[63,67,70] Compound **28** displayed very high selectivity: K_d(Gal-1)/K_d(Gal-3) = 524 and K_d(Gal-7)/K_d(Gal-3) = 1573 at RT or K_d(Gal-1)/K_d(Gal-3) = 1143 and K_d(Gal-7)/K_d(Gal-3) = 1500 at 4 °C.

This derivative was also used as probe for competitive fluorescence polarization assays at 0.1 µM with 1 µM galectin. Inhibitors **26** and **16** as well as TD139 as a positive control were assessed for binding affinity to Gal-1 C3S, Gal-3 and Gal-7 at 4 °C or RT. Compound **26** was much less recognized than **28** by these lectins, which supports the idea that the fluorescent tag facilitates galectin recognition,[28] having K_d values in the sub-micromolar range toward Gal-3. Noticeably, compound **26** was selective for Gal-3 over Gal-1 (K_d(Gal-1)/K_d(Gal-3) = 46) as well as highly selective over Gal-7, (K_d(Gal-7)/K_d(Gal-3) = 152. The same tendency was observed for compound **16** – Gal-3 over Gal-1 (K_d(Gal-1)/K_d(Gal-3) = 25.5 and Gal-3 over Gal-7 (K_d(Gal-7)/K_d(Gal-3) = 57. To ascertain these experimental data, TD139 was introduced as a positive control and the determined values compared to that reported in the literature. While determined K_d of TD139 for the galectin-3 was in good agreement with the values reported by Leffler *et al.*, some discrepancies were noted, in particular, regarding galectin-1[82] (**Table 3**). Indeed, TD139 was claimed not to discriminate between galectin-1 and galectin-3, what is in disagreement with our results. Although both series of data were obtained by fluorescence anisotropy assays, the use of different probes at different concentrations might explain the observed bias. However, our data correlate well with reported K_d values of TD139 for Gal-1, Gal-3 and Gal-7 determined by isothermal titration calorimetry (ITC).[51]

As we proved, careful choice of aromatic substituents (2-naphthyl)methyl or 3,5-dimethoxybenzyl at 3'-C position of Gal has enhanced both the affinity and the specificity toward galectin-3. As expected, methoxy-substituents at meta-position of the introduced aromatic ring of compound **16** facilitate the complexation between the tested inhibitor and CRD of Gal-3.[28] Interestingly, binding of compound 16 to Gal-7 or Gal-1 is in the same order or even less, respectively, than naked type II lactosamine, suggesting that oxazoline substituent is counter-productive to Gal-7 and Gal-1 recognition. This inhibitor can, however, be accommodated by Gal-3 CRD with a potency in the µM range. Thus, inhibitor **26** demonstrated 7.5 and 7.6 times higher affinity towards Gal-3 compared to oxazoline **16** at

4 °C and RT, correspondingly, designing the derivative **26** as a lead compound for evaluation of Gal-3 inhibition *in vivo*.

3.3. Development and characterization of Gal-3 inhibitor loaded NCs

To avoid a rapid removal of compound **26**, named as the Gal-3 inhibitor (Gal-3i), from the intra-articular cavity, we decided to load this derivative in the previously developed DDS (**Chapter 1**). Thus, first we designed, produced and characterized Gal-3i loaded NCs to be later incorporated into a HA-fibrin hydrogel.

Blank and Gal-3i-loaded HA NCs were successfully prepared using the simple solvent displacement technique. The particle size, zeta potential and encapsulation efficiency of the formulations are summarized in **Table 4**.

Table 4. Physicochemical characteristics of the nanocapsules (NCs) prepared with 700 kDa HA (mean ± SD; n = 3). PDI: polydispersity index, EE%:

Type of NCs	Particle size (nm)	PDI	ζ-potential (mV)	Drug concentration (mg/mL)	Drug EE%
Blank	121 ± 10	0.2	−30 ± 3	n/a	n/a
Gal-3i NCs	122 ± 11	0.2	−29 ± 5	0.53 ± 0.05	11 ± 2%

For the preparation of HA-based NCs, we used the following components: olive oil (OO), lecithin (Lec), oleylamine (OAm) and HA. The ratio Gal-3i/OO/Lec/OAm/HA was 0.9:4:1:0.2:0.44. In order to obtain small particle sizes, the preparation of the NCs was made injecting the organic phase over the aqueous phase through a needle. The particle size for drug loaded formulations, determined by DLS, was 122 ± 11 nm, PDI 0.2 and ζ-potential −29 ± 5 mV, encapsulation efficiency 11 ± 2% (531 ± 5 μg/mL).

3.4. Stability of the NCs

No drug leakage was observed upon 5 days storage of NCs and after 5 months 74 ± 19% of the initially encapsulated drug was detected.

3.5. NCs loading into in situ hydrogel

We have shown the capacity of HA-fibrin *in situ* hydrogels to load HA NCs (**Chapter 1**, *Section 3.1)*. Maximal incorporation capacity of Gal-3i loaded NCs to *in situ* HA-fibrin hydrogel was 30% (v/v). Gelation process of blank and NCs loaded hydrogels was monitored by turbidity analysis and verified by rheology studies. Complete characterization of NCs loaded hydrogels is given in the **Chapter 1** (*Section 3.2*).

None of the DDS components doses is suppose to cause any inflammatory response *in vivo*. Cirino *et al.* found that thrombin administrated intra-articularly mediates inflammation in the rat paw at doses 1-10 NIH-U/paw.[84] Although the hydrogel formation is activated by Thr at dose 0.2 NIH-U per injection, this value is 5 times below the limit causing transient edema or moderate inflammation.

3.6. In vivo studies

3.6.1. Carrageenan-induced acute knee joint synovitis

The homology between human and rat Gal-3 CRDs is about 96.5%, confirmed by structure-based sequence alignment of mammalian Gal-3s' CRD S4-S6 β-strands fragments,[64] which make the rat models appropriate for *in vivo* testing of human Gal-3 inhibitors.

There are different models of RA in rats: acute (short term inflammation) and chronic (long-lasting inflammation), that share similar features with human RA. Thus, acute models are induced by carrageenan (1% - 3% solutions)[62,85–95] or type-II collagen,[23,96–101] while chronic models include antigen-induced arthritis by methylated BSA,[102–105] adjuvant-induced arthritis by *Mycobacterium butyricum*[85,87] and fungal-induced arthritis by *Candida albicans.*[106]

Short term models are the preferred for drug screening and testing of cell therapies, they constitute useful tools to designed specific therapeutic interventions to suppress synovial inflammation.[85] Therefore, an acute carrageenan-induced synovitis model was selected for Gal-3i evaluation. Carrageenan-induced knee swelling is a two-step process: during 1 hour the release of histamine, serotonin and bradykinin is observed, as well as initial levels of prostaglandins. Later phase, after 1 hour, is associated with continuous prostaglandins

generation, polymorphonuclear leucocytes infiltration and release of pro-inflammatory markers, NO, and free radicals.[107,108] Finally, the peak of inflammation is observed at 4 hours after carrageenan injection.[62]

3.6.2. Anti-inflammatory activity of Gal-3 inhibitor in synovitis rat model

Intra-articular injections of carrageenan led to significant increase of the knee diameter of hindpaw (~ 40%) due to the swelling process, which correlates well with the results described by Ekundi-Valentim *et al.*[62] At 4 hours after carrageenan injection the knee diameter reached the maximum value (**Figure 5**). Interestingly, the treatment with blank NCs, Gal-3i NCs and "HA-fibrin hydrogel + 30% Gal-3i NCs" prevented this tendency. In this way, blank NCs showed to slightly diminish the inflammation. This can be explained by the rational selection of components; on the one hand, olive oil core presents anti-inflammatory functions, due to the high content of oleocanthal with ibuprofen-like activity.[94,109,110] On the other hand, the NCs shell polymer, 700 kDa HA, is known to be the most effective among hyaluronans of different MWs in reducing synovial inflammation.[111] Gal-3i NCs at the dose of 200 µg/kg reduced the inflammation in about 3.5 times at Δ4 hours compared to carrageenan control and 2 times compared with blank NCs. Noticeably, HA-fibrin hydrogel with 30% Gal-3i NCs caused an effective swelling inhibition in about 7 times compared to carrageenan control (**Figure 5**). This becomes more remarkable if we consider that the dose used for group 3 is considerably lower than for the group 2 (55 vs 200 µg/kg). Possibly, HA-fibrin hydrogel effectively keeps NCs within the articular cavity, modulates the release and by itself has a beneficial effect on joints healing even in the short inflammatory rat model.

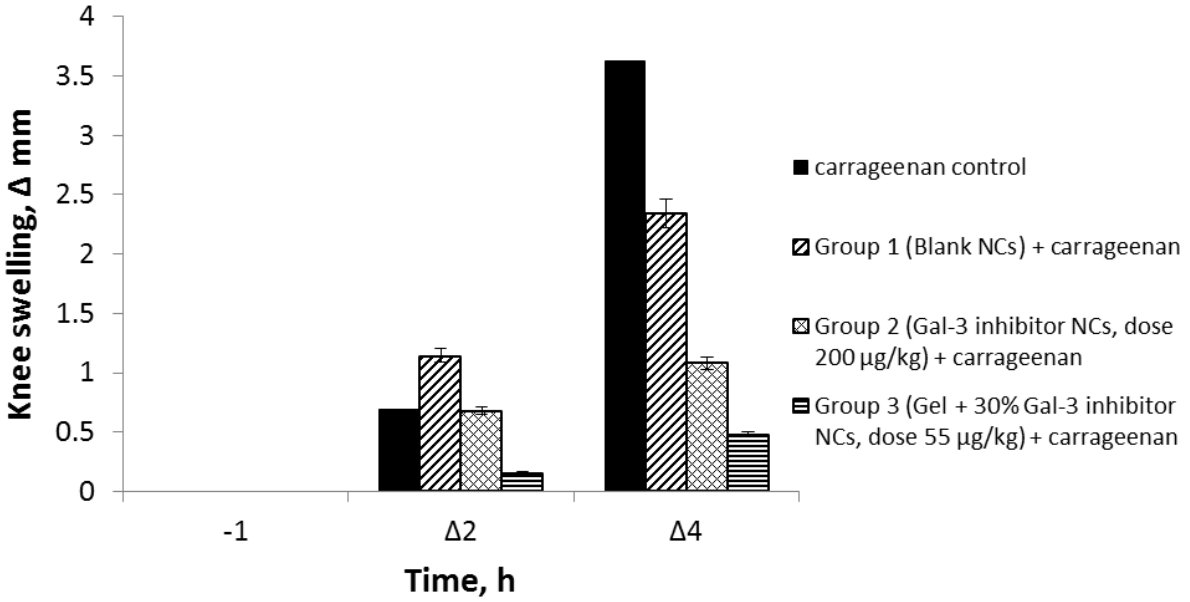

Figure 5. Effect of the treatment with Gal-3 inhibitor on the carrageenan-induced joint inflammation model using NCs, and NCs in a gel compared to blank NCs and carrageenan control (n = 5/6 for groups 1-3, n = 1 for carrageenan and gel control). Δ is the difference in knee diameter at different time points before and after injection of carrageenan, expressed in mm. Data is expressed as mean ± SEM.

3.6.3. Blood tests (immune cells level changes)

Blood samples were collected at 4 hours after carrageenan injection (n = 3), before the animals were euthanized, and analyzed on the same day. The total leucocytes formula and amount of lymphocytes, neutrophils and monocytes are presented in **Figure 6**, which illustrates the changes in cell levels.

The inflammation process is accompanied by rapid inversion of the leukogram ratio: decrease of lymphocytes and increase of neutrophils,[62] which in turn attract macrophages and dendritic cells,[112] presented at the **Figure 6** as total monocytes. Considering the obtained results, Gal-3i loaded NCs in the hydrogel is able to prevent this tendency, improving the total leucocytes amount, increasing the lymphocytes and reducing the neutrophils level.[1,97,112]

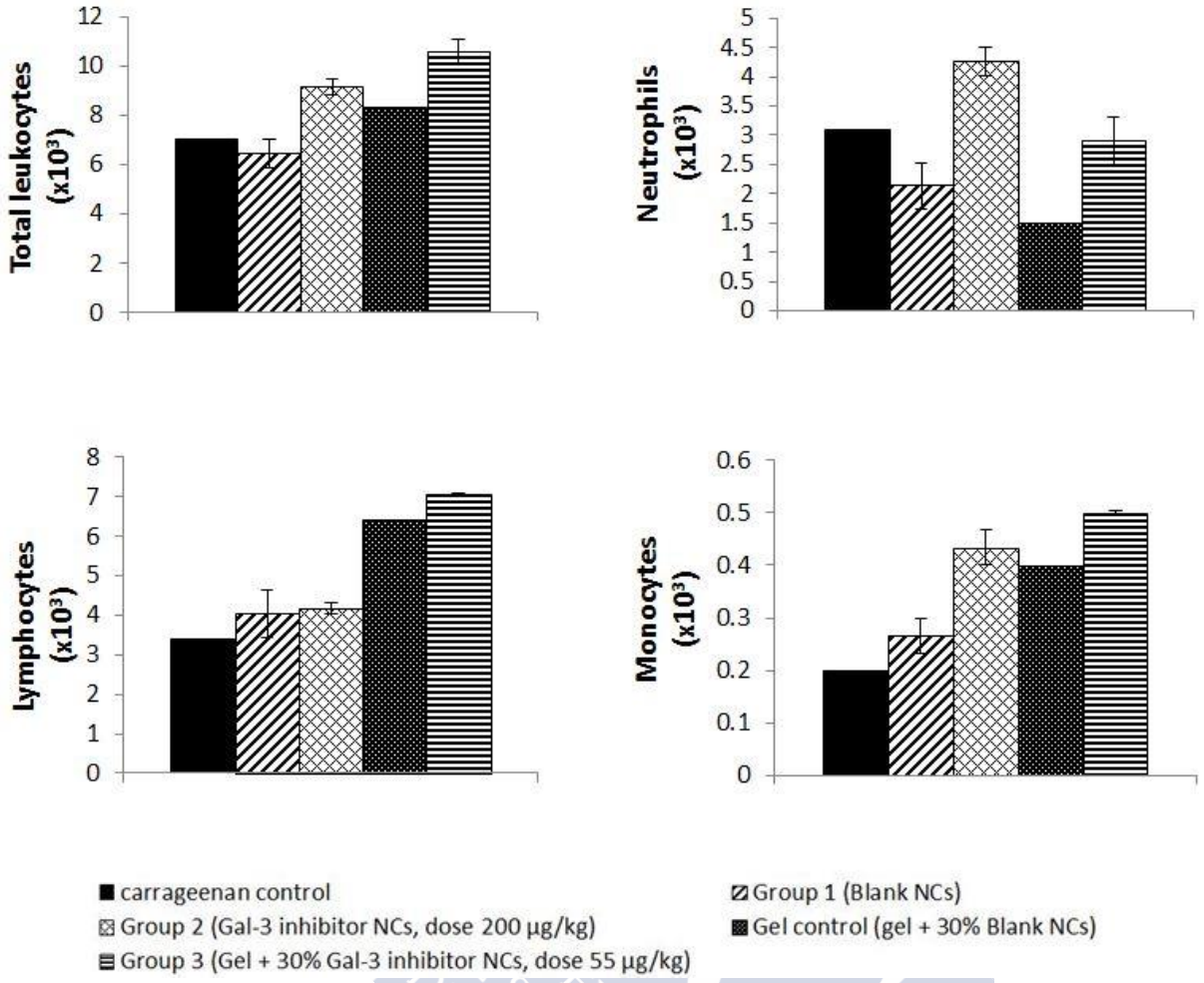

Figure 6. Effect of the treatment with Gal-3 inhibitor on leukocyte levels at the blood plasma at different doses administered in NCs, and the gel compared to blank NCs and carrageenan control (n = 5 for groups 1-3, n = 1 for carrageenan and gel control). Data expressed as mean ± SEM.

3.6.4. Histopathological scores

After decalcification process the rat hind paws and knees specimens were sliced, stained and analyzed by light microscopy (**Figure 7**).

Articular cartilage from carrageenan control rat had a normal histological appearance. Leukocytes margination and moderate infiltration of neutrophils and its accumulation in the synovial membrane surface, sometimes with synovial membrane surface cell loss were observed. Articular cavity included several neutrophil and fibrin agglomerates. In the surrounding tissues edema and neutrophil infiltration into the capsule and into the skeletal muscle were detected. Extensive synovitis lesions were found in the various synovial

membranes with great emphasis on vascular phenomena. Hence, carrageenan control exhibited a pronounced inflammatory response (**Figure 7A**), which is consistent with the reported histological data by other authors.[62,113]

The treated groups 1-3 revealed no microscopic changes in the articular cartilage. Congestion of synovial membranes was observed in all the groups, however accumulation of neutrophils and fibrin in the surface of synovial membrane was detected in both groups 1 (**Figure 7B**) and 2 (**Figure 7C**), while only light/moderate neutrophils infiltration was found in group 3 (**Figure 7E**). Additionally, loss of surface synovial cells was also present in groups 1 and 2. Similarly for these two groups, surrounding tissues lesion extension was presented as synovitis of variable intensity with neutrophil infiltration in the periarticular tissue, as well as disperse hemorrhages; however edema in group 2 was less intensive than in group 1. In contrast, in the case of group 3, only light edema and mild neutrophil infiltration in the periarticular tissue with no hemorrages were observed. Surrounding tissues from groups 1 and 2 reflected strong inflammatory reaction and neutrophil infiltration through the muscular tissue and periosteum. The articular cavity contained several neutrophil, erythrocytes and fibrin agglomerates for both group 1 and 2, while articular cavity of group 3 presented a few neutrophil agglomerates with no fibrin deposition and heterogeneous synovial membrane changes with no evidence of inflammatory reaction. Similar histological results were obtained by other autors in carrageenan-induced knee joint synovitis animal models.[62,114]

The rat knee, injected with Gel + 30% blank NCs with no carrageenan, did not show microscopic articular cartilage neither synovial membrane changes. Besides, articular cavity was free of neutrophils and no signs of cell infiltration were detected in the surrounding tissues (**Figure 7D**), suggesting that the DDS is well-tolerated *in vivo*.

In conclusion, the improvement on the histological level was gradually observed from group 1 to 3, suggesting that Gal-3i in its final DDS (Gel + 30% NCs) has the most detectable impact on the inhibition of synovial inflammation and the articular tissues integrity in rat synovitis model.

Of note, the current study is a preliminary and unprecedented *in vivo* evaluation of a novel galectin-3 inhibitor effects in short RA rat model. More tests are required to understand Gal-3 inhibitor behavior and its impact on the inflammatory cascade of RA in rat joints. For ethical and economical reasons further tests were not performed upon this study.

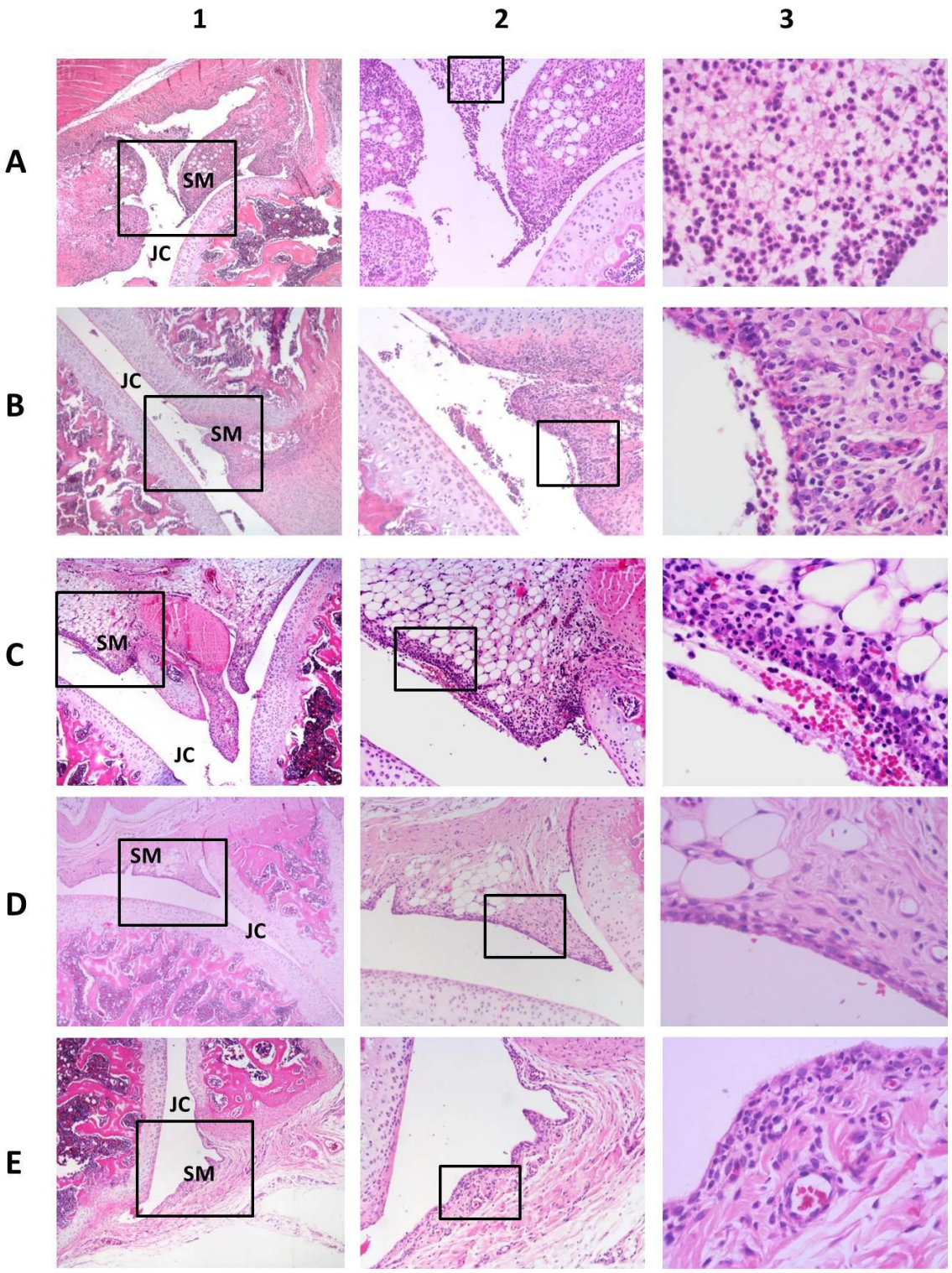

Figure 7. Microphotographs from rat knee joints stained with haematoxylin and eosin; low (40×), medium (100×) and high (400x) magnification (columns 1, 2 and 3 respectively). The square areas in the images reveal the amplified regions of the photograph. Groups: control of carrageenan (row **A**), blank NCs + carrageenan (row **B**), Gal-3i NCs + carrageenan (row **C**), blank NCs + gel (row **D**) and Gal-3i NCs + gel + carrageenan (row **E**). Abbreviations: **SM**, synovial membranes; **JC**, joint cavity.

As shown by a number of authors, HA-fibrin hydrogel is a perspective biocomposite with versatile functions, which alone or in combinations with other materials have also received major breakthrough at different biomedical applications,[43,115–119] in particular in tissue engineering (TE).[120] In the light of the above, Zhang *et al.* developed a HA-fibrin *in situ* hydrogel, prepared by orthogonal fibrinogenesis and disulfide crosslinking reaction between chemically modified HA-molecules and fibrinogen, designed for cell encapsulation. This hydrogel also included aprotinin (a synthetic inhibitor of fibrinolysis) aimed to prolong gel half-life and demonstrated complete degradation profile *in vitro* in the solution of nattokinase in 5 days, notably, 50% of degradation is observed between day 1 and 2, and complete degradation is between day 4 and 5.[118] Another HA-fibrin hydrogel for TE was developed by Lee and Kurisawa, where HA was modified with tyramine to improve the gel mechanical properties and prevent degradation by enzymes. These highly crosslinked gels incubated with low dose of plasmin or hyaluronidase showed 100% matrix stability *in vitro* during 7 days, despite they were able to support less amount of proliferated cells in its matrixes, compared to the gels that lost 50% in diameter within 2 days.[43] Park *et al.* designed fibroin-fibrin-HA hydrogel to create a mechanically strong and slowly degradable cell scaffold for cartilage regeneration. The authors showed maintenance of about 95% of initial gel volume in chondrocyte culture during 4 weeks.[119] Ultimately, the same group has also developed fortified fibrin-HA composite gel with chondrocytes for implantation. In order to inhibit the degradation, gels were fortified with FXIII and aprotinin and tested in nude mice subcutaneously and, thus, demonstrated huge endurance *in vivo* up to 4 weeks.[121] Clearly, reinforced by supplementary crosslinking agents and fibrinolysis inhibition factors HA-fibrin gel scaffolds demonstrate better performance *in vivo*.

Given that articular cartilage has limited ability to self-healing,[122] fortified HA-fibrin gel (designed and described in **Chapter 1**) may contribute to restore the integrity of cartilage in longer chronic rat inflammatory models, serving as a temporary matrix for *in vivo* cells encapsulation.[118] *In vivo* gel half-life time in rat joint was not evaluated in this study, but might be interesting for further exploration of DDS performance. Such a composite might result to a synergistic effect in tissue self-healing properties – HA-fibrin matrix plays a major role in the subsequent tissue regeneration processes.[123]

4. CONCLUSIONS AND FUTURE PERSPECTIVES

Despite the growing interest for the galectin family, to date only few reports mention the use of small molecule inhibitors to interfere with galectin-mediated biological processes.[131–135] Some of them made used of poor and unspecific inhibitors such as lactose, making necessary to apply high doses to observe significant effects.[136] In this work, a novel highly affine and potent monovalent Gal-3 inhibitor, composed of two different moieties assembled to a modified lactosamine core was designed and synthesized. The hydrophobic form of Gal-3 inhibitor was included within hyaluronic acid NCs although the encapsulation efficiency makes necessary a further optimization. Then, NCs were loaded into *in situ* HA-fibrin hydrogel designed for intra-articular administration. A pronounced anti-inflammatory activity was found in rat carrageenan-induced knee synovitis model for the inhibitor encapsulated in HA NCs included to the hydrogel. Treated rats showed improvement on the histological and white blood cells levels as well as in the knee swelling tests. The inhibition of galectin-3 is a promising strategy for the treatment of inflammatory knee diseases with particular interest for rheumatoid arthritis. These findings present Gal-3 inhibitor as a lead compound for anti-RA drug candidates. Efficiency of Gal-3 inhibitor could be further enhanced by preparation of multivalent inhibitors using synthetic scaffolds mimicking lactose units. Apart from joints pathologies, Gal-3 mono- or multivalent inhibitors could be applied for the treatment of other inflammatory conditions, *e.g.* cancer, bowel diseases, etc. increasing the range of therapeutic possibilities for these new compounds.

REFERENCES

1. Gibofsky, A. Overview of epidemiology, pathophysiology, and diagnosis of rheumatoid arthritis. *Am. J. Manag. Care* **18,** S295–302 (2012).

2. Li, S., Yu, Y., Koehn, C. D., Zhang, Z. & Su, K. Galectins in the pathogenesis of rheumatoid arthritis. *J Clin Cell Immunol* **4,** 164 (2013).

3. Nation Institute for Health and Care Excellence. *Rheumatoid arthritis The management of rheumatoid arthritis in*. 78 (2009).

4. Steiner, G. & Smolen, J. Autoantibodies in rheumatoid arthritis and their clinical significance. *Arthritis Res. Ther.* **4,** 1 (2002).

5. Hu, Y. *et al.* Advances in research on animal models of rheumatoid arthritis. *Clin. Rheumatol.* **32,** 161–165 (2013).

6. Quan, L.-D., Thiele, G. M., Tian, J. & Wang, D. The Development of Novel Therapies for Rheumatoid Arthritis. *Expert Opin. Ther. Pat.* **18,** 723–738 (2008).

7. Emry, P. *Atlas of Rheumatoid Arthritis*. 35–66 (2015).

8. Bua, S. *et al.* Design and Synthesis of Novel Nonsteroidal Anti-Inflammatory Drugs and Carbonic Anhydrase Inhibitors Hybrids (NSAIDs-CAIs) for the Treatment of Rheumatoid Arthritis. *J. Med. Chem.* **60,** 1159–1170 (2017).

9. Firestein, G. S. Evolving concepts of rheumatoid arthritis. *Nature* **423,** 356–61 (2003).

10. Turesson, C., O'Fallon, W. M., Crowson, C. S., Gabriel, S. E. & Matteson, E. L. Occurrence of extraarticular disease manifestations is associated with excess mortality in a community based cohort of patients with rheumatoid arthritis. *J. Rheumatol.* **29,** 62–67 (2002).

11. Ngo, S. T., Steyn, F. J. & McCombe, P. a. Gender differences in autoimmune disease. *Front. Neuroendocrinol.* **35,** 347–369 (2014).

12. Petit, A. In situ forming hydrogels for intra-articular delivery of celecoxib : from polymer design to in vivo studies. (2014).

13. Hu, Y., Yéléhé-Okouma, M., Ea, H. K., Jouzeau, J. Y. & Reboul, P. Galectin-3: A key player in arthritis. *Jt. Bone Spine* **84,** 15–20 (2017).

14. McInnes, I. The Pathogenesis of Rheumatoid Arthritis. *N. Engl. J. Med.* **365,** 2205–19 (2011).

15. Zuber, T. J. Knee joint aspiration and injection. *Am. Fam. Physician* **66,** 1497–1503 (2002).

16. Goronzy, J. J. *et al.* Prognostic markers of radiographic progression in early rheumatoid arthritis. *Arthritis Rheum.* **50,** 43–54 (2004).

17. Choy, E. H. S. & Panayi., G. S. Cytokine pathways and joint inflammation in rheumatoid arthritis. **344,** 907–916 (2001).

18. Fernández-Carballido, A., Herrero-Vanrell, R., Molina-Martínez, I. T. & Pastoriza, P. Biodegradable ibuprofen-loaded PLGA microspheres for intraarticular administration: Effect of Labrafil addition on release in vitro. *Int. J. Pharm.* **279,** 33–41 (2004).

19. Wernecke, C., Braun, H. J. & Dragoo, J. L. The Effect of Intra-articular Corticosteroids on Articular Cartilage: A Systematic Review. *Orthop. J. Sport. Med.* **3,** 1–7 (2015).

20. Brown, P. M., Pratt, A. G. & Isaacs, J. D. Mechanism of action of methotrexate in rheumatoid arthritis, and the search for biomarkers. *Nat. Rev. Rheumatol.* **12,** 731–742 (2016).

21. Takeuchi, T. & Kameda, H. The Japanese experience with biologic therapies for rheumatoid arthritis. *Nat. Rev. Rheumatol.* **6,** 644–652 (2010).

22. Soini, E. J., Leussu, M. & Hallinen, T. Administration costs of intravenous biologic drugs for rheumatoid arthritis. *Springerplus* **2,** 531 (2013).

23. De Oliveira, F. L. *et al.* Galectin-3 in autoimmunity and autoimmune diseases. *Exp. Biol. Med.* (2015).

24. Chen, H. Y., Liu, F.-T. & Yang, R.-Y. Roles of galectin-3 in immune responses. *Arch. Immunol. Ther. Exp. (Warsz).* **53,** 497–504 (2005).

25. Evans, C. H., Kraus, V. B. & Setton., L. A. Progress in intra-articular therapy. *Nat. Rev. Rheumatol.* **10,** 11–22 (2015).

26. Kang, M. L. & Im, G.-I. Drug delivery systems for intra-articular treatment of osteoarthritis. *Expert Opin. Drug Deliv.* **11,** 269–82 (2014).

27. Haudek, K. C. *et al.* Dynamics of galectin-3 in the nucleus and cytoplasm. *Biochim. Biophys. Acta - Gen. Subj.* **1800,** 181–189 (2010).

28. Sörme, P., Arnoux, P., Kahl-Knutsson, B. & Leffler, H. Structural and Thermodynamic Studies on Cation− Π Interactions in Lectin− Ligand Complexes: High-Affinity Galectin-3 Inhibitors through Fine-Tuning of an Arginine− *J Am Chem* 543–549 (2005).

29. Lepur, A. Functional properties of Galectin-3. Beyond the sugar binding. *Lund University, University of Zagreb* (2012).

30. Thiemann, S. & Baum, L. G. Galectins and Immune Responses—Just How Do They Do Those Things They Do? *Annu. Rev. Immunol* **34,** 243–64 (2016).

31. Vasta, G. R. *et al.* Galectins as self/non-self recognition receptors in innate and adaptive immunity: An unresolved paradox. *Front. Immunol.* **3,** 1–14 (2012).

32. Rabinovich, G. A. & Toscano, M. A. Turning 'sweet' on immunity: galectin-glycan interactions in immune tolerance and inflammation. *Nat. Rev. Immunol.* **9,** 338–352 (2009).

33. Than, N. G. *et al.* A primate subfamily of galectins expressed at the maternal-fetal interface that promote immune cell death. *Proc. Natl. Acad. Sci. U. S. A.* **106,** 9731–9736 (2009).

34. Joo, H. G. *et al.* Expression and function of galectin-3, a beta-galactoside-binding protein in activated T lymphocytes. *J. Leukoc. Biol.* **69,** 555–64 (2001).

35. Ohshima, S. *et al.* Galectin 3 and Its Binding Protein in Rheumatoid Arthritis. *Arthritis Rheum.* **48,** 2788–2795 (2003).

36. Janelle-Montcalm, A. *et al.* Extracellular localization of galectin-3 has a deleterious role in joint tissues. *Arthritis Res. Ther.* **9,** R20 (2007).

37. Aubin, J. E., Liu, F., Malaval, L. & Gupta, a. K. Osteoblast and chondroblast differentiation. *Bone* **17,** (1995).

38. Kimura, T. *et al.* Dedicated SNAREs and specialized TRIM cargo receptors mediate secretory autophagy. 1–19 (2016).

39. Mantovani, A., Sozzani, S., Locati, M., Allavena, P. & Sica, A. Macrophage polarization: Tumor-associated macrophages as a paradigm for polarized M2 mononuclear phagocytes. *Trends Immunol.* **23,** 549–555 (2002).

40. Forsman, H. *et al.* Galectin 3 aggravates joint inflammation and destruction in antigen-induced arthritis. *Arthritis Rheum.* **63,** 445–454 (2011).

41. Palmer, M., Stanford, E. & Murray, M. M. The effect of synovial fluid enzymes on the biodegradability of collagen and fibrin clots. *Materials (Basel).* **4,** 1469–1482 (2011).

42. Ortega, N., Behonick, D. J., Colnot, C., Douglas N.W. Cooper & Werb, and Z. Galectin-3 Is a Downstream Regulator of Matrix Metalloproteinase-9 Function during Endochondral Bone Formation. *Mol. Biol. Cell* **16,** 1–13 (2005).

43. Lee, F. & Kurisawa, M. Formation and stability of interpenetrating polymer network hydrogels consisting of fibrin and hyaluronic acid for tissue engineering. *Acta Biomater.* **9,** 5143–5152 (2013).

44. Masuko, K., Murata, M., Yudoh, K., Kato, T. & Nakamura, H. Anti-inflammatory effects of hyaluronan in arthritis therapy: Not just for viscosity. *Int. J. Gen. Med.* **2,** 77–81 (2009).

45. Page-McCaw, A., Ewald, A. J. & Werb, Z. Matrix metalloproteinases and the regulation of tissue. *Nat Rev Mol Cell Biol.* **8,** 221–233 (2007).

46. Klyosov, A., Zomer, E. & Platt, D. in *Glycobiology and Drug Design* **1102,** 89–130 (American Chemical Society, 2012).

47. Klyosov, A. a. Galectins as New Therapeutic Targets for Galactose-Containing Polysaccharides. *Bull. Georg. Natl. Acad. Sci.* **8,** 5–17 (2014).

48. ClinicalTrials. A New Agent GM-CT-01 in Combination With 5-FU, Avastin and Leucovorin in Subjects With Colorectal A New. 10–12 (2016).

49. Harrison, S. *et al.* Randomised clinical study: GR-MD-02, a galectin-3 inhibitor, vs. placebo in patients having non-alcoholic steatohepatitis with advanced fibrosis. *Aliment. Pharmacol. Ther.* **44,** 1183–1198 (2016).

50. ClinicalTrials. RCT (Randomized Control Trial) of TD139 vs Placebo in HV's (Human Volunteers) and IPF Patients Purpose. 10–12 (2016).

51. Hsieh, T. *et al.* Dual thio-digalactoside-binding modes of human galectins as the structural basis for the design of potent and selective inhibitors. *Sci. Rep.* **6,** 29457 (2016).

52. ClinicalTrials. An Open-Label , Phase 2a Study to Evaluate Safety and Efficacy of GR-MD-02 for Treatment of Psoriasis 12–14 (2017).

53. ClinicalTrials. Clinical Trial to Evaluation the Safety and Efficacy of GR-MD-02 for the Treatment of Liver Fibrosis and Resultant Portal Hypertension in Patients With Nash Cirrhosis (NASH-CX) 4–7 (2017).

54. Blanchard, H., Yu, X., Collins, P. M. & Bum-erdene, K. Galectin-3 inhibitors : a patent review (2008 -- present). *Expert Opin. Ther. Patents* 1–13 (2014).

55. Seetharaman, J. *et al.* X-ray crystal structure of the human galectin-3 carbohydrate recognition domain at 2.1-A resolution. *J. Biol. Chem.* **273,** 13047–13052 (1998).

56. Chen, Y.-X., Zhao, W., Zhao, L., Zhao, Y.-F. & Li, Y.-M. Facile synthesis of a pentasaccharide mimic of a fragment of the capsular polysaccharide of Streptococcus pneumoniae type 15C. *Carbohydr. Res.* **343,** 607–614 (2008).

57. Prego, C., Fabre, M., Torres, D. & Alonso, M. J. Efficacy and mechanism of action of chitosan nanocapsules for oral peptide delivery. *Pharm. Res.* **23,** 549–556 (2006).

58. Pascal, B. a, Annick, M. & Panteley, D. P. Hplc Analysis of Mono-and Disaccharides in Food Products. 761–765 (2013).

59. Anumula, K. R. New high-performance liquid chromatography assay for glycosyltransferases based on derivatization with anthranilic acid and fluorescence detection. *Glycobiology* **22,** 912–917 (2012).

60. Kupper, C. E. *et al.* Chemo-enzymatic modification of poly-N-acetyllactosamine (LacNAc) oligomers and N,N-diacetyllactosamine (LacDiNAc) based on galactose oxidase treatment. *Beilstein J. Org. Chem.* **8,** 712–725 (2012).

61. Intra-articular injection & Technique. Rat anterior cruciate ligament transection and intra-articular injection Surgical technique Intra-articular injection. 1–3 (2014).

62. Ekundi-Valentim, E. *et al.* Differing effects of exogenous and endogenous hydrogen sulphide in carrageenan-induced knee joint synovitis in the rat. *Br. J. Pharmacol.* **159,** 1463–1474 (2010).

63. Sörme, P., Kahl-Knutson, B., Wellmar, U., Nilsson, U. J. & Leffler, H. Fluorescence polarization to study galectin-ligand interactions. *Methods Enzymol.* **362,** 504–512 (2003).

64. Hsieh, T. J. *et al.* Structural basis underlying the binding preference of human galectins-1, -3 and -7 for Galβ1-3/4GlcNAc. *PLoS One* **10,** 1–19 (2015).

65. Roy, R., Murphy, P. V. & Gabius, H. J. Multivalent carbohydrate-lectin interactions: How synthetic chemistry enables insights into nanometric recognition. *Molecules* **21,** (2016).

66. Cumpstey, I., Sundin, A., Leffler, H. & Nilsson, U. J. C2-symmetrical thiodigalactoside bis-benzamido derivatives as high-affinity inhibitors of galectin-3: Efficient lectin inhibition through double arginine-arene interactions. *Angew. Chemie - Int. Ed.* **44,** 5110–5112 (2005).

67. Cumpstey, I., Salomonsson, E., Sundin, A., Leffler, H. & Nilsson, U. J. Studies of arginine-arene interactions through synthesis and evaluation of a series of galectin-binding aromatic lactose esters. *ChemBioChem* **8,** 1389–1398 (2007).

68. Atmanene, C. *et al.* Biophysical and structural characterization of mono/di-arylated lactosamine derivatives interaction with human galectin-3. *Biochem. Biophys. Res. Commun.* (2017). doi:10.1016/j.bbrc.2017.05.150

69. Cumpstey, I., Salomonsson, E., Sundin, A., Leffler, H. & Nilsson, U. J. Double affinity amplification of galectin-ligand interactions through arginine-arene interactions: synthetic, thermodynamic, and computational studies with aromatic diamido thiodigalactosides. *Chemistry* **14,** 4233–4245 (2008).

70. Van Hattum, H. *et al.* Tuning the preference of thiodigalactoside- and lactosamine-based ligands to galectin-3 over galectin-1. *J. Med. Chem.* **56,** 1350–1354 (2013).

71. André, S. *et al.* Combining carbohydrate substitutions at bioinspired positions with multivalent presentation towards optimising lectin inhibitors: case study with calixarenes. *Chem. Commun.* **47,** 6126 (2011).

72. Bernardi, S. *et al.* Clicked and long spaced galactosyl- and lactosylcalix[4]arenes: New multivalent galectin-3 ligands. *Beilstein J. Org. Chem.* **10,** 1672–1680 (2014).

73. Gautier, F.-M., Djedaïni-Pilard, F. & Grandjean, C. The iodosulfonamidation of peracetylated glycals revisited: access to 1,2-di-nitrogenated sugars. *Carbohydr. Res.* **346,** 577–587 (2011).

74. Mironov, Y. S. A. N. N. Homogeneous Azidophenylselenylation of glycals using. **45,** 117913 (2004).

75. Mironov, Y. V., Sherman, A. a. & Nifantiev, N. E. Homogeneous azidophenylselenylation of glucals. *Mendeleev Commun.* **18,** 241–243 (2008).

76. Ágoston, K., Dobó, A., Rákó, J., Kerékgyártó, J. & Szurmai, Z. Anomalous Zemplén deacylation reactions of α- and β-D-mannopyranoside derivatives. *Carbohydr. Res.* **330,** 183–190 (2001).

77. Zemplen, G. & Pascu, E. Verseifung acetylierler Zucker. 9–10 (1929).

78. Nagashima, N. & Ohno, M. An Efficient O-Monoalkylation of Dimethyl L-Tartrate via O-Stannylene Acetal with Alkyl Halides in the Presence of Cesium Fluoride. *Chem. Lett.* **16,** 141–144. (1987).

79. Sörme, P. *et al.* Structural and thermodynamic studies on cation-Pi interactions in lectin-ligand complexes: high-affinity galectin-3 inhibitors through fine-tuning of an arginine-arene interaction. *J. Am. Chem. Soc.* **127,** 1737–1743 (2005).

80. Sörme, P., Kahl-Knutsson, B., Huflejt, M., Nilsson, U. J. & Leffler, H. Fluorescence polarization as an analytical tool to evaluate galectin-ligand interactions. *Anal. Biochem.* **334,** 36–47 (2004).

81. Hirabayashi, J. & Kasai, K. Effect of amino acid substitution by sited-directed mutagenesis on the carbohydrate recognition and stability of human 14-kDa beta-galactoside-binding lectin. *J. Biol. Chem.* **266,** 23648–23653 (1991).

82. Delaine, T. *et al.* Galectin-3-Binding Glycomimetics that Strongly Reduce Bleomycin-Induced Lung Fibrosis and Modulate Intracellular Glycan Recognition. *ChemBioChem* **17,** 1759–1770 (2016).

83. Adamczyk, Z. & Weronski, P. Application of the DLVO theory for particle deposition problems. *Adv. Colloid Interface Sci.* **83,** 137–226 (1999).

84. Giuseppe Cirino, C. C. Thrombin Functions as an Inflammatory Mediator through Activation o f Its Receptor. *J. Exp. Med* **183,** (1996).

85. Santos, J. M. *et al.* The role of human umbilical cord tissue-derived mesenchymal stromal cells (UCX®) in the treatment of inflammatory arthritis. *J. Transl. Med.* **11,** 18 (2013).

86. Lam, F. Y. & Ferrell, W. R. Inhibition of carrageenan induced inflammation in the rat knee joint by substance P antagonist. *Ann. Rheum. Dis.* **48,** 928–32 (1989).

87. Radhakrishnan, R., Moore, S. a. & Sluka, K. a. Unilateral carrageenan injection into muscle or joint induces chronic bilateral hyperalgesia in rats. *Pain* **104,** 567–577 (2003).

88. Wang, M. T. *et al.* In vivo biodistribution, anti-inflammatory, and hepatoprotective effects of liver targeting dexamethasone acetate loaded nanostructured lipid carrier system. *Int. J. Nanomedicine* **5,** 487–497 (2010).

89. Mei, Z., Chen, H., Weng, T., Yang, Y. & Yang, X. Solid lipid nanoparticle and microemulsion for topical delivery of triptolide. *Eur. J. Pharm. Biopharm.* **56,** 189–196 (2003).

90. Xu, X. *et al.* Anti-inflammatory activity of injectable dexamethasone acetate-loaded nanostructured lipid carriers. *Drug Deliv.* **18,** 485–492 (2011).

91. Van Den Hoven, J. M. *et al.* Liposomal drug formulations in the treatment of rheumatoid arthritis. *Mol. Pharm.* **8,** 1002–1015 (2011).

92. Chime, S. a, Kenechukwu, F. C. & Attama, a a. Nanoemulsions — Advances in Formulation , Characterization and Applications in Drug Delivery. (2014). doi:10.5772/58673

93. Dumortier, G., Grossiord, J. L., Agnely, F. & Chaumeil, J. C. A review of poloxamer 407 pharmaceutical and pharmacological characteristics. *Pharm. Res.* **23,** 2709–2728 (2006).

94. Fezai, M., Senovilla, L., Jemaà, M., Ben-Attia, M. & Ben-Attia, M. Analgesic, Anti-Inflammatory and Anticancer Activities of Extra Virgin Olive Oil. *J. Lipids* **2013,** 1–7 (2013).

95. Kapoor, B., Singh, S. K., Gulati, M., Gupta, R. & Vaidya, Y. Application of liposomes in treatment of rheumatoid arthritis: Quo vadis. *Sci. World J.* **2014,** (2014).

96. Liu, H. *et al.* Remission of collagen-induced arthritis through combination therapy of microfracture and transplantation of thermogel-encapsulated bone marrow mesenchymal stem cells. *PLoS One* **10,** 1–18 (2015).

97. Tanaka, D., Kagari, T., Doi, H. & Shimozato, T. Essential role of neutrophils in anti-type II collagen antibody and lipopolysaccharide-induced arthritis. *Immunology* **119,** 195–202 (2006).

98. Mitragotri, S. & Yoo, J. W. Designing micro- and nano-particles for treating rheumatoid arthritis. *Arch. Pharm. Res.* **34,** 1887–1897 (2011).

99. Ye, J., Wang, Q., Zhou, X. & Zhang, N. Injectable actarit-loaded solid lipid nanoparticles as passive targeting therapeutic agents for rheumatoid arthritis. *Int. J. Pharm.* **352,** 273–279 (2008).

100. Barrera, P. *et al.* Synovial macrophage depletion with clodronate-containing liposomes in rheumatoid arthritis. *Arthritis Rheum.* **43,** 1951–1959 (2000).

101. Edwards, S. H. R., Cake, M. a, Spoelstra, G. & Read, R. a. Biodistribution and clearance of intra-articular liposomes in a large animal model using a radiographic marker. *J. Liposome Res.* **17,** 249–261 (2007).

102. Chandrupatla, D. M. S. H. *et al.* Sustained macrophage infiltration upon multiple intra-articular injections: An improved rat model of rheumatoid arthritis for PET guided therapy evaluation. *Biomed Res. Int.* **2015,** (2015).

103. Roth, A. *et al.* Intra-articular injections of high-molecular-weight hyaluronic acid have biphasic effects on joint inflammation and destruction in rat antigen-induced arthritis. *Arthritis Res. Ther.* **7,** R677–R686 (2005).

104. Riveiro-Naveira, R. R. *et al.* Resveratrol lowers synovial hyperplasia, inflammatory markers and oxidative damage in an acute antigen-induced arthritis model. 1–12 (2016).

105. Frey, O. *et al.* The role of regulatory T cells in antigen-induced arthritis: aggravation of arthritis after depletion and amelioration after transfer of CD4+CD25+ T cells. *Arthritis Res. Ther.* **7,** R291–R301 (2005).

106. Shan-Bin, G., Yue, T. & Ling-Yan, J. Long-term sustained-released in situ gels of a water-insoluble drug amphotericin B for mycotic arthritis intra-articular administration: preparation, in vitro and in vivo . *Drug Dev. Ind. Pharm.* **9045,** 1–10 (2014).

107. Bhattacharyya, S. *et al.* Specific effects of BCL10 Serine mutations on phosphorylations in canonical and noncanonical pathways of NF-{kappa}B activation following carrageenan. *Am. J. Physiol. Gastrointest. Liver Physiol.* **301,** G475–G486 (2011).

108. Sadeghi, H., Hajhashemi, V., Minaiyan, M., Movahedian, A. & Talebi, A. A study on the mechanisms involving the anti-inflammatory effect of amitriptyline in carrageenan-induced paw edema in rats. *Eur. J. Pharmacol.* **667,** 396–401 (2011).

109. Cecerale, S. in *Olive oil - Constituents, Health Properties and Bioconversions* (INTECH, 2011).

110. Berbert, a a, Kondo, C. R., Almendra, C. L., Matsuo, T. & Dichi, I. Supplementation of fish oil and olive oil in patients with rheumatoid arthritis. *Nutrition* **21,** 131–136 (2005).

111. Ghosh, P. & Guidolin, D. Potential mechanism of action of intra-articular hyaluronan therapy in osteoarthritis: Are the effects molecular weight dependent? *Semin. Arthritis Rheum.* **32,** 10–37 (2002).

112. Kaplan, M. J. Role of neutrophils in systemic autoimmune diseases. *Arthritis Res. Ther.* **15,** 219 (2013).

113. Matsukura, Y. *et al.* Mouse synovial mesenchymal stem cells increase in yield with knee inflammation. *J. Orthop. Res.* **33,** 246–253 (2015).

114. Liggins, R. T. *et al.* Intra-articular treatment of arthritis with microsphere formulations of paclitaxel: biocompatibility and efficacy determinations in rabbits. *Inflamm. Res.* **53,** 363–372 (2004).

115. Snyder, T. N., Madhavan, K., Intrator, M., Dregalla, R. C. & Park, D. A fibrin/hyaluronic acid hydrogel for the delivery of mesenchymal stem cells and potential for articular cartilage repair. *J. Biol. Eng.* **8,** 10 (2014).

116. Kim, D. Y. *et al.* Tissue-engineered allograft tracheal cartilage using fibrin/hyaluronan composite gel and its in vivo implantation. *Laryngoscope* **120,** 30–38 (2010).

117. Park SH, Park SR, Chung SI, Pai KS, M. B. Tissue-engineered Cartilage Using Fibrin/Hyaluronan Composite Gel and Its In Vivo Implantation. **29,** 838–860 (2005).

118. Zhang, Y., Heher, P., Hilborn, J., Redl, H. & Ossipov, D. a. Hyaluronic acid-fibrin interpenetrating double network hydrogel prepared in situ by orthogonal disulfide cross-linking reaction for biomedical applications. *Acta Biomater.* **38,** 23–32 (2016).

119. Park, S.-H. *et al.* Silk-Fibrin/Hyaluronic Acid Composite Gels for Nucleus Pulposus Tissue Regeneration. *Tissue Eng. Part A* **17,** 2999–3009 (2011).

120. Vilela, C. *et al.* Cartilage repair using hydrogels: a critical review of in vivo experimental designs. *ACS Biomater. Sci. Eng.* 150813111234008 (2015).

121. Park, S. H., Cui, J. H., Park, S. R. & Min, B. H. Potential of fortified fibrin/hyaluronic acid composite gel as a cell delivery vehicle for chondrocytes. *Artif. Organs* **33,** 439–447 (2009).

122. Ahearne, M., Buckley, C. T. & Kelly, D. J. A growth factor delivery system for chondrogenic induction of infrapatellar fat pad-derived stem cells in fibrin hydrogels. *Biotechnol. Appl. Biochem.* **58,** 345–352 (2011).

123. Weigel, P. H., Fuller, G. M. & LeBoeuf, R. D. A model for the role of hyaluronic acid and fibrin in the early events during the inflammatory response and wound healing. *J. Theor. Biol.* **119,** 219–234 (1986).

124. Kim, J. E. *et al.* Effect of self-assembled peptide-mesenchymal stem cell complex on the progression of osteoarthritis in a rat model. *Int. J. Nanomedicine* **9,** 141–157 (2014).

125. Anderson, G. D. *et al.* Selective inhibition of cyclooxygenase (COX)-2 reverses inflammation and expression of COX-2 and interleukin 6 in rat adjuvant arthritis. *J. Clin. Invest.* **97,** 2672–2679 (1996).

126. Zangerle, P. F. *et al.* Direct stimulation of cytokines (IL-1b, TNF-a, IL-6, IL-2, IFN and GM-CSF) in whole blood: II. Application to rheumatoid arthritis and osteoarthritis. *Cytokine* **4,** 568–575 (1992).

127. Gratacós, J. *et al.* Serum cytokines (Il-6, Tnf-a, Il-1a and Ifn) in ankylosing spondylitis: A close correlation between serum il-6 and disease activity and severity. *Rheumatology* **33,** 927–931 (1994).

128. Kutukculer, N., Caglayan, S. & Aydogdu, F. Clinical Rheumatology Juvenile Chronic Arthritis : Correlations with Clinical and Laboratory Parameters. *Clin. Rheumatol.* 288–292 (1998).

129. Kagari, T., Doi, H. & Shimozato, T. The Importance of IL-1beta and TNF-alpha, and the Noninvolvement of IL-6, in the Development of Monoclonal Antibody-Induced Arthritis. *J. Immunol.* **169,** 1459–1466 (2002).

130. Romano, M. *et al.* Carrageenan-induced acute inflammation in the mouse air pouch synovial model. Role of tumour necrosis factor. *Mediators Inflamm.* **6,** 32–8 (1997).

131. Delaine, T. *et al.* Galectin-inhibitory thiodigalactoside ester derivatives have antimigratory effects in cultured lung and prostate cancer cells. *J. Med. Chem.* **51,** 8109–8114 (2008).

132. Lin, C.-I. *et al.* Galectin-3 targeted therapy with a small molecule inhibitor activates apoptosis and enhances both chemosensitivity and radiosensitivity in papillary thyroid cancer. *Mol. cancer Res. MCR* **7,** 1655–1662 (2009).

133. André, S. *et al.* Combining carbohydrate substitutions at bioinspired positions with multivalent presentation towards optimising lectin inhibitors: case study with calixarenes. *Chem. Commun. (Camb).* **47,** 6126–6128 (2011).

134. Delaine, T. *et al.* Galectin-3-Binding Glycomimetics that Strongly Reduce Bleomycin-Induced Lung Fibrosis and Modulate Intracellular Glycan Recognition. *Chembiochem A Eur. J. Chem. Biol.* (2016). doi:10.1002/cbic.201600285

135. Mackinnon, A. C. *et al.* Regulation of transforming growth factor-β1-driven lung fibrosis by galectin-3. *Am. J. Respir. Crit. Care Med.* **185,** 537–546 (2012).

136. Toegel, S. *et al.* Galectin-1 Couples Glycobiology to Inflammation in Osteoarthritis through the Activation of an NF-κB-Regulated Gene Network. *J. Immunol. (Baltimore, Md. 1950)* **196,** 1910–1921 (2016).

USC
UNIVERSIDADE
DE SANTIAGO
DE COMPOSTELA

Overall discussion

Learn from yesterday, live for today, hope for tomorrow. The important thing is to not stop questioning.

Albert Einstein

USC
UNIVERSIDADE
DE SANTIAGO
DE COMPOSTELA

INTRODUCTION

The advances in the biopharmaceutical field along the past decades have allowed the development of drug delivery systems (DDS) that can display long residence at the biological media with controlled and prolonged drug release directly to the targeted place.[1,2] At the same time, the discovery of novel immunotherapeutic targets has triggered intensive efforts towards the development of highly specific small molecules-antagonists for effective therapies.[3–6]

In this work, we have focused our efforts on the design, development and characterization of a controlled release DDS that can be easily injectable to the intra-articular (IA) cavity and display sufficient residence time for the treatment of joints pathologies (**Figure 1**). We described a new system that involves a combination of an *in situ* formed hydrogel with polymeric nanocapsules (NCs) dispersed on it. The injectable *in situ* hydrogel consists of interpenetrating network (IPN) hyaluronic acid (HA) crosslinked with fibrin. HA NCs serve as multireservoirs for lipophilic drugs. Hence, *in situ* hydrogel protects NCs from the fast degradation in synovial fluid (SF), cell internalization and its elimination from the IA cavity, allowing prolonged and controlled release of the drug.

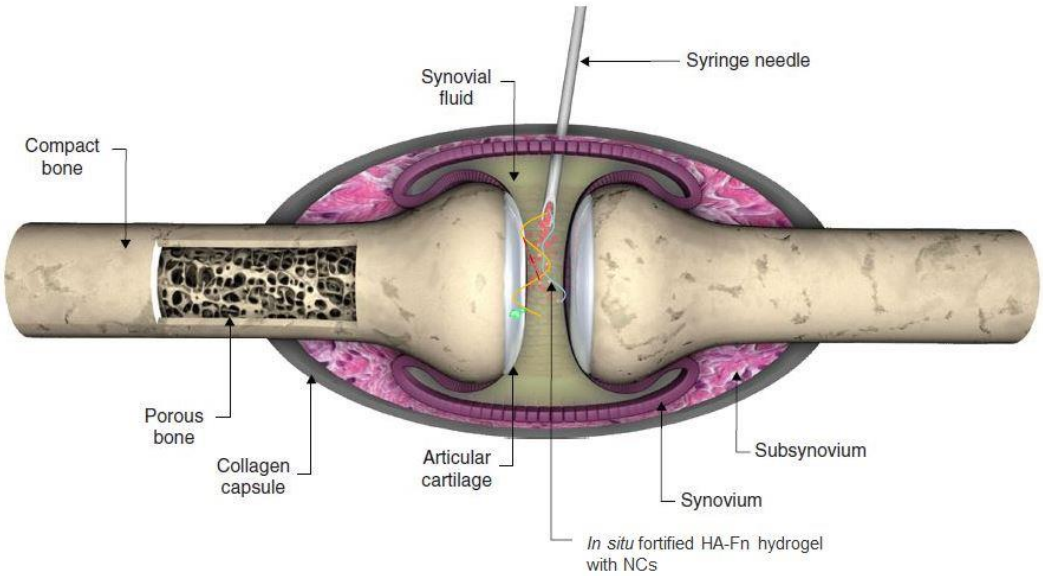

Figure 1. Schematic illustration of the structure of a synovial joint and intra-articular injection of *in situ* forming hydrogel combined with lipophilic drug-loaded nanocapsules. Adapted and modified from Burt *et al.*[7] with permission, Copyright© 2009, Taylor & Francis.

The developed hydrogel maintains good rheological properties and high resistance to deformations with a 30% (v/v) loading of NCs. The nanocarriers are homogenously

distributed and the final gel behaves similar to blank hydrogel, demonstrating features of both elastic and solid-like behavior material, displaying the designed hydrogel suitable for IA application. This formulation is intended to extend the NCs retention in the IA cavity, to control the delivery of the associated drug and to act as a viscosupplement with viscoinductive properties, potentially improving the knee homeostasis.

The physico-chemical characterization, encapsulation efficiency, and release profile of the IA DDS was firstly evaluated with a model lipophilic drug, dexamethasone (DXM). This anti-inflammatory and immunosuppressive corticosteroid drug is commonly used for systemic and local treatment of rheumatoid arthritis (RA).[1,8] Later on, the same technology was applied to a new galectin-3 inhibitor (Gal-3i) that we designed and synthesized as a potential anti-inflammatory drug for autoimmune diseases, in particular for RA.

Galectin-3 (Gal-3), a β-galactoside binding lectin, is an appealing protein to target due to its presence in most of the tissues and its participation in many pathologies.[9–16] In this work, we focused on one of the most important extracellular functions of Gal-3**,** supporting the control of immune and inflammatory response by triggering the pro-inflammatory cascade. Noticeably, Gal-3 expression is up-regulated in synovial tissues in RA,[17] its concentration in SF increases from about 50 up to 130-300 ng/mL,[15] amplifying the inflammation[9–15] and contributing to the joint degradation.[18,19] Inhibition of extracellular Gal-3 by highly affine ligands based on β-galactoside motifs has recently seen major breakthrough. Thus, aiming to develop a potent Gal-3i, aromatic substituents have been introduced at positions 3'-C of galactose and 2-C of glucosamine residues of type II lactosamine core [Galβ(1→4)-GlcN], selected as starting material. Such modifications result in considerably enhanced affinity and selectivity due to the establishment of cation-π interactions between the arene substituents of the inhibitor and guanidinium ions of two key arginine residues (Arg144 and Arg186), adjacent to the binding site of the Gal-3 carbohydrate-recognition domain (CRD).

Gal-3 inhibitor was further encapsulated in the developed NCs to be later included in the hydrogel. Anti-inflammatory properties of Gal-3i and performance of DDS were evaluated *in vivo* in a rat carrageenan-induced knee synovitis model. Finally, we discussed some prospects on the challenges to be addressed for the further success of the novel immunotherapeutic antagonist – Gal-3i and its DDS that may further be explored for multiple applications for various arthropathies and tissue regeneration.

1. Development and characterization of IA DDS: *in situ* hydrogel containing drug-loaded NCs

Aiming at prolonging drug release in the joint cavity, reducing the cell internalization and rapid efflux from the synovial cavity,[1,7] we decided to develop a DDS composed of NCs dispersed in an *in situ* hydrogel. Thus, primarily we designed, produced and characterized NCs to be later incorporated during the gel formation. Among the possible components for NCs preparation we selected: i) extra pure virgin olive oil (OO) due to its anti-inflammatory properties[20,21] and because of its capacity to solubilize DXM;[22] ii) soy lecithin (Lec) and oleylamine (OAm), as surfactants, in order to produce cationic nanoemulsions to which the HA molecules could be attached;[23,24] iii) HA (700 kDa) as a shell polymer due to its anti-inflammatory responses[25] (**Figure 2A**).

Two prototypes of drug-loaded HA NCs, differed by the amount of OO and surfactants, were successfully prepared using the simple solvent displacement technique, as previously described in our laboratory.[26] We intended to develop NCs with a size close to 100 nm that are not expected to cause cartilage or other mechanical damage in the joint[27] and to load them with drugs prior to their incorporation into a hydrogel. We developed NCs with an average particle size of 122 ± 11 nm (Gal-3i NCs for extracellular Gal-3 targeting) and 135 ± 9 nm (DXM NCs for multiple extracellular targeting). The particle size, zeta potential and encapsulation efficiency of the formulations are summarized in **Table 1**.

The size of the NCs, obtained by DLS, was compared with TEM data. Resulting TEM images revealed the spherical shape, which is one of the key parameters for IA drug delivery at RA[28,29] and regular morphology of these nanosystems with considerably smaller particle size values and homogeneity compared to DLS data (**Figure 2B**). These results can be explained considering that TEM requires detection of NCs in a dry state, whereas DLS analyzes NCs in aqueous suspension, measuring the hydrodynamic diameter.[30]

NCs maintained their stability only in water and aggregated in PBS and simulated synovial fluid (SSF). Thus, we developed an injectable *in situ* hydrogel, formed in presence of the NCs to improve their stability, along with their retention in the articular cavity (avoiding cell-internalization and a fast drainage) and allow prolonged drug release.

Table 1. Physicochemical characteristics of the blank and drug-loaded nanocapsules prepared with 700 kDa HA (mean ± SD; n = 6). PDI: polydispersity index.

Type of NCs			OO (mg)	Lec (mg)	OAm (mg)	Particle size (nm)	PDI	ζ-potential (mV)	Drug concentration (mg/mL)
Blank		prototype 1	15	3.75	0.75	128 ± 13	0.2	−27 ± 3	n/a
		prototype 2	22	5.625	1.125	121 ± 10	0.2	−30 ± 3	n/a
Drug-loaded	DXM	prototype 1	15	3.75	0.75	160 ± 12	0.2	−20 ± 4	0.75 ± 0.125
		prototype 2	22	5.625	1.125	135 ± 9	0.2	−31 ± 5	5.60 ± 0.40
	Gal-3i	prototype 2	22	5.625	1.125	122 ± 11	0.2	−29 ± 5	0.53 ± 0.05

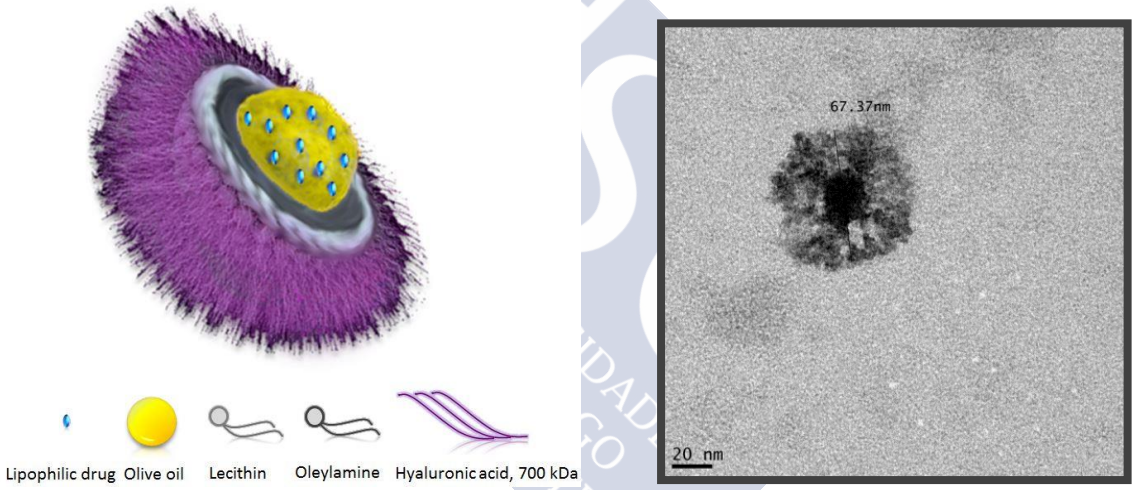

A B

Figure 2. (A) Representation of the structure of drug-loaded hyaluronic acid nanocapsule; **(B)** TEM images of hyaluronic acid blank nanocapsule: at magnification 50,000×.

At this step, among the variety of potential materials for gel preparation, we selected biopolymers HA and fibrin that allowed us to form an interpenetrating 3D network,[31–35] using the affinity of high MW HA to fibrin.[36,37] Later on, the gel was fortified with cross-linker factor XIII (FXIII) and with α2-antiplasmin (α2-AP), to gain advanced mechanical stability and prevent fast degradation by enzymes of pathological synovial fluid.[38–46]

The hydrogel formation, that relies on the enzymatic activation of fibrinogen by thrombin (Thr), let us to stepwise design an IPN in the presence of HAs, fibrin-stabilizing agents (FXIII and α2-AP), and drug-loaded NCs. We could modulate the gelation time by

adjusting different parameters, such as the temperature, the amount of thrombin, the MW and concentration of HA, the concentration of Ca^{2+} and FXIII. The targeted gelation lag-time was 2 minutes, a time that was sufficient to provide an adequate syringeability of the hydrogel for *in vivo* experiments.

We developed two DDS compositions of hydrogels to be tested in acute- and chronic-RA rat models: "HA-fibrin gel" and "fortified HA-fibrin gel" (fortified with cross-linker FXIII and with α2-AP, both of them with a 30% NCs. The gel formation was monitored by turbidity analysis (at λ = 350 nm) and rheology studies that allowed us to detect the starting gelation point (**Figure 3**), by observing the gel evolution in time and the endpoint at which the gel is completely formed.

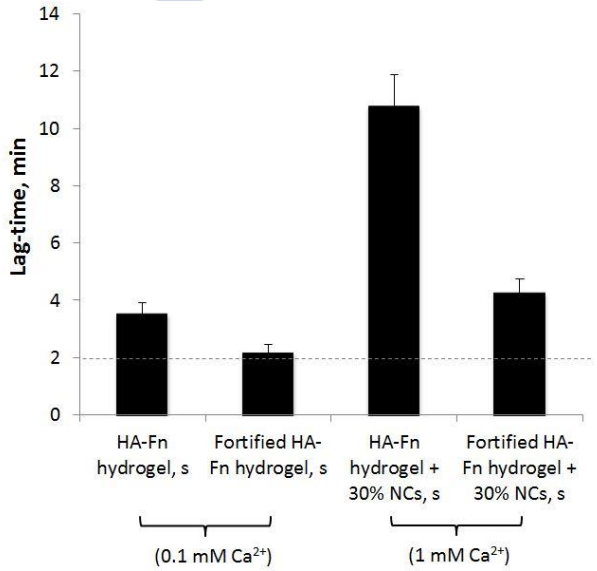

Figure 3. Summary of gelation time point determination by rheological measurements in different systems: HA-fibrin (HA-Fn) and fortified HA-Fn blank and 30% NCs loaded gels. For blank gels fibrinogen was always taken at 1 mg/mL concentration, activity of thrombin (Thr) = 1 NIH-U/mL. For 30% NCs loaded gels fibrinogen was always taken at 1.5 mg/mL concentration, activity of Thr = 2 NIH-U/mL. The dash-and-dot line reflects the 2 minutes lag-phase requirements. The measurements were carried out at 37 °C. Expressed as mean ± SD; n = 3.

The viscosity values of the HA-fibrin mixture (without no thrombin addition) at 20 °C and 37 °C are 118.9 mPa·s and 81.3 mPa·s, respectively, much lower compared to the commercial viscosupplementation agents.[47,48] Thereby the mixed solutions necessary to form the *in situ* gelling systems are expected to be easily injected intra-articularly *in vivo*.

The rheological behavior of both non-fortified and fortified HA-fibrin gels was tested in oscillatory strain and frequency sweeps tests and the results indicated that the gel has high elasticity and resistance against applied deformations. Interestingly, gels loaded with 30% of NCs showed higher moduli of deformations than blank gels and, thus, longer persistence, which could be explained by additional crosslinking of IPN by NCs, due to ionic interactions between shell polymer of NCs and fibrin network of the hydrogel. The behavior of the elastic modulus against the oscillatory frequency exhibited a plateau-type in the range of 0.1-3 Hz, which is indicative of stable cross-linked networks. Thus, fortified HA-fibrin gel + 30% of NCs, combines features of both elastic and solid-like behavior material and displays long persistence, making this DDS appropriate for intra-articular application.

Topographic characterization of HA-fibrin and fortified HA-fibrin blank and loaded with 30% of NCs was performed by interferometric microscopy to evaluate the changes in the surface structure and the pores sizes caused by the NCs and fibrin-stabilizing components. All the gel samples presented quite homogenous and well-determined pores with a low value of pore size distribution, which is the evidence of a well-organized architecture. According to data in **Table 2**, fortified HA-fibrin gels (both blank and NCs loaded) appeared to be more crosslinked compared to non-fortified ones. Moreover, the average pore diameter of fortified HA-fibrin NCs loaded gels (4.88 μm) is only slightly larger than for blank fortified HA-fibrin gels (3.26 μm), meaning that FXIII provides sufficient crosslinking to maintain the microarchitecture of the NCs-loaded gels.

Table 2. Mean pore size and depth of the different hydrogel compositions.

Sample	Mean pore diameter (μm)	Depth (μm)
HA-fibrin hydrogel	4.23 ± 0.89	1.07 ± 0.18
HA-fibrin hydrogel + 30% NCs	7.29 ± 1.23	0.7 ± 0.17
Fortified HA-fibrin hydrogel	3.26 ± 1.01	1.07 ± 0.41
Fortified HA-fibrin hydrogel + 30% NCs	4.88 ± 1.12	0.98 ± 0.12

These data correlate well with morphology studies of the gels injected by syringes to PBS buffer, and incubated at 37 °C during 20 hours, lyophilized and analyzed by scanning electron microscopy (SEM/FESEM) (**Figure 4A-D**). Analysis of the SEM images allowed us to visually evaluate the differences in non- and fortified HA-fibrin gels structure. Thus, SEM/FESEM studies confirmed that fortified HA-fibrin gel has more compact structure of the

network, as porosity data indicated. Gel fibrils revealed the proper fibrils thickness of 1-2 μm in diameter, belonging to stable fibrin hydrogels.[49,50]

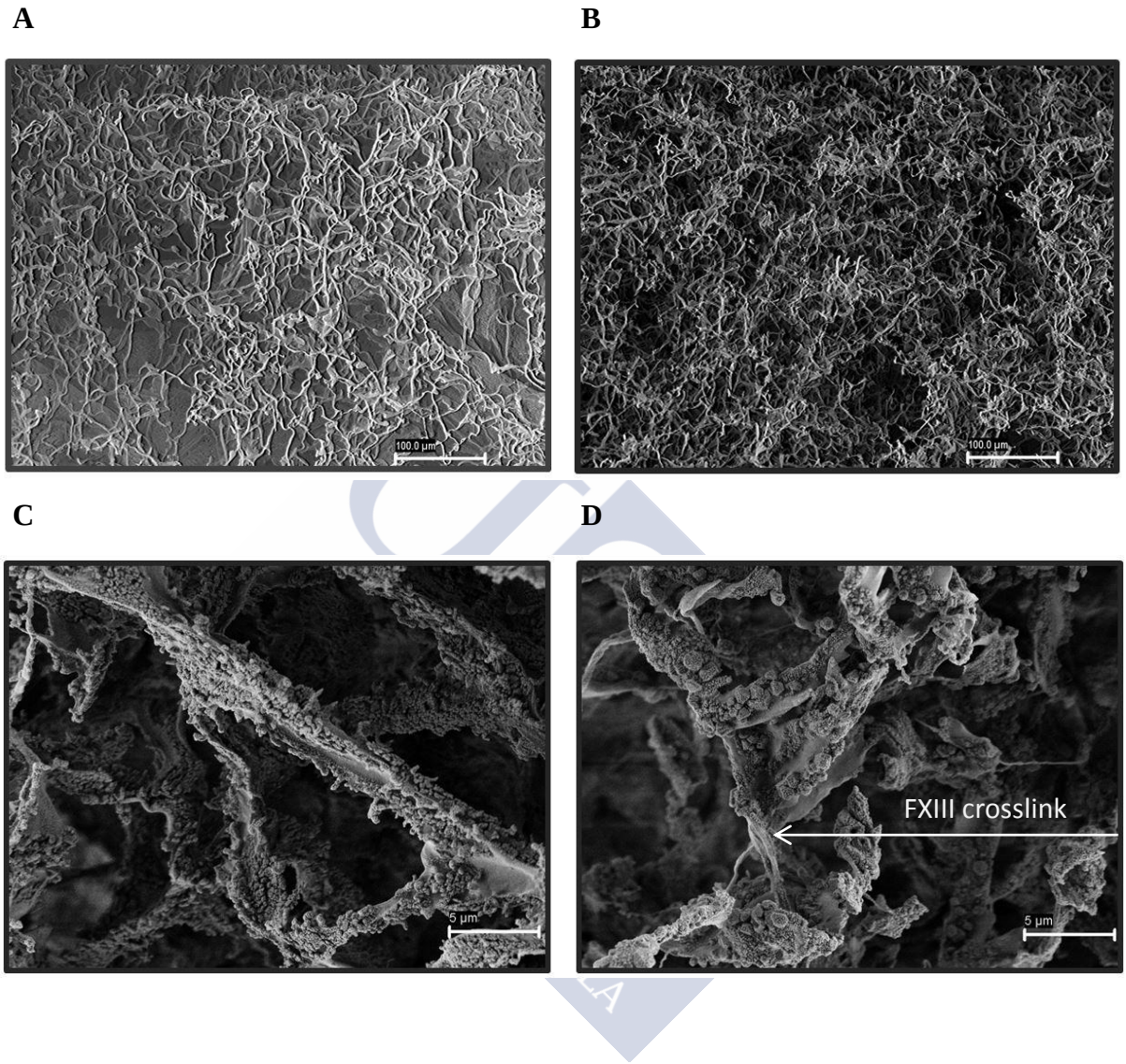

Figure 4. SEM images of (**A**) the blank HA-fibrin and (**B**) blank fortified HA-fibrin hydrogels at magnification is 500×. FESEM images of (**C**) the blank HA-fibrin and (**D**) blank fortified HA-fibrin hydrogels at magnification is 10,000×.

The distribution of Nile Red labeled NCs within the HA-fibrin hydrogel (30% loading) was observed by confocal electron microscopy on the deepness 50 μm and 490 μm at different magnification, as illustrated in **Figure 5A** and **B**. The images indicate that HA NCs are randomly dispersed in the hydrogel network and, possibly, interact with the positively charged regions of fibrin and stay adhered to the fibrils.

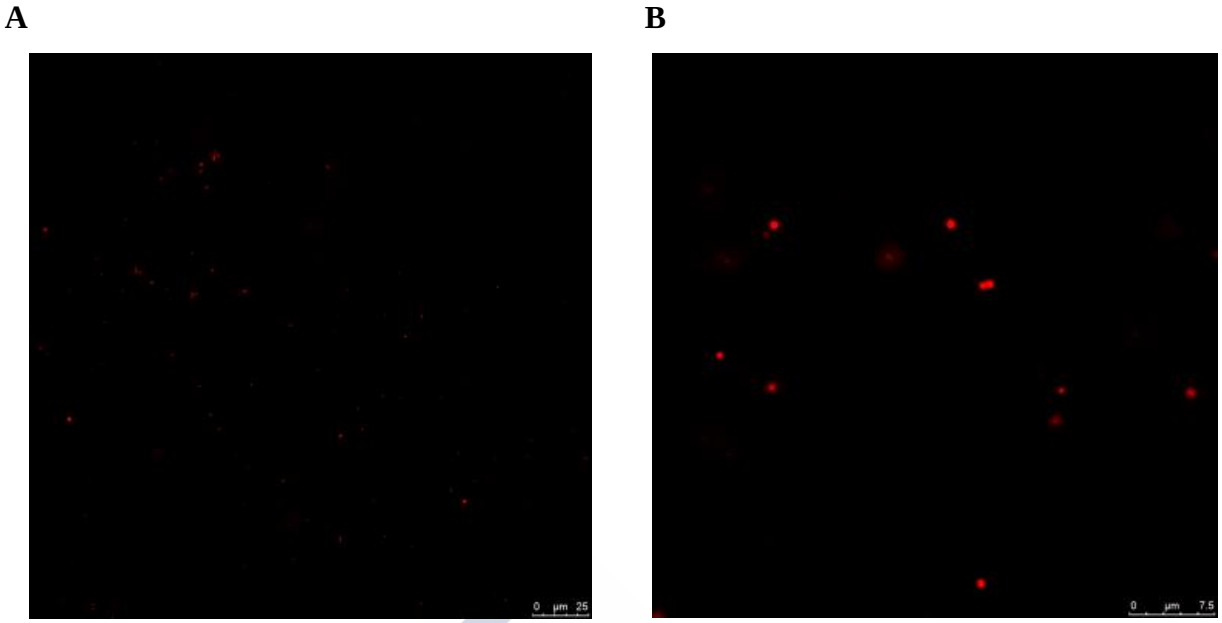

Figure 5. Confocal microscopy images of Nile Red-labeled HA NCs dispersed in the HA-fibrin hydrogel (30% loading). Magnification is 320× (**A**), 1600× (**B**).

Finally, the release studies of DXM were carried out under sink conditions for both, NCs and 30% NCs-loaded hydrogel, in simulated synovial fluid (SSF, RI = 1.334) at 37 °C. In the case of the free NCs, a burst of approximately 70% DXM release was observed in the first hour of incubation in SSF, reaching 100% after 24 hours *(data not shown)*. In contrast, in the case of NCs loaded into the HA-fibrin hydrogel a slow release profile was observed in SSF (**Figure 6**), characterized by an initial ~30% DXM release, followed by a slow release up to ~50% within 24 hours. In the next phase (24-60 h), the drug was released very slowly till 60%, and finally 100% of DXM release was reached at the last time point (72 h) after the gel started to slowly decrease in volume (between 60-72 h). Overall, the results underline the importance of the hydrogel in controlling the release of the drug that was incorporated within the NCs. Hence, both, the NCs and the hydrogel have a role in terms of controlling the release of DMX.

These *in vitro* release results are in line with other previously reported in the literature. For example, Ranch *et al.* described a fast release of DMX from Carbopol® 940-gellan gum gels, ranging from 5 to 25 hours depending on the composition,[51] whereas Borden *et al.* reported a 72 h *in vitro* release profile.[52] On the other hand, Webber *et al.* reported the longest *in vitro* controlled release of DXM conjugated to a peptide-based nanofiber gels

during 32 days.[53] Similar results were shown by Wu *et al.* with 1 month *in vitro* release profile of DXM from micelles loaded into a PEG-PCL-PEG hydrogel.[54]

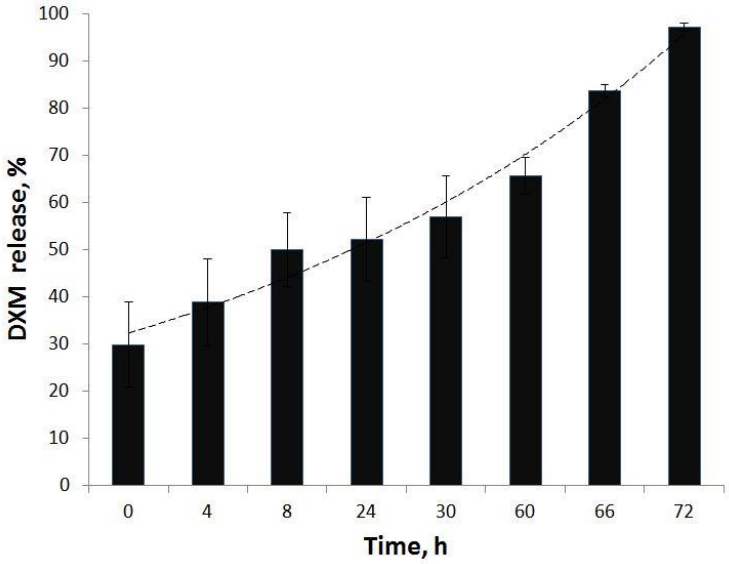

Figure 6. Dexamethasone (DXM) release from the hyaluronic acid-fibrin hydrogel with 30% loaded nanocapsules to simulated synovial fluid, 37 °C, 72 h.

It is expected that the release from the fortified HA-fibrin hydrogel might be more prolonged due to slower rate of degradation. In this case, FXIII and α2-AP enzyme should retard the gel decomposition[45] at simulated and physiological environments. Even though the results of the *in vitro* release studies cannot be directly extrapolated to the *in vivo* conditions, the fact that a certain amount of DXM (> 35%) remains encapsulated in the NCs after 60 h would be highly advantageous for intra-articular drug delivery of small molecule drugs that are known to be eliminated from the joints within few hours after administration.[1]

In summary, we developed an *in situ* hydrogel for IA delivery that contains HA NCs as multireservoirs for anti-inflammatory lipophilic drugs (*e.g.* DXM, Gal-3i). The 30% of NCs are dispersed within the HA-fibrin IPN. On the other hand, the gel is aimed to protect NCs from the rapid decomposition in SF, to reduce the elimination from the synovial cavity and the cell internalization, allowing at the same time a controlled drug release.

2. A novel Gal-3i as the lead compound for immunotherapeutic drugs for RA treatment

Taking into account the involvement into pathophysiology of RA, Gal-3 appears a novel potential immunotherapeutic target. Currently, only three Gal-3 antagonists among the reported inhibitors have entered clinical trials for the treatment of different pathologies.[16,55–61]

However, none of them was designed or tested for RA treatment so far. The chemical structures of a natural poly-saccharide inhibitor (GM-CT-01), a small sugar-derived molecule inhibitor *bis*-3-[(3-fluorophenyl)triazolyl] thiodigalactoside (TD139, approved by FDA) and two of the inhibitors synthesized in this work (oxazoline and Gal-3i) are gathered in **Figure 7.**

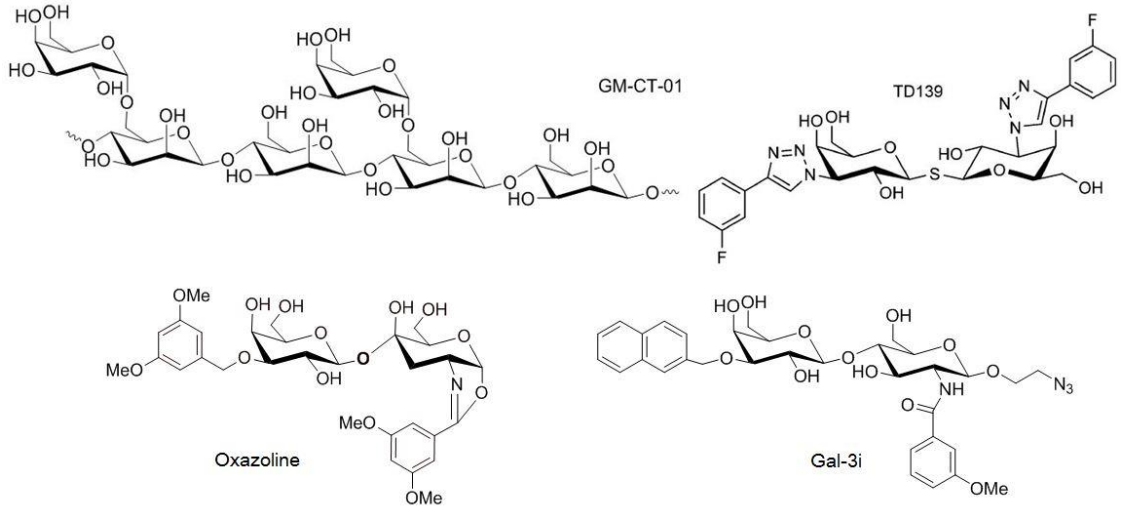

Figure 7. Structures of two commercial Gal-3 inhibitors: GM-CT-01 (DAVANAT®), TD139 and developed oxazoline (compound **16**) and Gal-3i (compound **26**).

Given that the Gal-3 CRD domain has a canonical structure as other galectin family members, all of them bind the same β-galactoside motifs with similar K_d values for these ligands.[62–64] Thus, to design highly selective and affine Gal-3 inhibitor new binding contacts with two nonconserved Arg144 and Arg186 residues, adjacent to the binding site of Gal-3 CRD,[65,66] were established. For this purpose, type II lactosamine core [Galβ(1→4)GlcN], due to its higher intrinsic affinity to Gal-3 over type I,[62,67] was modified with different aromatic substituents at 3'-C position of Gal and 2-C position of the GlcN residues, respectively. Such modifications allowed to greatly improve the binding affinity of inhibitors to CRD of Gal-3 helped by cation-π interactions establishment between guanidinium ions of Args and arenes.[10,66] Three different synthetic approaches (**A, B,** and **C**), were evaluated to obtain Gal-3i – derivative **26**, (2-Azidoethyl [3-*O*-(2-naphthyl)methyl-β-D-galactopyranosyl]-(1-4)-2-

deoxy-2-(3-methoxybenzamido)-β-D glucopyranoside), that was further transformed to a fluorescent probe **28** (**Scheme 1**).

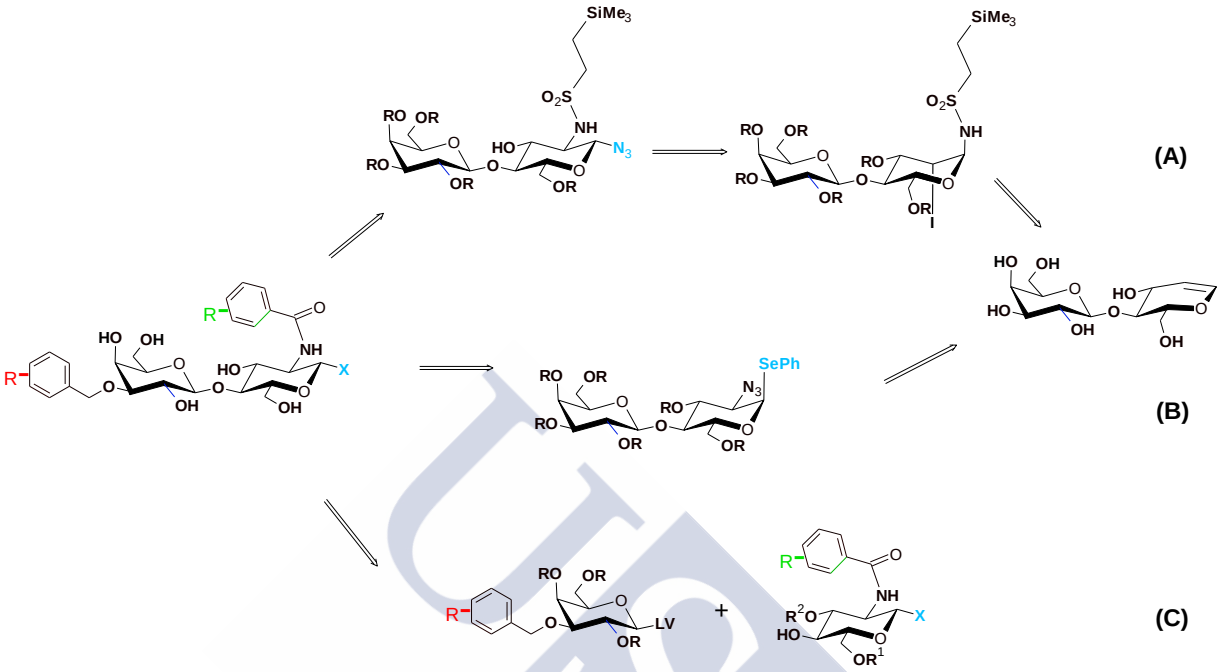

Scheme 1. A short scheme of derivatives preparation by 3 approaches: iodosulfonamidation (**A**), azidophenylselenation (**B**) and 1+1 glycosylation (a donor-acceptor coupling approach) (**C**).

The affinity studies were held with the fluorescein-labeled Gal-3i **28** (shown in **Chapter 2**, *Section 2.2*), an oxazoline (compound **16**), Gal-3i (compound **26**) and TD139 (**Figure 7**) (a positive control) by direct and competitive fluorescence polarization assay towards recombinant human Gal-1 C3S, Gal-3 and Gal-7, expressed in *E.coli*, at two different temperatures (**Table 3**).

We found that all the tested compounds were selective to Gal-3, what is an evident observing lower K_d values compared to Gal-1 or Gal-7 ones. Considering that the fluorescein tag contributes to the binding to galectins,[64,69,70] fluorescein-labelled Gal-3i displayed very high affinity to Gal-3 (K_d = 14 nM at 4 °C) and selectivity: or K_d(Gal-1)/K_d(Gal-3) = 1143 and K_d(Gal-7)/K_d(Gal-3) = 1500 at 4 °C. In turn, its intact analogue Gal-3i has K_d = 590 nM at 4 °C and showed selectivity K_d(Gal-1)/K_d(Gal-3) = 46 and K_d(Gal-7)/K_d(Gal-3) = 152. The same tendency was observed for oxazoline **16** with K_d = 4.4 μM and selectivity: (K_d(Gal-1)/K_d(Gal-3) = 25.5 and (K_d(Gal-7)/K_d(Gal-3) = 57 at 4 °C. As expected, compared to the parental derivative LacNAc-β-OMe, methoxy-substituents at meta-position of the introduced

aromatic ring of compound **16** greatly facilitate the complexation between the tested inhibitor and CRD of Gal-3.[10] However, larger π-systems as (2-naphtyl)methyl of compound **26** are more polarizable and form stronger interactions with Arg144 that is capable to accommodate such substituents, resulting to the higher affinity and better selectivity between Gal-3/Gal-1/Gal-7.[64] Thus, an inhibitor **26** demonstrated 7.5 and 7.7 times higher affinity towards Gal-3 than oxazoline **16** at 4 °C and room temperature, correspondingly, designing the derivative **26** as a lead compound for evaluation of Gal-3 inhibition *in vivo*.

Table 3. Dissociation constants of FITC-labeled compound **16,** compound **26**, compound **28** and **TD139** and galectin-1 C3S, galectin-3 and galectin-7.

	K_d (μM)[a]			
Compound	**Galectin-1**[b]	**Galectin-3**	**Galectin-7**	**Affinity**
	Temperature 4 °C			
LacNAc-β-OMe [c]	65 ± 28	n.d.	550 ± 98	+
16	112 ± 7	4.4 ± 0.25	249 ± 21	++
26	27 ± 5	0.59 ± 0.11	90 ± 35	+++
28	16 ± 1	0.014 ± 0.005	21 ± 1	++++
TD139	2.2 ± 1.4	0.036 ± 0.023	32 ± 17	++++
TD139[e]	0.012 ± 0.003	0.014 ± 0.003	1.9 ± 0.38	++++
	RT			
LacNAc-β-OMe [c]	n.d.	59 ± 12	n.d.	+
16	n.d.	23 ± 0.31	n.d.	++
26	n.d.[d]	2.99 ± 0.17	n.d.	+++
28	43 ± 4	0.082 ± 0.014	129 ± 18	++++
TD139	n.d.	0.166 ± 0.091	n.d.	++++
TD139 [f]	0.22 ± 0.05	0.068 ± 0.01	38 ± 0.71	++++

[a] Mean values from two assays; [b] Galectin-1: galectin-1 C3S (this study) or native galectin-1 (last two rows) [c] Determined by fluorescence polarization (from reference[64]); [d] n.d. = not determined; [e] Measured by fluorescence polarization at RT except for Gal-7 (from ref.[68]); [f] Determined by ITC at 24.8 °C (from ref.[59]).

3. *In vivo* anti-inflammatory activity of Gal-3 inhibitor at carrageenan-induced acute knee joint synovitis

The homology between human and rat Gal-3 CRDs is about 96.5%,[62] which make the rat models appropriate for *in vivo* testing of human Gal-3 inhibitors. To evaluate the activity

of the Gal-3i we synthesized we used an acute carrageenan-induced synovitis model. This is a short-term model usually used for drug screening and testing of cell therapies. Besides, these models constitute useful tools to design specific therapeutic interventions to suppress synovial inflammation.[71]

Before testing the activity of the Gal-3i, a syringeability test was done with one rat receiving 100 µL of HA-fibrin *in situ* gel with 30% blank NCs and without further inflammation induction. In order to see the influence of the DDS and the activity of the Gal-3i, an *in vivo* experiment was done in rats with induced synovitis. Another animal was induced with carrageenan, acting as a disease control. Other rats were distributed between three groups according to the received treatment (100 µL, IA): blank NCs used as vehicle control (group 1), Gal-3i loaded NCs at dose 200 µg/kg (group 2) and HA-fibrin *in situ* gel with 30% Gal-3i loaded NCs at dose 55 µg/kg (group 3). The drug activity was monitored at 4 hours after synovitis induction, when the peak of inflammation is reached.[72] Knee swelling measurements, whole blood tests, and histopathological analysis data demonstrated pronounced anti-inflammatory activity of Gal-3i. Knee swelling data (**Figure 8**) exhibited reduction of knee diameter in: 1.6 times (group 1), 3.5 times (group 2) and 7 times (group 3) compared to carrageenan control.

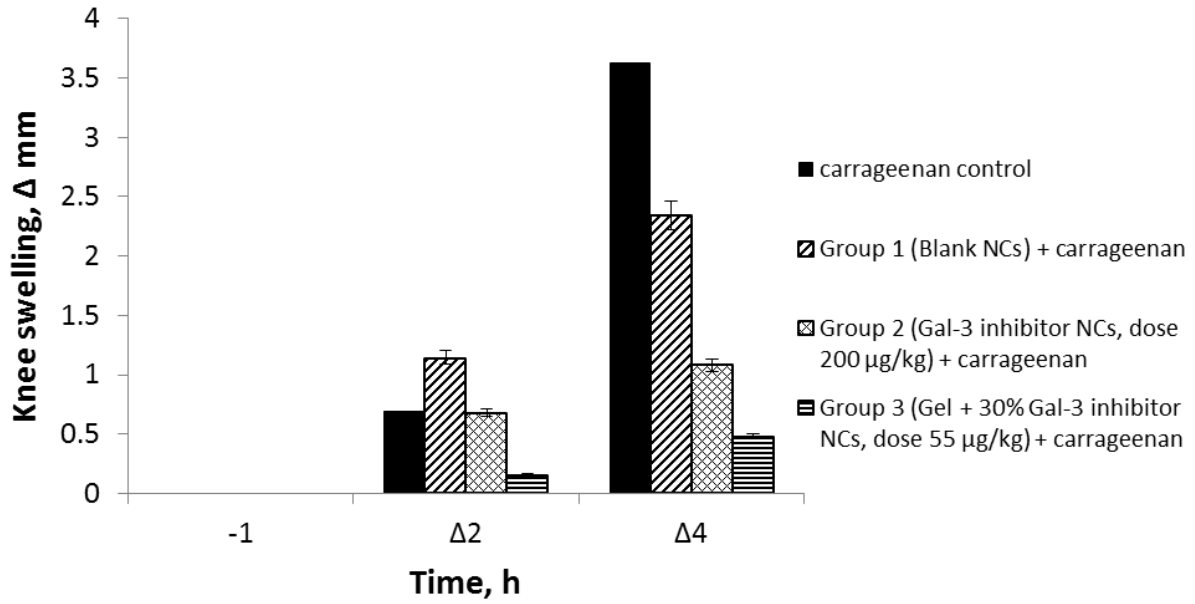

Figure 8. Effect of the treatment with Gal-3 inhibitor on the carrageenan-induced joint inflammation model using NCs, and NCs in a gel compared to blank NCs, a gel with blank NCs and carrageenan control (n = 5 for groups 1-3, n = 1 for carrageenan control). Δ is the difference in knee diameter at different time points before and after injection of carrageenan, expressed in mm. Data expressed as mean ± SEM.

This becomes more remarkable if we consider that the dose used for group 3 is considerably lower than for the group 2 (55 vs 200 µg/kg). Possibly, HA-fibrin hydrogel effectively keeps NCs within the articular cavity, modulates the release and by itself has a beneficial effect on joints healing even in the short inflammatory rat model.

The inflammation process is accompanied by rapid inversion of the leukogram ratio: decrease of lymphocytes and increase of neutrophils,[72] which in turn attract macrophages and dendritic cells expressed as total monocytes in **Figure 9**. Considering the obtained results, Gal-3i loaded NCs in the hydrogel is able to prevent this tendency, improving the total leucocytes amount, increasing the lymphocytes and reducing the neutrophils level.[73–75]

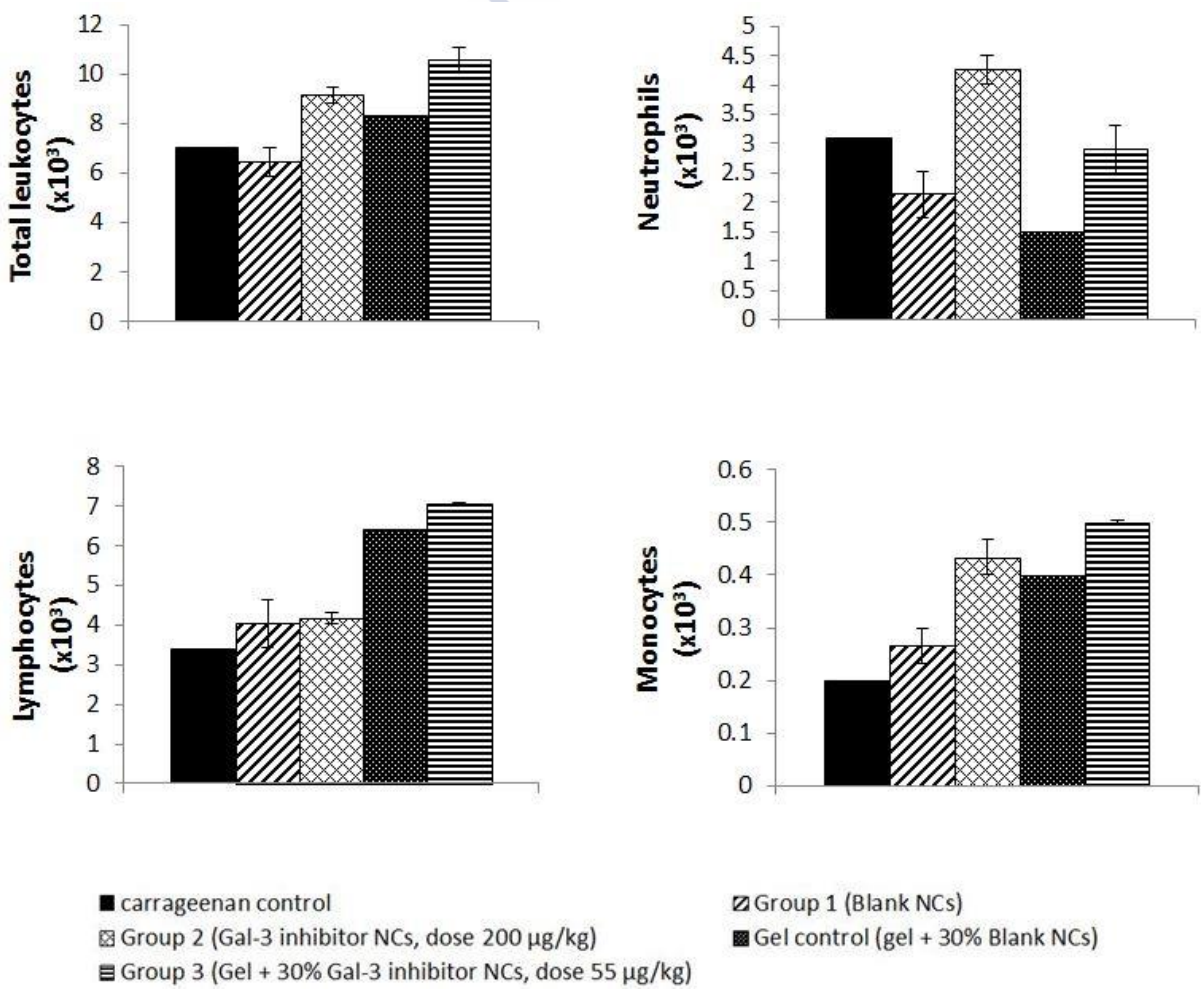

Figure 9. Effect of the treatment with Gal-3 inhibitor on leukocyte levels at the blood plasma at different doses administered in NCs, and the gel compared to blank NCs and carrageenan control (n = 5 for groups 1-3, n = 1 for carrageenan and gel control). Data expressed as mean ± SEM.

Supplementary, after a decalcification process the rat hind paws and knees were sliced, stained and analyzed by light microscopy (**Figure 10 A-D**). The improvement on the histological level was gradually observed from carrageenan control to group 3, suggesting that Gal-3i in its final DDS (Gel + 30% NCs) has the most detectable impact on the inhibition of synovial inflammation and the articular tissues integrity in rat synovitis model. Group 3 has less synovial membrane changes than other groups, besides, the articular cavity was free of neutrophils and no signs of cell infiltration were detected in the surrounding tissues.

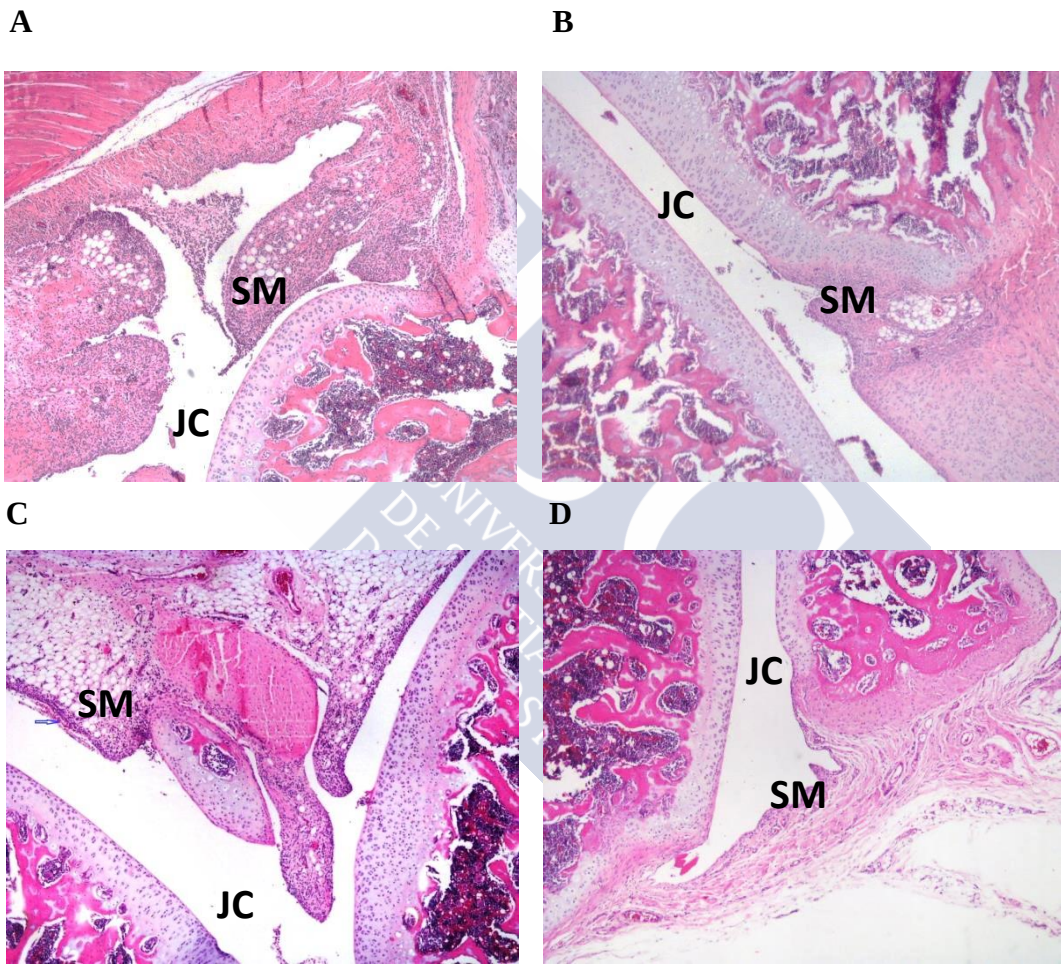

Figure 10. Microphotographs from rat knee joints stained with haematoxylin and eosin; low (40×), medium (100×) and high (400x) magnification (columns 1, 2 and 3 respectively). The square areas in the images reveal the amplified regions of the photograph. Groups: control of carrageenan (row **A**), blank NCs + carrageenan (row **B**), Gal-3i NCs + carrageenan (row **C**), and Gal-3i NCs + gel + carrageenan (row **D**) (row **E**). Abbreviations: **SM**, synovial membranes; **JC**, joint cavity.

Given that articular cartilage has limited ability to self-healing,[76] fortified HA-fibrin gel may contribute to restore the integrity of cartilage in longer chronic rat inflammatory

models, serving as a temporary matrix for *in vivo* cells encapsulation.[35] *In vivo* gel half-life time in rat joint was not evaluated in this study, but might be interesting for further exploration of DDS performance. Such a composite might result to a synergistic effect in tissue self-healing properties – HA-fibrin matrix plays a major role in the subsequent tissue regeneration processes.[37]

In summary, this work highlights the development of a new nanotechnology-based platform for an efficient treatment of joint pathologies (*e.g.* rheumatoid arthritis). An intra-articular injectable *in situ* hydrogel consisting of an IPN of HA and fibrin crosslinked with FXIII and α2-AP, containing drug loaded NCs (30%). The system presents well-organized structure and rheological behavior typical for stable gel networks, with features of both elastic and solid-like materials desired for IA application. HA NCs, dispersed in the gel, serve as multireservoirs for lipophilic anti-inflammatory drugs and they control and prolong the release of the encapsulated drug. The physicochemical evaluation of the drug delivery system was performed for DXM, as a model drug, and later on applied to a synthetized highly affine and specific Gal-3i.

The results obtained in a preliminary *in vivo* acute knee synovitis rat model showed a remarkable suppression of inflammation by Gal-3 inhibitor encapsulated within hydrogel and administrated intra-articular at microgram scale doses. Treated rats showed improvement on the knee swelling, at the histological and at the white cells levels. These findings present a promising strategy for the treatment of inflammatory knee diseases by the inhibition of galectin-3 and Gal-3 inhibitor as a lead compound for immunotherapeutic drug candidate in particular for RA. Efficiency of Gal-3 inhibitor could be further enhanced by preparation of multivalent inhibitors using synthetic scaffolds mimicking lactose units. Apart from joints pathologies, Gal-3 mono- or multivalent inhibitors could be applied for the treatment of other inflammatory conditions, *e.g.* cancer, inflammatory bowel disease, etc. increasing the range of therapeutic possibilities for these new compounds. At the same time, we showed the potential of a new *in situ* hydrogel as an IA DDS. The developed hydrogel might also have self-healing properties, behaving as a viscosupplement and could work as an *in situ* cell scaffold, all these properties being of interest for the treatment of the degenerative joint diseases.

REFERENCES

1. Evans, C. H., Kraus, V. B. & Setton., L. A. Progress in intra-articular therapy. *Nat. Rev. Rheumatol.* **10,** 11–22 (2015).

2. Kang, M. L. & Im, G.-I. Drug delivery systems for intra-articular treatment of osteoarthritis. *Expert Opin. Drug Deliv.* **11,** 269–82 (2014).

3. Klyosov, A. A. in *Galectin Therapeutics* (2012).

4. Roy, R., Murphy, P. V. & Gabius, H. J. Multivalent carbohydrate-lectin interactions: How synthetic chemistry enables insights into nanometric recognition. *Molecules* **21,** (2016).

5. Oberg, C. T., Leffler, H. & Nilsson, U. J. Inhibition of galectins with small molecules. *Chimia (Aarau).* **65,** 18–23 (2011).

6. St-Pierre, C. *et al.* Galectin-1-specific inhibitors as a new class of compounds to treat HIV-1 infection. *Antimicrob. Agents Chemother.* **56,** 154–162 (2012).

7. Burt, H. M., Tsallas, A., Gilchrist, S. & Liang, L. S. Intra-articular drug delivery systems: Overcoming the shortcomings of joint disease therapy. *Expert Opin. Drug Deliv.* **6,** 17–26 (2009).

8. Zhang, Z. *et al.* Intra-articular injection of cross-linked hyaluronic acid-dexamethasone hydrogel attenuates osteoarthritis: An experimental study in a rat model of osteoarthritis. *Int. J. Mol. Sci.* **17,** (2016).

9. Haudek, K. C. *et al.* Dynamics of galectin-3 in the nucleus and cytoplasm. *Biochim. Biophys. Acta - Gen. Subj.* **1800,** 181–189 (2010).

10. Sörme, P., Arnoux, P., Kahl-Knutsson, B. & Leffler, H. Structural and Thermodynamic Studies on Cation− Π Interactions in Lectin− Ligand Complexes: High-Affinity Galectin-3 Inhibitors through Fine-Tuning of an Arginine− *J Am Chem* 543–549 (2005).

11. Lepur, A. Functional properties of Galectin-3. Beyond the sugar binding. *Lund University, University of Zagreb* (2012).

12. Thiemann, S. & Baum, L. G. Galectins and Immune Responses—Just How Do They Do Those Things They Do? *Annu. Rev. Immunol* **34,** 243–64 (2016).

13. Vasta, G. R. *et al.* Galectins as self/non-self recognition receptors in innate and adaptive immunity: An unresolved paradox. *Front. Immunol.* **3,** 1–14 (2012).

14. Rabinovich, G. A. & Toscano, M. A. Turning 'sweet' on immunity: galectin-glycan interactions in immune tolerance and inflammation. *Nat. Rev. Immunol.* **9,** 338–352 (2009).

15. Hu, Y., Yéléhé-Okouma, M., Ea, H. K., Jouzeau, J. Y. & Reboul, P. Galectin-3: A key player in arthritis. *Jt. Bone Spine* **84,** 15–20 (2017).

16. Klyosov, A. a. Galectins as New Therapeutic Targets for Galactose-Containing Polysaccharides. *Bull. Georg. Natl. Acad. Sci.* **8,** 5–17 (2014).

17. Chen, H. Y., Liu, F.-T. & Yang, R.-Y. Roles of galectin-3 in immune responses. *Arch. Immunol. Ther. Exp. (Warsz).* **53,** 497–504 (2005).

18. Quan, L.-D., Thiele, G. M., Tian, J. & Wang, D. The Development of Novel Therapies for Rheumatoid Arthritis. *Expert Opin. Ther. Pat.* **18,** 723–738 (2008).

19. Page-McCaw, A., Ewald, A. J. & Werb, Z. Matrix metalloproteinases and the regulation of tissue. *Nat Rev Mol Cell Biol.* **8,** 221–233 (2007).

20. Fezai, M., Senovilla, L., Jemaà, M., Ben-Attia, M. & Ben-Attia, M. Analgesic, Anti-Inflammatory and Anticancer Activities of Extra Virgin Olive Oil. *J. Lipids* **2013,** 1–7 (2013).

21. Cecerale, S. in *Olive oil - Constituents, Health Properties and Bioconversions* (INTECH, 2011).

22. Moghimipour, E., Salimi, A., Karami, M. & Isazadeh, S. Preparation and characterization of dexamethasone microemulsion based on pseudoternary phase diagram. *Jundishapur J. Nat. Pharm. Prod.* **8,** 105–112 (2013).

23. Chime, S. a, Kenechukwu, F. C. & Attama, a a. Nanoemulsions — Advances in Formulation , Characterization and Applications in Drug Delivery. (2014).

24. Mourdikoudis, S. & Liz-Marzán, L. M. Oleyamine in Nanoparticle Synthesis. *Chem. Mater.* **25,** 1465 (2013).

25. Ghosh, P. & Guidolin, D. Potential mechanism of action of intra-articular hyaluronan therapy in osteoarthritis: Are the effects molecular weight dependent? *Semin. Arthritis Rheum.* **32,** 10–37 (2002).

26. Oyarzun-Ampuero, F., Rivera-Rodriguez, G. R., Alonso, M. J. & Torres, D. Hyaluronan nanocapsules as a new vehicle for intracellular drug delivery. *Eur. J. Pharm. Sci.* **49,** 483–490 (2013).

27. Morgen, M. *et al.* Nanoparticles for improved local retention after intra-articular injection into the knee joint. *Pharm. Res.* **30,** 257–268 (2013).

28. Butoescu, N., Jordan, O. & Doelker, E. Intra-articular drug delivery systems for the treatment of rheumatic diseases: A review of the factors influencing their performance. *Eur. J. Pharm. Biopharm.* **73,** 205–218 (2009).

29. Butoescu, N. *et al.* Dexamethasone-containing biodegradable superparamagnetic microparticles for intra-articular administration: Physicochemical and magnetic

properties, in vitro and in vivo drug release. *Eur. J. Pharm. Biopharm.* **72,** 529–538 (2009).

30. Chernyshev, V. S. *et al.* Size and shape characterization of hydrated and desiccated exosomes. *Anal. Bioanal. Chem.* **407,** 3285–3301 (2015).

31. Weigel, P. H., Frost, S. J., McGary, C. T. & LeBoeuf, R. D. The role of hyaluronic acid in inflammation and wound healing. *Int. J. Tissue React.* **10,** 355–365 (1988).

32. Frost, S. J. & Weigel, P. H. Binding of hyaluronic acid to mammalian fibrinogens. *BBA - Gen. Subj.* **1034,** 39–45 (1990).

33. Yang, C. L., Chen, H. W., Wang, T. C. & Wang, Y. J. A novel fibrin gel derived from hyaluronic acid-grafted fibrinogen. *Biomed. Mater.* **6,** 025009 (2011).

34. Lee, F. & Kurisawa, M. Formation and stability of interpenetrating polymer network hydrogels consisting of fibrin and hyaluronic acid for tissue engineering. *Acta Biomater.* **9,** 5143–5152 (2013).

35. Zhang, Y., Heher, P., Hilborn, J., Redl, H. & Ossipov, D. a. Hyaluronic acid-fibrin interpenetrating double network hydrogel prepared in situ by orthogonal disulfide cross-linking reaction for biomedical applications. *Acta Biomater.* **38,** 23–32 (2016).

36. LeBoeuf, R. D., Raja, R. H., Fuller, G. M. & Weigel, P. H. Human fibrinogen specifically binds hyaluronic acid. *J. Biol. Chem.* **261,** 12586–12592 (1986).

37. Weigel, P. H., Fuller, G. M. & LeBoeuf, R. D. A model for the role of hyaluronic acid and fibrin in the early events during the inflammatory response and wound healing. *J. Theor. Biol.* **119,** 219–234 (1986).

38. Francis W and Marder, J. Increased resistance to plasmic degradation of fibrin with highly crosslinked alpha-polymer chains formed at high factor XIII concentrations. *Blood* **71,** (1988).

39. Muszbek, L., Bereczky, Z., Bagoly, Z., Komáromi, I. & Katona, É. Factor XIII: a coagulation factor with multiple plasmatic and cellular functions. *Physiol. Rev.* **91,** 931–972 (2011).

40. Lovejoy, A. E. *et al.* Safety and pharmacokinetics of recombinant factor XIII-A 2 administration in patients with congenital factor XIII deficiency. *Hematology* **108,** 57–62 (2006).

41. Greenberg, C. S. & Shumang, M. A. The Zymogen Forms of Blood Coagulation Factor XIII Bind Specifically to Fibrinogen. *J. Biol. Chem.* **257,** 6096–6101 (1982).

42. Tsurupa, G., Yakovlev, S., McKee, P. & Medved, L. Noncovalent interaction of alpha(2)-antiplasmin with fibrin(ogen): localization of alpha(2)-antiplasmin-binding sites. *Biochemistry* **49,** 7643–7651 (2010).

43. Carpenter, S. L. & Mathew, P. α2-antiplasmin and its deficiency: Fibrinolysis out of balance. *Haemophilia* **14,** 1250–1254 (2008).

44. Lee, K. N. *et al.* Antiplasmin-cleaving enzyme is a soluble form of fibroblast activation protein. *Blood* **107,** 1397–1404 (2006).

45. Mosesson, M. W. *et al.* Evidence that a2-antiplasmin becomes covalently ligated to plasma fibrinogen in the circulation: A new role for plasma factor XIII in fibrinolysis regulation. *J. Thromb. Haemost.* **6,** 1565–1570 (2008).

46. Janmey, P. a, Winer, J. P. & Weisel, J. W. Fibrin gels and their clinical and bioengineering applications. *J. R. Soc. Interface* **6,** 1–10 (2009).

47. *Instruction For Use Synvisc® (hylan G-F 20).* 1–6 (2014).

48. Eymard, F. *et al.* Predictors of response to viscosupplementation in patients with hip osteoarthritis: results of a prospective, observational, multicentre, open-label, pilot study. *BMC Musculoskelet. Disord.* **18,** 1–8 (2017).

49. Chiu, C. L., Hecht, V., Duong, H., Wu, B. & Tawil, B. Permeability of Three-Dimensional Fibrin Constructs Corresponds to Fibrinogen and Thrombin Concentrations. *Biores. Open Access* **1,** 34–40 (2012).

50. Lugovskoy, E.V. , Makogonenko, E.M., Komisarenko, S. . *Molecular Mechanisms of formation and degradation of fibrin*. 2013 (2013).

51. Ranch, K. *et al.* Development of in situ ophthalmic gel of dexamethasone sodium phosphate and chloramphenicol: A viable alternative to conventional eye drops. *J. Appl. Pharm. Sci.* **7,** 101–108 (2017).

52. Borden, R. C. *et al.* Hyaluronic acid hydrogel sustains the delivery of dexamethasone across the round window membrane. *Audiol. Neurotol.* **16,** 1–11 (2010).

53. Webber, M. J., Matson, J. B., Tamboli, V. K. & Stupp, S. I. Controlled release of dexamethasone from peptide nanofiber gels to modulate inflammatory response. *Biomaterials* **33,** 6823–6832 (2012).

54. Wu, Q. *et al.* Thermosensitive hydrogel containing dexamethasone micelles for preventing postsurgical adhesion in a repeated-injury model. *Sci. Rep.* **5,** 13553 (2015).

55. Klyosov, A., Zomer, E. & Platt, D. in *Glycobiology and Drug Design* **1102,** 89–130 (American Chemical Society, 2012).

56. ClinicalTrials. A New Agent GM-CT-01 in Combination With 5-FU, Avastin and Leucovorin in Subjects With Colorectal A New. 10–12 (2016).

57. Harrison, S. a. *et al.* Randomised clinical study: GR-MD-02, a galectin-3 inhibitor, vs. placebo in patients having non-alcoholic steatohepatitis with advanced fibrosis. *Aliment. Pharmacol. Ther.* **44,** 1183–1198 (2016).

58. ClinicalTrials. RCT (Randomized Control Trial) of TD139 vs Placebo in HV's (Human Volunteers) and IPF Patients Purpose. 10–12 (2016).

59. Hsieh, T. *et al.* Dual thio-digalactoside-binding modes of human galectins as the structural basis for the design of potent and selective inhibitors. *Sci. Rep.* **6,** 29457 (2016).

60. ClinicalTrials. An Open-Label, Phase 2a Study to Evaluate Safety and Efficacy of GR-MD-02 for Treatment of Psoriasis An Open-Label,12–14 (2017).

61. ClinicalTrials. Clinical Trial to Evaluation the Safety and Efficacy of GR-MD-02 for the Treatment of Liver Fibrosis and Resultant Portal Hypertension in Patients With Nash Cirrhosis (NASH-CX) 4–7 (2017).

62. Hsieh, T. J. *et al.* Structural basis underlying the binding preference of human galectins-1, -3 and -7 for Galβ1-3/4GlcNAc. *PLoS One* **10,** 1–19 (2015).

63. Cooper, D. N. W. Galectinomics: Finding themes in complexity. *Biochim. Biophys. Acta - Gen. Subj.* **1572,** 209–231 (2002).

64. Cumpstey, I., Salomonsson, E., Sundin, A., Leffler, H. & Nilsson, U. J. Studies of arginine-arene interactions through synthesis and evaluation of a series of galectin-binding aromatic lactose esters. *ChemBioChem* **8,** 1389–1398 (2007).

65. Blanchard, H., Yu, X., Collins, P. M. & Bum-erdene, K. Galectin-3 inhibitors : a patent review (2008 -- present). *Expert Opin. Ther. Patents* 1–13 (2014).

66. Cumpstey, I., Salomonsson, E., Sundin, A., Leffler, H. & Nilsson, U. J. Double affinity amplification of galectin-ligand interactions through arginine-arene interactions: synthetic, thermodynamic, and computational studies with aromatic diamido thiodigalactosides. *Chemistry* **14,** 4233–4245 (2008).

67. Seetharaman, J. *et al.* X-ray crystal structure of the human galectin-3 carbohydrate recognition domain at 2.1-A resolution. *J. Biol. Chem.* **273,** 13047–13052 (1998).

68. Delaine, T. *et al.* Galectin-3-Binding Glycomimetics that Strongly Reduce Bleomycin-Induced Lung Fibrosis and Modulate Intracellular Glycan Recognition. *ChemBioChem* **17,** 1759–1770 (2016).

69. Sörme, P., Kahl-Knutson, B., Wellmar, U., Nilsson, U. J. & Leffler, H. Fluorescence polarization to study galectin-ligand interactions. *Methods Enzymol.* **362,** 504–512 (2003).

70. Van Hattum, H. *et al.* Tuning the preference of thiodigalactoside- and lactosamine-based ligands to galectin-3 over galectin-1. *J. Med. Chem.* **56,** 1350–1354 (2013).

71. Santos, J. M. *et al.* The role of human umbilical cord tissue-derived mesenchymal stromal cells (UCX®) in the treatment of inflammatory arthritis. *J. Transl. Med.* **11,** 18 (2013).

72. Ekundi-Valentim, E. *et al.* Differing effects of exogenous and endogenous hydrogen sulphide in carrageenan-induced knee joint synovitis in the rat. *Br. J. Pharmacol.* **159,** 1463–1474 (2010).

73. Gibofsky, A. Overview of epidemiology, pathophysiology, and diagnosis of rheumatoid arthritis. *Am. J. Manag. Care* **18,** S295–302 (2012).

74. Tanaka, D., Kagari, T., Doi, H. & Shimozato, T. Essential role of neutrophils in anti-type II collagen antibody and lipopolysaccharide-induced arthritis. *Immunology* **119,** 195–202 (2006).

75. Kaplan, M. J. Role of neutrophils in systemic autoimmune diseases. *Arthritis Res. Ther.* **15,** 219 (2013).

76. Ahearne, M., Buckley, C. T. & Kelly, D. J. A growth factor delivery system for chondrogenic induction of infrapatellar fat pad-derived stem cells in fibrin hydrogels. *Biotechnol. Appl. Biochem.* **58,** 345–352 (2011).

Conclusions

If you can't explain it simply, you don't understand it well enough.

Albert Einstein

USC
UNIVERSIDADE
DE SANTIAGO
DE COMPOSTELA

CONCLUSIONS

This thesis project comprised the design, development and characterization of a novel injectable nanotechnology-based system intended to prolong and control the release of the associated drug in the intra-articular (IA) cavity. The system is composed of an *in situ* forming hydrogel loaded with polymeric nanocapsules, which serve as multireservoirs for different lipophilic anti-inflammatory drugs, namely i) a model drug – dexamethasone; and ii) a novel synthesized drug candidate – galectin-3 (Gal-3) antagonist. The obtained experimental results led to following conclusions:

1) A novel highly affine, potent and selective monovalent Gal-3 inhibitor, composed of two different moieties assembled to a modified lactosamine core was developed and synthetized in this study. Its K_d to Gal-3, measured by direct and competitive fluorescence polarization assay, was 0.59 µM at 4 °C (2.99 µM at 25 °C), while fluorescein-labelled Gal-3 inhibitor displayed very high affinity to Gal-3, K_d = 14 nM at 4 °C (82 nM at 25 °C), certainly higher than a reported commercial Gal-3 inhibitor DAVANAT® has. An important feature of this compound is the ability to discriminate between Gal-1/Gal-3/Gal-7, while DAVANAT® could hardly discriminate between Gal-1 and Gal-3. On the other hand, a first low MW Gal-3 antagonist TD139, approved by FDA, with modified thio-digalactoside core, measured in the same assay, has been experimentally confirmed to have high affinity K_d(Gal-3) = 0.036 µM at 4 °C (0.166 µM at 25 °C) and high selectivity among Gal-1/Gal-3/Gal-7. Considering the success of TD139, the low MW Gal-3 inhibitor that we developed might receive future pharmaceutical advancement.

2) Polymeric NCs consisting of an olive oil core and a HA coating were successfully prepared using a simple solvent displacement method. The NCs can be loaded with dexamethasone (5.6 ± 0.4 mg/mL) or Gal-3 inhibitor (531 ± 5 µg/mL), have nanometric size (135 ± 9 nm and 122 ± 11 nm, correspondingly), negative surface charge and regular spherical shape.

3) Two injectable *in situ* forming hydrogel systems were developed. One of them is composed of HA and fibrin interpenetrating network, and the other one contains HA and fibrin additionally crosslinked and fortified with factor XIII and α2-antiplasmin in

order to have an increased half-life time. The hydrogels showed an easily adjustable gelation time, a well-defined microstructure and adequate mechanical properties. In addition, the gels could load 30% (v/v) of NCs during their self-assembly. The initial viscosity of the gelling system was significantly lower compared to commercial viscosupplementations agents, thus allowing its good syringeability. The rheological studies revealed the resistance of the hydrogels to high deformations, and showed both, elastic and solid-like behavior, adequate for IA sustainability. Regarding its structure, the formulation has well-defined pores with NCs randomly dispersed within the gel. This IA drug delivery system (DDS) exhibited a controlled and prolonged *in vitro* drug release profile.

4) Preliminary *in vivo* studies performed in carrageenan-induced acute knee joint synovitis rat model demonstrated a remarkable suppression of inflammation by Gal-3 inhibitor. Both, the group with drug-loaded NCs and the group with drug-loaded NCs in the gel, administrated IA at microgram scale doses (55 and 200 μg/kg), performed significantly better compared with the non-treated control. These findings presented Gal-3 inhibitor as a lead compound for immunotherapeutic drug candidate for inflammatory knee diseases, in particular for rheumatoid arthritis. Noticeably, blank NCs also showed a tendency to contribute to joints healing by reducing the synovial inflammation.

Overall, the work presented here describes the development and characterization of a new biodegradable *in situ* forming hydrogel adapted for IA administration. The hydrogel serves as a depot for drug-loaded NCs, preventing their fast elimination from the joint cavity and allowing prolonged drug release profile. The rheological properties of the initial system enabled good syringeability and desirable mechanical properties for intra-articular application. Preliminary *in vivo* activity of galectin-3 inhibitor confirmed galectin-3 as a potential immunotherapeutic target for inflammatory joints diseases as rheumatoid arthritis.

Annex

(Permissions and Reprints)

USC
UNIVERSIDADE
DE SANTIAGO
DE COMPOSTELA

1. Ethical permission for *in vivo* studies, Chapter 2:

GOVERNO DE PORTUGAL | MINISTÉRIO DA AGRICULTURA E DO MAR

dgav Direção Geral de Alimentação e Veterinária

Ex ma Senhora
Doutora Sandra Isabel Dias Simões
Faculdade de Farmácia da Universidade de Lisboa
Departamento de Farmácia Galénica e Tecnologia Farmacêutica
Campus do Lumiar
Estrada do poço do Lumiar, 22
Edifício F, R/C
1649 – 038 LISBOA

2014-05-22 011974

Nossa referência	Vossa referência	Vossa data
0421/000/000 /2014		

Assunto: **PROTEÇÃO DOS ANIMAIS UTILIZADOS PARA FINS EXPERIMENTAIS E/OU OUTROS FINS CIENTÍFICOS – PEDIDO DE AUTORIZAÇÃO PARA REALIZAÇÃO DE PROJECTO DE EXPERIMENTAÇÃO ANIMAL**

Na sequência do pedido efetuado por V. Exª no sentido de poder ser autorizada a realização do projeto experimental designado **"PRIMED-UCX – Pré-Condicionamento de células mesenquimatosas da matriz do cordão umbilical (UCX®) como forma de incrementar a potência terapêutica para a artrite reumatóide"**, de que é a investigadora responsável, cabe-me informar que o mesmo foi avaliado de acordo com o Artigo 44º do Decreto-Lei nº 113/2013, de 7 de Agosto, relativo à "proteção dos animais utilizados para fins científicos".

Mais se informa V. Exª que, depois de esclarecidas as dúvidas que a sua análise nos levantou, o projeto em apreço recebeu uma **avaliação favorável** e foi **autorizado** de acordo com o nº 1, do Artigo 42º do mesmo diploma legislativo.
No entanto, e dado os procedimentos serem classificados como "Moderado", é primordial fazer-se, no decorrer do desenvolvimento do projeto, uma adequada monitorização dos sinais de dor, sofrimento ou angústia dos animais submetidos aos procedimentos, por forma a poder fazer-se uma atualização sobre o nível de dor efetiva a que os mesmos possam ficar sujeitos.

Finalmente, resta-me especificar, de acordo com o discriminado no nº 2, do Artigo 46º, do atrás referido Decreto-Lei, o seguinte:

- **O utilizador que realiza o projeto:** Senhor Diretor da Faculdade de Farmácia da universidade de Lisboa;
- **A pessoa responsável pela execução global do projeto e pela sua conformidade com a autorização do mesmo:** Doutora Sandra Isabel Dias Simões;
- **O estabelecimento onde o projeto vai ser realizado:** Biotério de pequenos roedores da Faculdade de Farmácia da Universidade de Lisboa, no Campus do Lumiar.

Com os melhores cumprimentos,

O Diretor-Geral

As) Álvaro Pegado Mendonça

DBEA/APM

SEDE : LARGO DA ACADEMIA NACIONAL DE BELAS ARTES, 2 – 1249-105 LISBOA TELEF. 21 323 95 00 FAX. 21 346 35 18

Permission to use graphical material as Figure 2 in Chapter Resumen in *exteno*, Figure 2 in Chapter Résumé, Figure 1 in Chapter 1, and Figure 1 in Chapter Overall discussion.

https://s100.copyright.com/AppDispatchServlet#formTop

Copyright Clearance Center RightsLink®

Home | Create Account | Help

informa healthcare

Title: Intra-articular drug delivery systems: overcoming the shortcomings of joint disease therapy

Author: Helen M Burt, Antonia Tsallas, Samuel Gilchrist, et al

Publication: Expert Opinion on Drug Delivery

Publisher: Taylor & Francis

Date: Jan 1, 2009

Copyright © 2009 Taylor & Francis

LOGIN

If you're a copyright.com user, you can login to RightsLink using your copyright.com credentials. Already **a RightsLink user** or want to learn more?

Thesis/Dissertation Reuse Request

Taylor & Francis is pleased to offer reuses of its content for a thesis or dissertation free of charge contingent on resubmission of permission request if work is published.

BACK | CLOSE WINDOW

Copyright © 2017 Copyright Clearance Center, Inc. All Rights Reserved. Privacy statement. Terms and Conditions.
Comments? We would like to hear from you. E-mail us at customercare@copyright.com

Permission to use graphical material as Figure 1, Chapter Introduction.

PERMISSION LICENSE: EDUCATIONAL PRINT & ELECTRONIC USE

Request ID/Invoice Number: NAT052690320-1

Date: February 09, 2018

To: Nataliya Storozhylova
University of Santiago de Compostela
CIMUS
Avda. de Barcelona s/n, Campus Vida
Santiago de Compostela
A CORUNA 15782
Spain
"Licensee"

McGraw-Hill Education Material

Author: Chew and Golden
Title: The Permanent Pain Cure: The Breakthrough Way to Heal Your Muscle and Joint Pain for Good
ISBN: 9780071627139
Edition: 1
Description of material: Figure 2.1 on Page 22 (1 figure ONLY)

Fee: "Waived"

Purpose of Reproduction

School: Universty Of Santiago De Compostela
Purpose of use: For use in a doctoral dissertation titled "New potential nanotechnology-based therapies for the treatment of rheumatoid arthritis"
Format: Print and Electronic (Electronic- open access website)
Number of Copies: 20 printed copies
Distribution: One-time educational use for the above purposes only.

Permission to use to use graphical material as Figure 2, Chapter Introduction.

reprint permission

Support <support@mdpi.com> 29 січня 2018 р. о 10:15
Кому: Nataliya Storozhylova <nstorozhylova@gmail.com>

Dear Nataliya,

Thank you for your enquiry. /Polymers/ is an open access journal and its articles are published under an open access (CC BY) license. It means you are free to re-use and copy content, including figures, on condition the original source is cited properly. You do not need formal permission for using the Figure (https://creativecommons.org/licenses/by/4.0/).

Kind regards,
Luca Rasetti
-MDPI Support

Permission to use graphical material as Figure 3, Chapter Introduction.

Permission to use graphical material as Figure 4-5, Chapter Introduction.

ELSEVIER LICENSE
TERMS AND CONDITIONS

Jul 21, 2017

This Agreement between Ms. Nataliya Storozhylova ("You") and Elsevier ("Elsevier") consists of your license details and the terms and conditions provided by Elsevier and Copyright Clearance Center.

License Number	4153721135768
License date	Jul 21, 2017
Licensed Content Publisher	Elsevier
Licensed Content Publication	Biochimica et Biophysica Acta (BBA) - General Subjects
Licensed Content Title	Galectin-3: An open-ended story
Licensed Content Author	Jerka Dumic,Sanja Dabelic,Mirna Flögel
Licensed Content Date	Apr 1, 2006
Licensed Content Volume	1760
Licensed Content Issue	4
Licensed Content Pages	20
Start Page	616
End Page	635
Type of Use	reuse in a thesis/dissertation
Portion	figures/tables/illustrations
Number of figures/tables /illustrations	2
Format	both print and electronic
Are you the author of this Elsevier article?	No
Will you be translating?	No
Original figure numbers	Fig. 1. Fig. 2.
Title of your thesis/dissertation	New potential nanotechnology-based therapies for the treatment of rheumatoid arthritis
Expected completion date	Sep 2017
Estimated size (number of pages)	220
Requestor Location	Ms. Nataliya Storozhylova Rua Garcia Prieto 54-56, 2B Santiago de Compostela, 15706 Spain Attn: Ms. Nataliya Storozhylova
Publisher Tax ID	GB 494 6272 12
Total	0.00 EUR
Terms and Conditions	

Permission to use graphical material as Figure 6, Chapter Introduction.

Permission to use graphical material as Figure 7A, Chapter Introduction.

ELSEVIER LICENSE
TERMS AND CONDITIONS

Jul 21, 2017

This Agreement between Ms. Nataliya Storozhylova ("You") and Elsevier ("Elsevier") consists of your license details and the terms and conditions provided by Elsevier and Copyright Clearance Center.

License Number	4153731472905
License date	Jul 21, 2017
Licensed Content Publisher	Elsevier
Licensed Content Publication	Biochemical and Biophysical Research Communications
Licensed Content Title	Biophysical and structural characterization of mono/di-arylated lactosamine derivatives interaction with human galectin-3
Licensed Content Author	Cédric Atmanene,Céline Ronin,Stéphane Téletchéa,François-Moana Gautier,Florence Djedaïni-Pilard,Fabrice Ciesielski,Valérie Vivat,Cyrille Grandjean
Licensed Content Date	Jul 29, 2017
Licensed Content Volume	489
Licensed Content Issue	3
Licensed Content Pages	6
Start Page	281
End Page	286
Type of Use	reuse in a thesis/dissertation
Portion	figures/tables/illustrations
Number of figures/tables /illustrations	1
Format	both print and electronic
Are you the author of this Elsevier article?	No
Will you be translating?	No
Original figure numbers	Fig.1
Title of your thesis/dissertation	New potential nanotechnology-based therapies for the treatment of rheumatoid arthritis
Expected completion date	Sep 2017
Estimated size (number of pages)	220
Requestor Location	Ms. Nataliya Storozhylova Rua Garcia Prieto 54-56, 2B Santiago de Compostela, 15706 Spain Attn: Ms. Nataliya Storozhylova
Publisher Tax ID	GB 494 6272 12
Total	0.00 EUR
Terms and Conditions	

Permission to use graphical material as Figure 7B, Chapter Introduction.

Permission to use graphical material as Figure 1 in Chapter 2.

Reuse of Content Within a Thesis or Dissertation

Content (full-text or portions thereof) may be used in print and electronic versions of a dissertation or thesis without formal permission from the Massachusetts Medical Society (MMS), Publisher of the *New England Journal of Medicine*.

The following credit line must be printed along with the copyrighted material:

> Reproduced with permission from (scientific reference citation), Copyright Massachusetts Medical Society.

Permission to use graphical material as Figure 2 in Chapter 2.

11200 Rockville Pike
Suite 302
Rockville, Maryland 20852

August 19, 2011

American Society for Biochemistry and Molecular Biology

To whom it may concern,

It is the policy of the American Society for Biochemistry and Molecular Biology to allow reuse of any material published in its journals (the Journal of Biological Chemistry, Molecular & Cellular Proteomics and the Journal of Lipid Research) in a thesis or dissertation at no cost and with no explicit permission needed. Please see our copyright permissions page on the journal site for more information.

Best wishes,

Sarah Crespi

American Society for Biochemistry and Molecular Biology
11200 Rockville Pike, Rockville, MD
Suite 302
240-283-6616
JBC | MCP | JLR

CONFLICT OF INTEREST

I declare no conflict of interest regarding the context of this thesis, entitled "New potential nanotechnology-based therapies for the treatment of rheumatoid arthritis".

Sgd. Nataliya Storozhylova